



Griffin, Sinead Gael (2020) *Investigating the role of sex and the right ventricle in the development and treatment of experimental pulmonary hypertension*. PhD thesis.

<http://theses.gla.ac.uk/81645/>

Copyright and moral rights for this work are retained by the author

A copy can be downloaded for personal non-commercial research or study, without prior permission or charge

This work cannot be reproduced or quoted extensively from without first obtaining permission in writing from the author

The content must not be changed in any way or sold commercially in any format or medium without the formal permission of the author

When referring to this work, full bibliographic details including the author, title, awarding institution and date of the thesis must be given

Enlighten: Theses

<https://theses.gla.ac.uk/>  
[research-enlighten@glasgow.ac.uk](mailto:research-enlighten@glasgow.ac.uk)

**Investigating the role of sex and the right ventricle  
in the development and treatment of experimental  
pulmonary hypertension**

**Sinéad Gael Griffin**

**BSc (Hons), MRes**

Submitted in fulfilment of the requirements for the degree of Doctor of  
Philosophy in the Institute of Cardiovascular and Medical Sciences, University of  
Glasgow

Institute of Cardiovascular and Medical Sciences

College of Medical, Veterinary and Life Sciences

University of Glasgow

September 2020

## Author's Declaration

I declare that this thesis has been written entirely by myself and is a record of the work performed by me, except where acknowledgement has been made. Margaret Nilsen and Dr. Craig Docherty provided assistance during the Anastrozole and FK506 *in vivo* studies. The protein expression analysis in rat pulmonary artery smooth muscle cells was generated by Dr. Katie Harvey. Development of the pulmonary artery banding model was carried out in collaboration with Margaret Nilsen and Michael Dunne. This thesis has not previously been submitted for a higher degree. The research was carried out in the Institute of Cardiovascular and Medical Sciences, College of Medical, Veterinary and Life Sciences at the University of Glasgow under the supervision of Prof. Stuart A. Nicklin and Dr. Christopher M. Loughrey.

Sinéad G. Griffin

January 2020

## Acknowledgements

Firstly, I would like to thank my supervisors Prof. Stuart Nicklin and Dr. Christopher Loughrey for their support and advice throughout my PhD studies, particularly during my final year in the lab. I also have to thank them for their continued encouragement and support in ensuring I completed my thesis.

I would also like to thank all my fellow lab members from Lab 427 - Lynn, Mags, Craig, Kirsty, Nina, Gerry, Teja, Afshan, Katie, Dawid, Alasdair and Claire. You all taught me so much and helped me develop as a scientist. As well as all the great laughs and nights out! A special thanks to Mags for her help with all things *in vivo*! Also, thank you to Mags and Mike for all their help with developing the PAB model. Thanks to the Nicklin and Loughrey groups for all their support during the final year when I was trying to learn a lot of new techniques and I had no idea where to start.

I don't look back on my PhD studies with many fond memories but the experience allowed me to work with some great people and gave me amazing friends and for that I am very grateful! To my lab mum Lynn, thank you so much for your friendship and all your support within and out with the lab. I couldn't have done it without you and I will be eternally grateful to you (so will my mum!). Steph, you were a constant support and a great friend to me throughout Undergrad, Masters and PhD, thank you so much. I'm incredibly proud of you and the courage you've shown. I know you'll be absolutely amazing in your new venture!

The final thanks go to my family - Mum, Dad, Seán and Niamh - and my husband Chris. I would not have managed this had it not been for your absolute faith in me. I feel very lucky to have a family and husband that whole heartedly believe I can achieve anything I put my mind to. You would not let me give up and you gave me the courage I needed to keep going. You have been there for me in so many ways throughout this whole journey and for that I can't thank you enough. Chris, you've been by my side throughout my whole university career, your support has been unwavering and you've done your very best to keep me sane during it all! Thank you.

# Table of Contents

AUTHOR'S DECLARATION .....	II
TABLE OF CONTENTS .....	IV
LIST OF FIGURES.....	XI
LIST OF TABLES.....	XIV
LIST OF PUBLICATIONS, PRESENTATIONS AND AWARDS .....	XV
DEFINITIONS/ABBREVIATIONS .....	XVI
SUMMARY .....	XX
CHAPTER 1.....	1
1 INTRODUCTION .....	1
1.1 Pulmonary circulation.....	2
1.2 The right ventricle.....	3
1.3 Pulmonary Hypertension .....	5
1.3.1 WHO Classifications .....	5
1.3.2 Clinical definitions .....	8
1.3.3 Epidemiology .....	8
1.3.4 Pathophysiology.....	9
1.3.4.1 Pulmonary artery remodelling .....	9
1.3.4.2 Right ventricular remodelling and failure .....	13
1.4 Genetic predisposition .....	16
1.4.1 Bone morphogenetic protein receptor signalling .....	16
1.4.2 Bone morphogenetic protein receptor 2 mutations as a risk factor for PAH .....	18
1.5 PAH Therapeutics .....	19
1.5.1 Current PAH therapeutics .....	19

1.5.1.1	Calcium channel blockers.....	21
1.5.1.2	Prostacyclin Analogues .....	21
1.5.1.3	Prostacyclin IP receptor agonist .....	22
1.5.1.4	Endothelin Receptor Antagonists .....	22
1.5.1.5	Phosphodiesterase 5 Inhibitors.....	23
1.5.2	Potential therapeutics .....	23
1.5.2.1	FK506 .....	23
1.5.2.2	Aromatase inhibitors .....	26
<b>1.6</b>	<b>Estrogen.....</b>	<b>28</b>
1.6.1	Estrogen biosynthesis and metabolism .....	28
1.6.2	Estrogen signalling .....	31
1.6.2.1	Nuclear signalling .....	32
1.6.2.2	Non-genomic estrogen signalling .....	32
<b>1.7</b>	<b>Sex differences in the cardiovascular system.....</b>	<b>33</b>
1.7.1	Downstream effects of estrogen in the cardiovascular system.....	33
1.7.2	Sex differences in pulmonary hypertension .....	33
1.7.3	Estrogen in Pulmonary Hypertension .....	34
1.7.3.1	Estrogen in the pulmonary vasculature.....	34
1.7.3.2	Estrogen in the right ventricle .....	34
1.7.4	Sex differences in BMPR2 in pulmonary hypertension .....	35
<b>1.8</b>	<b>Animal models of pulmonary hypertension + right ventricular dysfunction .....</b>	<b>36</b>
1.8.1	Chronic hypoxia model .....	37
1.8.2	Sugen Hypoxia model .....	37
1.8.3	Monocrotaline model.....	38
1.8.4	Pulmonary artery banding model .....	39
<b>1.9</b>	<b>Hypothesis and Aims .....</b>	<b>40</b>
<b>CHAPTER 2.....</b>	<b>.....</b>	<b>42</b>
<b>2</b>	<b>MATERIALS AND METHODS .....</b>	<b>42</b>
<b>2.1</b>	<b>Chemicals and Reagents .....</b>	<b>43</b>

<b>2.2</b>	<b>Ethical Approval</b> .....	<b>43</b>
<b>2.3</b>	<b>Animals</b> .....	<b>43</b>
2.3.1	Animal welfare.....	43
2.3.2	Sprague Dawley Rats.....	44
2.3.3	Wistar Rats.....	44
2.3.4	C57Bl/6 mice.....	44
<b>2.4</b>	<b>Animal Models of Pulmonary Hypertension</b> .....	<b>44</b>
2.4.1	Hypobaric Hypoxic Chamber.....	44
2.4.2	Chronic Hypoxia Rat Model.....	45
2.4.3	Chronic Hypoxia Mouse Model.....	45
<b>2.5</b>	<b>Preparation of drugs</b> .....	<b>45</b>
2.5.1	FK506.....	45
2.5.2	Anastrozole.....	46
<b>2.6</b>	<b>Administration of Drugs</b> .....	<b>46</b>
2.6.1	FK506 administration.....	46
2.6.2	Anastrozole administration.....	48
<b>2.7</b>	<b>Assessment of Pulmonary Hypertension Phenotype</b> .....	<b>48</b>
2.7.1	Anaesthesia.....	48
2.7.2	Haemodynamic Measurements.....	49
2.7.2.1	Right Ventricular Pressure.....	49
2.7.2.2	Systemic Arterial Pressure and Left Ventricular Pressure.....	51
2.7.2.3	Volume calibration.....	53
2.7.2.4	Analysis of haemodynamic measurements.....	54
2.7.3	Tissue collection.....	54
2.7.3.1	FK506 rat study.....	54
2.7.3.2	Anastrozole mouse study.....	55
2.7.4	Right ventricular hypertrophy.....	55
2.7.5	<i>In vivo</i> studies acknowledgements.....	56
<b>2.8</b>	<b>Histology</b> .....	<b>57</b>
2.8.1	Tissue Processing.....	57
2.8.2	Elastin picrosirius red staining.....	59
2.8.3	Pulmonary artery remodelling.....	59

<b>2.9</b>	<b>Cell Culture .....</b>	<b>60</b>
2.9.1	Primary cell isolations .....	60
2.9.1.1	Adult rat cardiomyocyte isolation .....	60
2.9.1.2	Neonatal rat cardiac cell isolation .....	63
2.9.1.3	Adult rat pulmonary artery smooth muscle cell isolation .....	66
2.9.2	Passaging and plating cells.....	66
2.9.2.1	Charcoal stripped serum .....	68
2.9.3	Estrogen Stimulations of Neonatal Cardiac Fibroblasts.....	68
2.9.4	Migration Assay .....	69
<b>2.10</b>	<b>Analysis of RNA .....</b>	<b>70</b>
2.10.1	RNA extraction.....	70
2.10.2	Quantification of RNA.....	70
2.10.3	Complementary DNA preparation .....	71
2.10.4	Quantitative Polymerase Chain Reaction (qPCR) .....	73
<b>2.11</b>	<b>Western Blotting.....</b>	<b>76</b>
2.11.1	Protein Extraction .....	76
2.11.2	Quantification of protein.....	76
2.11.3	Sodium dodecyl sulphate-polyacrylamide gel electrophoresis .....	76
2.11.4	Protein transfer and visualisation.....	77
2.11.5	Immunoblotting .....	77
<b>2.12</b>	<b>Development of the Pulmonary Artery Banding Surgical Model .....</b>	<b>80</b>
<b>2.13</b>	<b>Statistical Analysis .....</b>	<b>80</b>
<b>CHAPTER 3.....</b>	<b>81</b>	
<b>3</b>	<b>THE EFFECT OF FK506 TREATMENT ON PARAMETERS OF EXPERIMENTAL PULMONARY HYPERTENSION. ....</b>	<b>81</b>
<b>3.1</b>	<b>Introduction.....</b>	<b>82</b>
<b>3.2</b>	<b>Results.....</b>	<b>85</b>
3.2.1	Hypoxia but not treatment with FK506 significantly affects the body weight gain of male rats .....	86

3.2.2	Hypoxia or treatment with FK506 does not significantly affect the body weight gain of female rats .....	88
3.2.3	Treatment with FK506 had no significant effect on RVSP in male rats . .....	90
3.2.4	Treatment with FK506 had no significant effect on RVSP in female rats .....	92
3.2.5	FK506 did not reverse pulmonary artery remodelling in hypoxic male rats .....	94
3.2.6	FK506 did not reverse pulmonary artery remodelling in hypoxic female rats .....	96
3.2.7	Systemic blood pressure in male rats is not influenced by treatment with FK506.....	98
3.2.8	Systemic blood pressure in female rats is not affected by treatment with FK506 but hypoxia significantly influenced the systemic circulation ...	100
3.2.9	Treatment with FK506 had no effect on LVSP in male rats housed in normoxic or hypoxic conditions .....	102
3.2.10	Treatment with FK506 had no effect on LVSP in female rats housed in normoxic or hypoxic conditions .....	104
<b>3.3</b>	<b>Discussion.....</b>	<b>106</b>
<b>CHAPTER 4.....</b>		<b>110</b>
<b>4</b>	<b>SEX DIFFERENCES IN RIGHT VENTRICLE IN EXPERIMENTAL PULMONARY HYPERTENSION AND THE EFFECT OF FK506 TREATMENT.....</b>	<b>110</b>
<b>4.1</b>	<b>Introduction.....</b>	<b>111</b>
<b>4.2</b>	<b>Results.....</b>	<b>113</b>
4.2.1	The effect of hypoxia and FK506 treatment on right ventricular hypertrophy in male rats .....	114
4.2.2	The effect of hypoxia and FK506 treatment on right ventricular hypertrophy in female rats .....	116
4.2.3	Sex differences in right ventricular remodelling in experimental pulmonary hypertension.....	118
4.2.4	Identification of an appropriate housekeeping gene for RV gene expression analysis .....	118

4.2.5	The effect of hypoxia on the expression of genes involved in <i>Bmpr2</i> and <i>Tgfβ</i> pathway in RV tissue from male rats .....	121
4.2.6	The effect of hypoxia on the expression of genes involved in cardiac remodelling in RV tissue from male rats.....	123
4.2.7	The effect of hypoxia on the expression of genes involved in <i>Bmpr2</i> and <i>Tgfβ</i> pathway in RV tissue from female rats.....	125
4.2.8	The effect of hypoxia on the expression of genes involved in cardiac remodelling in RV tissue from female rats .....	127
4.2.9	The effect of FK506 treatment on the expression of <i>Bmpr2</i> and <i>Tgfβ1</i> in RV tissue from male and female rats.....	129
4.2.10	The effect of FK506 treatment on the expression of cardiac remodelling associated genes in the male RV.....	131
4.2.11	Differential gene expression between the male and female normoxic RV. ....	133
4.2.12	Differential gene expression between the male and female hypoxic RV. ....	135
4.2.13	Development of <i>in vitro</i> models to investigate the role of sex in the right ventricle.....	137
4.2.14	Investigation of neonatal rat cardiac fibroblasts .....	137
<b>4.3</b>	<b>Discussion.....</b>	<b>140</b>
<b>CHAPTER 5.....</b>		<b>144</b>
<b>5</b>	<b>THE ROLE OF SEX AND ESTROGEN IN THE DEVELOPMENT OF EXPERIMENTAL PULMONARY HYPERTENSION AND THEIR EFFECT IN THE RV</b>	<b>144</b>
<b>5.1</b>	<b>Introduction.....</b>	<b>145</b>
<b>5.2</b>	<b>Results.....</b>	<b>148</b>
5.2.1	Investigation of the effect of Anastrozole on RVSP and BMPR2 expression in the female mouse lung .....	150
5.2.2	Treatment with Anastrozole had no significant effect on RV or LV+S mass in the chronic hypoxia female mouse model .....	152
5.2.3	Anastrozole does not significantly affect RV or LV+S mass in male chronic hypoxia mice .....	154
5.2.4	Expression studies in the male and female mouse RV. ....	156

5.2.5	Protein expression of Id1 and Id3 is significantly different between the male and female normoxic RV.....	156
5.2.6	CYP1b1, ER- $\alpha$ and Aromatase are expressed in the male and female mouse RV but expression is not significantly different between males and females .....	159
5.2.7	Investigation of the effect of estrogen on the migration of pulmonary artery smooth muscle cells .....	162
5.2.7.1	The expression of ER- $\alpha$ and ER- $\beta$ in male and female rat PASMCs. ....	162
5.2.7.2	The effect of varying serum conditions on the migration of rat PASMCs. ....	164
5.2.7.3	The effect of 17 $\beta$ -estradiol and 16 $\alpha$ -OHE1 on the migration of PASMCs .....	167
5.3	Discussion.....	170
6	GENERAL DISCUSSION .....	175
6.1	General Discussion.....	176
6.2	Future perspective .....	181
7	APPENDICES .....	183
7.1	Development of a protocol to isolate cardiomyocytes from the adult rat right ventricle.....	183
7.2	Development of the pulmonary artery banding rat model .....	188
	BIBLIOGRAPHY .....	192

## List of Figures

Figure 1.1 - Pulmonary artery remodelling. ....	12
Figure 1.2 - Right Ventricle Adaptation in Pulmonary Arterial Hypertension. ....	15
Figure 1.3 - Canonical BMPR2 signalling pathway. ....	17
Figure 1.4 - Proposed mechanism of action for the activation of BMPR2 signalling by FK506. ....	25
Figure 1.5 - Estrogen metabolism. ....	30
Figure 2.1 - Schematic diagram showing FK506 study protocol and dosing regimen. ....	46
Figure 2.2 - Schematic diagram showing Anastrozole study protocol and dosing regimen. ....	48
Figure 2.3 - Right ventricular pressure traces ....	51
Figure 2.4 - Left ventricular pressure traces ....	53
Figure 2.5 - Right ventricular remodelling in PH. ....	56
Figure 2.6 - Pulmonary artery remodelling. ....	60
Figure 3.1- Schematic diagram showing FK506 study protocol and dosing regimen. ....	85
Figure 3.2. The body weight (g) of male rats throughout the duration of the study protocol. ....	87
Figure 3.3. The weight (g) of female rats throughout the duration of the study protocol. ....	89
Figure 3.4. Right Ventricular Systolic Pressure (RVSP) in male rats housed in normoxia or hypoxia and treated with placebo or FK506 (0.05mg/kg/day). ....	91
Figure 3.5. Right Ventricular Systolic Pressure (RVSP) in female rats housed in normoxia or hypoxia and treated with placebo or FK506 (0.05mg/kg/day). ....	93
Figure 3.6. The effect of hypoxia and FK506 treatment on pulmonary artery remodelling. ....	95
Figure 3.7. The effect of hypoxia and FK506 treatment on pulmonary artery remodelling. ....	97
Figure 3.8. The effect of hypoxia and treatment with FK506 (0.05mg/kg/day) on systemic pressure in male rats. ....	99
Figure 3.9. The effect of hypoxia and treatment with FK506 (0.05mg/kg/day) on systemic pressure in female rats. ....	101

Figure 3.10. Left Ventricular Systolic Pressure (LVSP) in male rats housed in normoxia or hypoxia and treated with placebo or FK506 (0.05mg/kg/day). ...	103
Figure 3.11. Left Ventricular Systolic Pressure (LVSP) in female rats housed in normoxia or hypoxia and treated with placebo or FK506 (0.05mg/kg/day). ...	105
Figure 4.1 - Schematic diagram showing FK506 study protocol and dosing regimen. ....	113
Figure 4.2. The effect of hypoxia and treatment with FK506 on right and left ventricular mass in male rats. ....	115
Figure 4.3. The effect of hypoxia and treatment with FK506 on right and left ventricular mass in female rats. ....	117
Figure 4.4 . Identification of the most appropriate housekeeping gene for qRT-PCR analysis of RV tissue. ....	120
Figure 4.5. The effect of hypoxia on the gene expression of Tgf $\beta$ pathway and Bmpr2 pathway in the male RV. ....	122
Figure 4.6. The effect of hypoxia on the expression of gene involved in cardiac hypertrophy and cardiac fibrosis in the male RV. ....	124
Figure 4.7. The effect of hypoxia on the gene expression of Tgf $\beta$ pathway and Bmpr2 pathway in the female RV. ....	126
Figure 4.8. The effect of hypoxia on the expression of gene involved in cardiac hypertrophy and cardiac fibrosis in the female RV. ....	128
Figure 4.9. FK506 treatment significantly reduces expression of Tgf $\beta$ 1 in the male hypoxic RV. ....	130
Figure 4.10 FK506 treatment has no significant effect on the expression of genes involved in cardiac remodelling. ....	132
Figure 4.11. Differential gene expression between the male and female normoxic RV. ....	134
Figure 4.12. Differential gene expression between the male and female hypoxic RV. ....	136
Figure 4.13 The effect of estrogen on Tgf- $\beta$ 1 gene expression in Ang II stimulated NRCFs. ....	139
Figure 5.1- Schematic diagram showing Anastrozole study protocol and dosing regimen. ....	149
Figure 5.2. RVSP and lung BMPR2 expression in the female chronic hypoxia mouse model. ....	151

Figure 5.3. The effect of hypoxic and treatment with Anastrozole (3mg/kg/day) on RV and LV+S mass in female C56Bl/6 mice. ....	153
Figure 5.4. The effect of hypoxic and treatment with Anastrozole (3mg/kg/day) on RV and LV+S mass in male C56Bl/6 mice. ....	155
Figure 5.5. Differential gene expression between the male and female normoxic mouse RV. ....	157
Figure 5.6 Protein expression of BMPR2, ID1 and ID3 in the normoxic male and female mouse RV. ....	158
Figure 5.7. Cyp1b1 gene expression in the male and female normoxic mouse RV. ....	160
Figure 5.8 Protein expression in the male and female mouse normoxic RV. ...	161
Figure 5.9. Expression of ER- $\alpha$ and ER- $\beta$ in male and female rat PSMCs. ....	163
Figure 5.10. The effect of serum and DMEM on the migration of male rat PSMCs. ....	165
Figure 5.11. The effect of serum and DMEM on the migration of male rat PSMCs. ....	166
Figure 5.12. The effect of 17 $\beta$ -estradiol and 16 $\alpha$ -OHE1 on the migration of male and female rat pulmonary artery smooth muscle cells in charcoal stripped serum. ....	168
Figure 5.13. The effect of 17 $\beta$ -estradiol and 16 $\alpha$ -OHE1 on the migration of male and female rat pulmonary artery smooth muscle cells in charcoal stripped serum and FBS. ....	169
Figure 7.1 Representative image showing the rod shaped and ball shaped cells following adult rat RV cardiomyocyte isolation protocol. ....	185

## List of Tables

Table 1 - Updated clinical classification of PH. ....	6
Table 2 - Functional classification of pulmonary hypertension in adults. ....	7
Table 3 - Tissue Processing Schedule for embedding rat lung tissue and rat heart tissue in paraffin wax. ....	58
Table 4 - Krebs-Henseleit Solution contents ....	62
Table 5 - ADS buffer contents. ....	65
Table 6 - Neonatal heart digestion protocol ....	65
Table 7 - Plating media contents ....	65
Table 8 - TaqMan Reverse Transcription Reagents. ....	72
Table 9 - Mouse TaqMan Primers (Thermo Scientific, UK). ....	74
Table 10 - Rat TaqMan Primers (Thermo Scientific, UK). ....	75
Table 11 - Western Blotting protocols. ....	79
Table 12. Development of adult rat RV cardiomyocyte isolation in Wistar Hans male rats. ....	186
Table 13. Development of adult rat RV cardiomyocyte isolation in Wistar Hans female rat. ....	187
Table 14. Development of the pulmonary artery banding rat model protocol. ....	189
Table 15. Summary of the phenotype and haemodynamic measurements of Pulmonary Artery Banding Sham surgery model. ....	191

# List of Publications, Presentations and Awards

## Publication

Docherty C.K., Harvey K.Y., Mair K.M., **Griffin S.**, Denver N., MacLean M.R. (2018) The Role of Sex in the Pathophysiology of Pulmonary Hypertension. In: Kerkhof P., Miller V. (eds) Sex-Specific Analysis of Cardiovascular Function. *Advances in Experimental Medicine and Biology* 1065:511-528. Springer, Cham

## Poster Presentation

**Griffin S.**, Docherty C.K., Nilsen M., Loughrey C.M. and Nicklin S.A. Sex differences in right ventricular remodelling in experimental pulmonary hypertension and the effect of FK506 (tacrolimus) treatment. British Heart Foundation Student Conference, Edinburgh, UK.

## Awards

Graham Wilson Travelling Scholarship, May 2017.

## Definitions/Abbreviations

(v/v)	volume/volume
(w/v)	weight/volume
16 $\alpha$ -OHE1	16 $\alpha$ -hydroxyestrone
ANG II	Angiotensin II
ANOVA	Analysis of variance
ANP	Atrial natriuretic peptide
B2M	$\beta$ 2-microglobulin
BMP	Bone morphogenetic protein
BMPR2	Bone morphogenetic protein receptor 2
BNP	Brain natriuretic peptide
BSA	Bovine serum albumin
BW	Body weight
cDNA	Complementary deoxyribonucleic acid
CI	Cardiac index
CMC	Carboxymethyl cellulose
CO	Cardiac output
COL1A1	Collagen type 1 alpha 1 chain
COL3A1	Collagen type 3 alpha 1 chain
CRF	Central Research Facility
CSS	Charcoal Stripped Serum
CT	Cycle Threshold
CTGF	Connective tissue growth factor
CVRU	CardioVascular Research Unit
CYP	Cytochrome P450
CYP1a1	Cytochrome P450 1A1
CYP1B1	Cytochrome P450 1B1
DMEM	Dulbecco's Modified Eagle's Medium
DMSO	Dimethyl Sulfoxide
DNA	Deoxyribonucleic acid
E1	Estrone
E2	17 $\beta$ -Estradiol
E3	Estriol
ECL	Enhanced chemiluminescence

EDTA	Ethylenediaminetetraacetic acid
EndMT	Endothelial-to-mesenchymal transition
ER- $\alpha$	Estrogen receptor- $\alpha$
ER- $\beta$	Estrogen receptor- $\beta$
ERE	Estrogen response element
ET-1	Endothelin 1
EtOH	Ethanol
FBS	Fetal Bovine Serum
GAPDH	Glyceraldehyde phosphate dehydrogenase
GPER	G protein-coupled estrogen receptor 1
HD	High detergent
HIF1 $\alpha$	Hypoxia-inducible factor 1-alpha
hPASCs	Human pulmonary artery smooth muscle cells
Hr	Hour
HRP	Horseradish peroxidase
Id1	Inhibitor of DNA binding protein 1
Id3	Inhibitor of DNA binding protein 3
IL-1 $\beta$	Interleukin-1 $\beta$
IP	Intra-peritoneal
Klf15	Krüppel-like factor 15
Krebs	Krebs-Henseleit solution
LM	Lauryl Maltoside
LV	Left ventricle
LV+S	Left ventricle + septum
LVP	Left ventricular pressure
LVSP	Left ventricular systolic pressure
MDD	Matrix driven delivery
mins	Minutes
mmHg	Millimetres of mercury
MPVS	Millar Pressure Volume System
Myh7	Myosin heavy chain 7
NBF	Neutral buffered formalin
NIH	National Institute of Health
Nppa	Natriuretic Peptide A
Nppb	Natriuretic Peptide B

OHE	Hydroxyestradiol
PAB	Pulmonary artery banding
PAH	Pulmonary arterial hypertension
PAP	Pulmonary arterial pressure
PASMCs	Pulmonary artery smooth muscle cells
PBS	Phosphate buffered saline
PenStrep	Penicillin + Streptomycin
PH	Pulmonary hypertension
Ppib	Peptidyl-prolyl cis-trans isomerase B
pSmad	Phospho-Smad
PV	Pressure-Volume
PVDF	Polyvinylidene fluoride
PVR	Pulmonary vascular resistance
qPCR	Quantitative polymerase chain reaction
RNA	Ribonucleic acid
RPM	Rotations per minute
RQ	Relative quantification
RT	Reverse Transcription
RV	Right Ventricle
RVEF	Right ventricular ejection fraction
RVH	Right ventricular hypertrophy
RVP	Right ventricular pressure
RVSP	Right ventricular systolic pressure
SAP	Systemic arterial pressure
SD	Sprague Dawley
SDS	Sodium dodecyl sulphate
SDS PAGE	SDS-polyacrylamide gel electrophoresis
SEM	Standard error of the mean
SMC	Smooth muscle cell
SNP	Single nucleotide polymorphism
SuHx	Sugen 5416/Hypoxia
TBS	Tris-Buffered Saline
TBST	Tris-buffered saline + 0.1% (v/v) Tween20
TGF- $\beta$ 1	Transforming Growth Factor Beta 1
TGFBR1	Transforming Growth Factor Beta Receptor 1

TNF- $\alpha$	Tumour necrosis factor $\alpha$
UK	United Kingdom
USA	United States of America
VEGF-a	Vascular Endothelial Growth Factor a
WGA	Wheat Germ Agglutinin
WKY	Wistar Kyoto
WMB	West Medical Building

## Summary

Pulmonary arterial hypertension (PAH) is a rare disease characterised by pathological remodelling of the pulmonary vasculature resulting in increased pulmonary vasculature resistance and pulmonary artery pressure. This eventually results in maladaptive changes within the right ventricle (RV) leading to RV dysfunction and ultimately RV failure. Investigations of heritable PAH identified mutations in *BMPR2* as a major risk factor for disease development.

Approximately 75% of heritable cases and 20% of idiopathic cases are associated with heterozygous mutations in this gene. However, penetrance rates are low, suggesting the involvement of other endogenous and environmental factors in triggering the development of disease.

PAH patient registries have highlighted an increased female to male ratio within the patient population, in some registries the ratio is as high as 4:1. This indicated the female sex was associated with increased risk of disease and encouraged investigation into the role of sex hormones in the development of disease. Estrogen ( $17\beta$ -estradiol) and estrogen metabolites have been a focus of recent research, however, studies have produced conflicting results on the protective or pathological effect of estrogen in the pulmonary vasculature. This research is further complicated by the finding that although fewer males develop PAH, male PAH patients tend to have poorer clinical outcomes. This is thought to be associated with more rapid decline in RV function. These contradictions are known within the field as the “estrogen paradox”.

Currently, the therapies licenced for the treatment of PAH only target the vasoconstriction of the pulmonary vasculature, therefore, there is a need to identify new therapeutic targets. The role of sex in the development of disease highlights a need to investigate the sex specific effects of potential PAH therapies. The main aim of this thesis was to investigate the sex-specific effects of two potential therapies for PAH patients - FK506 (tacrolimus) and Anastrozole (aromatase inhibitor). An additional aim was to characterise the male and female RV and identify sex-specific differences that may contribute to disease progression.

Firstly, the effect of FK506 treatment (0.05 mg/kg/day) was investigated in the chronic hypoxia rat model. To our knowledge, this was the first time FK506 treatment had been investigated in this model. Administration of FK506 in male and female chronic hypoxia rats had no significant effect on right ventricular systolic pressure (RVSP), pulmonary artery remodelling or RV/LV+S. However, further investigation of the RV indicated that RV mass and RV mass/body weight were significantly decreased in the hypoxic FK506 treated males. This led to a gene expression study to investigate the effect of hypoxia and FK506 treatment in the male and female RV, as well as a direct comparison between the male and female RV. The key finding from this study was that hypoxia increased expression of *Tgfβ1* in the male RV only and treatment with FK506 significantly reduced expression. Furthermore, *Tgfβ1* expression is significantly higher in the male RV in normoxia and hypoxia compared with the female RV. Expression of genes associated with cardiac remodelling - *Col1a1*, *Ctgf*, *Nppa* and *Myh7* - were all differentially expressed between the hypoxic male and female RV, with males displaying increased expression. These results are preliminary but could indicate a differential response to hypoxia by the male and female RV, which could be associated with disease progression. A model to isolate adult rat RV cardiomyocytes is under development during this thesis in order to investigate these findings further in male and female cells.

The next study involved investigation of treatment with Anastrozole in the chronic hypoxia mouse model. This study was focused on female mice as Anastrozole had previously been shown to reverse pulmonary hypertension (PH) in female mice. However, Anastrozole had no significant effect on RVSP or RV/LV+S in female mice and had no significant effect on RV/LV+S in male mice. As the first study in this thesis had highlighted key differences in the male and female RV in adult rats, the male and female mouse RV was compared to understand if these findings were due to differences across species. These investigations showed that Id1 and Id3 proteins, downstream components of the BMPR2 signalling pathway, were expressed at significantly lower levels in the female normoxic RV. This again highlighted differences in a key signalling pathway in PAH that could contribute to the differences in susceptibility and progression of disease between males and females.

Continuing to assess the role of estrogen in the development of PAH, final investigations carried out in rat pulmonary artery smooth muscle cells (PASMCs) investigated the effects of  $17\beta$ -estradiol (E2) and  $16\alpha$ -hydroxyestrone ( $16\alpha$ -OHE1) on cell migration. These results highlighted that although the use of charcoal stripped serum is preferred for in vitro investigations involving steroid hormones, the stripping process may also remove factors that promote cell migration. E2 and  $16\alpha$ -OHE1 did not stimulate migration of male or female rat PASMCs.

In summary, this thesis provides preliminary evidence that there are significant differences between the male and female RV which could contribute to disease development, progression and the success of treatment. In future, it would be important to confirm these findings and the downstream effects of differential gene and protein expression utilising appropriate cell models. It is important that the sex-specific effects of potential PAH therapeutics are investigated as well as the lung and RV specific effects. PAH patients may benefit from sex-specific treatment protocols which could ultimately reduce disease burden and mortality rates.

# Chapter 1

## 1 Introduction

## 1.1 Pulmonary circulation

The roles of the pulmonary circulation and systemic circulation differ significantly and therefore the structure and function of the two circulatory systems are also significantly different. The systemic circulation is a high pressure, high resistance system, with systolic pressures of approximately 120 mmHg and a mean pressure of approximately 100 mmHg (Hlastala and Berger, 2001). The function of the systemic circulation is to deliver oxygenated blood to all peripheral tissues. Despite high blood volumes, the pulmonary circulation is a low pressure, low resistance system (Yuan and Rubin, 2001). It carries deoxygenated blood from the right ventricle (RV) to the right and left lungs and allows for high volume gaseous exchange (Rizzo et al., 2015). The primary function of the pulmonary circulation is to allow for gaseous exchange to take place between inspired air within the lungs and the blood in the capillaries surrounding the terminal alveoli of the right and left lung. Systolic pressures within the pulmonary circulation are approximately 25 mmHg and mean pressures approximately 15 mmHg, significantly lower than the systemic pressure (Hlastala and Berger, 2001). Venous blood is received into the right atrium, via the vena cava, where it then passes into the RV through the tricuspid valve. During contraction of the heart, blood from the RV is ejected into the main pulmonary artery, which subsequently branches to form the left pulmonary artery and right pulmonary artery distributing blood to the right and left lung. The left and right pulmonary arteries enter the left and right lung parenchyma, respectively, and continue to branch to cover the entirety of the terminal alveoli at the most distal areas of the lung. The right pulmonary artery branches into 3 vessels in order to supply the 3 lobes of the right lung - inferior, middle and superior. The left pulmonary artery branches into 2 vessels supplying the 2 lobes of the left lung - superior and inferior.

Huang *et al.* (1996) describes 15 orders of pulmonary artery from the main pulmonary artery down to the capillaries surrounding the terminal alveoli (Huang et al., 1996). Order 15 describes the main pulmonary artery which is approximately 15.1 mm in diameter whereas order 1 pre-capillary vessels are only 20  $\mu$ m in diameter. The diameter of the pulmonary vessels decreases rapidly with the order. Only the most proximal vessels (order 15-12) are greater than 2 mm in diameter. The structure and compliance of the vessels adapts as

they branch from the main pulmonary artery to the capillaries. In general, the higher order vessels are compliant with a developed elastic lamina, medium order vessels have increased muscularisation and the low order vessels have relatively lower numbers of smooth muscle cells and an increased number of endothelial cells comparatively (Elliott and Reid, 1965; Rizzo et al., 2015).

## **1.2 The right ventricle**

Primarily, the role of the RV is to receive the venous return from the vena cava via the right atrium. Then, during each contraction of the heart muscle, eject the blood allowing the pulmonary circulation to deliver it to the right and left lungs. The RV must do this without increasing the pressure experienced by the right atria (Pinsky, 2016). Venous return under steady state is equal to cardiac output. As cardiac output, and therefore venous return, is dependent on physiological conditions such as stress or exercise, the RV has the capacity to respond to significant changes in blood flow (Pinsky, 2016). The pressure within the thoracic cavity also changes instantaneously with the movement of the chest during each breath and therefore venous return is also influenced by this pressure gradient (Pinsky, 1984). When functioning normally, the pulmonary vasculature can cope with these transient and prolonged changes in blood flow from the RV without a significant increase in pulmonary arterial pressure.

It was assumed that the RV functioned similarly to the left ventricle (LV) but on a smaller and weaker scale. However, more recent investigations into the structure and function of the RV have shown it to be significantly different. Studies have investigated the relationship between RV volumes and RV pressure (Tyberg et al., 1986) (Pinsky et al., 1992). It is hypothesised that under normal conditions the RV fills without an increase in RV pressure or wall stretch. This feature of the RV is thought to be associated with a change in RV shape (Pinsky, 2016).

The contraction of the muscle fibres also differs between the left and right ventricle due to the orientation of the 3D network of myocardial fibres that make up the myocardium. Primarily, fibres of the LV are in a circumferential orientation. Contraction of these circumferential fibres is the main cause of a decrease in LV diameter, whereas, the oblique fibres contribute by shortening

the overall length of the ventricle (Sheehan and Redington, 2008). Contraction of the LV can be described as a twisting action as the muscle fibres of both the oblique and longitudinal axis contract (Pinsky, 2016). On the surface of the RV there are also circumferential muscle fibres which are a continuation of the myofiber tracts shared with the LV. However, the fibres which are most significantly involved in the contraction of the RV are longitudinal (Sakuma et al., 2002). These are positioned deeper within the RV myocardium in the subendocardial region (Rich, 2012; Geva et al., 1998). The interventricular septum also contributes to RV contraction and the subsequent ejection of blood. This is also via shortening of longitudinally oriented fibres. RV contraction creates a wave like “peristaltic” motion moving between the RV inflow tract, mid wall and outflow tract (Dell'Italia, 1991). It takes approximately 25-50 milliseconds (ms) for the contraction to travel between the inflow and outflow regions (Pinsky, 2016). It is also thought that the RV free wall moves inwards and protrusion of the septum into the RV during LV contraction all contribute to the pumping action of the RV (Kovacs et al., 2019). It is not only during the peak in systolic pressure within the RV that blood is ejected, it is estimated that almost 60% of the blood is ejected following the peak in pressure. The compliant and low resistance pulmonary circulation allows for this. Furthermore, the pulmonary artery is dilated and prepared to receive the blood as a result of the peristaltic contraction of the RV (Redington et al., 1990).

The LV is better adapted to changes in afterload as a result of its more muscular phenotype. However, it is less capable than the RV to cope with changes in pre-load. As described, even under normal physiological conditions, drastic changes in pre-load will take place when exercise is commenced for example. During these changes the RV doesn't stretch but maintains its shape and therefore can continue to function normally. The ability of the RV to cope with alterations in preload is exemplified by the fact that it can continue to function normally even under pathological conditions of prolonged preload (Rich, 2012). On the contrary, it is much less capable of coping with changes in afterload compared to the LV. In pathological conditions involving a sustained increase in afterload, such as in pulmonary hypertension (PH), the RV falls into a state of dysfunction and eventually failure.

## 1.3 Pulmonary Hypertension

Pulmonary hypertension (PH) is used to describe a group of pathologies associated with the pulmonary vasculature. Often there is a combination of different pathological changes which occur in the pulmonary vasculature. These pathological changes lead to an increase in pulmonary artery pressure (PAP), an increase in pulmonary vascular resistance and vasoconstriction of the pulmonary arteries. All of these factors contribute to constriction of the vessel lumen and, in some cases, complete obliteration of the vessel. The vascular changes ultimately lead to an increase in afterload experienced by the RV which in turn results in right ventricular dysfunction and subsequently right ventricular failure. These pathogenic changes can have fatal consequences.

### 1.3.1 WHO Classifications

Pulmonary hypertension can result from a wide range of clinical conditions and is classified into 5 categories depending on the mechanism of disease (Table 1). An updated version of the World Health Organisation (WHO) clinical classifications were published by Simonneau *et al.* in 2019 (Simonneau *et al.*, 2019). Similar pathological changes occur to all 5 groups, however, classification aids with the diagnosis, prognosis and treatment of PH patients. Pulmonary Arterial Hypertension (PAH) is classified as Group 1. This grouping includes idiopathic PAH (iPAH), heritable PAH (hPAH), drug and toxin induced PAH and associated PAH (aPAH). aPAH incorporates PAH resulting from other systemic conditions and diseases. The WHO have also published guidelines for the functional classification of pulmonary hypertension in adult patients (Galie *et al.*, 2009b). The classification is based on the New York Heart Association (NYHA) classification of heart failure. Patients are assigned to 1 of 4 groups dependent on their symptoms and their capability to perform any type of physical activity (Table 2). Class I describes PH patients with no limitation to physical activity. Class IV describes PH patients who experience symptoms even at rest and are incapable of carrying out any physical activity without experiencing symptoms. The classifications are very broad, for example, class III could describe many PH patients with variable capacities for physical activity. However, it is thought to be useful in developing treatment strategies and predicting patient survival.

Updated clinical classifications of PH	
Group 1	Pulmonary Arterial Hypertension
	1.1 Idiopathic PAH
	1.2 Heritable PAH
	1.2.1 BMPR2
	1.2.2 ALK1, ENG, SMAD9, CAV1, KCNK3
	1.2.3 Unknown
	1.3 Drug- and Toxin-induced PAH
	1.4 PAH associated with
	1.4.1 Connective tissue disease
	1.4.2 HIV infection
	1.4.3 Portal hypertension
	1.4.4 Congenital heart disease
	1.4.5 Schistosomiasis
	1.5 Persistent PH of the newborn
	1.6 Pulmonary veno-occlusive disease and/or pulmonary capillary hemangiomatosis
	1.7 PAH long-term responders to calcium channel blockers
Group 2	Pulmonary hypertension due to left heart disease
	2.1 Systolic dysfunction
	2.2 Diastolic dysfunction
	2.3 Valvular heart disease
	2.4 Congenital/acquired left heart inflow/outflow tract obstruction and congenital cardiomyopathies
Group 3	Pulmonary hypertension due to lung disease and or/hypoxia
	3.1 Chronic obstructive pulmonary disease
	3.2 Restrictive lung disease
	3.3 Other pulmonary diseases with mixed restrictive and obstructive pattern
	3.4 Hypoxia without lung disease
	3.5 Developmental lung diseases
Group 4	Pulmonary hypertension due to pulmonary artery obstructions
	4.1 Chronic thromboembolic PH
	4.2 Other pulmonary artery obstructions
Group 5	Pulmonary hypertension with unclear multifactorial mechanisms
	5.1 Haematological disorders: chronic haemolytic anaemia, myeloproliferative disorders, splenectomy
	5.2 Systemic disorders: sarcoidosis, pulmonary histiocytosis, lymphangioleiomyomatosis
	5.3 Metabolic disorders: glycogen storage disease, Gaucher disease, thyroid disorders
	5.4 Other: tumoral obstruction, fibrosing mediastinitis, chronic renal failure, segmental PH.
	5.5 Complex congenital heart disease

**Table 1 - Updated clinical classification of PH.**

*World Health Organisation (WHO) Classification of Pulmonary Hypertension (Simonneau et al., 2019).*

<b>Functional classification of pulmonary hypertension in adults</b>	
<b>Class I</b>	Patients with PH but without limitation of physical activity. Ordinary physical activity does not cause undue dyspnoea, fatigue chest pain or near syncope
<b>Class II</b>	Patients with PH resulting in slight limitation of physical activity. Comfortable at rest. Ordinary physical activity causes undue dyspnoea, fatigue, chest pain or near syncope
<b>Class III</b>	Patients with pulmonary hypertension resulting in marked limitation of physical activity. Comfortable at rest. Less than ordinary activity causes dyspnoea or fatigue, chest pain or near syncope
<b>Class IV</b>	Patients with pulmonary hypertension resulting in inability to carry out any physical activity without symptoms. These patients manifest symptoms of right heart failure. Dyspnoea and/or fatigue may be present even at rest. Discomfort is increased by any physical activity undertaken. Syncope or near syncope can occur.

*Table 2 - Functional classification of pulmonary hypertension in adults.*

*WHO functional classification of pulmonary hypertension in adults (Galie et al., 2009b).*

### 1.3.2 Clinical definitions

Clinically, PAH is defined as sustained elevation in pulmonary vascular resistance (PVR) and a mean pulmonary arterial pressure (PAP) > 25mmHg at rest and > 30mmHg during exercise (Mair et al., 2014a). The clinical symptoms of PAH include: fatigue, breathlessness during exercise, dizziness and chest pain. As the symptoms are non-specific, diagnosis is often delayed and the disease is well established, with significant haemodynamic and functional impairment, when a patient presents at clinic (Ling et al., 2012).

### 1.3.3 Epidemiology

Understanding the clinical features and disease development of a rare and complex disease, such as PAH, is challenging and, therefore, information is based on the data collected in registries. The first PAH register was developed in the 1980s by the National Institute of Health (USA) (Rich et al., 1987). There are now many different PAH registries in countries including: USA, UK, Spain, China and France. However, it is suggested that in order to advance our understanding of this complex disease, more still needs to be done to create a world-wide, centralised approach to PAH registries (Awdish and Cajigas, 2016).

The prevalence of PAH is relatively low, a study by Ling *et al.* (2012) which investigated the UK registry estimated the prevalence as 6.6 adults per million in the UK/Ireland in 2009 (Ling et al., 2012). An early study of PAH in Scottish centres described the prevalence as 25 adults per million (Peacock et al., 2007). Finally, the French National Registry described 15 cases per million adults in 2003 (Humbert et al., 2006). All of these studies show a low prevalence of PAH across different populations. Ling *et al.* (2012) also highlighted changes in the patient cohort within recent years suggesting that patients were now diagnosed at an older age, with more obesity and with a greater number of co-morbidities. The mean age of diagnosis in the data collected from the 8 PAH centres across the UK and Ireland was 50 years of age (Ling et al., 2012). This is in keeping with other recent studies based on the French and REVEAL registries which showed the mean age of diagnosis to be 50 and 53 years of age, respectively (Humbert et al., 2006; Badesch et al., 2010). In comparison, the NIH register from the 1980s showed the mean age of diagnosis to be 36 years of age (Rich et al.,

1987). Ling *et al.* (2012) also suggested that 2 distinct patient cohorts were becoming apparent. A younger patient cohort that were described as having worse haemodynamic profiles but fewer co-morbidities and better survival in comparison to the older patient cohort. There was a similar proportion of male and females patients with the 2 age-dependent cohorts (Ling *et al.*, 2012).

The proportion of female patients within the PAH patient cohort has also been revised over the years as the data collected from registries has advanced. The first registry showed 62.5% of the patient cohort were female (Rich *et al.*, 1987). More recent studies have shown 70% (UK and Ireland), 65% (French registry) and 80% (REVEAL registry) to be female (Ling *et al.*, 2012; Humbert *et al.*, 2006; Badesch *et al.*, 2010). The reason behind the increased prevalence of PAH in females is the focus of current research and is not yet fully understood. The 3 year survival rate was only 58.2% in 2010 (Humbert *et al.*, 2010) but a more recent study of patients in a German PAH centre found the 3 year survival rate to have improved to 72.3% (Gall *et al.*, 2017).

### **1.3.4 Pathophysiology**

#### **1.3.4.1 Pulmonary artery remodelling**

In PAH there is disruption to the normally controlled proliferation and migration of the cells that make up the pulmonary vasculature (Rabinovitch, 2008). It is understood that the pathological remodelling associated with PAH first develops in the most distal pulmonary arteries. It has been shown in the context of both experimental and clinical studies, that pathogenic alterations in endothelial cells (ECs) occurs prior to the muscularisation of the vessel (Rabinovitch *et al.*, 1986; Rosenberg and Rabinovitch, 1988). The mechanisms which initiate these pathogenic changes are not fully understood, however, studies have shown that both the cellular environment and genetic factors contribute to the instability of the EC layer within the vessel. For example, both hypoxia (Block *et al.*, 1989) and reactive oxygen species (Thies and Autor, 1991) have been shown to damage the membrane of ECs which could drive the instability of the endothelial layer. Also, genetic factors such as dysfunctional bone morphogenetic protein receptor 2 (BMPR2) signalling within the ECs can lead to increased apoptosis, again compromising the EC layer (Teichert-Kuliszewska *et al.*, 2006).

Furthermore, a process known as endothelial-to-mesenchymal transition (EndMT) can contribute to alterations in ECs. During EndMT, ECs gain mesenchymal properties and their gene expression profile becomes more similar to that of smooth muscle cells (SMCs), in particular, the induction of  $\alpha$ -smooth muscle actin ( $\alpha$ -SMA) expression (Hemnes and Humbert, 2017; Xiong, 2015). Co-expression of EC and SMC markers, such as von Willebrand factor and  $\alpha$ -SMA, has been identified in the pulmonary endothelium of both PH rodent models and PH patients indicating EndMT has taken place (Good et al., 2015). Transforming growth factor- $\beta$  (TGF- $\beta$ ) in combination with inflammatory cytokines, tumour necrosis factor- $\alpha$  (TNF- $\alpha$ ) and interleukin-1 $\beta$  (IL-1 $\beta$ ), have been shown to activate this process using a pulmonary artery EC *in vitro* model (Good et al., 2015). Mechanical stresses experienced by the pulmonary artery endothelium such as high pulsatile flow and shear stress are also thought to activate EndMT as well as an acute inflammatory response (Elliott et al., 2015). A number of recent studies suggest this process is key in pulmonary artery remodelling in PH (Good et al., 2015; Ranchoux et al., 2015; Hopper et al., 2016).

The proliferation and migrations of SMCs also plays a significant role in pulmonary artery remodelling. The release of fibroblast growth factor 2 (FGF2), serotonin and vasoconstrictor endothelin-1 (ET-1) from ECs are thought to be key stimulators of SMC proliferation (Thompson and Rabinovitch, 1996; Dewachter et al., 2006; Davie et al., 2002). At the site of the alveoli, pericytes within the pulmonary arteries have been shown to differentiate into SMCs (Meyrick and Reid, 1980). SMCs are thought to play a key role in the pathological cell proliferation and migration observed in PAH as many of the cells responsible for the thickening of pulmonary vessels stain positive for  $\alpha$ -smooth muscle actin ( $\alpha$ -SMA) (Jones et al., 1997). It is well established that hypoxia can induce pulmonary artery SMCs (PASMCs) migration, however, there remains a lack of understanding of the different mechanisms by which migration and proliferation are induced (Shimoda and Laurie, 2013). In addition, endothelial nitric oxide synthase (eNOS) present within ECs, is responsible for the production of the vasodilatory factor nitric oxide (NO) which can act to prevent SMC proliferation. The ECs of PAH patients produce lower levels of NO which again contributes to the pathological phenotype (Xu et al., 2004). Furthermore, there is an increase in the ratio of vasoconstrictor to vasodilatory agents in the pulmonary

vasculature, for example with lower levels of prostacyclin compared to thromboxane (Christman et al., 1992). All of these combined factors drive pathological changes to take place within the pulmonary vasculature, particularly the distal pulmonary arteries early in the process. SMCs can migrate from the larger, muscularised vessels to the distal vessels and contribute to their muscularisation (Sheikh et al., 2014). The remodelling process leads to the formation of a double elastic lamina (Rabinovitch, 1998; Todorovich-Hunter et al., 1988) (Figure 1.1A). This is the phenotypic feature used to identify remodelled vessels in experimental models of PH. These processes all lead to the complete loss of small and medium sized distal pulmonary arteries, a process known as vascular pruning (Mair et al., 2014a). However, it is not only the distal arteries which undergo remodelling, stiffening of the large elastic vessels also occurs (Humbert et al., 2019). These pathological changes lead to the muscularisation of previously non-muscular arteries with thickening of the medial layer and intimal hyperplasia (Figure 1.1B). Subsequently, this leads to narrowing of the lumen and eventually the lumen can become completely occluded with the formation of complex or plexiform vascular lesions (Figure 1.1C). Plexiform lesions are made up of proliferative endothelial cells forming complex vascular channels (St Croix and Steinhorn, 2016) and are often symptomatic of end stage disease (Cool et al., 1999). All of these pathological changes contribute to the high pressure, high resistance pulmonary vasculature system associated with PAH.

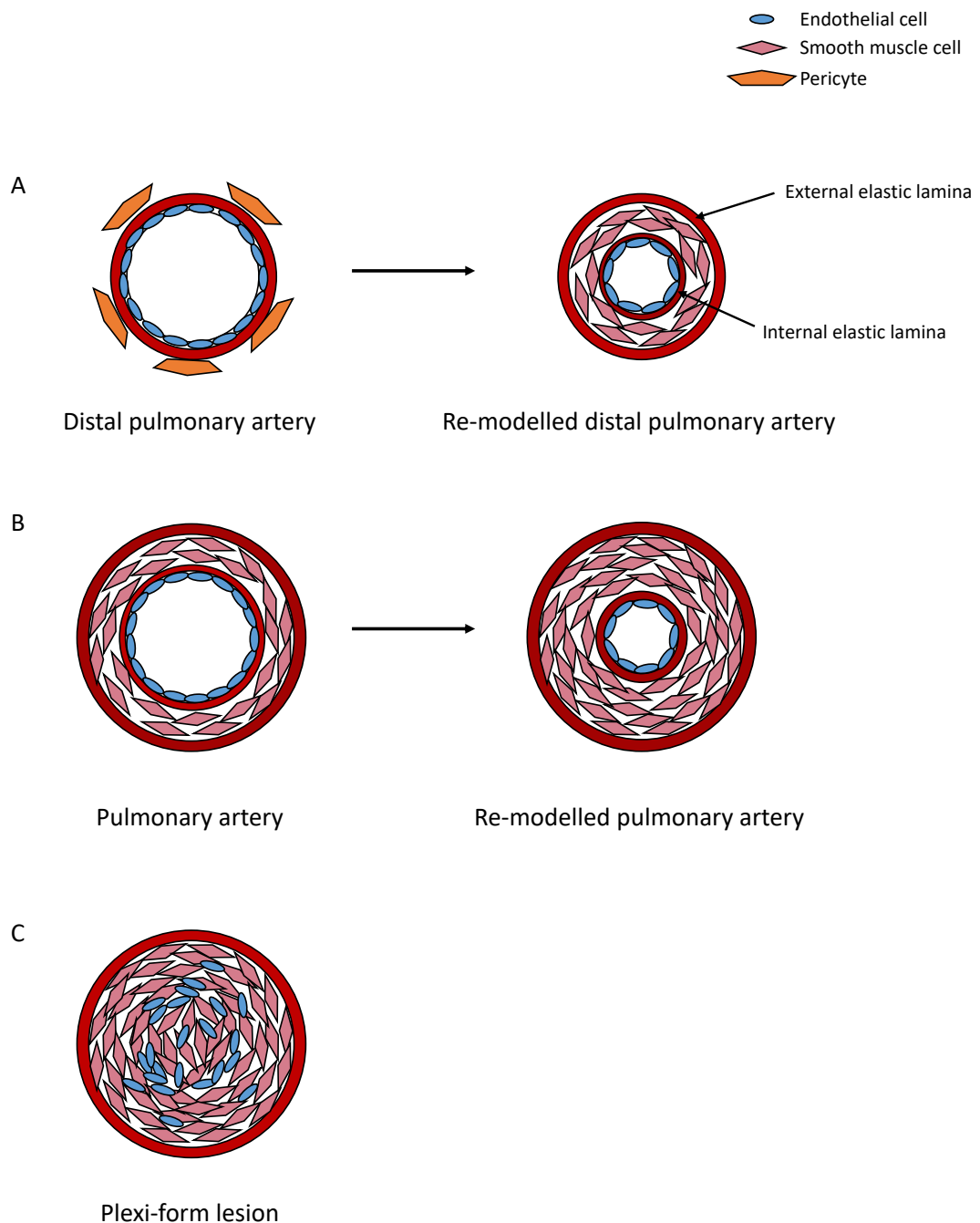


**Figure 1.1 - Pulmonary artery remodelling.**

A) Distal pulmonary artery with single elastic lamina. Remodelling results in muscularised distal pulmonary artery with double elastic lamina. B) Pulmonary artery with open lumen. Pulmonary artery remodelling involves hypertrophy of the medial smooth muscle cell layer as a result of increased smooth muscle cell migration and proliferation. This causes a significant decrease in lumen diameter. C) Plexiform lesion with complete loss of the vessel lumen.

### 1.3.4.2 Right ventricular remodelling and failure

Pulmonary vascular remodelling and the resultant high pressure, high resistance system causes an increase in the afterload experienced by the RV (Bogaard et al., 2009). RV afterload describes the RV wall stress during ejection which, in general, is proportional to the pressure in the RV (Tedford, 2014). It is well established that increased afterload is the initial trigger for RV adaptations. Increased afterload leading to increased RV wall stress negatively impacts myocardial perfusion and increases the oxygen demand of the myocardium (Bogaard et al., 2009). In order to compensate for increases in RV wall stress, the RV increases wall mass, a process known as hypertrophy. Initially this concentric RV hypertrophy (RVH), which is defined by an increased mass to volume ratio, is adaptive as it can help to maintain contractile function, cardiac output (CO) and RV ejection fraction (RVEF) by partially compensating for the increased PVR (Lahm et al., 2018; Fang et al., 2012). RV-PA coupling, which describes this adaptation of RV contractility to match RV afterload, means that with minimal energy expenditure, the RV can continue to function at a high level (Vonk Noordegraaf et al., 2017). However, it will reach a stage when the RV is no longer able to maintain optimal contractility with increasing afterload and at this stage adaptations to the RV become maladaptive (Bogaard et al., 2009). The heart rate can increase in an attempt to compensate for decreased stroke volume but unfortunately this leads to further increases in afterload. At this point RV-PA uncoupling occurs as is seen in late stage disease or under the physiological stresses of exercise in disease. The changes occurring at this stage in disease development are maladaptive and RV dilatation and RV fibrosis develop and right heart function becomes impaired (Vonk-Noordegraaf et al., 2013). A decrease in cardiomyocyte function is thought to occur as a result of changes in extracellular matrix components, an increase in reactive oxygen species, differential energy metabolism and electrical remodelling (Bogaard et al., 2009; Piao et al., 2010). Prolongation of action potential duration (Lee et al., 1997) and downregulation of potassium repolarisation channels (Lee et al., 1999) have been shown to occur in RVH, both affecting cardiac contractility. The pressure overload experienced by the RV can also influence the LV as septal flattening and bowing causes the formation of a “D-shaped” LV (Sanz et al., 2012) (Figure 1.2). The RV is known to have a more rapid progression to failure than the LV due to a reduced capillary density, increased susceptibility to

oxidative stress and likeliness to activate cell death pathways (Reddy and Bernstein, 2015). In RV failure, the RV is no longer capable of maintaining perfusion of the pulmonary circulation at a level that is necessary to ensure LV filling while maintaining normal diastolic pressures (Ryan et al., 2015). It is the main cause of mortality in PAH patients and the extent of right heart impairment is used in determining a prognosis in PAH (Mair et al., 2014a).

However, following lung transplantation in PAH patients, the RV is able to recover which suggests that RV failure may be reversible (Bogaard et al., 2009). Patients with advanced disease who had PAPs of more than 60 mmHg and had the associated cardiac remodelling including large right atrium and RV, septal flattening and RV dysfunction were investigated for their cardiac response to bilateral lung transplantation (Kasimir et al., 2004). The PAP in all patients had returned to normal within only 12 weeks post-transplant. RV dysfunction had reversed completely. The heart and tricuspid valve were able to function normally. One factor which is thought to contribute to the remarkable ability of the RV of PAH patients to recover so effectively post lung transplant is the pattern of fibrosis. Fibrosis within the RV differs significantly compared with the fibrosis pattern of an LV experiencing pressure overload. There is much less extensive fibrosis of the RV and the fibrosis tends only to appear at the RV-septal insertion points (Vonk-Noordegraaf et al., 2013; Clapham et al., 2019).

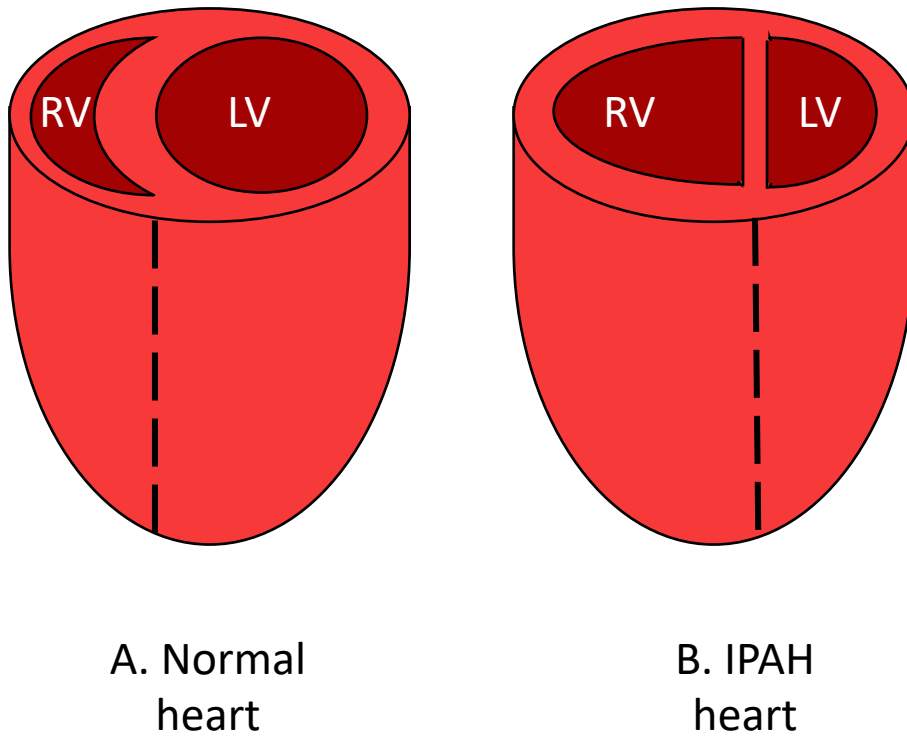


***Figure 1.2 - Right Ventricle Adaptation in Pulmonary Arterial Hypertension.***

*A) Normal, thin walled RV. B) Adapted RV as a result of PAH. The RV free wall has undergone hypertrophy. The RV chamber has also increased in size (dilatation) and caused the formation of a D-shaped LV.*

## 1.4 Genetic predisposition

Family studies which took place in the 1950s suggested that PAH could be inherited and the idea of genetic predisposition to disease development led to investigations in this area. However, the role of the *BMP2* gene in heritable PAH was not identified until the year 2000 (Deng et al., 2000). Since then investigations have also demonstrated that mutations in activin receptor-like kinase 1 (ALK-1) and potassium channel subfamily K, member 3 (*KCNK3*) are also a risk factor for PAH. Studies have shown that patients with heritable PAH are more likely to present at a younger age and with more severe haemodynamic profiles than those who develop idiopathic PAH (Sztrymf et al., 2008). The female to male ratio is also increased within the heritable PAH patient population suggesting that sex also plays a role in the prevalence of the disease (Humbert et al., 2006; Rich et al., 1987; Loyd et al., 1995).

### 1.4.1 Bone morphogenetic protein receptor signalling

*BMP2* belongs to the transforming growth factor (TGF)- $\beta$  family (Garcia de Vinuesa et al., 2016). It is described as a serine/threonine transmembrane type II receptor. BMP signalling via *BMP2* plays a role in early development right through to adulthood (Wang et al., 2014). It plays a role in early processes such as embryogenesis and also late processes such as adult tissue homeostasis. The binding of the BMP ligands results in hetero-dimerisation between *BMP2* and a type I receptor (Machado et al., 2006). The formation of the hetero-dimer, and the resultant phosphorylation of the type I receptor, triggers a signalling cascade. The first step in the signalling cascade is the phosphorylation of the Smad 1/5/8 proteins. These proteins then act to upregulate the expression of inhibitors of DNA binding proteins 1 and 3 (*Id1/Id3*) (Yang et al., 2013) (Figure 1.3). These proteins have transcription factor activity which acts to inhibit cellular proliferation. However, not only is cellular proliferation influenced by BMP signalling, migration and apoptosis of both ECs and SMCs are also affected (Garcia de Vinuesa et al., 2016).

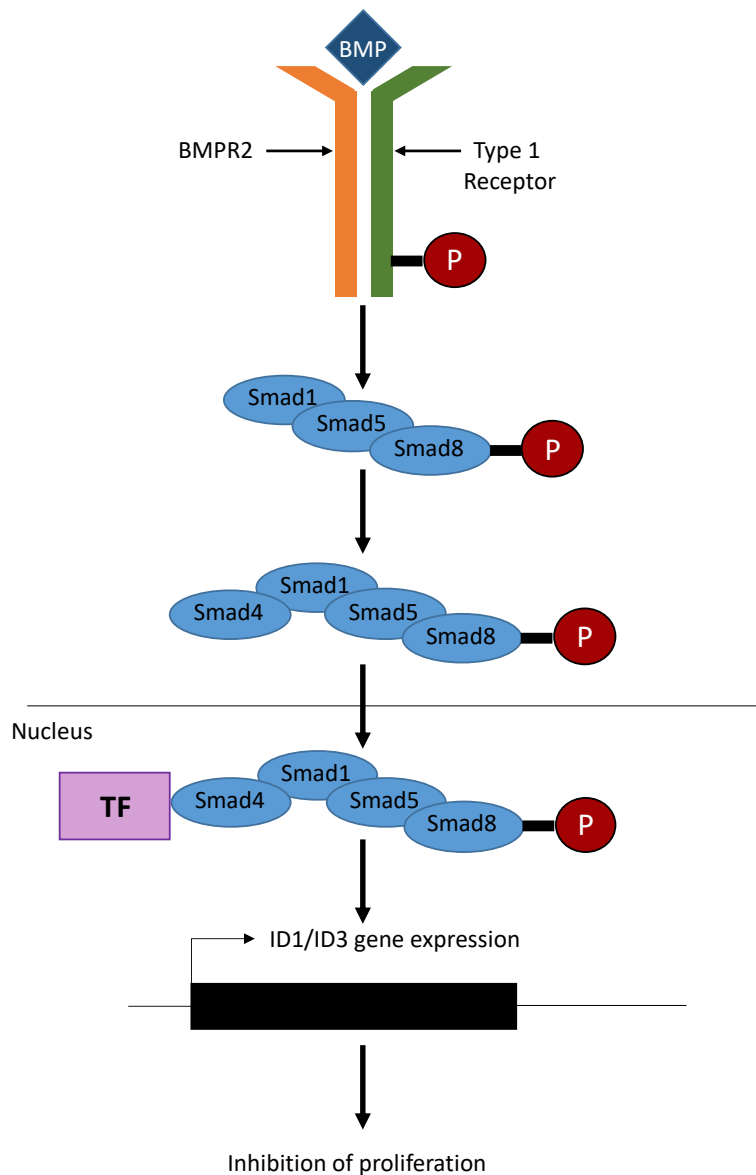


**Figure 1.3 - Canonical BMPR2 signalling pathway.**

*Binding of BMP ligand to BMPR2 dimerized to Type 1 receptor (e.g. ALK1, BMPR1) results in phosphorylation of Type 1 Receptor activating signalling cascade which leads to phosphorylation of Smad1/5/8 complex known as a signal transducer protein. This complex binds Smad4 and is translocated to the nucleus where it binds to other transcription factors (TF) and transcriptional activators leading to transcription regulation including expression of ID1 and ID3. ID1 and ID3 are known to inhibit proliferation. BMP - bone morphogenetic protein, BMPR2 - bone morphogenetic protein receptor 2 P -phosphorylation. ID - inhibitors of DNA binding proteins. TF - transcription factors.*

### **1.4.2 Bone morphogenetic protein receptor 2 mutations as a risk factor for PAH**

The most well-established risk factor for the development of PAH is harbouring mutations in BMPR2. Mutations in BMPR2 are involved in both familial and idiopathic PAH, however, the proportion of familial cases with a heterozygous BMPR2 mutation are much higher at ~75% in comparison to ~20% for idiopathic cases (Machado et al., 2009). Molecular analysis of PAH patients has identified over 300 different mutation sites within the BMPR2 gene affecting the ligand-binding, kinase and cytoplasmic domains. Mutations can affect interaction with the cytoskeleton as well as result in aberrant receptor function and therefore dysregulated downstream signalling. Dysregulated signalling involves a decrease in the phosphorylation of the Smad 1/5 proteins and consequently reduced expression of anti-proliferative Id1 and Id3 (Yang et al., 2013). The phenotypic effect of decreased Id1/3 expression is better understood in the pulmonary vasculature than in the RV. Within the pulmonary vasculature, decreased Id1/3 expression can lead to increased proliferation of the PASMCs and consequently pathological remodelling of the pulmonary vasculature (Morrell et al., 2009). The presence of a mutation in BMPR2 has a significant impact on the diagnosis and prognosis of a patients. BMPR2 mutant patients tend to be younger and have worse haemodynamic profiles when they present at diagnosis than those patients without a mutation (Evans et al., 2016a). The more severe presentation of the disease means that the patients are more likely to be in need of a lung transplant and their survival rates are poorer. With regard to the RV, recent studies have begun to elucidate the effect of dysfunctional BMPR2 signalling. A study of PAH patients comparing BMPR2 mutation carriers with non-carriers suggested that BMPR2 mutations were correlated with decreased RV functionality despite similar afterload measurements and cardiac remodelling between the two groups (van der Bruggen et al., 2016). Therefore, the potential involvement of BMPR2 signalling in RV dysfunction in PAH must be better understood.

Although BMPR2 mutations are well-established as a risk factor for PAH, their presence is not sufficient for disease development. Mutations in BMPR2 are inherited in an autosomal dominant pattern but only 20% of BMPR2 mutation carriers develop PAH - the penetrance of these mutations are particularly low

(Newman et al., 2004). However, the importance of BMPR2 in the development of iPAH is emphasised by the finding that all patients have reduced expression of BMPR2 protein even in the absence of a BMPR2 mutation (Atkinson et al., 2002). The reduced penetrance of BMPR2 mutations indicates that there must be other genetic and environmental factors involved that also contribute to disease development. One of the factors affecting penetrance of the disease is thought to be the alternative splicing of BMPR2. There are two isoforms of BMPR2 - the full transcript and one lacking exon 12 - these result from alternative splicing of BMPR2 (Machado et al., 2006). The removal of exon 12 from the transcript is significant as it encodes a cytoplasmic domain and it is the largest of the exons within BMPR2. The transcript lacking exon 12 is known as isoform B and the full transcript is isoform A. Studies have shown that PAH patients have an increased isoform B: isoform A ratio when compared to those who carry a BMPR2 mutation but are unaffected. This suggests that alternative splicing could be involved in the penetrance of the disease (Cogan et al., 2012). As sex has been shown to play a significant role in the development of PAH, studies have also investigated the effect of estrogen metabolism in the penetrance of disease. Investigations involving individuals with BMPR2 mutations have shown that the penetrance of disease can also be influenced by genetic variation in the estrogen metabolizing enzyme cytochrome P450 1B1 (CYP1B1) and the metabolites it produces (Austin et al., 2009).

## **1.5 PAH Therapeutics**

### **1.5.1 Current PAH therapeutics**

There are several different factors which contribute to the challenges associated with the development of PAH therapeutics. PAH is a complex, multifactorial disease and many of the molecular pathways which contribute to its development are not yet fully understood, making it difficult to identify potential therapeutic targets. Furthermore, as patients do not present at clinic until the onset of symptoms, the disease is well established when treatment begins. Therefore, the development of therapeutics has to be aimed at slowing the progression of the disease or reversing the pathological changes. The epidemiology of the disease has also changed significantly in recent years. PAH patients are more elderly and present with more co-morbidities making

treatment even more challenging. Current pharmacological interventions are based on pathological mechanisms that were identified many years ago. The increase in 5 year survival rates, from 36% in the NIH registry in the 1980s (Rich et al., 1987) to 60% in the UK and Ireland registry in 2012 (Ling et al., 2012), suggests that the current therapies have played a role in prolonging the life of PAH patients. Current therapies primarily target the increased vasoconstriction of the pulmonary vasculature (Ryan et al., 2015) and they are unable to reverse the remodelling of the pulmonary vasculature or the right ventricle. Therefore, there is a real need to develop our understanding of this disease in order to identify new therapeutic targets and work towards further reducing the mortality rate.

Current pharmacological interventions target 3 main pathways - prostacyclin, endothelin-1 (ET-1) and nitric oxide - that contribute to increased vasoconstriction and the pro-proliferative and anti-apoptotic phenotype of the pulmonary vascular in PAH (Lau et al., 2017). There are 5 classes of drug that are currently approved that target these pathways: prostacyclin IP receptor agonist, prostacyclin analogues, phosphodiesterase type 5 (PDE5) inhibitors, soluble guanylate cyclase stimulator and endothelin-1 receptor antagonists (ERAs) (Lau et al., 2017). Calcium channel blockers are also currently prescribed as therapy for patients with PAH (Medarov and Judson, 2015).

Treatment with a combination of therapies from the point of diagnosis has been shown to have improved clinical outcomes in PAH patients (Sitbon et al., 2016; Galie et al., 2015; Galie et al., 2016). The clinical outcomes following duo-combination therapy of ERA (ambrisentan) and PDE 5 inhibitor (tadalafil) were improved in comparison to mono-therapy (Galie et al., 2015). There is currently a clinical trial underway investigating the clinical outcomes associated with a triple combination therapy with an ERA, PDE 5 inhibitor and a prostacyclin IP receptor agonist (TRITON study, Clinical trial no. NCT02558231). The 2015 ECS/ERS guidelines for the treatment of PAH advise that prior to selecting a treatment protocol, patients should be risk stratified. It is recommended that patients who fall into the high-risk category be treated with combination therapy from diagnosis and patients that fall into low- or medium-risk categories can be treated with dual or mono-therapy (Galie et al., 2015). However,

patients must be continually monitored and where low-risk status is not achieved, additional therapies should be added to their treatment protocol. In the past, patients were treated with different therapies on a sequential basis and only when the initial treatment was deemed to have unsatisfactory clinical outcomes would the therapy subsequently be changed to a different therapy (Sitbon et al., 2016; Galie et al., 2015; Galie et al., 2016).

#### **1.5.1.1 Calcium channel blockers**

The role of pulmonary artery vasoconstriction in the pathogenesis of PAH is well established. Therefore, the effect of vasodilators on disease progression has been investigated for many years. Vasoconstriction is dependent on the levels of intracellular calcium  $Ca^{2+}$  and influx of calcium to the vascular SMC (VSMC) via L-type calcium channels (Godfraind, 2017; Medarov and Judson, 2015). The use of calcium channel blockers (CCBs) in the pulmonary vasculature can prevent vasoconstriction by blocking voltage gated calcium channels and stopping the influx of  $Ca^{2+}$  into the PASM (McMurtry et al., 1976). This in turn prevents an increase in PVR. Studies conducted by Rich et al. in 1987 and 1992 suggested that treatment strategies involving high doses of calcium channel blockers (CCBs), such as diltiazem or nifedipine, could significantly reduce PAP and PVR in a subset of patients described as “responders” (Rich and Brundage, 1987; Rich et al., 1992). Since then CCBs have been used clinically as a therapeutic for PAH. More recent studies have since indicated those who respond positively to acute vasodilatory testing with CCBs tend to respond well to CCBs in the long term. However, long term responders to CCBs only make up <10% of the iPAH population (Sitbon et al., 2005). Therefore, the clinical impact of CCBs is limited and this type of therapy is only beneficial for a small proportion of the patient population.

#### **1.5.1.2 Prostacyclin Analogues**

Prostacyclin is produced in endothelial cells by the action of prostacyclin synthase on arachidonic acid (Olschewski et al., 2001). It has anti-proliferative and immunomodulatory effects and therefore prostacyclin analogues are very useful in the treatment of patients with PAH. Prostacyclin analogues, such as epoprostenol and treprostinil, target the prostacyclin receptor leading to

activation of downstream pathways involved in cAMP production and vasodilation (Coleman et al., 1994). Epoprostenol is the key therapy for patients with severe PAH. In these patients, epoprostenol has been shown to improve haemodynamic profiles and survival rates after only 3 months of administration (Barst et al., 1996). Administration of this drug is challenging, primarily due to its extremely short half-life of 2-3 minutes (Lau et al., 2017), meaning it can only be administered intravenously as a continuous infusion. This type of drug administration can impact patient quality of life and also requires education of patients and highly skilled medical staff. There are more options available for the administration of trepostinil such as oral, subcutaneous and intravenous administration as well as via inhalation (Lau et al., 2017). However, these routes of administration also come with restrictions and challenges. Subcutaneous administration is associated with infusion site pain and oral and inhaled trepostinil is restricted to specific patient groups (Jing et al., 2013; McLaughlin et al., 2010).

#### **1.5.1.3 Prostacyclin IP receptor agonist**

Recently identified as a therapy for PAH is the prostacyclin IP receptor agonist selexipag (Asaki et al., 2015). Selexipag must be converted to its active form by hydrolysis in the liver (Lau et al., 2017). It is thought the side effects of this drug are reduced in comparison to other prostacyclin analogues due to the receptor specificity, however, its safety had to be investigated following the death of five patients who had been administered this drug. Findings of the investigation conducted by the European Medicines Agency (EMA) in 2017 concluded that mortality rates were not affected by the use of selexipag as death rates were similar across different treatment groups (EMA, 2017). However, patients administered this drug continue to be monitored.

#### **1.5.1.4 Endothelin Receptor Antagonists**

ET-1 was first identified as a potent vasoconstrictor in 1988 by Yanagisawa et al. (1988) (Yanagisawa et al., 1988). ET-1 is produced primarily in endothelial cells but it has also been identified in a number of other cell types including: SMCs and cardiac myocytes (Sakurai et al., 1991). There are 2 receptor subtypes within the endothelin pathway that ET-1 acts upon - endothelin A receptor (ET<sub>A</sub>)

and endothelin B receptor (ET<sub>B</sub>). ET<sub>A</sub> is more highly expressed in VSMCs and ET<sub>B</sub> is expressed in both VSMCs and ECs (Seo et al., 1994). In PAH patients, there is increased expression of ET-1 in both circulating levels and local expression in the lung (Bauer et al., 2002; Behr and Ryu, 2008; Giaid et al., 1993). ET-1, acting at both the ET<sub>A</sub> and ET<sub>B</sub> receptor, can lead to increased proliferation and the activation of vasoconstriction in isolated pulmonary artery smooth muscle cells (PASMCs) and pulmonary artery endothelial cells (PAECs) (MacLean et al., 1994; Davie et al., 2002).

The three drugs designed to target the receptors of the endothelin pathway are: bosentan, macitentan and ambrisentan. Bosentan and macitentan target both receptors while ambrisentan targets ET<sub>A</sub> only (Lau et al., 2017). Liver dysfunction is a side effect associated with the use of bosentan in up to 10% of PAH patients (Humbert et al., 2007). However, these adverse side effects do not continue when drug use is stopped.

#### **1.5.1.5 Phosphodiesterase 5 Inhibitors**

Phosphodiesterase (PDE) enzymes regulate the breakdown of an intracellular second messenger known as cGMP. cGMP is involved in controlling SMC relaxation and therefore plays a role in vasoconstriction of the pulmonary vasculature in PAH patients. One of the PDE enzymes, known as PDE5, is highly expressed in the pulmonary vasculature and is involved in the hydrolysis of cGMP. PDE5 inhibitors, such as sildenafil and tadalafil, have been developed which block the catalytic domain of PDE5 and therefore prevent hydrolysis of cGMP and control its endogenous levels (Rybalkin et al., 2003). Sildenafil and tadalafil are different structurally and in terms of their half-life. Sildenafil has a much shorter half-life meaning it requires 3 times daily dosing whereas tadalafil can be taken once a day (Galie et al., 2009a; Galie et al., 2005).

### **1.5.2 Potential therapeutics**

#### **1.5.2.1 FK506**

A recent high throughput study identified that the FDA approved immunosuppressive drug FK506 (tacrolimus) was able to increase expression of BMPR2 (Spiekerkoetter et al., 2013). This suggested that FK506 had the potential

to be used as a therapy for PAH as the reduced BMPR2 expression in PAH patients, even those without a loss of function mutation, is thought to be a key driver in the development of disease. FK506 induced BMPR2 signalling through its action as a calcineurin inhibitor and through its binding to FK-binding protein 12 which is a repressor of bone morphogenetic protein (BMP) signalling. The mechanism of action proposed by Spiekerkoetter et al (2013) is shown below in Figure 1.4. Treatment with FK506 in the monocrotaline rat model and the Sugen hypoxia (SuHx) rat model showed improvements in all parameters of PH (Spiekerkoetter et al., 2013). FK506 significantly reduced RVSP, RVH (as measured by RV/LV + Septum) and pulmonary artery remodelling in all models investigated. However, this study was performed in male mice and rats only and therefore was lacking any investigation into the sex-dependent effects of this treatment.

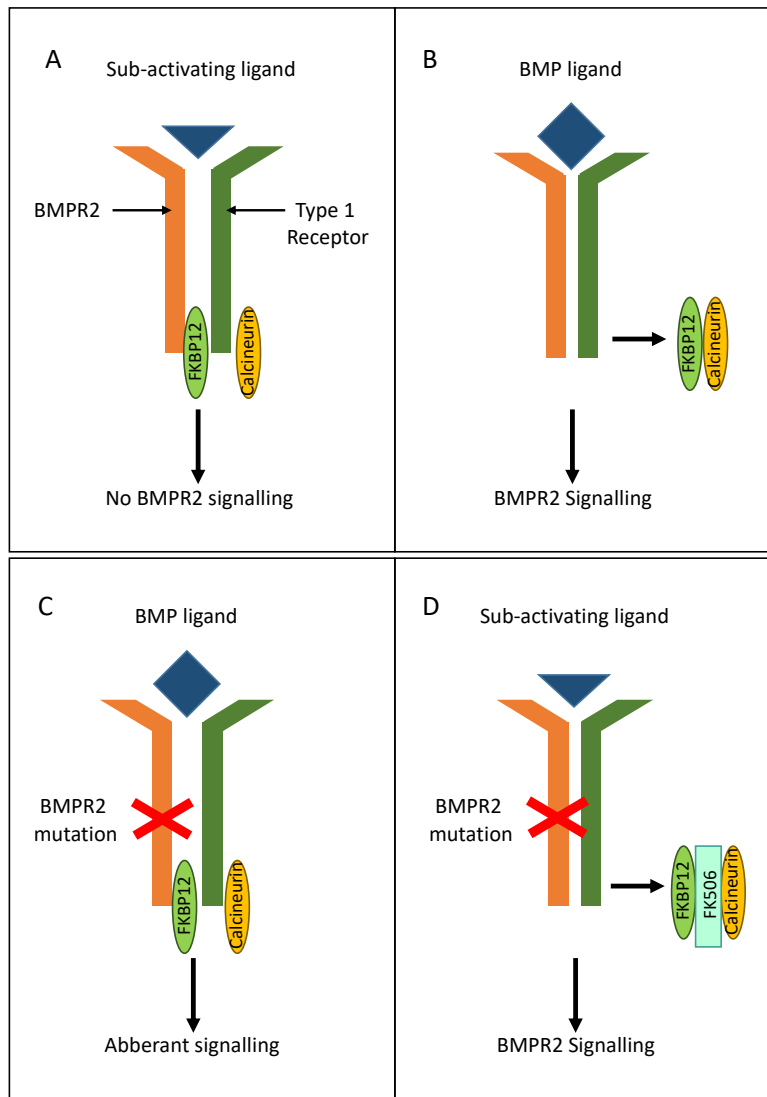


**Figure 1.4 - Proposed mechanism of action for the activation of BMPR2 signalling by FK506.**

A-B) Ligand is bound to BMPR2 dimerized with Type 1 Receptor. A) A sub-activating ligand binding does not lead to BMPR2 signalling. B) Activating BMP ligand binds leading to FKBP12 and Calcineurin dissociating from receptor and normal BMPR2 signalling. C-D) Ligand binds to mutant BMPR2 dimerized with Type 1 Receptor. C) Activating BMP ligand binds resulting in abberant BMPR2 signalling. D) Sub-activating ligand binds in the presence of FK506. FK506 acts to inhibit calcineurin and binds FKBP12. This releases inhibitory effect on BMPR2 signalling even in the presence of BMPR2 mutation. BMP - bone morphogenetic protein. BMPR2 - bone morphogenetic protein receptor 2. FKBP12 - FK binding protein 12.

The same group also went on to trial compassionate use of low dose FK506 in patients with late stage, severe PAH for whom there are no other treatment options available (Spiekerkoetter et al., 2015). Three female patients aged 36, 50 and 55 were treated with FK506 and monitored throughout the treatment regime. At 12 months, 2 of the 3 patients showed improved or stable RV function in relation to ejection fraction, stroke volume index and cardiac output index. Neither of the patients had a PAH related hospitalisation within the 12-month period. The third patient unfortunately had to discontinue FK506 treatment as a result of significant clinical worsening, however, once stabilised the patient voluntarily started on FK506 once again and at 12 months of round 2 of FK506 also hadn't had any PAH related hospitalisations. This study showed promise that FK506 could significantly improve the quality of life and survival rates of PAH patients.

A Phase IIa clinical trial conducted by the same group in the USA was published in 2017 (Spiekerkoetter et al., 2017). This trial aimed to determine the safety and tolerability of low dose-FK506 in PAH patients. Although the study showed that FK506 was reasonably well tolerated in all patients with nausea/diarrhoea being reported as the most common side effect, expression of BMPR2 and parameters of PAH were not significantly improved across the patient cohort. There was a trend towards improvement in 6 min walk distance and in measurements associated with heart failure however only in some patients and the changes did not reach significance. It was suggested that a phase IIb efficacy trial would be appropriate but, currently, there is not a trial underway.

### **1.5.2.2 Aromatase inhibitors**

Aromatase inhibitors act to prevent the production of endogenous estrogen from the androgens - androstenedione and testosterone (Kelly and Buzdar, 2010; Grodin et al., 1973). As studies have indicated a pathogenic effect of estrogen in the pulmonary vasculature, aromatase inhibitor - Anastrozole - is being considered as a therapeutic for the treatment of PAH. Anastrozole is currently licenced for the treatment of hormone receptor positive breast cancer (Geisler et al., 1996; Baum et al., 2002). It reversibly binds to the haem group of aromatase inhibiting its catalytic activity (Kelly and Buzdar, 2010). The half-life of the drug is approximately 50 hours and within 7- 10 days a steady level within

the plasma can be achieved (Kelly and Buzdar, 2010). As this therapy is already licenced for the treatment of breast cancer and its efficacy is well studied and it is already known to have limited side effects this makes it an attractive therapeutic for PAH patients.

Initial pre-clinical studies showed that treatment with Anastrozole at 3 mg/kg/day significantly reversed PH disease phenotype in female chronic hypoxia mice and female Sugen hypoxia rats (Mair et al., 2014b). This finding was not replicated in male mice. Anastrozole treatment in female BMPR2 mutant mice showed its ability to improve parameters of metabolic dysfunction (Chen et al., 2017). The demographics of PAH patients has changed in recent years with more patients presenting with other co-morbidities such as obesity. These patients will have significantly more adipose tissue which is a well-established site of estrogen production. Treatment with anastrozole significantly improved RVSP in *ob/ob* male and female mice that spontaneously develop PH (Mair et al., 2019). Almost a third of PAH patients are clinically obese when they present at diagnosis, therefore these findings are relevant to the treatment of the current PAH population (Farber et al., 2015).

These findings in pre-clinical models led to a small Phase II trial in male and female PAH patients to assess the safety and tolerability (Kawut et al., 2017). Anastrozole successfully reduced circulating 17 $\beta$ -estradiol levels by approximately 40% after 3 months of treatment. The study indicated that Anastrozole was well tolerated by PAH patients and was capable of improving 6 min walk distance in these patients. The effect of Anastrozole on other disease parameters assessed such as functional class or adverse events was not as clear. One potential limitation of the use of Anastrozole to treat PAH patients is that estrogen has been shown to be cardioprotective (Iorga et al., 2017) and although treatment may improve lung pathology it may have a detrimental effect on the RV function, the main determinant in PAH patient survival. This small Phase II did not highlight any adverse effects of Anastrozole treatment on RV function predominantly assessed by tricuspid annular plane systolic excursion (TAPSE) measurements. This study indicated a larger scale clinical trial was appropriate. The PHANTOM Phase II clinical trial is currently recruiting patients (NCT03229499). This clinical trial will investigate the effect of Anastrozole

versus placebo treatment on 6 min walk distance and other clinical parameters of PAH during a 6-month period. The safety and tolerability of the drug will also be investigated over a 12-month dosing period.

## 1.6 Estrogen

Estrogens are a group of sex hormones made up of estrone (E1),  $17\beta$ -estradiol (E2) and estriol (E3). E2 has been described as the most potent and predominant of the estrogen subtypes, E1 is most significant post-menopause and E3 is important during pregnancy when it plays a role in maintaining a healthy uterine lining (Khosla et al., 1997; Stricker et al., 2006). The estrogens are the primary female sex hormones produced predominantly in the ovaries in females and at lower levels in the testes of males, specifically in the Leydig cells and the seminiferous epithelium (Cooke et al., 2017). Estrogens are required for female reproductive system development and maintenance and in postmenopausal women, the E2 concentration within the serum drops significantly (Becker, 2008). Recently, there has been a greater understanding of the role estrogens play in other systems within the body, including the cardiovascular system. Younger women have been shown to be protected from cardiovascular disease and this is thought to be associated with the role of estrogen in the cardiovascular system as when women reach postmenopausal age this cardio protection is lost (Blenck et al., 2016).

### 1.6.1 Estrogen biosynthesis and metabolism

Estrogen metabolism is a large enzymatic pathway involving many of the cytochrome P450 (CYP) enzymes. CYP enzymes are a large family of heme-containing mono-oxygenases that are responsible for catalysing the metabolism of endogenous and exogenous substances such as steroids and hormones as well as any drugs or chemicals consumed by the body (Nelson et al, 1996). Estrogens and the other sex hormones are biosynthesised from cholesterol (Tofovic and Jackson, 2020). The full metabolism pathway involved in the production of estrogen metabolites from cholesterol is shown in Figure 1.5. Briefly, cholesterol is converted to pregnenolone by the action of the CYP enzyme CYP11A1. The metabolism of pregnenolone to progesterone is by 3-hydroxysteroid dehydrogenase (HSD). CYP17A1 then catalyses the conversion of pregnenolone to

androstenedione. At this point, androstenedione can be metabolised straight to estrone (E1) by the action of CYP19A1, also known as aromatase, or converted to the androgen, testosterone, by 17 $\beta$ -hydroxysteroid dehydrogenase (HSD) (Tofovic and Jackson, 2020). 17 $\beta$ -HSD can catalyse both the forward and reverse reaction between androstenedione and testosterone. Estradiol (E2) is produced by the action of aromatase on testosterone or the action of 17 $\beta$ -HSD on estrone (Tofovic and Jackson, 2020). Aromatisation of both androstenedione and testosterone results in the production of estrone and estradiol, respectively (Grodin et al., 1973). E1 and E2 are interconverted by the action of 17 $\beta$ -HSD enzymes. E1 is further metabolised to an intermediate 16 $\alpha$ -hydroxyestrone (16 $\alpha$ OHE) before the synthesis of E3 estriol (Tofovic and Jackson, 2020). Although, 16 $\alpha$ OHE is an intermediate between estrone and estriol, this metabolite has also been shown to exert its own effects as is the case with many of the metabolites of estrogen. Estrogens can be excreted from the body in urine and faeces, they are converted to inactive metabolites prior to excretion. These are mainly sulphated and glucuronidated derivatives (Liu et al., 2009; Thomas and Potter, 2013).

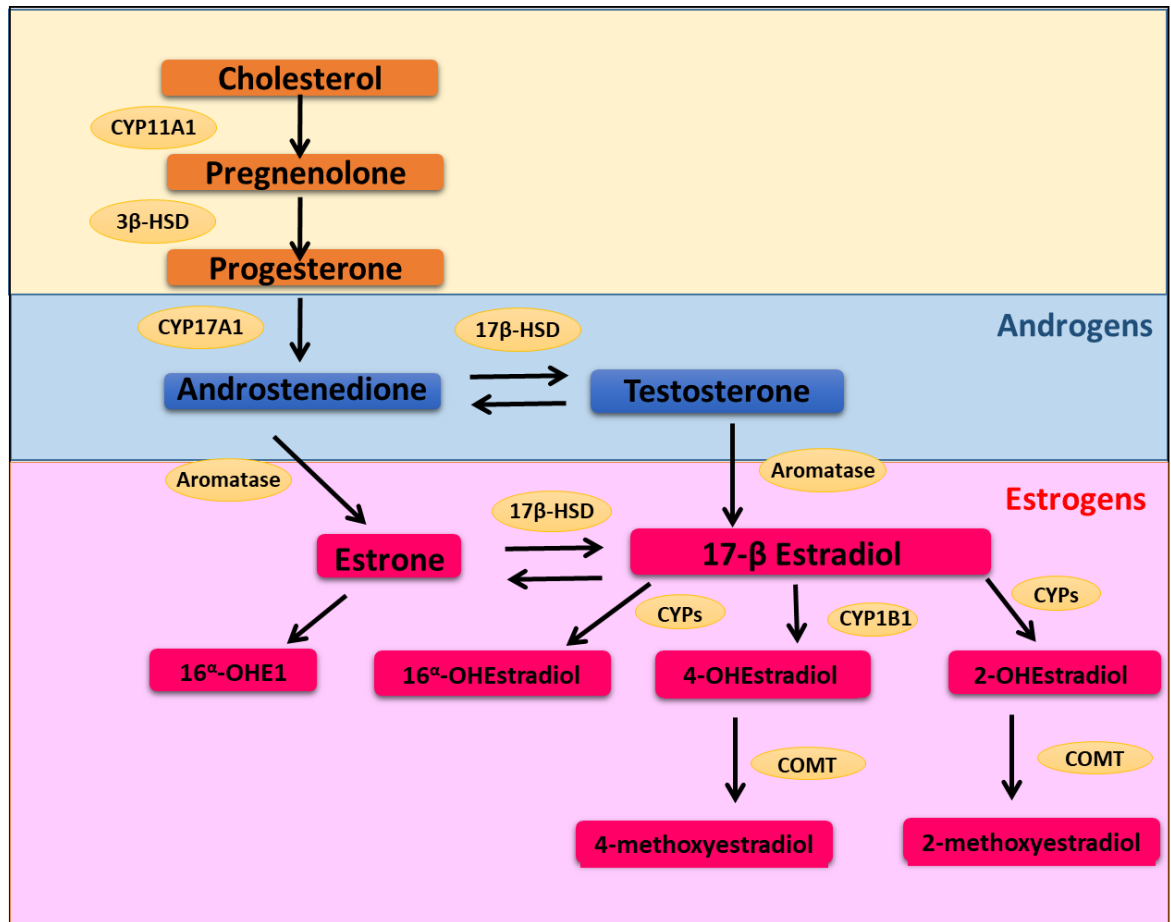


**Figure 1.5 - Estrogen metabolism.**

Both androgens and estrogens are metabolised from cholesterol. Cholesterol is converted to the androgen androstenedione by the action of CYP11A1, 3β-HSD and CYP17A1. Androstenedione can then either be converted to testosterone by 17β-HSD or estrone by aromatase also known as CYP19A1. Testosterone is the main precursor for all the estrogen metabolites. Again aromatase is responsible for the conversion of testosterone to 17β estradiol. From there various CYP enzymes including CYP1B1 can metabolise 17β estradiol to 16<sup>α</sup>-, 4- and 2- OHEstradiol. These metabolites can then be further metabolised by COMT to 4- or 2- methoxyestradiol. CYP - cytochrome P450, HSD - hydroxysteroid dehydrogenase, OHEstradiol - hydroxyestradiol and COMT - catechol-O-methyltransferase.

As stated previously, the primary site for estrogen production in pre-menopausal women is the ovaries. However, there are other key sites of estrogen production such as the adrenal glands, brain, skin, adipose tissue and the liver (Cui et al., 2013; Barakat et al., 2016). The expression of aromatase in many different tissues throughout the body has suggested that estrogen can be synthesised from androgens locally. The synthesis of estrogen has been shown to take place in the SMCs of the vasculature (Harada et al., 1999), including the pulmonary vasculature (Mair et al., 2014b). Estrogen production within the vasculature is thought to be associated with its role in maintaining vascular homeostasis and arterial vasodilation (Novella et al., 2019). It is also known that estrogen can be stored in tissues as estrone-sulfate. It is synthesised from E1 estrone by the enzyme estrogen sulfotransferase, when required the conversion of estrone-sulfate to estrone is controlled by steroid sulfatase (Thomas and Potter, 2013).

### **1.6.2 Estrogen signalling**

The classic estrogen signalling pathway involves the binding of estrogen to either estrogen receptor- $\alpha$  (ER- $\alpha$ ) or estrogen receptor- $\beta$  (ER- $\beta$ ). The genes ESR1 and ESR2 encode for ER- $\alpha$  and ER- $\beta$  respectively. ER- $\alpha$  and ER- $\beta$  are not located on the cell membrane but are located within the cytoplasm or nucleus. As estrogens are lipophilic, they can easily cross the cell membrane in order to exert their effects on the receptors. The activation of ERs results in both genomic and non-genomic signalling (Vrtačnik et al., 2014). Both ERs are expressed in vascular SMCs and ECs (Lindner et al., 1998; Andersson et al., 2001; Mendelsohn and Karas, 1999). ER- $\alpha$  has been shown to have 3 different isoforms, a full-length isoform at 68 kDa and two truncated versions that are only 46 kDa and 36 kDa (Heldring et al., 2007). It is thought that the different isoforms could play a role in the different types of signalling that ER- $\alpha$  is capable of. Another estrogen receptor known as G protein-coupled estrogen receptor (GPER1) has more recently been identified. Expression of GPER1 has also been identified in both vascular SMCs and ECs (Lindsey et al., 2011) as well as many other tissue types including heart and lung (Otto et al., 2008).

### 1.6.2.1 Nuclear signalling

Following ligand binding, there is the formation of hetero- or homo-dimers and activation of the receptors. The receptor dimer then translocates to the nucleus where it can act to influence gene expression via the estrogen response elements present in the promoter region of many different genes (Vrtačnik et al., 2014). The recruitment of additional transcription factors as well as activators and repressors can influence the action of the ER. The estrogen response element itself can also either act to enhance or repress transcription of the target gene (Hall et al., 2001). However, ERs have also been shown to bind to other transcription factors and modulate the transcription of genes which do not contain the estrogen response element (Vrtačnik et al., 2014). Examples of other transcription factors that facilitate estrogen signalling include: nuclear factor  $\kappa$ B (NF- $\kappa$ B), GATA binding protein 1 (GATA1) and signal transducer and activator of transcription 5 (STAT5) (Bjornstrom and Sjoberg, 2005).

### 1.6.2.2 Non-genomic estrogen signalling

Estrogen receptor signalling has also been shown to exert rapid signalling effects, faster than those that could be achieved via normal genomic signalling and therefore must also initiate non-genomic effects. It occurs via the activation of cytosolic signalling pathways and involves second messengers. GPER1, a G-protein coupled receptor (GPCR) with seven transmembrane domains, has been identified which binds to 17- $\beta$  estradiol and results in estrogen dependent signalling. Its binding affinity for 17 $\beta$ -estradiol is lower than that of the two nuclear ERs (Thomas et al., 2005). Signalling via GPER1 can activate ERK signalling (Gonzalez de Valdivia et al., 2017), however, this finding is not replicated across all cell types (Evans et al., 2016b). The G proteins, Gs and Gi, are coupled to GPER1 and signalling is mediated through these proteins. Gs and Gi proteins modulate the intracellular cAMP levels through positive and negative regulation of adenylyl cyclase (Filardo et al., 2000; Filardo et al., 2002).

## **1.7 Sex differences in the cardiovascular system**

### **1.7.1 Downstream effects of estrogen in the cardiovascular system**

The protective effects of estrogen in the cardiovascular system are reinforced by the lower rates of cardiovascular disease in premenopausal women compared to age-matched men (Mendelsohn and Karas, 1999; Stampfer and Grodstein, 1994). There has been evidence to suggest that estrogen exerts many different protective effects on the cardiovascular system including preventing vascular inflammation (Nathan et al., 1999), and stimulating vasodilation via the release of NO (Chen et al., 1999) as well as protecting against the uncontrolled proliferation of vascular SMCs (Pare et al., 2002). Signalling via ER- $\alpha$  has been shown to be responsible for many of these protective effects as well as playing a key role in the response to vascular injury such as stimulating vascular re-endothelialisation (Pare et al., 2002; Brouchet et al., 2001).

### **1.7.2 Sex differences in pulmonary hypertension**

The REVEAL registry identified a 4:1 ratio of females to males within the PAH population, suggesting increased female susceptibility (Badesch et al., 2010). Several other registries have also identified a female predominance however not all to the same extent as the REVEAL registry (Rich et al., 1987; Humbert et al., 2006; Ling et al., 2012). Despite the increased female to male ratio, there are currently no approved therapies that are targeted specifically towards males or females. The REVEAL registry highlighted other sex-specific differences in the manifestation of PAH. For example, it showed that females often present with a lower mean PAP than males and have a better 5 year survival rate at 62% compared to only 52% for males (Shapiro et al., 2012). Male sex has been identified as an independent predictor of worse survival and this is thought to be associated with increased and accelerated RV dysfunction (Jacobs et al., 2014; Kawut et al., 2009). This conflict between susceptibility and survival rate is known as the “estrogen paradox” (Lahm et al., 2014). The estrogen paradox has been a focus for many different research groups for many years. Investigations have attempted to identify the role of sex and estrogen in the initiation and development of PAH.

### 1.7.3 Estrogen in Pulmonary Hypertension

#### 1.7.3.1 Estrogen in the pulmonary vasculature

Experimentally, there is conflicting evidence as to whether estrogen is pathogenic or protective in the pulmonary vasculature. The protective effects of 17- $\beta$  estradiol have been shown in the male chronic hypoxia rat model (Xu et al., 2010; Lahm et al., 2012) and the inflammatory monocrotaline model (Farhat et al., 1993). However, inhibiting endogenous estrogen production with an aromatase inhibitor (Anastrozole) was shown to attenuate the pulmonary hypertension (PH) phenotype in female chronic hypoxic mice and female Sugen 5416/Hypoxia (SuHx) rats (Mair et al., 2014b). This suggests that estrogen plays a pathogenic role in the development of PH in females. Estrogen can be metabolised by the cytochrome P450 family of enzymes - CYP1A1, CYP1A2 and CYP1B1. E2 can be hydroxylated to 2-hydroxyestradiol (OHE), 4-OHE and 16 $\alpha$ -hydroxyestradiol (16 $\alpha$ -OHE2) (Samavat and Kurzer, 2015). These metabolites have been shown to have opposing effects in the pulmonary vasculature with 2-OHE having a protective effect (Tofovic et al., 2008) and 16 $\alpha$ -OHE1 inducing proliferation of human PASMCs (White et al., 2012). The dissociation between clinical and experimental findings adds to the complexity of deciphering the interaction between sex hormones and the development of PAH.

#### 1.7.3.2 Estrogen in the right ventricle

It is important to gain an understanding of the effect of sex on the healthy RV and also the effect of sex on the diseased RV. Understanding factors which affect RV function is vitally important for PAH as RV failure is ultimately the cause of death in PAH patients. Although more females develop PAH, the male sex has been identified as an independent predictor of worse survival. This is thought to be associated with increased and accelerated RV dysfunction (Kawut et al., 2009; Jacobs et al., 2014). This observation highlights that there are sex-specific differences in RV function. Research into the effects of estrogen on RV function is still very much in its infancy. Initial clinical and experimental studies have suggested a protective effect of estrogen on RV function. In control groups, higher estradiol levels are associated with increased RVEF in postmenopausal women using hormone replacement therapy (Ventetuolo et al., 2011). A recent study identified single nucleotide polymorphisms (SNPs) in the CYP1B1 gene that

are associated with RVEF and showed higher urinary estradiol metabolite levels were associated with significantly increased RVEF in white subjects (Ventetuolo et al., 2016b). Experimentally, female SuHx rats have been shown to have increased cardiac index (CI) in comparison to the male SuHx rats and male rats treated with 17- $\beta$  estradiol showed improvements in RV function and structure. This study also suggested an inverse correlation between estrogen receptor- $\alpha$  (ER- $\alpha$ ) RV expression and right ventricular systolic pressure (RVSP) and RVH (Frump et al., 2015). Additionally, in a SuHx mouse model, estrogen was shown to improve RVEF and CI through increasing RV contractility, suggesting an inotropic effect of estrogen on the RV myocardium (Liu et al., 2014). These studies are very much preliminary studies, however, they underline the importance of the role of estrogen in RV function and therefore survival in PAH.

The potentially pathogenic effect of estrogen in the pulmonary vasculature versus its protective effect in the RV could make targeting estrogen as a therapeutic for PAH particularly challenging as therapies would have to be targeted to the RV. Additionally, using experimental models of PH it may be difficult to identify if the effect of estrogen on RV function is secondary to the effect on the pulmonary vasculature or if it is a result of direct action on the myocardium. Further work is required in order to understand the mechanism by which estrogen influences RV function and structure and how this can be exploited.

#### **1.7.4 Sex differences in BMPR2 in pulmonary hypertension**

A greater number of females develop PAH, in some registries the female to male ratio is as high as 4:1 (Badesch et al., 2010). There are sex-specific differences in the expression and activity of BMPR2, even under basal conditions, which could contribute to the greater number of females within the PAH patient population (Mair et al., 2015). Female human pulmonary artery smooth muscle cells (hPASMCs) obtained from non-PAH controls have been shown to have reduced expression of BMPR2 at both a gene and protein level when compared to male hPASMCs obtained from non-PAH controls (Mair et al., 2015). Furthermore, the downstream factors in the BMPR2 signalling pathway, Smad 1 and Id1/3, were also down regulated in female hPASMCs. This suggests that females could be pre-disposed to PAH because they have basally lower levels of BMPR2.

Interestingly, when male non-PAH control hPASMCs were stimulated with estrogen there was no change in the expression of BMPR2 and Smad 1 but there was a reduction in mRNA and protein levels of the Id genes (Mair et al., 2015). These findings suggest that estrogen could be responsible for driving the suppression of the BMPR2 pathway and the predisposition of females to PAH. Sex-specific differences in BMPR2 expression have also been highlighted in PAH patients. For example, BMPR2 gene expression in lymphocytes was approximately 20% lower in female patients than in male patients (Austin et al., 2012). These observations are also apparent in experimental models. For example, when comparing whole lung BMPR2 expression in male and female mice, BMPR2 gene expression was lower in the female mouse compared to male mouse (Austin et al., 2012). This same study also highlighted an estrogen response element (ERE) in the BMPR2 promoter. This ERE was found to be a highly conserved functional binding site for estrogen receptor alpha (ER- $\alpha$ ). Based on these findings, it was suggested that estrogen is able to reduce expression of BMPR2 through the direct binding of ER- $\alpha$  to the BMPR2 promoter. This strengthens the hypothesis that estrogen can cause sex-specific differences in BMPR2 expression, which ultimately results in the predisposition of females to PAH.

At the moment, there is very little known about sex-specific differences in BMPR2 expression in the RV and the potential effects this might have on RV function in PAH.

## **1.8 Animal models of pulmonary hypertension + right ventricular dysfunction**

Despite the number of rodent models that have been developed for the study of PAH, no one model completely recapitulates all of the severe disease phenotypes and disease progression that is seen in humans. The different animal models can represent aspects of the disease phenotype. However, this also highlights the disparate nature of the different PH subtypes and that the initiating pathophysiology is likely to influence the development of the disease. Mouse models have the benefit of being genetically modifiable, however, it is understood that rat models display a more robust PH phenotype than mouse models.

### **1.8.1 Chronic hypoxia model**

Rodents can be exposed to chronic hypoxia via either normobaric hypoxia or hypobaric hypoxia. Muscularisation of the distal pulmonary arteries, associated with an increase in smooth muscle actin (Stenmark et al., 2009), and infiltration with inflammatory cells (Burke et al., 2009) are key features of this model. The extent to which chronic hypoxia induces the PH phenotype is variable, muscularisation of pulmonary arteries ranges from mild to moderate across different mouse strains (Gomez-Arroyo et al., 2012). Increases in RV mass and RVSP are modest in chronic hypoxia mice (Gomez-Arroyo et al., 2012). Some studies investigating the C57Bl6 chronic hypoxia mouse model report an increase of 5 mmHg in RVSP with no corresponding increase in RV mass (Vanderpool et al., 2011). However, numerous studies have shown an increase in RVSP, RV mass and pulmonary artery remodelling (Mair et al., 2014b; Mair et al., 2015). The use of a mouse model does allow for genetic manipulation and the effect of hypoxia on the transgenic mice to be investigated. Induction of chronic hypoxia is relatively easy and although there are some variations in the exact phenotype, relatively speaking the overall phenotype is reproducible meaning this is a popular model in research.

The rat model of chronic hypoxia has been shown to be more robust than the mouse model (Colvin and Yeager, 2014). Exposure of rats to chronic hypoxia results in remodelling of the pulmonary vasculature, particularly hypertrophy of the medial layer, and an increase in PAP (Hislop and Reid, 1976; Rabinovitch et al., 1979; Stenmark et al., 2006). RV hypertrophy will develop in this model, however, there is no evidence of RV failure (Stenmark et al., 2009) and therefore pathobiology obviously differs between this model and human disease development. However, there are also strain dependent phenotypes that exist within rat chronic hypoxia models. It is well characterised that the fawn hooded strain of rat will develop a more severe phenotype than other strains (Sato et al., 1992).

### **1.8.2 Sugen Hypoxia model**

Another agent which is used in the development of PH rodent models is Sugen 5416, a vascular endothelial growth factor receptor (VEGFR) 1/2 antagonist

(Taraseviciene-Stewart et al., 2001; Nicolls et al., 2012). Rats which have been administered Sugen 5416 by subcutaneous injection and exposed to chronic hypoxia for a period of 3 weeks, followed by a further period of 10-11 weeks of normoxia develop a severe PH phenotype. The disease phenotype continues to progress even after the animals have been returned to normoxia (Nicolls et al., 2012; Taraseviciene-Stewart et al., 2001). This model is thought to best represent the pathological changes that occur in human pulmonary vasculature as there is development of angio-obliterative lesions similar to the plexiform lesions of iPAH (Abe et al., 2010). These lesions develop during the period of normoxia that follows the 3-week hypoxic period. Delivery of a pan-caspase inhibitor to SuHx rats was able to prevent the development of these lesions and therefore it is thought that apoptosis plays an essential role in lesion development (Taraseviciene-Stewart et al., 2001). Histopathological analysis of the lesions in SuHx rats shows similarities to the plexiform lesions in the human disease (Abe et al., 2010). This progressive PH phenotype is specific to the Sugen-Hypoxia (Su-Hx) model, other models such as the chronic hypoxia model will eventually show reversal of the pathological changes after being returned to normoxia.

### **1.8.3 Monocrotaline model**

Monocrotaline (MCT) is an alkaloid agent with overall lung toxicity which is delivered to rats as a model of the pathophysiological changes that occur in the lung during the development of PH (Kay et al., 1967). The effects are characterised by an increase in cell proliferation within the pulmonary vasculature (Meyrick and Reid, 1982). The exact mechanism by which MCT induces a pathological response is unknown but there has been evidence to suggest it is due to endothelial damage (Jasmin et al., 2001) and inflammation (Wilson et al., 1989). Due to the toxic nature of MCT and how this influences the development of the disease-like phenotype, it is likely that MCT will have other toxic effects which are unrelated to the PH phenotype. Studies have described pathological effects in the liver and the heart with the presence of occlusive lesions within veins of the liver (Roth et al., 1981) and RV and LV myocarditis (Miyachi et al., 1993). Furthermore, the development of the pathological changes in pulmonary vasculature will not be representative of disease development in humans and therefore provides a limited understanding of the

pathways involved in disease development and the potential effects of therapies. Monocrotaline treated rats develop RV failure (Hessel et al., 2006) and therefore for animal welfare reasons these animals must be monitored carefully.

#### **1.8.4 Pulmonary artery banding model**

The pulmonary artery banding model has been developed as both a rat and mouse model applicable for the study of RV hypertrophy, dysfunction and failure (Rockman et al., 1994; Dias et al., 2002; Bogaard et al., 2011). The right ventricle is subjected to a continued increase in afterload as a result of banding the main pulmonary artery either through the use of suture or a clip. The outcomes of this model very much depend on the extent of the constriction. Mild constrictions will result in a RV dysfunction phenotype with increased RVSP and RVH (Faber et al., 2006). A more severe constriction will result in features more similar to RV failure and there are normally high mortality rates within these groups (Borgdorff et al., 2015b). This model has been described as a model that recapitulates the continual pressure overload of the RV and eventual RV failure (Borgdorff et al., 2015a). The surgical procedure has recently been described in both mice and rats (Tarnavski et al., 2004; Mendes-Ferreira et al., 2016). However, the surgical methodology varies across the different studies both in how the pulmonary artery is accessed and how it is banded. Tarnavski et al. (2004) suggests a left thoracotomy and the use of a suture and a blunted needle as a guide to constrict the artery in a PAB mouse model. The use of a surgical clip to constrict the pulmonary artery in a rat model was recently described (Hirata et al., 2015). This method was associated with lower intra-surgical mortality rates and increased RV dysfunction and RV fibrosis. Tarnavski et al., 2004 describes the challenges associated with the surgical procedure as a result of the physiology of the RV and pulmonary artery (Tarnavski et al., 2004). The RV is less capable of withstanding the stress associated with the manipulation of the thin walled pulmonary artery by the operator. The position of the atria over the pulmonary artery presents further technical complexities as the atria are in constant motion and are also unable to withstand any pressure as a result of manipulation. In addition, any manipulation of the artery can lead to momentary disruption of the blood flow from the RV to the lungs. This can lead to

respiratory and cardiac distress which in turn reduces the intra-operative survival rates of animals involved in a study.

## 1.9 Hypothesis and Aims

PAH is a devastating disease which has a serious detrimental effect on the patient's quality of life and has poor survival rates. The vague symptoms of PAH mean that the disease is often already established when a patient presents at clinic. Development of PAH involves irreversible, pathogenic remodelling of the pulmonary vasculature which leads to the development of a high pressure, high resistance pulmonary system. The increased afterload experienced by the RV leads to RV dysfunction and eventually failure. RV failure is the main cause of death in PAH patients. There are currently no curative therapies available for PAH and none of the current therapies target the pathological changes which take place in the RV despite this being the main cause of death in patients. Limited research has been conducted into the factors influencing the RV and how these might be targeted as therapeutics.

Furthermore, the gender disparity that is evident within the PAH population is not yet fully understood. The increased number of female patients is evident across all registries (Humbert et al., 2006; Rich et al., 1987; Ling et al., 2012) and is as high as 4:1 in the REVEAL registry (Badesch et al., 2010) suggesting that the female sex plays a role in susceptibility of disease. There is strong evidence to suggest that estrogen can have a pathogenic effect in the pulmonary vasculature (Mair et al., 2014b; White et al., 2012; Wright et al., 2015). There is a further estrogen paradox that exists within PAH in that although there are more females within the patient population, males tend to have poorer haemodynamic profiles, increased RV dysfunction and poorer survival rates. The role of estrogen in the RV and how this contributes to the presentation of disease in male and female patients is not well understood. Furthermore, PAH patients are currently not stratified for treatment based on sex and the sex-dependent effects of current therapeutics are not fully understood. Therefore, there is a real need to develop our understanding of the role of sex and estrogen in the development and progression of PAH and how to treat it.

The hypothesis of this thesis was that sex and, in particular, estrogen influence the development of PAH and independently also influence the RV which could be related to the sex-dependent presentation of disease within the PAH population. Furthermore, it was also hypothesised that potential therapies for PAH would have sex-dependent effects which should be considered during the development of new therapeutics.

The central aim of this thesis was to develop our understanding of the effect of sex and estrogen in the RV, on the development of PAH and on the response to potential PAH therapies. There were several research aims identified in order to investigate this:

- The characterisation of right ventricular gene expression in male and female rodents.
- The characterisation of the right ventricle in response to chronic hypoxia in male and female rats.
- The characterisation of the sex dependent effects of FK506 (tacrolimus) treatment on parameters of experimental PH.
- The development of a surgical model of right ventricular dysfunction in rats.

By developing our understanding of these areas, we hope to better understand the sex differences in the development and progression of PAH in order to identify new therapeutic targets and develop new therapies for this devastating disease.

## **Chapter 2**

### **2 Materials and methods**

## 2.1 Chemicals and Reagents

All chemicals and reagents were supplied by Sigma-Aldrich (Dorset, United Kingdom (UK)) or ThermoFisher Scientific (Paisley, UK) unless otherwise stated. Materials and reagents required for ribonucleic acid (RNA) analysis were supplied by Qiagen (Manchester, UK). Cell culture plastics were supplied by Corning (Flintshire, UK). Anastrozole used for *in vivo* experiments was supplied by Tocris (Bristol, UK) and FK506 used for *in vivo* experiments was supplied by Cayman Chemical via Cambridge BioScience (Cambridge, UK).

## 2.2 Ethical Approval

All animal procedures performed were approved by the Home Office according to regulations regarding experiments with animals in the UK (United Kingdom Animal Procedures Act 1986). All animal experimentation also adhered to the “Guide for the Care and Use of Laboratory Animals” produced by the United States National Institutes of Health (NIH). Experiments were performed at the University of Glasgow under the personal licence I85F0A9AF and the project licence 60/4404 or the project licence of Dr. C.M. Loughrey (60/4503 and PO5FE1F82).

## 2.3 Animals

### 2.3.1 Animal welfare

Animals were housed across three different licensed facilities within the University of Glasgow: Central Research Facility (CRF), West Medical Building (WMB) or Cardiovascular Research Unit (CVRU). All animals received a normal diet (Rat and mouse No.1 maintenance diet, Special Diet Services) and had access to food and water *ad libitum*. Animals were housed in a controlled environment - controlled lighting (7am to 7pm) and temperature maintained at  $21\pm 3^{\circ}\text{C}$ . Animals were randomly selected from the cage and allocated to a study group. Age and sex matched controls were utilised where appropriate. Experimental groups were blinded to the investigator during the acquisition and analysis of haemodynamic data.

### **2.3.2 Sprague Dawley Rats**

Male and female Sprague Dawley rats (CD IGS CrI:CD(SD)) were obtained from Charles River (UK). Rats were initially housed in either the CRF or the CVRU (University of Glasgow) and monitored during a 7-day acclimatisation period before use in any experimental procedures. During experimental procedures, rats were housed in either the WMB or the CVRU.

### **2.3.3 Wistar Rats**

Male and female Wistar Hans rats were obtained from Envigo (Oxon, UK). Rats were housed in either the CRF or the CVRU, University of Glasgow, and monitored during a 7-day acclimatisation period before use in any experimental procedures.

### **2.3.4 C57Bl/6 mice**

C57Bl/6 mice were obtained from Envigo (Oxon, UK). All mice were initially housed in the CRF and monitored during a 7-day acclimatisation period before use in any experimental procedures. During experimental procedures mice were housed either in the WMB or the CRF.

## **2.4 Animal Models of Pulmonary Hypertension**

### **2.4.1 Hypobaric Hypoxic Chamber**

Hypobaric hypoxic chambers were used to create a chronic hypoxia environment. On day 1, pressure within the chamber was slowly reduced from atmospheric pressure (1013mbar) to 750mbar and left overnight to allow for a period of acclimatisation. On Day 2, the pressure within the chamber was slowly reduced to 550mbar, approximately half of atmospheric pressure (1013mbar). This low oxygen environment results in vasoconstriction and the development of a pulmonary hypertension phenotype (Mair et al., 2014b). Chambers were brought back to atmospheric pressure slowly when required. Food and water were replenished as needed and bedding was changed every 7 days. The temperature and humidity within the chamber were monitored each day to ensure they remained within appropriate limits. Male and female rats were housed in

different hypoxic chambers. Male and female mice were also housed in different hypoxic chambers. Rat and mouse studies did not overlap to ensure that mice and rats were not housed in the same area at the same time.

### **2.4.2 Chronic Hypoxia Rat Model**

Male and female Sprague Dawley rats were placed in the hypobaric hypoxic chambers at approximately 100g and 175g total body mass, respectively. This was in an attempt to ensure rats weighed approximately 220g after 2 weeks of chronic hypoxia. Rats were acclimatised at 750mbar for 24 hrs. The hypobaric chambers were then maintained at 550mbar for the remainder of the 35 days. This study was extended to 35 days, instead of the standard 28-day model, in order to be in alignment with a previous study conducted by Spiekerkoetter *et al*, 2015. As described, chambers were brought back to atmospheric pressure slowly when required.

### **2.4.3 Chronic Hypoxia Mouse Model**

Male and female C57Bl/6 mice were recruited to the study at 6-8 weeks old. Mice were placed in the hypobaric hypoxic chambers and acclimatised at 750mbar for 24 hrs. The hypobaric chambers were then maintained at 550mbar for the remainder of the 28 days. The standard hypoxic mouse model within the field is 28 days. As described, chambers were brought back to atmospheric pressure slowly when required.

## **2.5 Preparation of drugs**

### **2.5.1 FK506**

Preparation of FK506 (Cayman Chemical via Cambridge BioScience, CAY10007965) in pellet form was completed by Innovative Research of America (Florida, USA). Innovative Research of America prepared FK506 in a pellet containing a matrix of the carrier binder consisting of cholesterol, lactose, celluloses, phosphates and stearates. The pellet was designed to release FK506 at a dose of 0.05 mg/kg/day for 21 days. The dose was based on an animal body weight of 220g therefore each FK506 pellet contained 231µg of FK506. Placebo pellets consisted of the matrix only.

## 2.5.2 Anastrozole

Carboxymethyl cellulose (CMC) (sodium salt, low viscosity - Sigma-Aldrich, C-5678) was dissolved in distilled water to create a 1% CMC (w/v) solution. Anastrozole (Tocris Bioscience, 3388) was then suspended in the appropriate volume of 1% CMC to create a solution at 0.3 mg/mL. Even distribution was achieved by sonication. 1% CMC and Anastrozole solutions were frozen at -20°C and defrosted as required. The 0.3 mg/mL Anastrozole solution allowed 100µL per 10 g of body weight to be distributed to each mouse achieving a final dose of 3 mg/kg/day (Mair et al., 2014b).

## 2.6 Administration of Drugs

### 2.6.1 FK506 administration

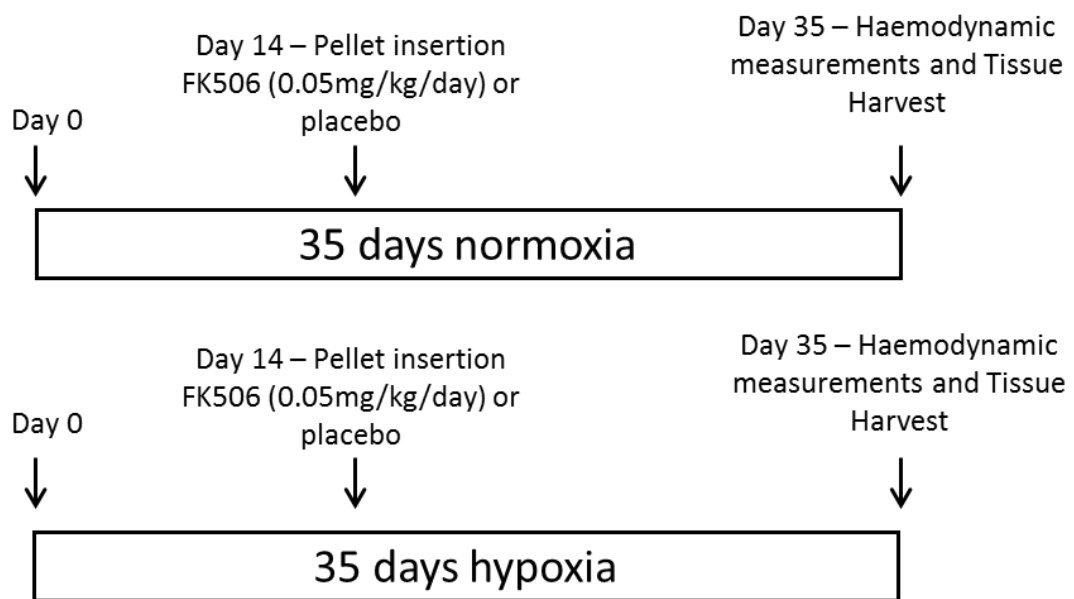


*Figure 2.1 - Schematic diagram showing FK506 study protocol and dosing regimen.*

*Male and female Sprague Dawley rats were kept in normoxic or hypoxic conditions for a period of 35 days. On day 14, FK506 pellets (0.05mg/kg/day) or placebo pellets were administered, and the rats returned to normoxia or hypoxia. On day 35 haemodynamic measurements were collected and the animals humanely killed prior to tissue harvesting.*

This study aimed to investigate the effect of FK506 on an established hypoxic phenotype, this is known as a reversal study. Therefore, rats were housed in hypoxia for 14 days prior to subcutaneous pellet insertion. Subcutaneous pellet insertion took place on day 14 of the study with the aim of dosing all rats, both male and female, at approximately 220g body weight. However, on day 14 the body weight of rats ranged between 180-250g. Body weight (g) was recorded at the time of pellet insertion. Rats were anaesthetised in an anaesthetic box with 4% (v/v) isoflurane (Abbot Laboratories, Berkshire, UK) in oxygen. Rats were then transferred to a face mask and maintained on 3% (v/v) isoflurane in oxygen at a rate of 1L/min. Rats were placed in the prone position and the fur at the dorsal neck behind the ears was removed. A small incision was made using sterile scissors and a subcutaneous pocket created. The pellet was placed on a sterile MP-182 10 Gauge Precision Trochar (Innovative Research of America) and inserted into the small subcutaneous pocket. When the trochar was removed the wound was closed using wound glue (3M, Bracknell, UK). Animals were allowed to fully recover from anaesthesia before being returned into hypoxic conditions. The matrix driven delivery (MDD) allowed FK506 to be released continuously at a rate of 0.05 mg/kg/day for 21 days. Placebo control pellets were inserted in the same manner. Age and sex matched controls were kept under normoxic conditions and dosed using the same dosing regimen (Figure 2.1). Haemodynamic assessment, followed by tissue harvest, was performed on day 35 of the study.

## 2.6.2 Anastrozole administration

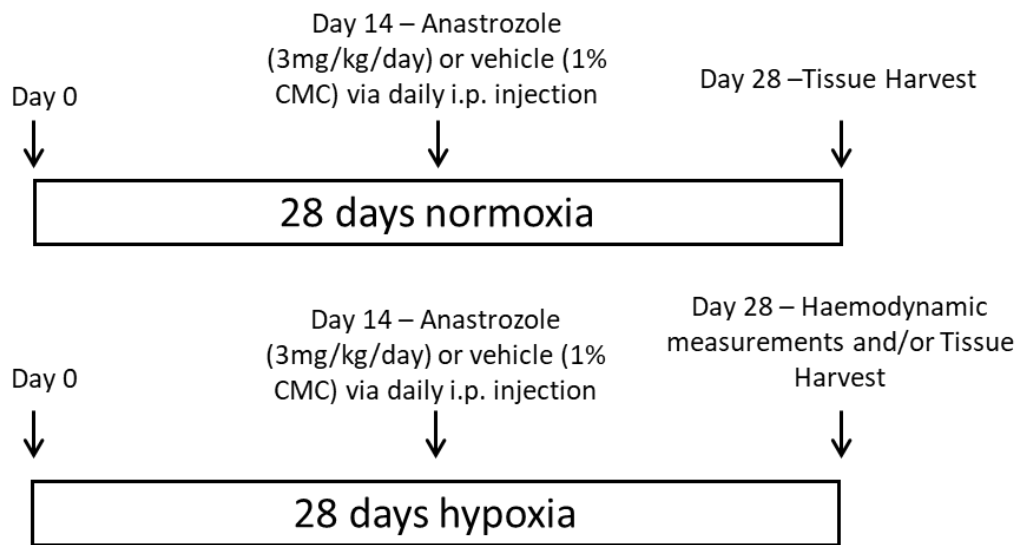


**Figure 2.2 - Schematic diagram showing Anastrozole study protocol and dosing regimen.**

Male and Female C57Bl/6 mice were kept in normoxia or hypoxia for a period of 28 days. On day 14 daily intra-peritoneal (i.p.) injections of Anastrozole (3mg/kg/day) or vehicle (1% CMC) began in normoxic and hypoxic mice for the remainder of the 28 days. On day 28 tissue was harvested from the normoxic group and the male hypoxic group. Haemodynamic assessment and tissue harvest were completed for the female hypoxic group.

This study aimed to investigate the effect of Anastrozole on an established hypoxic phenotype, this is known as a reversal study. Therefore, mice were housed in hypoxia for 14 days prior to intraperitoneal (i.p.) dosing. Dosing began on Day 14 of the study. Mice were dosed via i.p. injection with 3mg/kg/day of Anastrozole or the equivalent volume of vehicle (1% CMC) every day - a total of 14 doses. Age and sex matched controls were kept under normoxic conditions and dosed using the same dosing regimen (Figure 2.2).

## 2.7 Assessment of Pulmonary Hypertension Phenotype

### 2.7.1 Anaesthesia

Rats were anaesthetised in an induction chamber using 4% (v/v) isoflurane (Abbot Laboratories, Berkshire, United Kingdom) in oxygen at a flow rate of

1L/min. Mice were anaesthetised in an induction chamber using 3% (v/v) isoflurane in oxygen at a flow rate of 0.5L/min. Body weight (g) was recorded immediately after the induction of anaesthesia, prior to haemodynamic measurements. Animals were then placed in the supine position on the procedure table and anaesthesia maintained via a face mask. Rats were supplied with 3% (v/v) isoflurane and mice were supplied with 1.5% (v/v) isoflurane in oxygen at a flow rate of 1L/min and 0.5L/min, respectively, in order to maintain anaesthesia. Rats were placed on a heat mat while under anaesthesia and a rectal temperature probe (RS components, Corby, UK) was used to monitor body temperature. Hind limb reflex was assessed to confirm sufficient level of anaesthesia before beginning any experimental procedure. Hind limb reflex, breathing rate, the depth of each breath and heart rate were continually monitored throughout the procedure.

## **2.7.2 Haemodynamic Measurements**

Right ventricular pressure (RVP), left ventricular pressure (LVP) and systemic arterial pressure (SAP) were measured using a Millar Ultra Pressure Volume Loop System (MPVS) and the appropriate pressure volume (PV) catheter. Different models of the Mikro-Tip® ultra-miniature PV loop catheters (Millar, Texas, USA) were utilised for different studies. The SPR 869 PV catheter was utilised for rat studies, the PVR 1030 PV catheter was used for mouse right ventricle (RV) measurements and the PVR 1045 PV catheter was used for mouse left ventricle (LV) measurements. The PVR 1030 PV catheter and the PVR 1045 PV catheter differ in the electrode spacing, 3mm on the 1030 and 4.5mm on the 1045. It was recommended that due to the smaller size of the RV the 1030 PV catheter with the smaller spacing was used. Data was collected using Powerlab 8/35 data acquisition system (AD instruments, Oxford, UK) and interpreted using LabChart 7 software (AD instruments, Oxford, UK).

### **2.7.2.1 Right Ventricular Pressure**

Once appropriate anaesthesia was established, a small area of skin and fur was removed from the ventral side of the neck, exposing the muscular layer beneath the skin. The muscle and connective tissue were bluntly dissected ensuring minimal damage to the tissue. The right jugular vein was exposed and the vein

carefully isolated from the surrounding tissue. Surgical nonsterile suture (Harvard Apparatus, Massachusetts, USA, size 3-0 for rats and size 5-0 for mice) was placed under the vein and the suture tied off at the superior end to prevent blood flow through the vein. The suture was taped down to create tension along the length of the vein and a small incision was made in the vein using a 25G needle (Harvard Apparatus, 72-2251). The appropriate catheter was then fed into the right jugular vein, in some cases a second suture was passed under the vein and was used to tie the catheter in place. The catheter was then advanced towards the RV. Correct placement of the catheter within the RV was confirmed with a characteristic right ventricular pressure trace (Figure 2.3). When satisfied with the placement of the catheter, right ventricular pressure was recorded. The closed chest approach allowed the most physiologically relevant measurements to be obtained, however, it was more challenging to ensure the correct placement within the ventricle. Correct placement within the chamber is required to ensure a clean pressure trace therefore, it was not always possible to achieve the high-quality exemplar pressure traces. The pressure trace was recorded for as long as was necessary to achieve a stable pressure trace recording, on average between 2 and 10 mins.

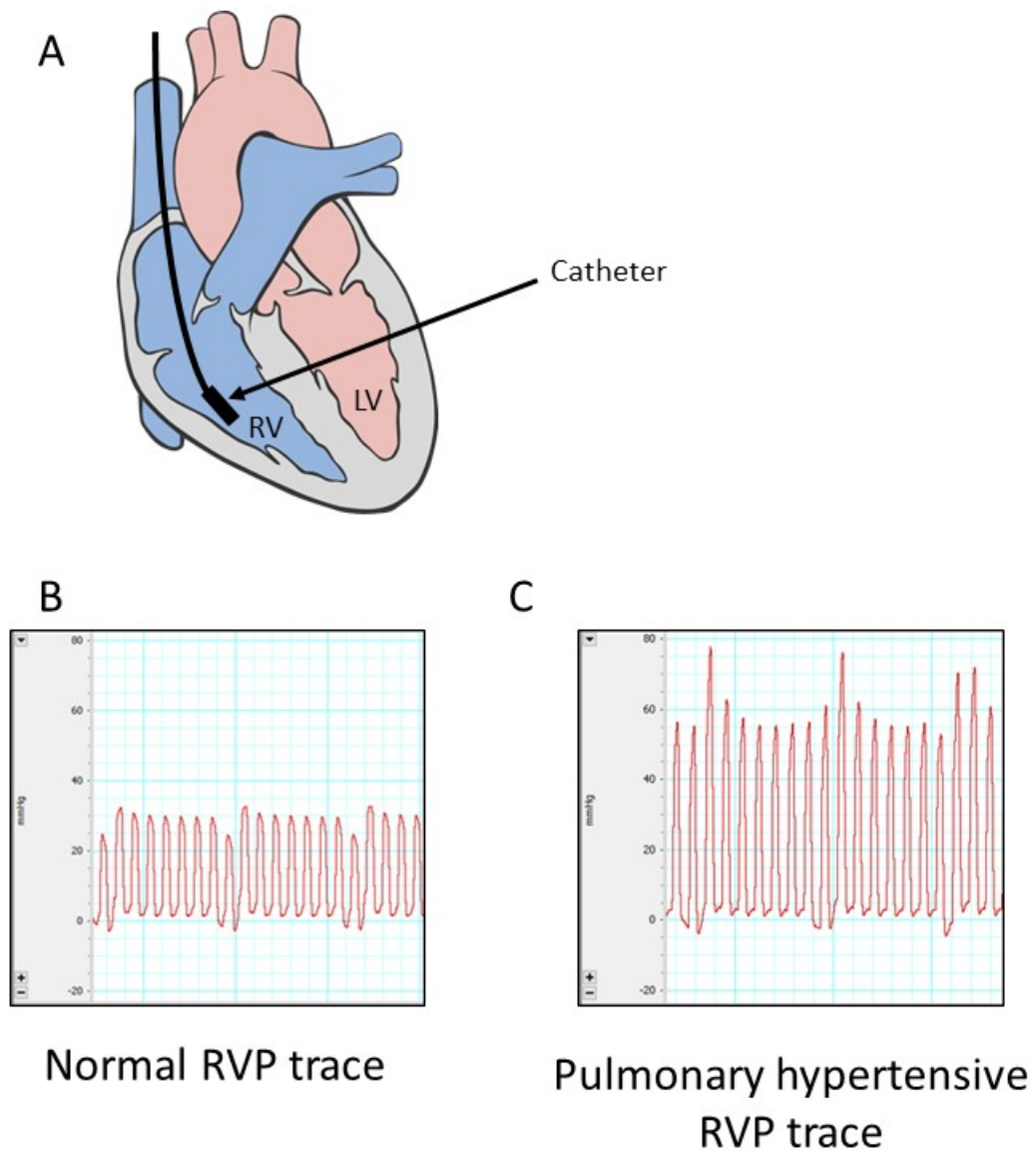


**Figure 2.3 - Right ventricular pressure traces**

Representative right ventricular pressure traces. A) Diagram to represent the placement of the catheter within the RV. B) Normal right ventricular pressure (RVP) trace obtained from a rat housed in normoxia (time on x-axis plotted against mmHg on the y axis). C) Pulmonary hypertensive right ventricular pressure (RVP) trace obtained from a rat housed in hypoxia (time on x-axis plotted against mmHg on the y axis).

### 2.7.2.2 Systemic Arterial Pressure and Left Ventricular Pressure

Following the recording of RV pressure, the catheter was removed from the jugular vein and the vein remained tied off. Further blunt dissection allowed

identification of the right carotid artery. The artery was isolated from the surrounding connective tissue and the vagus nerve was carefully separated from the artery. A tie was placed on the superior end of exposed artery using surgical nonsterile suture (Harvard Apparatus, Massachusetts, USA, size 3-0 for rats and size 5-0 for mice). This allowed the artery to be manipulated in order to expose the required length. A surgical micro-clip (Fine Science Tools, Heidelberg, Germany, FST#18055-04) was then placed at the most inferior end to prevent blood flow through the artery. Using surgical spring scissors, a small incision was made in the artery and the catheter was fed into the artery. Another suture was placed around the catheter in the artery to hold in place. The clip was released, the catheter quickly advanced and the suture tightened to hold the catheter in the artery and prevent blood loss. Systemic pressure was recorded in the carotid artery. Following a period of pressure recording within the artery, the catheter was advanced slowly until it reached the LV. Correct placement of the catheter within the LV was confirmed by a characteristic left ventricular pressure trace (Figure 2.4). When satisfied with the placement of the catheter, left ventricular pressure was recorded. The pressure trace was recorded for as long as was necessary to achieve a stable pressure trace recording, on average between 2 and 10 mins.

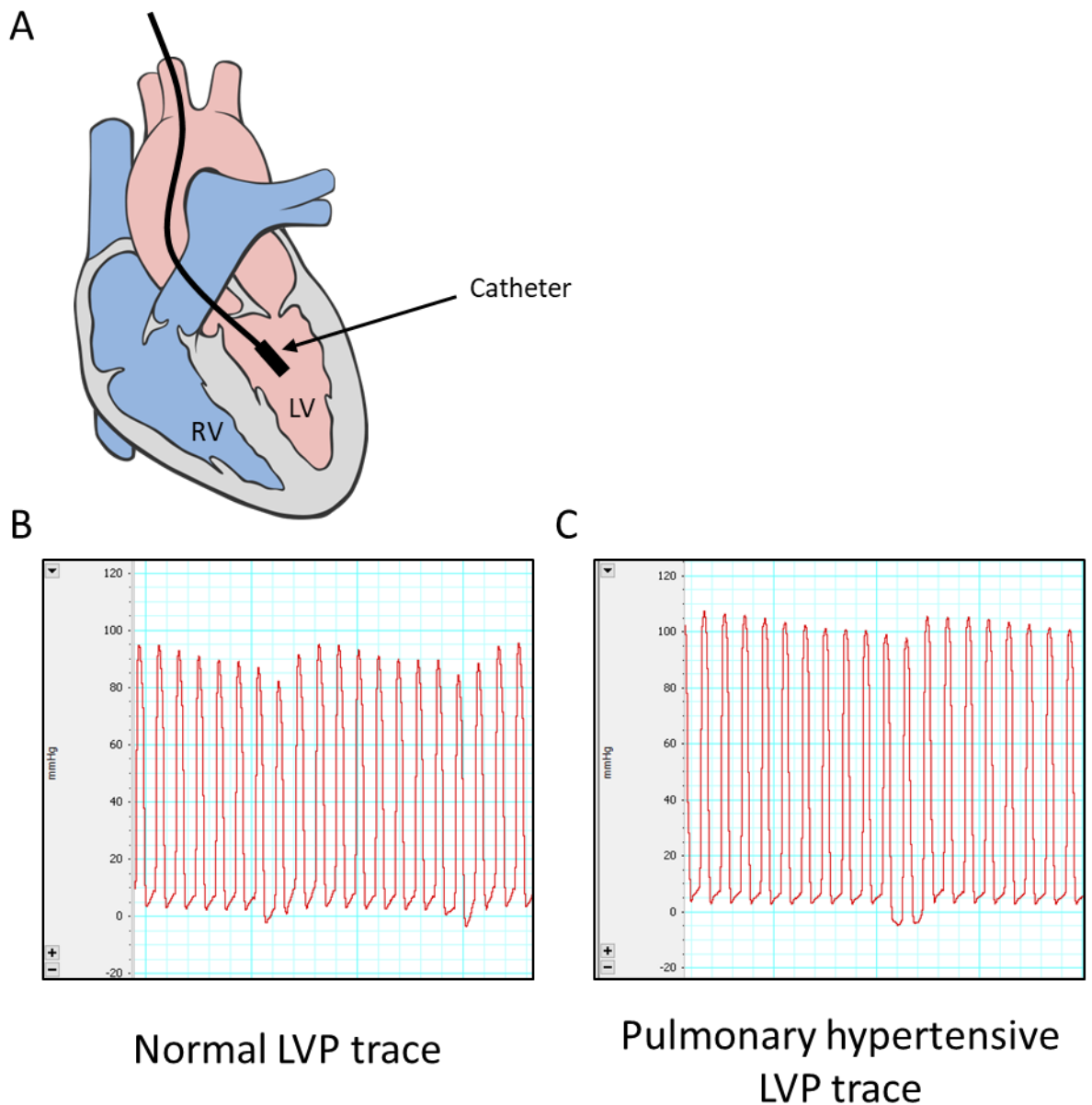


**Figure 2.4 - Left ventricular pressure traces**

A) Diagram to represent the placement of the catheter within the LV. B) Normal left ventricular pressure (LVP) trace obtained from a rat housed in normoxia (time on x-axis plotted against mmHg on the y axis). C) Pulmonary hypertensive left ventricular pressure (LVP) trace obtained from a rat housed in hypoxia (time on x-axis plotted against mmHg on the y axis).

### 2.7.2.3 Volume calibration

Post-surgery a cuvette calibration was performed using the volume calibration cuvette (AD instruments, Oxford, UK) in order to calibrate the volume

measurements collected by the Millar PV loop system. Blood was collected from the animal after removal of the catheter from the carotid artery using a 1 mL syringe. The collected blood was used to fill wells of known volumes in the cuvette. The catheter was then inserted into each well and the conductivity recorded. This was performed quickly in order to ensure minimal clotting of the blood, however, this was a challenge associated with performing the technique in this manner. The LabChart software then generated a standard curve from the conductivity of the blood within a known volume. The standard curve was then extrapolated in order to determine blood volume within the ventricle and subsequently cardiac output.

#### **2.7.2.4 Analysis of haemodynamic measurements**

At the end of the study, all pressure traces were collected for analysis. The most stable section of the pressure trace was selected for analysis. The analysis for the rat study consisted of a 20 second section of the most stable RV pressure trace and systemic pressure trace and a 1 min section of stable trace was analysed for the left ventricular pressure. The analysis for the mouse study consisted of a 1 min section of stable pressure trace from the RV, LV and the systemic circulation. Where it was not possible to obtain 20 seconds or 1 minute of steady trace, the longest possible steady trace was selected. The mean maximum pressure was calculated from the maximum pressure reached in each systole during the length of the recording. Mean maximum pressure was displayed describing the right ventricular systolic pressure (RVSP) and the left ventricular systolic pressure (LVSP). The mean maximum and minimum pressure of the systemic arterial pressure (SAP) trace was displayed showing systolic and diastolic systemic blood pressure. In addition, developed pressure (systolic-diastolic pressure) and mean SAP were also calculated.

### **2.7.3 Tissue collection**

#### **2.7.3.1 FK506 rat study**

On removing the catheter from the carotid artery, blood was collected. Blood was used to perform the cuvette calibration associated with the Millar PV loop system as described above. The remainder of the blood was collected in ethylenediaminetetraacetic acid (EDTA) tubes and stored on ice before

centrifugation at 1700 g for 10mins at 4°C. The plasma supernatant was then collected and snap frozen in liquid nitrogen. Post-mortem, the right lung lobes were tied off at the right bronchus using surgical nonsterile suture (Harvard Apparatus, Massachusetts, USA, size 3-0). The right bronchus had to be tied off as the left lung lobe was inflated at a later stage and an open right bronchus would have resulted in leakage of the liquid and failure to inflate the left lobe. The three right lobes were then removed and snap frozen in liquid nitrogen. A lobe of the liver, the right kidney and the spleen were also collected and snap frozen in liquid nitrogen for future analyses. Hearts were removed from the cadaver and collected for right ventricular hypertrophy measurements. In an attempt to better visualise the morphological features of the lungs using histological techniques, the left lung lobe was inflated using 10% (v/v) neutral buffered formalin (NBF) until the whole lobe appeared maximised in size and then removed from the cadaver ensuring not to deflate the lung. The lung lobe was then submerged in 10% (v/v) NBF and stored at room temperature until required for processing. Where possible, urine was also collected and snap frozen in liquid nitrogen. All tissues snap frozen in liquid nitrogen were then stored at -80°C until required. This tissue was used for protein and RNA analysis.

### **2.7.3.2 Anastrozole mouse study**

Mice were sacrificed on Day 28 of the study. Post-mortem, heart and lungs were removed, and the 3 right lung lobes snap frozen in liquid nitrogen. The heart was used to measure right ventricular hypertrophy and the RV and left ventricle + septum (LV+S) were then snap frozen in liquid nitrogen for protein/RNA analysis. A lobe of the liver was also collected and snap frozen in liquid nitrogen. Tissue was stored at -80°C until required.

### **2.7.4 Right ventricular hypertrophy**

Right ventricular hypertrophy (as shown in Figure 2.5) was investigated in all hearts from the rat FK506 study and the mouse Anastrozole study. In order to collect the right ventricular hypertrophy measurement, blood vessels and connective tissue were removed from the heart, followed by the right and left atria. The wall of the RV was finely dissected from the LV+S with the use of a microscope when required. Both the RV and LV+S were then blotted dry and

weighed separately. The ratio of the RV free wall mass to the LV+S mass is one of the standard measures for right ventricular hypertrophy and is known as the Fulton's Index (Fulton et al., 1952). The Fulton's index (RV mass/LV+S mass) is displayed, however, further analysis was included for the FK506 study in order to accurately determine cardiac hypertrophy including: RV mass, LV+S mass, RV mass/body weight and LV+S mass/body weight. Following RVH analysis, hearts were then collected for either protein/RNA analysis or histological analysis. From each group of the FK506 study n=4 RV and LV+S were snap frozen and n=2 RV and LV+S were submerged and stored in 10% NBF for histological analysis. All RV and LV+S tissue from the mouse Anastrozole study was snap frozen in liquid nitrogen.

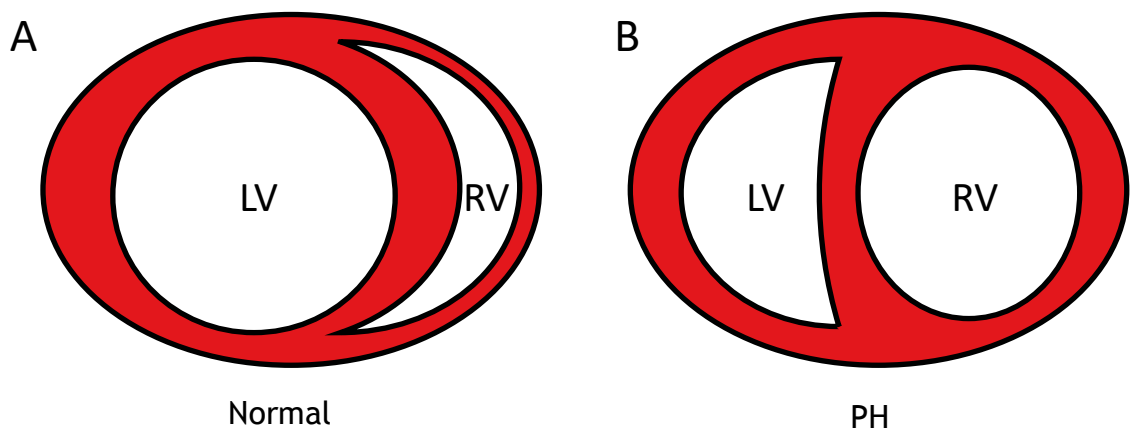


**Figure 2.5 - Right ventricular remodelling in PH.**

*Schematic diagram showing a transverse section of the heart. A) Normal heart with thin walled RV. B) Adapted RV as a result of PAH. The RV free wall has undergone hypertrophy. The RV chamber has also increased in size (dilatation) causing septal flattening and the formation of a D-shaped LV.*

### **2.7.5 In vivo studies acknowledgements**

Assistance in the administration of drugs, haemodynamic assessment and tissue harvest was provided in the Anastrozole mouse study by Margaret Nilsen and the FK506 rat study by Margaret Nilsen and Dr. Craig Docherty.

## 2.8 Histology

### 2.8.1 Tissue Processing

As stated, the left lung lobes and hearts were stored in 10% NBF at room temperature until required. The lung lobes were cut into 4-5 sections and placed into biopsy cassettes. RV and LV+S tissue was cut along the transverse axis into 2-3 sections. Lung and heart tissue were washed under running water to remove excess 10% NBF before being dehydrated through an ethanol gradient then immersed in histoclear and finally paraffin wax using the Citadel 1000 Tissue processor (Thermo Fisher, UK). Rat heart and lung tissues underwent the same processing protocol (Table 3). Following processing, the lung sections and heart sections were embedded in paraffin blocks, using a Shandon Histocenter 3 (ThermoFisher Scientific, Leicestershire, UK). Lung and LV tissue were wax embedded in an orientation that would allow for transverse lung sections. RV tissue was embedded in 2 different orientations that would allow for transverse and longitudinal sections. Paraffin embedded tissues were stored at room temperature however immediately prior to sectioning, wax blocks were placed at -20°C to improve the quality of sections. Tissues were cut at 5 µm sections using a Leica RM2125 microtome (Leica Microsystems, Milton Keynes, United Kingdom) and mounted on to poly-l-lysine (Sigma-Aldrich, P4707) coated glass microscope slides. Sections of the RV were created from at least two distinct areas to provide a better analysis across the heart. Slides with lung sections were stored at room temperature.

Solution	Incubation period
70% Ethanol	1.5 hrs
80% Ethanol	1.5 hrs
95% Ethanol	2 hrs
95% Ethanol	2.5 hrs
100% Ethanol	2 hrs
100% Ethanol	2 hrs
100% Ethanol	2 hrs
HistoClear	1.5 hrs
HistoClear	1.5 hrs
Paraffin wax	1 hr
Paraffin wax	1 hr

*Table 3 - Tissue Processing Schedule for embedding rat lung tissue and rat heart tissue in paraffin wax.*

### **2.8.2 Elastin picrosirius red staining**

A modified Miller's Elastin staining protocol was utilised to assess pulmonary artery remodelling (Miller, 1971). The sections were deparaffinised in HistoClear (Fisher Scientific Ltd, Leicestershire, UK) and rehydrated through an ethanol gradient 100% ethanol, 90% ethanol and 70% ethanol for 5 minutes at each gradient, before being washed in distilled water. Oxidation of the sections was achieved using 0.5% (w/v) potassium permanganate solution for 5 minutes. Sections were washed in running tap water for 5 minutes and then immersed in a 1% (w/v) oxalic acid solution for 2-3 minutes to decolourise the sections before another wash in running tap water and 95% ethanol. Sections were then immersed in Miller's elastin stain (Thermo Scientific, UK), which stains elastin fibres black, for 2 hrs. Following staining, sections were once again rinsed in 95% ethanol and running tap water. Sections were briefly counterstained using picrosirius red (solution of Sirius red in picric acid) (Sigma-Aldrich, Dorset, UK) before rinsing with running tap water once again. Finally, sections were immediately dehydrated in an ethanol gradient 1 minute in 70% ethanol, 1 minute in 90% ethanol and 2 x 5 minutes in 100% ethanol before 2 x 5 minutes in HistoClear. Slides were then mounted using DPX mounting medium (Sigma-Aldrich, Dorset, UK) and covered with cover slips.

### **2.8.3 Pulmonary artery remodelling**

Lung sections were microscopically assessed for remodelled and non-remodelled pulmonary arteries approximately  $<80\ \mu\text{M}$  in diameter using a light microscope. Remodelled pulmonary arteries were identified as those with a double elastic lamina (Figure 2.6). The percentage of remodelled pulmonary arteries was then calculated as the number of remodelled arteries/the total number of pulmonary arteries within the section.

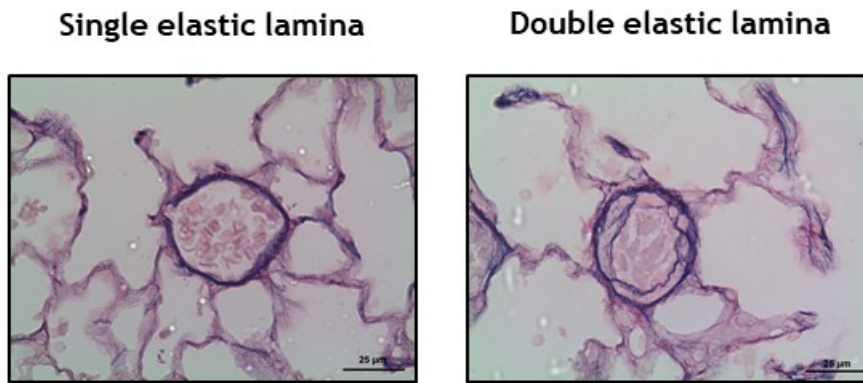


**Figure 2.6 - Pulmonary artery remodelling.**

*Representative images of a normal, unremodelled (single elastic lamina) pulmonary artery and a remodelled (double elastic lamina) pulmonary artery. Scale bar = 25  $\mu$ M, magnification x40.*

## 2.9 Cell Culture

All cell culture was performed under sterile conditions within a class II laminar flow cabinet. Cells were maintained in Corning flasks and plates (Flintshire, UK) in a humidified incubator at 37°C and 5% (v/v) carbon dioxide.

### 2.9.1 Primary cell isolations

#### 2.9.1.1 Adult rat cardiomyocyte isolation

Prior to beginning the cell isolation, Krebs-Henseleit (Krebs) solution was made up as described in Table 4. The pH of the Krebs solution was increased to pH 7.68 at room temperature using sodium hydroxide. The solution was then stored in the fridge until required. On the day of use, 11.1 mM glucose was added to the solution immediately prior to use.

Adult rat cardiomyocytes were isolated from male and female Wistar Hans rats (Envigo, Oxon, UK). A Langendorff perfusion with collagenase digestion was utilised. Rats were killed by cervical dislocation and the hearts rapidly excised and placed into chilled Krebs solution. The cull and heart excision were performed by staff in the Cardiovascular Research Unit (CVRU). Any lung tissue

or connective tissue was removed and the aorta isolated. The heart was quickly cannulated via the aorta on the Langendorff perfusion set up. Perfusion with Krebs solution warmed to 37°C at a flow rate of 7 mL/minute was performed for several minutes until the perfusate ran clear. At this point, 0.025g of Collagenase Type I (Worthington Biochemical via Lorne Laboratories, UK, 260units/mg Cat No: LS004196 Lot:47K17730B) and 0.002g of protease type XIV (P5147 - Sigma-Aldrich, UK) was added to 30 mL of Krebs solution to be perfused through the heart, resulting in a final concentration of 0.7 mg/mL collagenase and 0.06 mg/mL protease. The hearts were perfused with the digestion mix for varying time periods before perfusion with a 0.5% BSA in Krebs solution for varying time periods. Development of this protocol is described in Appendix 7.1. Perfusion with BSA aided the termination of enzymatic activity. At the end of the perfusion steps, the heart was cut down from the cannula and the vessels and atria removed. The RV was then carefully dissected from the LV and the RV and LV was then placed into separate weight boats with 0.5% BSA in Krebs solution. From this point onwards the RV and LV were treated separately. The RV and LV were cut into small pieces and then transferred to 15 mL tubes (Corning, Flintshire, UK) containing approximately 6 mL and 10 mL of 0.5% BSA Krebs solution, respectively. Using a flame blunted plastic Pasteur pipette the pieces of tissue were agitated in order to gently release the cells from the tissues. When the solution appeared straw coloured, indicating a release of cells, the tissue was allowed to settle to the bottom of the 15 mL tube and half the volume of BSA/Krebs solution was transferred to a new 15mL tube. Fresh BSA/Krebs solution was added to the original tube to increase the volume to the starting volume and the process began again. The process was repeated 4-5 times until the tissue had been successfully broken up and the majority of cells released. The cell suspension from each 15 mL tube containing RV and LV cells was then examined under a microscope to inspect the quality of the digestion indicated by the number of viable rod-shaped cardiomyocytes. The 15 mL tubes with the greatest number of viable rod-shaped cardiomyocytes as visible by eye were selected for the remainder of the experiment and the 15 mL tubes combined. The calcium concentration of the cell suspension was then increased to 1mM in gradual increments by adding 1µL of 100mM calcium chloride (CaCl<sub>2</sub>) per 1 mL of cell suspension every 5mins. This incremental addition of CaCl<sub>2</sub>

reduces hypercontraction of the cardiomyocytes as a result of rapid calcium influx.

Salt	Supplier and Catalogue Number	Final Concentration required (mM)	In 1L distilled water (g)
NaCl	<i>Fisher Chemical</i> S/3161/53	120	7.0128
HEPES	<i>Sigma-Aldrich</i> H3375 250g	20	4.7656
KCl	<i>VWR</i> 26764.260 500G	5.4	0.4026
NaH <sub>2</sub> PO <sub>4</sub>	<i>Fisher Scientific</i> 13472-35-0	0.52	0.0624
MgCl <sub>2</sub> ·6H <sub>2</sub> O	<i>VWR</i> 25108.260 500G	3.5	0.7114
Taurine	<i>Sigma-Aldrich</i> T0625-100G	20	2.5020
Creatine	<i>Sigma-Aldrich</i> C0780- 100G	10	1.4912
***Glucose (anhyd)	<i>Fisher Chemical</i> G/0500/53	11.1	2

*Table 4 - Krebs-Henseleit Solution contents*

### 2.9.1.2 Neonatal rat cardiac cell isolation

Wistar Kyoto (WKY) rat breeding cages were set up in the Cardiovascular Research Unit (CVRU) to provide neonatal pups. WKY rats were obtained through the internal breeding programme at the University of Glasgow. Both neonatal rat cardiac fibroblasts and neonatal rat cardiomyocytes were isolated from neonatal hearts through a process involving enzymatic digestion and differential plating.

Male and female neonatal rats were culled by decapitation on day 3-5. All the hearts from the litter were collected together. Hearts were quickly excised from the chest cavity and placed into chilled ADS buffer on ice. ADS buffer contents are as described (Table 5). The contents were added to 1 L of distilled water and the pH increased to 7.35 using sodium hydroxide. The buffer was then filtered and stored at 4°C. Hearts in ADS buffer were then moved into a sterile laminar flow hood and the remainder of the protocol was completed under sterile conditions. The atria and connective tissue were removed and the hearts washed in clean ADS buffer. The ventricles were then cut into small pieces and transferred to a 100 mL Duran bottle by Pasteur pipette. Any remaining ADS buffer was carefully removed and the enzyme mix was added. The enzyme mix was made up of 0.03 g collagenase type II (ThermoFisher Scientific, 17101-015) and 0.03 g pancreatin from porcine pancreas (Sigma-Aldrich, P3292-25G) in approximately 50 mL ADS buffer. The enzyme solution was filter sterilised before use. The appropriate volume of enzyme mix was added to the neonatal heart pieces and the Duran bottle placed in a shaking water bath at 37°C with a specific stroke speed and duration (Table 6). The digestion step was repeated several times as detailed (Table 6). Following the first digestion, the supernatant was removed and discarded. After each of the subsequent digestions (digestions 2-6), the supernatant was collected and transferred to a sterile 50 mL tube (Corning, Flintshire, UK) containing 2 mL FBS. The 50 mL tube was then centrifuged at 900xg for 5 mins. The supernatant was discarded and the pellet containing the fibroblasts and myocytes was gently re-suspended in 4 mL of FBS. This cell suspension was then pooled in 50 mL tube was then stored in the cell culture incubator with the lid slightly loosened. The resuspended pellet was then added to the same tube after each digestion. Therefore, all cells from each digestion were collected in a 50 mL tube which was then centrifuged at 900xg for 6 minutes. Following the final centrifugation, the cell pellet was re-

suspended in plating media (Table 7) and plated onto poly-L-lysine (Sigma-Aldrich, P4707) coated 10 cm cell culture dishes (Corning, 430167). The plates were placed in the incubator for at least 1 hr to allow the neonatal cardiac fibroblasts to adhere to the plate. The plates were then washed gently using the plating media within the plate, and the plating media removed. This media contained the neonatal cardiac myocytes that did not adhere to the poly-L-lysine coated plates. Plating media was replaced on the neonatal cardiac fibroblasts and the cells stored in the cell culture incubator. After 24 hrs, the plating media was changed to DMEM (Thermo Fisher Scientific, 41966-029) supplemented with 20% (v/v) FBS, 100 U/mL penicillin and 100 µg/mL streptomycin (ThermoFisher Scientific, 15140-122).

Salt	Catalogue number (Sigma-Aldrich)	Final concentration required (mM)	In 1L of distilled water (g)
NaCl	S9888	116	6.8
HEPES	H4034	20	4.76
NaH <sub>2</sub> PO <sub>4</sub>	S3139	1	0.12
Glucose	G7528	5.5	1.0
KCl	P3911	5	0.4
MgSO <sub>4</sub>	M2643	0.8	0.1

*Table 5 - ADS buffer contents*

Digest	Volume of the enzyme mix (mL)	Time (minutes)	Speed (strokes/min)
1	10	5	160
2	10	20	150
3	8	25	150
4	8	25	150
5	6	25	150
6	6	25	150

*Table 6 - Neonatal heart digestion protocol*

	Supplier	mL/500mL	Final concentration
DMEM	ThermoFisher Scientific	340	68% (v/v)
M199	ThermoFisher Scientific	85	17% (v/v)
Horse Serum	ThermoFisher Scientific	50	10% (v/v)
FBS	ThermoFisher Scientific	25	5% (v/v)
Penicillin + Streptomycin	ThermoFisher Scientific	5	1% (v/v) 100 U/mL Penicillin 100 µg/mL

*Table 7 - Plating media contents*

### **2.9.1.3 Adult rat pulmonary artery smooth muscle cell isolation**

The digestion mixture was made up of a ratio of 1:3:17:17 of Elastase (Sigma-Aldrich, Dorset, UK): Soyabean trypsin inhibitor (Sigma-Aldrich, Dorset UK): Collagenase type 1 (Lorne Laboratories, Reading, UK): BSA (Sigma-Aldrich, Dorset, UK). The digestion mix was stored at 4 °C until required. Post mortem, the left lung lobe was collected from male and female Wistar rats (Envigo, Oxon, UK). Lungs were collected in DMEM supplemented with 10% (v/v) FBS and 1% (v/v) antibiotic antimycotic solution (10,000units penicillin, 10,000 µg streptomycin and 25 µg amphotericin B., Sigma-Aldrich, UK). The main pulmonary artery in the left lung lobe was carefully dissected and placed into a glass bottle containing the digestion mix with 25 mL of Nutrient Mixture F-12 Ham (Sigma-Aldrich, UK, 6658) and a magnetic stirrer bar. The bottle was then placed on a heated stirrer plate. Temperature was monitored to ensure the mixture was kept at approximately 37 °C. Pulmonary arteries were digested until they appeared “hairy”. Following this, the digestion mix containing cells was filtered through 100 µm sterile filter. The mixture was centrifuged at 220 g for 1 minute at room temperature. The cell pellet was resuspended in complete DMEM and plated in T25 flasks. Media was changed after 24-48 hrs to remove dead cells.

### **2.9.2 Passaging and plating cells**

Once the rat PSMCs or the neonatal cardiac fibroblast cells had reached the appropriate confluency (the coverage of the cell monolayer on the surface of the flask) the media was removed from the flask. Cells were washed with sterile 1 x PBS warmed to 37 °C to ensure all serum was removed from the cells. Following the PBS wash, 2-3 mL of Trypsin-EDTA (0.5%) solution (ThermoFisher Scientific, 15400-054), warmed to 37 °C, was then added to the cells for approximately 5 minutes and the flask placed in the incubator during this time. Trypsin is a proteolytic enzyme which acts to detach the cells from the flask. EDTA within the solution acts as a chelator for calcium ions which further aids the process of cell detachment. Cell detachment from the flask was confirmed by assessing the cells under a microscope and DMEM containing FBS was then added to neutralise the action of trypsin-EDTA solution. The cell suspension was then transferred to a sterile tube and the cell suspension centrifuged at 210 g for 5 mins at room

temperature. The supernatant containing the Trypsin-EDTA solution was then removed and the cell pellet resuspended in the appropriate volume of DMEM. Cells were then plated into fresh flasks. When passaging neonatal rat cardiac fibroblasts, the cells were passaged at a ratio of 1:2 or 1:3. For example, the cells from 1 flask were split into 2 flasks (1:2).

When experimental set up required a specific number of cells to be seeded in 6, 12, 24 or 96 well plates, the cells within the cell suspension were counted. Once the pellet had been resuspended the cell suspension was mixed well and 10  $\mu$ L of the cell suspension was added to a haemocytometer. The number of cells within each of the 4 quadrants, made up of 16 large squares, were counted. The mean cell count across the 4 quadrants was calculated. The haemocytometer is designed such that the number of cells in 1 quadrant is equivalent to the number of cells  $\times 10^4$  per mL. Each quadrant has an area of 1 mm<sup>2</sup> and the depth between the grid and the coverslip is 0.1 mm therefore the volume of cell suspension in this area is 0.1  $\mu$ L. Therefore, the mean number of cells in a quadrant is equal to the same number  $\times 10^4$  cells/mL.

The volume of cell suspension required was calculated as:

$$\frac{\textit{The cell density required (cells/ml)}}{\textit{The number of cells/ml of cell suspension}}$$

The cell suspension was then mixed well before plating the appropriate volume into the wells.

When required cells were cryopreserved for short- and long-term storage. Cells were trypsinised and subjected to centrifugation as described above. The supernatant was removed and the cell pellet remained. Normally, the cell pellet from 1 x T75 cm<sup>2</sup> flask was resuspended in 1 mL of 10% (v/v) dimethyl sulfoxide (DMSO, Fisher Scientific) in FBS. The cell suspension was then quickly transferred to a cryopreservation vial and then vial either wrapped in bubble wrap and placed into -80°C or placed into a freezing container with 100% isopropanol and then into -80°C. Both methods help to slow the freezing process to help prevent cell rupture which can result from rapid freezing. The freezing container allows cooling at a rate of approximately 1°C per minute. For short term storage, cells

were stored in  $-80^{\circ}\text{C}$  and for longer term storage cells were transferred to liquid nitrogen storage tanks.

### **2.9.2.1 Charcoal stripped serum**

Charcoal stripped serum (CSS) was kindly gifted by Dr. Craig Docherty, University of Glasgow. FBS was stripped of endogenous estrogens with the use of dextran-activated charcoal (Johansen, 2014). The charcoal stripping process allows non-polar components, such as hormones, to be selectively removed from the serum. Dextran-activated charcoal was added to FBS at 0.1 g/10 mL. It was then gently shaken overnight at  $4^{\circ}\text{C}$  before being subjected to centrifugation at 1811 g for 30 mins at  $4^{\circ}\text{C}$ . The serum was then filtered using a  $0.22\ \mu\text{M}$  filter and the process repeated. After this step the serum was aliquoted and frozen at  $-20^{\circ}\text{C}$  until required.

### **2.9.3 Estrogen Stimulations of Neonatal Cardiac Fibroblasts**

Neonatal cardiac fibroblasts were plated into 6 well plates at a density of  $2 \times 10^5$  cells per well. Cells were maintained in DMEM supplemented with 20% (v/v) FBS and 100 U/mL penicillin and 100  $\mu\text{g}/\text{mL}$  streptomycin (ThermoFisher Scientific, 15140-122) for 24 or 48 hrs until cells reached 70-80% confluency. Once confluent, cells were serum starved for 24 hrs in serum free, phenol red free DMEM (ThermoFisher Scientific, UK, 21063029) supplemented with 100 U/mL penicillin and 100  $\mu\text{g}/\text{mL}$  streptomycin (ThermoFisher Scientific, 15140-122) and 1 nM sodium pyruvate (ThermoFisher Scientific, UK, S8636). This process of quiescence allowed for growth arrest and synchronisation of the cell cycle. Any experiment which involved stimulation with estrogen or an estrogen metabolite utilised phenol red free media from the quiescence stage onwards. Phenol red is a weak estrogenic mimic which could have influenced the action of exogenous estrogen added to stimulate the cells. Cells were stimulated for 24 hrs, unless otherwise indicated, with Angiotensin II (Ang II) (Sigma-Aldrich, Dorset, UK) at 100 nM and  $\beta$ -estradiol (Sigma-Aldrich, UK, E2758-250MG) at 1 nM or 10 nM in phenol red free DMEM described above.  $\beta$ -estradiol was resuspended in 100% ethanol to create a 10 mM stock solution. At the end of the stimulation, DMEM was removed and the cells washed twice with PBS.

## 2.9.4 Migration Assay

Rat PSMCs (Passage 2) were plated onto 24 well plates at high confluence. Cells were initially cultured with DMEM (ThermoFisher Scientific, 41966-029) supplemented with 10% FBS. When the cells appeared 90-100% confluent they were quiesced using Phenol Red Free media (Life technologies, 21063-029) containing either no serum or 0.5% FBS/0.5% CSS for 24 hrs in order to achieve growth arrest and synchronisation of the cell cycle. From this point onwards, cells were cultured in phenol red free media as phenol red is a weak estrogenic mimic (Welshons et al., 1988) which could have influenced the results. After 24 hrs in low serum media scratches were made in the cell monolayer down the centre of the well using a P10 pipette tip inserted over a P200 pipette tip. The pipette tip was placed against a ruler in an attempt to increase reproducibility of the scratches. Media was then removed, the plates inverted, and lines drawn horizontally across the bottom of the plates in the middle of the wells. These lines were used as guides for the position at which to measure migration. Phenol red free media with the appropriate serum concentration was added to the wells. 17 $\beta$ -Estradiol (E2) (Steraloids, New England, USA, E0950-000) was dissolved in 100% ethanol (EtOH) to create a 1 mM stock solution and stored at -20°C. 16 $\alpha$ -hydroxyestrone (16 $\alpha$ -OHE1) (Steraloids, New England, USA, E1250-000) was also dissolved in 100% EtOH to create a 1 mM stock solution and stored at -20°C. E2 and 16 $\alpha$ -OHE1 were diluted in media to create a final concentration in the well of 10 nM ( $1 \times 10^{-8}$  M) and 1 nM ( $1 \times 10^{-9}$  M). Each condition was repeated in duplicate. An unstimulated control was included with the same percentage serum containing media. As positive controls, 10% serum (FBS/CSS) were included and EtOH vehicle negative controls were also included and were repeated in either duplicate or triplicate, depending on the wells available. Photographs were taken using a Moticam ST 5.0MP camera and Motic Images Plus 2.0 software. 0 hr photographs were then taken at the point indicated by the line/s drawn on the bottom of the wells. During initial experiments only 1 photograph was taken per well, whereas for later experiments 2 photographs were taken at different points in each well. Cells were incubated with the appropriate treatment for 24 hr and images were captured in the same manner at approximately the same position as the 0 hr image. Using Image J software, the area of a small section of the scratch indicated by the line was calculated in

both 0 hr and 24 hr photographs. The percentage wound closure was then calculated by the equation  $(0 \text{ hr area} - 24 \text{ hr area} / 0 \text{ hr area}) * 100 = \text{percentage of wound closure}$ . The area was therefore always relevant to the initial area measured in the 0 hr photograph.

## **2.10 Analysis of RNA**

### **2.10.1 RNA extraction**

Total RNA was extracted from RV tissue, LV tissue or cells harvested at the end of the study. Approximately half of the RV tissue and one quarter of the LV tissue was selected for RNA analysis. For tissue RNA extraction, a 5 mm stainless steel bead (Qiagen, UK, 69989) and 700  $\mu\text{L}$  of QIAzol lysis reagent (Qiagen, UK, 79306) was added to each sample. Samples were then homogenised in the Tissue Lyser II (Qiagen, UK, 85300). RNA extraction from cells was performed by cells first being washed with PBS and then 700  $\mu\text{L}$  of QIAzol lysis reagent was added to each well. The bottom of the wells was then scraped to remove the cells from the surface of the well and the cells in the QIAzol suspension were then transferred to RNase free microcentrifuge tubes. Samples from both tissue and cells were incubated at room temperature for 5 mins after which 140  $\mu\text{L}$  of chloroform was added and the microcentrifuge tubes shaken vigorously. Microcentrifuge tubes were subjected to centrifugation at 12,000 g for 15 mins at 4°C. Further extraction and purification were performed using the miRNeasy extraction kit (Qiagen, UK, 217004) as per the manufacturer's instructions. A DNase digestion step was performed to prevent contamination of the RNA sample with deoxyribonucleic acid (DNA). Next, 10  $\mu\text{L}$  of the DNase digestion enzyme and 70  $\mu\text{L}$  of the RDD buffer (Qiagen, UK, 79254) were mixed and added to the mini spin column and incubated for between 20 - 40 mins. Finally, RNA was eluted in 33  $\mu\text{L}$  of RNase free water (Qiagen, UK) and passed through the column twice to maximise RNA yield. RNA samples were then immediately placed on ice or stored at -80°C.

### **2.10.2 Quantification of RNA**

RNA was quantified using a NanoDrop ND-1000 spectrophotometer (Thermo Scientific, UK). Each sample was assessed for RNA concentration (ng/mL) and

the quality indicated by the 260/280 ratio. A 260/280 ratio of 2.0 indicates high quality RNA and the ratio of the majority of samples fell within the range of 1.95-2.05. However, a few samples outwith this range were included in final analysis due to the small number of samples. Each sample was analysed twice and a mean concentration calculated.

### **2.10.3 Complementary DNA preparation**

Reverse transcription (RT) of RNA to produce complementary DNA (cDNA) was carried out using the TaqMan Reverse Transcription Reagents kit (Applied Biosystems, USA, N808-0234) with 40  $\mu$ L reactions performed for each sample. 500 ng, 1  $\mu$ g or 1.5  $\mu$ g of RNA was added to the reaction. The different concentrations were due to differences in RNA concentration between cells, RV tissue and LV tissue and low volumes of RNA towards the end of the study. No comparisons were made across different cDNA plates. Reaction mixtures (*Table 8*) and RNA were added to 96 well plates. Plates were sealed with an adhesive sheet before brief centrifugation which ensured all components were mixed at the bottom of the well. RT was performed using the Veriti 96 well fast Thermal Cycler (Applied Biosystems, UK) or the Peltier Thermal Cycler PTC-225 (MJ Research). The following cycling conditions were selected: 10 mins at 25°C, 30 mins at 48°C and 5 mins at 95°C. 96 well plates containing cDNA were then stored at -20°C.

Solution	Volume ( $\mu\text{L}$ )	Final Concentration
10 x RT Buffer	4	1 x RT buffer
25 mM $\text{MgCl}_2$	8.8	5.5 mM
dNTPs	8	2 mM
Random hexamers	2	2.5 $\mu\text{M}$
RNase Inhibitor	0.8	0.4 U/ $\mu\text{L}$
Multiscribe enzyme	1	1.25 U/ $\mu\text{L}$
RNA + RNase free water	15.4	

***Table 8 - TaqMan Reverse Transcription Reagents.***

*Reverse Transcription reagents, the volume used in each 40  $\mu\text{L}$  reaction and the final concentration of reagents.*

#### 2.10.4 Quantitative Polymerase Chain Reaction (qPCR)

TaqMan reaction mixtures with 10  $\mu$ L volumes were produced with TaqMan Universal master mix II, no UNG (Applied Biosystems, USA, 4440040), the appropriate primer (Life Technologies, UK) (*Table 9, Table 10*), RNase free water (Qiagen, UK) and cDNA sample. Samples were repeated in triplicate on the same 384 well plate in order to account for technical errors. Non-template controls containing RNase free water instead of cDNA sample were also included for each primer to ensure there was no contamination of the master mix. After the addition of all the components, plates were sealed with an optical adhesive sheet and briefly centrifuged to remove all air bubbles and mix the components at the bottom of the well. The ViiA7 Real Time PCR system was used to perform quantitative real-time PCR (qRT-PCR). The cycling conditions were as follows: 50°C for 2 mins, 95°C for 10 mins and then 40 cycles of 95°C for 15 secs, 60°C for 1 min. Beta-2-microglobulin (B2M) was used as the housekeeper gene. The  $2^{-\Delta CT}$  method (Schmittgen and Livak, 2008) was used to calculate and display levels of gene expression.

Gene	Gene name	Species	Code
B2M	B2m	Mouse	Mm00437762_m1
BMPR2	bmpr2	Mouse	Mm00432134_m1
Col1a1	Col1a1	Mouse	Mm00801666_g1
Col3a1	Col3a1	Mouse	Mm01254476_m1
CTGF	Ctgf	Mouse	Mm01192933_g1
Cyp1b1	Cyp1b1	Mouse	Mm00487229_m1
Id1	Id1	Mouse	Mm00775963_g1
Id3	Id3	Mouse	Mm01188138_g1 Mm00492575_m1
Smad 1	Smad1	Mouse	Mm00484723_m1
TGF $\beta$ 1	Tgf $\beta$ 1	Mouse	Mm01178820_m1
TGF $\beta$ R1	Tgf $\beta$ R1	Mouse	Mm00436964_m1

***Table 9 - Mouse TaqMan Primers (Thermo Scientific, UK).***

*The mRNA target, gene name and catalogue number for each primer.*

Gene	Gene name	Species	Code
$\beta$ -Actin	Actb	Rat	Rn00667869_m1
ANP	Nppa	Rat	Rn00664637_g1
B2M	B2M	Rat	Rn00560865_m1
BMPR2	Bmpr2	Rat	Rn01437214_m1
B-myosin heavy chain	Myh7	Rat	Rn01488777_g1
BNP	Nppb	Rat	Rn00676450_g1
Col1a1	Col1a1	Rat	Rn01463848_m1
Col3a1	Col3a1	Rat	Rn01437681_m1
CTGF	CTGF	Rat	Rn01537279_g1
Id1	Id1	Rat	Rn00562985_s1
Id3	Id3	Rat	Rn04219390_g1
Ppib	Ppib	Rat	Rn00574762_m1
Smad 1	Smad1	Rat	Rn00565555_m1
TBF $\beta$ 1	TBF $\beta$ 1	Rat	Rn00572010_m1
TGF $\beta$ R1	TGF $\beta$ R1	Rat	Rn00688966_m1

*Table 10 - Rat TaqMan Primers (Thermo Scientific, UK).*

*The mRNA target, gene name and catalogue number for each primer.*

## 2.11 Western Blotting

### 2.11.1 Protein Extraction

Protein was extracted from RV tissue, LV tissue and lung tissue harvested on Day 28 of the mouse Anastrozole study. A small section of each tissue was used for protein extraction, normally, half of the mouse RV, one quarter of the mouse LV and one of the right lung lobes. The tissue was moved into a fresh, cold 2 mL microcentrifuge tube and placed on ice. A 5 mm stainless steel bead (Qiagen, UK), 300  $\mu$ L of 1% lauryl maltoside/PBS (LM buffer) (Abcam, UK) and Halt™ Protease Inhibitor Cocktail (ThermoFisher Scientific, 78429) was added to each sample. Samples were homogenised in the Tissue Lyser II (Qiagen, UK) at 25 Hz for 4 x 30 secs with 30 secs rest in between each homogenisation, this helped to prevent heating of the sample. The homogenised samples were then left on ice for 30 mins. Samples were then subjected to centrifugation at 10,600 g for 10mins at 4°C. Following centrifugation, the supernatant was then transferred to a new pre-cooled microcentrifuge tube and moved immediately onto ice or stored at -80°C.

### 2.11.2 Quantification of protein

Protein was quantified using a NanoDrop ND-1000 spectrophotometer (Thermo Scientific, UK). The Protein A280 setting was selected and each sample was assessed for the protein concentration (mg/mL). Each sample was analysed twice and a mean concentration calculated.

### 2.11.3 Sodium dodecyl sulphate-polyacrylamide gel electrophoresis

Sodium dodecyl sulphate-polyacrylamide gel electrophoresis (SDS PAGE) allows the separation of proteins across a gel due to their molecular weight. Protein samples were prepared for western blotting with NuPAGE reducing agent (Life technologies, UK) and NuPAGE sample loading buffer (Life technologies, UK) at a ratio of 5:1:2, respectively. Samples were then heated to 70°C for 10 mins to disrupt the tertiary protein structure and denature the proteins. This was followed by centrifugation at 10,600 g for 1 min. Samples were then stored at -20°C until required. On the day of the western blotting experiment, samples

were loaded into NuPAGE Novex 4-12% Bis-Tris Mini gels (Life Technologies, UK) and SeeBlue Plus2 (Invitrogen, UK) was used as a molecular weight ladder. Approximately 20 µg of protein was loaded into each well of the gel. When appropriate, 20 µg of positive control tissue, prepared in the same way, was also loaded on to the gel. The gel tanks were filled with 5% (v/v) NuPAGE MOPS buffer (Life technologies, UK) in distilled water. A voltage of 150 V was applied to the gel tanks for approximately 1.5 hrs or until adequate separation of the molecular weight ladder was visualised. The sample loading buffer and the molecular weight ladder allowed the progress of the proteins through the gel to be monitored.

#### **2.11.4 Protein transfer and visualisation**

Following gel electrophoresis, proteins were transferred onto a polyvinylidene fluoride (PVDF) microporous membrane (Millipore, USA). PVDF membranes were activated with 100% methanol prior to use. The transfer buffer was as follows: 5% (v/v) NuPAGE transfer buffer (Life technologies, UK), 20% (v/v) Methanol and (v/v) 75% distilled water. Sponges used in the transfer tanks were soaked in transfer buffer prior to use and a roller was used to exclude all air bubbles from the sponges which could affect the successful transfer of proteins. The transfer tanks were set up using sponges, paper, PVDF membrane and the gel containing the proteins. The transfer was run at 35 V for approximately 2 hrs and 15 mins, during this time the proteins migrated from the gel onto the PVDF membrane. After termination of the transfer, membranes were stained with 0.1% (w/v) Ponceau S in 5% (v/v) acetic acid solution to ensure the presence of proteins on the membrane. The PVDF membranes were then washed using tris-buffered saline with 0.1% (v/v) Tween20 (TBST) (ThermoFisher Scientific, UK) 3 times for 10 mins. This ensured all Ponceau S had been removed from the membrane. Membranes were then blocked to prevent non-specific antibody binding, using a non-fat milk solution made up of 5% Milk powder (w/v) in TBST.

#### **2.11.5 Immunoblotting**

The identification of proteins on the membrane was achieved by exposing the membrane to a protein-specific antibody. Membranes were washed for 3 x 10 minutes in TBST before primary antibodies were added (Table 11). All primary

antibodies were made up in 5% (w/v) (BSA)/TBST, with the exception of  $\alpha$ -tubulin which was made up in 5% (w/v) milk powder (Milk powder)/TBST. Membranes were incubated with primary antibodies overnight at 4°C on a shaker. Membranes were washed 3 times in TBST to remove all excess primary antibody that had not bound to its specific protein prior to the addition of an appropriate secondary antibody (Table 11). Secondary antibodies were conjugated with horse radish peroxidase (HRP) to allow detection of the antibody using an enhanced chemiluminescence (ECL) method. Secondary antibodies were made up in 5% milk powder or high detergent (HD) 5% milk powder (per 5 mL: 3.7 mL water, 0.5 mL 5% Milk powder, 0.5 mL 10x PBS 0.25 mL 20% Triton-x-100 and 0.05 mL 10% sodium dodecyl sulphate (SDS)). Membranes were incubated with secondary antibodies for approximately 1 hr at room temperature on a shaker. Protein bands were visualised using ECL solutions with either Immobilon western chemiluminescence horseradish peroxidase (HRP) substrate (Merck Millipore, USA) or Pierce ECL (ThermoFisher Scientific, UK). This allowed visualisation of the protein bands following exposure of the membrane to x-ray film. Following this, membranes were washed for 3 x 10 minutes in TBST before membranes were stripped using Restore Western Blot Stripping buffer (Thermo Scientific, UK) for 15 mins at room temperature on a shaker. The same protocol was then followed for the loading control which was either glyceraldehyde phosphate dehydrogenase (GAPDH),  $\alpha$ -tubulin or  $\alpha$ -actin. Protein bands on the x-ray film were quantified by densitometry analysis using Image Studio Lite Version 5.2 software (Licor, UK). The ratio of the protein of interest to loading control was calculated.

Primary Antibody	Dilution	Secondary Antibody	Dilution	ECL
BMPR2 (BD Biosciences, 612292)	1:500 in 5% BSA	Anti-mouse (Sigma-Aldrich, A9044/ Calbiochem, 401215)	1:10,000 in 5% Milk powder/TBST	Millipore
Id1 (CalBioreagents, M085)	1:1000 in 5% BSA	Anti-rabbit (Calbiochem, 401315)	1:10,000 in 5% Milk powder/TBST	Millipore
Id3 (CalBioreagents, M100)	1:1000 in 5% BSA	Anti-rabbit (Calbiochem, 401315)	1:10,000 in 5% Milk powder/TBST	Millipore
ER- $\alpha$ (Abcam, 32063)	1:1000 in 5% BSA	Anti-rabbit (Calbiochem, 401315)	1:20,000 in HD 5% Milk powder/TBST	Millipore
CYP1B1 (Abcam, 78044)	1:1000	Anti-rabbit (Calbiochem, 401315)	1:10,000 in 5% Milk powder/TBST	Millipore/ ThermoFisher
Aromatase (Abbexa)	1:500 in 5% BSA	Anti-rabbit (Calbiochem, 401315)	1:20,000 in 5% Milk powder/TBST	Millipore
$\alpha$ -tubulin (Abcam, ab7291)	1:10,000 in 5% Milk powder	Anti-mouse (Sigma-Aldrich, A9044)	1:10,000/1:20,000 in 5% Milk powder/TBST	ThermoFisher
$\alpha$ -Actin Sigma-Aldrich, A9357)	1:10,000 in 5% BSA	Anti-mouse (Sigma-Aldrich, A9044)	1:10,000 in 5% Milk powder/TBST	ThermoFisher

***Table 11 - Western Blotting protocols.***

*Primary and secondary antibodies with dilutions and the appropriate ECL.*

## 2.12 Development of the Pulmonary Artery Banding Surgical Model

Work was completed to develop a pulmonary artery banding (PAB) model at the University of Glasgow. The team developing this model included myself, Margaret Nilsen and Michael Dunne. The Named Veterinary Surgeon also provided advice regarding the surgical procedure and intra-operative/post-operative analgesics. The staff in the CVRU also provided assistance with animal welfare following surgery. The sham surgery was also undergoing development to act as a control. The full development of the surgical procedure is described in Appendix 7.2. Briefly, the surgery was being developed to include the following main steps: a lateral thoracotomy to expose the pulmonary artery, the positioning of a suture under the pulmonary artery using a ligation aid, constriction of the pulmonary artery with the suture and the use of a blunted needle to guide the diameter of the tie and finally closure of the wound. 1 male Wistar rat (Envigo, Oxon, UK) and 1 male Sprague Dawley rat (Charles River, UK) successfully recovered from sham surgery and were haemodynamically assessed at 6 weeks and 4 weeks post-surgery, respectively.

## 2.13 Statistical Analysis

All data is displayed as mean  $\pm$  standard error of the mean (S.E.M.). Protein results are displayed as the ratio of the densitometry measurements for the protein of interest to the loading control. Gene expression data is displayed as  $2^{-\Delta CT}$  relative to the housekeeping gene B2M. Data was analysed using unpaired t-test (two-tailed) or one-way analysis of variance (ANOVA) with Bonferroni post-hoc test, with the mean of pre-selected groups compared, as indicated. Statistical analysis was performed using GraphPad Prism Software version 7 and 8 (GraphPad Software Inc., California, USA). P values of  $< 0.05$  were considered statistically significant. The significant differences between the pre-selected groups have been shown. Significant differences are displayed \*  $p < 0.05$ , \*\*  $p < 0.01$ , \*\*\*  $p < 0.001$  and \*\*\*\*  $p < 0.0001$ .

## **Chapter 3**

### **3 The effect of FK506 treatment on parameters of experimental pulmonary hypertension.**

### 3.1 Introduction

An understanding of the genetic factors contributing to the development of disease allows potential drug targets to be identified. Mutations in *BMP2R* are the most well understood risk factor in the development of PAH. Over 400 different mutations across the ligand binding domain, kinase domain and cytoplasmic domain have been identified in the *BMP2R* gene (Austin and Loyd, 2014). The majority of mutations identified in PAH patients are nonsense and frameshift mutations that render the protein non-functional. Therefore, it is thought that haploinsufficiency of *BMP2R* contributes to the pathogenesis of the disease (Southgate et al., 2020).

Despite the role of *BMP2R* being well established in PAH, there are no therapies which currently target it. A recent study identified FDA approved compounds which increased the expression of *BMP2R* (Spiekerkoetter et al., 2013) an approach which might be useful to investigate for PAH. Repurposing drugs which are FDA approved for other conditions is a particularly useful approach for rare, orphan diseases such as PAH as often the appropriate funding is not available within the pharmaceutical industry to identify new therapeutic targets. The compound FK506 (tacrolimus) is currently used as an immunosuppressive drug and is often used to treat patients who are undergoing an organ transplant (Fung and Starzl, 1995). The Spiekerkoetter et al. (2013) study highlighted that treatment with low dose FK506 (tacrolimus) was able to increase *BMP2R* expression in an *in vitro* setting and reverse the PH phenotype in several different animal models (Spiekerkoetter et al., 2013). FK506 was able to mediate these effects via interaction with its pharmacological target FKBP12 which in turn prevented FKBP12 binding to the BMP receptors. It was also shown to activate *BMP2R* mediated signalling even in the absence of BMP ligands. The encouraging results in the pre-clinical setting meant that investigations into FK506 as a potential therapy to treat PAH have progressed to clinical investigations. The first study involved compassionate use of low dose FK506 in 3 female patients with late stage disease (Spiekerkoetter et al., 2015). Two out of the three patients appeared to respond to treatment with improved or stable RV function and neither patient had a PAH related hospitalisation during the 12 months of treatment. This then led to a Phase IIa clinical trial investigating safety and tolerability (Spiekerkoetter et al., 2017). Although within the patient

cohort FK506 was generally well tolerated and there was no concern over the safety or toxicity of the compound, neither an improvement in PAH parameters nor an increase in BMPR2 expression were observed. Although one of the outcomes of the study was that a phase IIb clinical trial was appropriate, recruitment for a phase IIb trial has not yet begun.

Another well-established risk factor in the development of PAH is the female sex. PAH registries show a female to male ratio of up to 4:1 (Badesch et al., 2010). Therefore, the role of sex in the pathological processes of PAH must be considered. This finding must also be considered during the development of new therapies as it is possible that the therapy related clinical outcomes may differ between men and women. Studies have shown sex-specific differences in the expression of BMPR2 and BMPR2 mediated signalling within PAH (Austin et al., 2012; Mair et al., 2015). Furthermore, sex-specific differences in the penetrance of BMPR2 mutations has also been highlighted. Females have shown approximately 42% penetrance and males only 14% penetrance (Larkin et al., 2012). Therefore, understanding the sex-specific effects of a potential PAH therapeutic is key to understanding its potential effect on the clinical outcomes of the PAH patient population. The study by Spiekerkoetter et al. (2013) in which treatment with FK506 was investigated in multiple animal models was only conducted using male animals (Spiekerkoetter et al., 2013). Therefore, there is a need to fully investigate the effects of treatment with FK506 in female animals as the majority of the PAH patient population who will be treated with this potential therapy are female.

Here, the effect of FK506 (0.05mg/kg/day) on parameters of experimental pulmonary hypertension was investigated in a rat model of chronic hypoxia.

The aims of this investigation were:

To characterise the chronic hypoxia model in both male and female rats. The effect on haemodynamic parameters along with the associated pathological changes in the pulmonary vasculature were assessed.

To assess the effects of FK506 treatment (0.05mg/kg/day) on these parameters.

To assess the effects of FK506 treatment (0.05mg/kg/day) on systemic and left ventricular pressure in order to identify any potential off target, systemic effects.

### 3.2 Results

Sprague Dawley rats were placed in a hypobaric hypoxic chamber for 35 days. On day 14 of the study drug releasing pellets were inserted subcutaneously in the neck. The pellets either released FK506 at a dose of 0.05 mg/kg/day or a placebo. The placebo consisted of cholesterol, lactose, celluloses, phosphates and stearates which made the matrix of the carrier binder in the FK506 pellets. Rats were returned to the hypoxic chamber for the remainder of the study. Age and sex matched controls were kept under normoxic conditions and followed the same dosing regimen. On day 35 of the study rats were haemodynamically assessed using the Millar PV loop system, humanely killed and tissues were then collected (Figure 3.1).

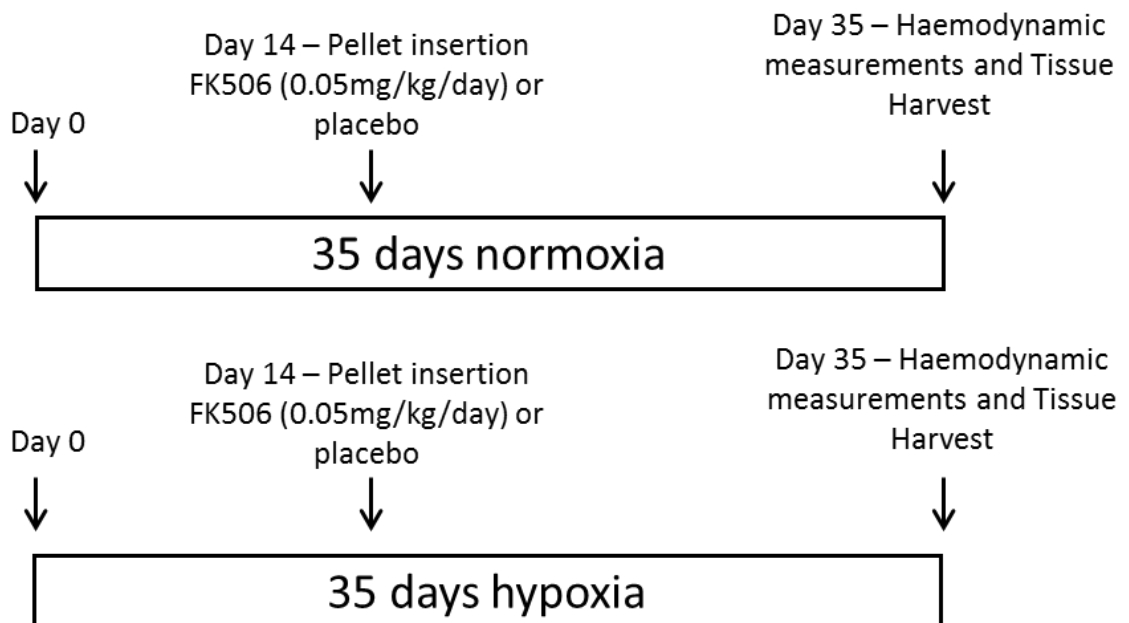


**Figure 3.1- Schematic diagram showing FK506 study protocol and dosing regimen.**

*Male and female Sprague Dawley rats were kept in normoxic or hypoxic conditions for a period of 35 days. On day 14, FK506 pellets (0.05mg/kg/day) or placebo pellets were administered, and the rats returned to normoxia or hypoxia. On day 35 haemodynamic measurements were collected and the animals humanely killed prior to tissue harvesting.*

### **3.2.1 Hypoxia but not treatment with FK506 significantly affects the body weight gain of male rats**

As standard, body weight is monitored for the duration of the study in order to monitor animal welfare and also ensure dosing regimens are appropriate for the weight of the animals. The pellets were designed to slowly release FK506 at a dose of 0.05 mg/kg/day. The concentration of FK506 released was based on an average body weight of 220 g. Therefore, the aim was to insert the pellets subcutaneously when the rats weighed approximately 220 g. Rats were weighed prior to beginning the administration of FK506 (Figure 3.2A) and at the end of the 3 week dosing period (Figure 3.2B). The average weight gain for each of the animals was then calculated (Figure 3.2C). No significant difference in the weight gain of male rats dosed with FK506 (0.05 mg/kg/day) or placebo was observed. However, hypoxia significantly reduced the weight gain in both treatment groups (normoxic placebo group  $135 \pm 9.0$ g vs hypoxic placebo group  $103.5 \pm 4.5$ g, \* $p < 0.05$ , normoxic FK506 group  $138.5 \pm 5.3$ g vs hypoxic FK506 group  $94.3 \pm 6.6$ g, \*\* $p < 0.01$ ,  $n=6$ ).

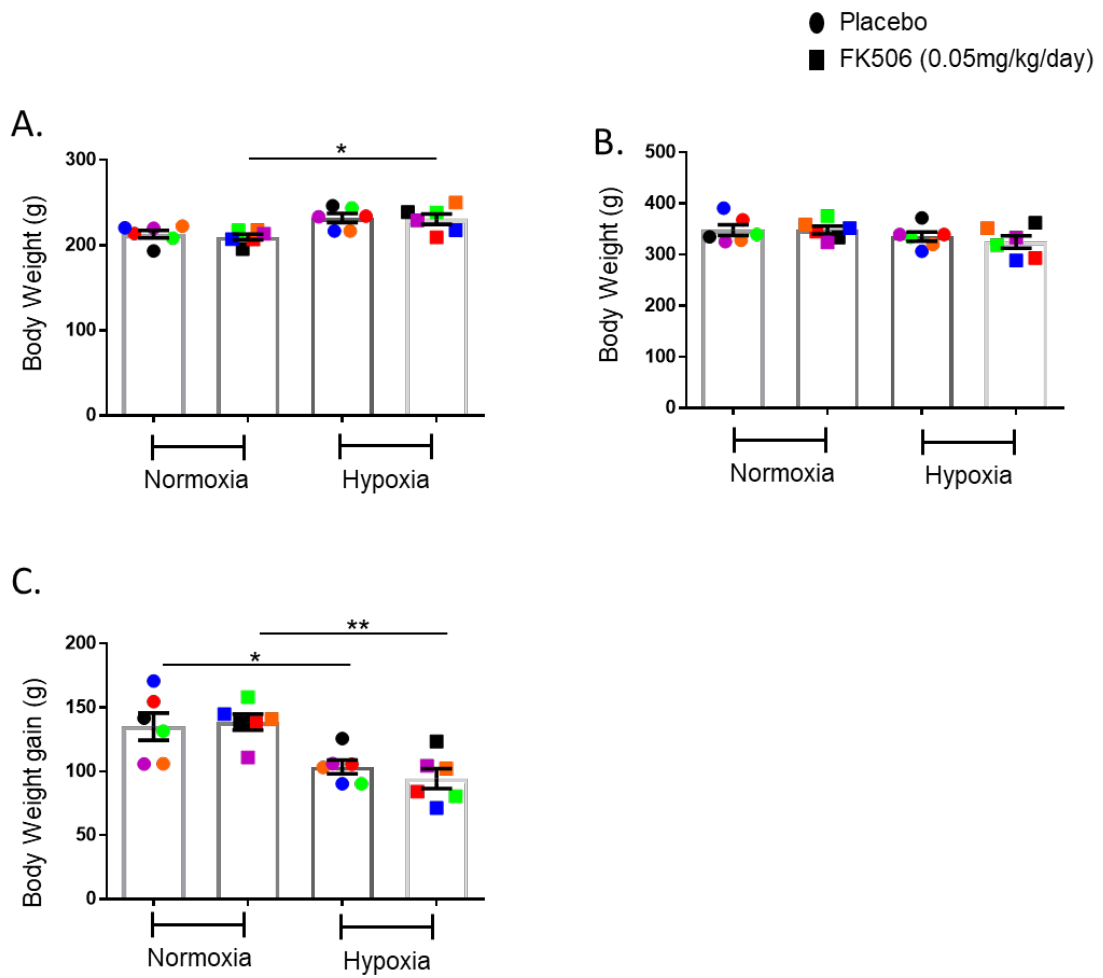


**Figure 3.2.** The body weight (g) of male rats throughout the duration of the study protocol.

A) Body weight (g) of male rats at the time of pelleting. B) Body weight (g) of male rats at the end of the study. C) Body weight gain (g) in male rats throughout the duration of the dosing period.  $n=6$ ,  $*p<0.05$ ,  $**p<0.01$ .

Statistical analysis was performed using one-way ANOVA followed by Bonferroni post-hoc test. Data is displayed with the bar representing the mean  $\pm$  S.E.M.

The measurement from each individual animal is also represented.

### **3.2.2 Hypoxia or treatment with FK506 does not significantly affect the body weight gain of female rats**

The weight of female rats was also monitored and the weights at the start (Figure 3.3A) and end of the treatment regime (Figure 3.3B) recorded. The rats within the hypoxic FK506 treatment group had a significantly lower body weight prior to starting the dosing regimen compared to the placebo treatment group ( $221.5 \pm 3.8\text{g}$  vs  $200.3 \pm 2.2\text{g}$  \* $p < 0.05$ ,  $n=6$ ). However, by the end of the dosing period there was no significant difference between the groups. The weight gain across the 3 week dosing period was then calculated. Treatment with FK506 had no significant effect on the weight gain under either normoxic or hypoxic conditions (Figure 3.3C). The weight gain of female rats housed in normoxia vs hypoxia was not significantly different.

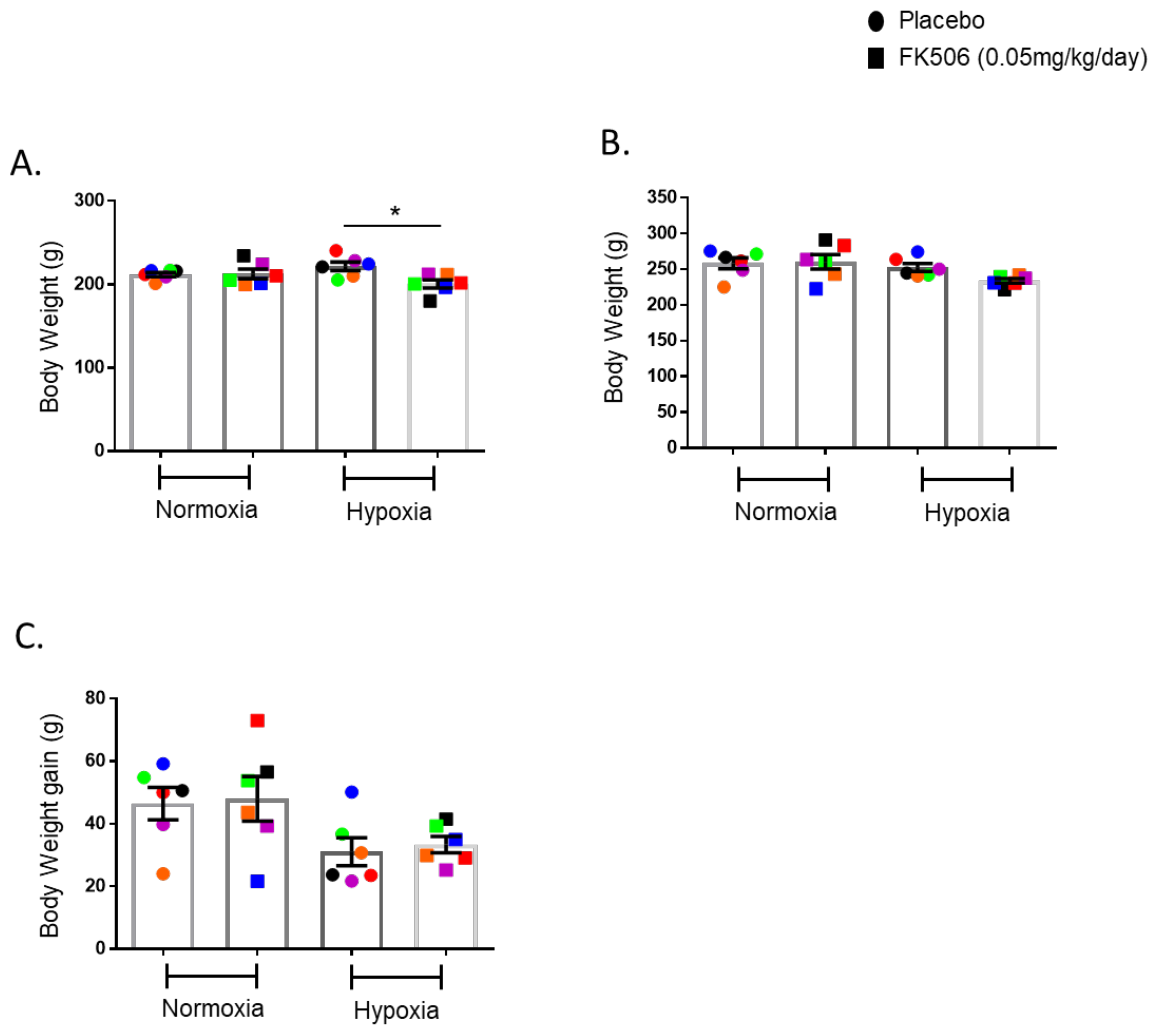


**Figure 3.3.** The weight (g) of female rats throughout the duration of the study protocol.

A) Weight (g) of female rats at the time of pelleting. B) Weight (g) of female rats at the end of the study. C) Weight gain (g) in female rats throughout the duration of the dosing period.  $n=6$ ,  $*p<0.05$ . Statistical analysis was performed using one-way ANOVA followed by Bonferroni post-hoc test. Data is displayed with the bar representing the mean  $\pm$  S.E.M. The measurement from each individual animal is also represented.

### **3.2.3 Treatment with FK506 had no significant effect on RVSP in male rats**

Haemodynamic measurements were recorded using the Millar PV loop system. RVSP (mmHg) was assessed as a parameter of experimental PH and to confirm the hypoxia regime induced a PH phenotype. The effect of treatment with FK506 on RVSP was also assessed. In the placebo treated male rat group, hypoxia significantly increased RVSP ( $27.9 \pm 1.7$  mmHg vs  $45.3 \pm 3.9$  mmHg,  $*p < 0.05$ ,  $n=6$ ) as expected indicating that a PH phenotype had been induced in these animals (Figure 3.4). However, there was no significant difference in the RVSP between the placebo and FK506 hypoxic groups, indicating treatment with FK506 (0.05mg/kg/day) was not sufficient to reverse the increase in RVSP induced by hypoxia in these animals. Heart rate (HR) was also assessed during the period of the RVSP recording (Figure 3.4C). There was no significant difference in heart rate across the 4 groups of male rats. Previous studies have shown heart rate in male Sprague Dawley rats under 3% isoflurane to be approximately 360bpm (Kato et al., 2016), therefore the HR across all groups was as expected. This indicates that hypoxia and FK506 did not influence the heart rate. This finding also confirms that any change in RVSP is not associated with increased HR or a change in cardiac output as a result of increased heart rate.

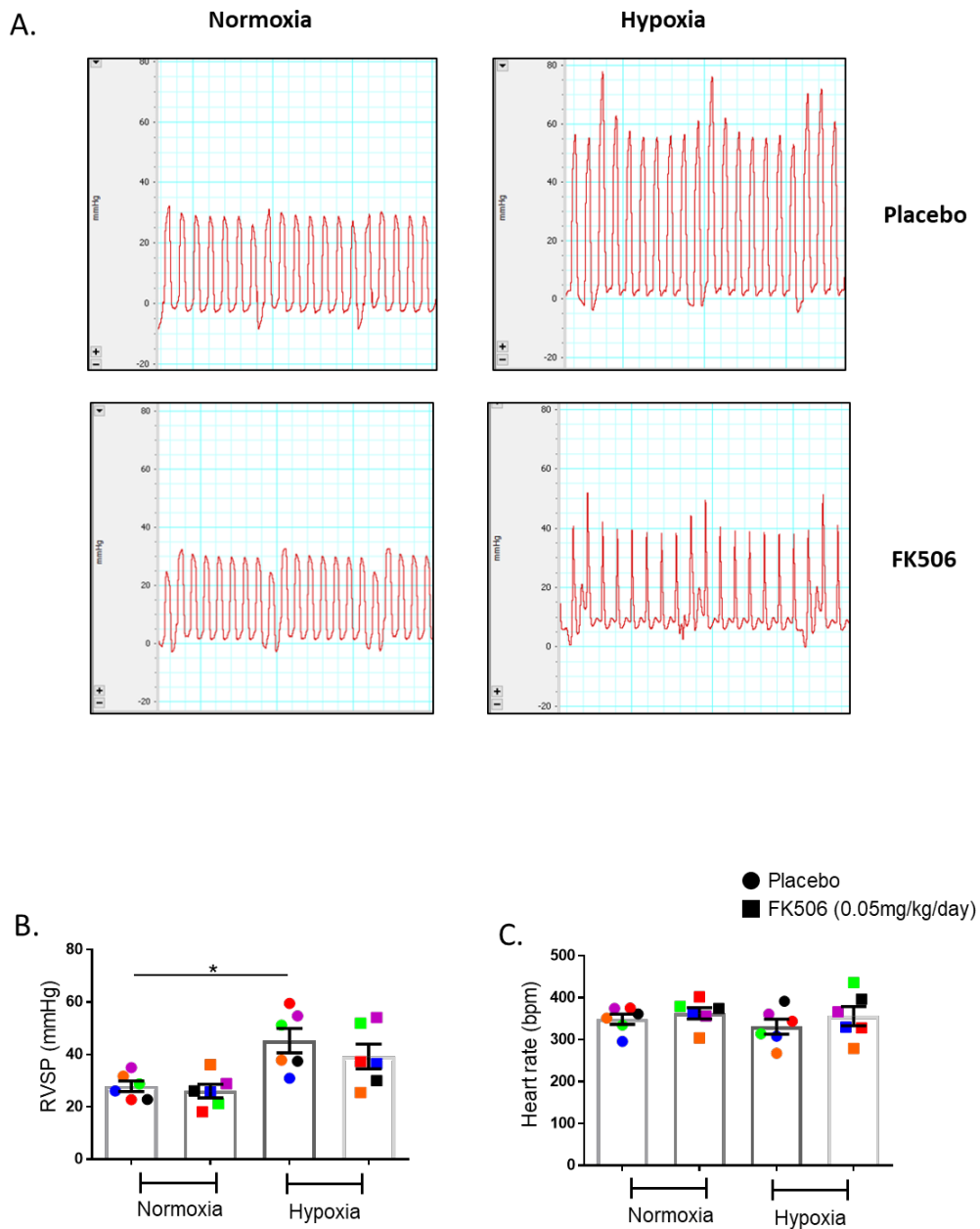


**Figure 3.4. Right Ventricular Systolic Pressure (RVSP) in male rats housed in normoxia or hypoxia and treated with placebo or FK506 (0.05mg/kg/day).**

A) Representative images showing the right ventricular systolic pressure traces collected by Millar PV loop system and AD Instruments software. B) RVSP (mmHg) in male rats housed in normoxia or hypoxia treated with placebo or FK506 (0.05mg/kg/day). C) Heart rate (beats per minute, bpm) during the RVSP recording.  $n=6$ ,  $*p<0.05$ . Statistical analysis was performed using one-way ANOVA followed by Bonferroni post-hoc test. Data is displayed with the bar representing the mean  $\pm$  S.E.M. The measurement from each individual animal is also represented.

### **3.2.4 Treatment with FK506 had no significant effect on RVSP in female rats**

RVSP (mmHg) was assessed in placebo and FK506 treated female rats exposed to normoxic or hypoxic conditions. Hypoxia significantly increased RVSP in female rats (placebo group  $28.0 \pm 0.9$  mmHg vs  $54.9 \pm 4.5$  mmHg, \*\*\*\* $p < 0.0001$ , FK506 group  $25.9 \pm 1.1$  mmHg vs  $44.3 \pm 3.1$  mmHg, \*\* $p < 0.01$ ,  $n=5-6$ ) (Figure 3.5). Again, FK506 treatment had no significant effect on RVSP in female rats suggesting that treatment with FK506 at 0.05 mg/kg/day does not reverse the increase in RVSP associated with exposure to hypoxia. There were no significant differences in HR across the 4 groups (Figure 3.5C). Again, this suggests that increased RVSP is associated with pathological changes related to exposure to hypoxia and not as a result of increased heart rate.

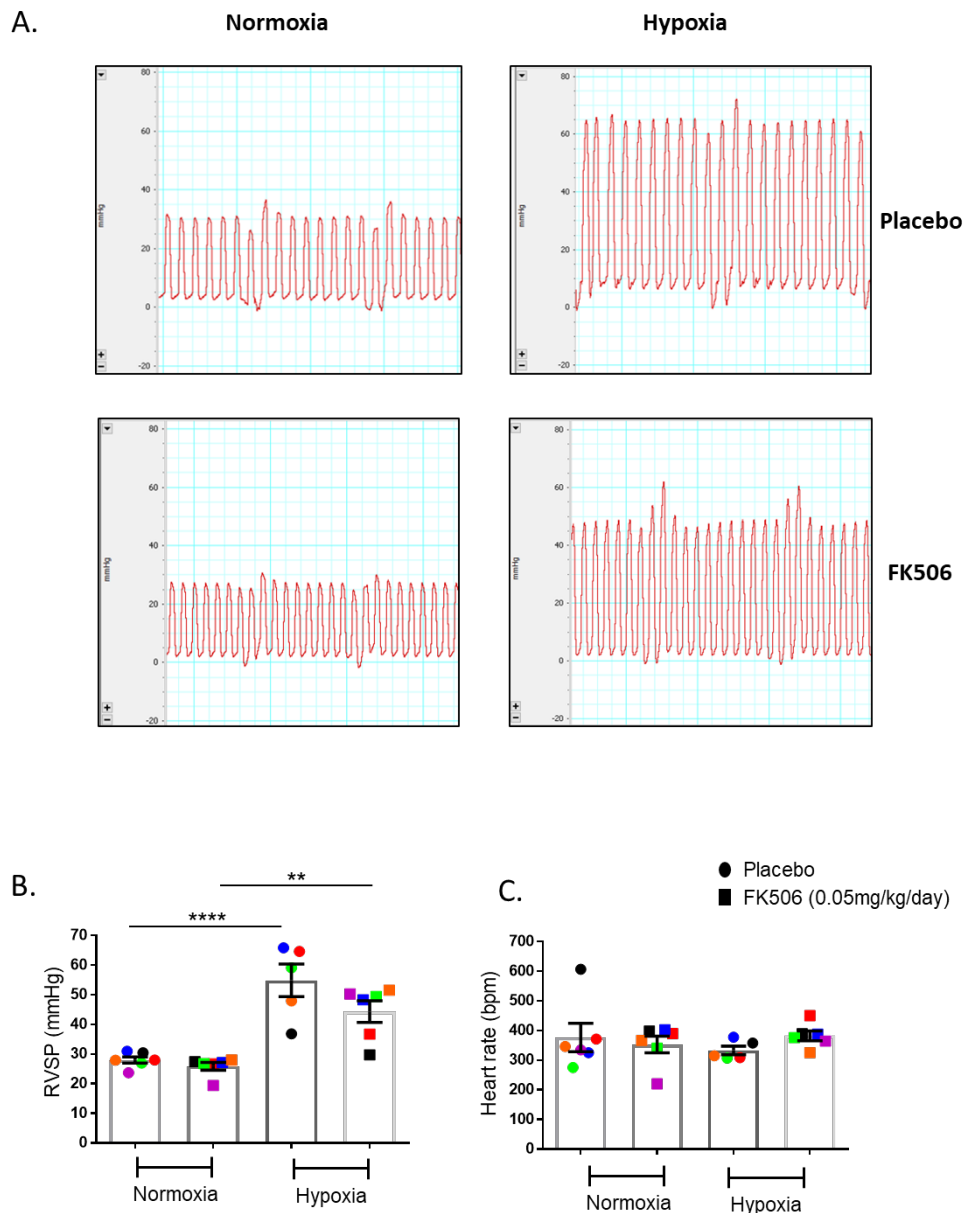


**Figure 3.5. Right Ventricular Systolic Pressure (RVSP) in female rats housed in normoxia or hypoxia and treated with placebo or FK506 (0.05mg/kg/day).**

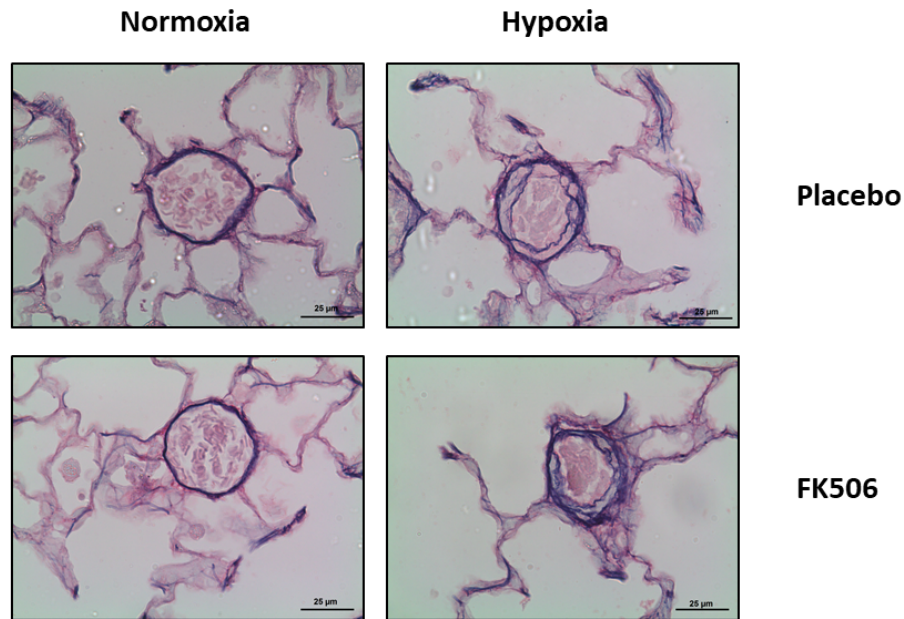
A) Representative images showing the right ventricular systolic pressure traces collected by Millar PV loop system and AD Instruments software. B) RVSP (mmHg) in female rats housed in normoxia or hypoxia treated with placebo or FK506 (0.05mg/kg/day). C) Heart rate (beats per minute, bpm) during the RVSP recording.  $n=5-6$ ,  $**p<0.01$   $****p<0.0001$ . Statistical analysis was performed using one-way ANOVA followed by Bonferroni post-hoc test. Data is displayed with the bar representing the mean  $\pm$  S.E.M. The measurement from each individual animal is also represented.

### **3.2.5 FK506 did not reverse pulmonary artery remodelling in hypoxic male rats**

Remodelled pulmonary arteries were defined as pulmonary arteries exhibiting a double elastic lamina, visualised by staining with Miller's elastin stain.

Pulmonary artery remodelling was assessed by the number of remodelled pulmonary arteries as a percentage of the total number of pulmonary arteries in a lung section. Hypoxia significantly increased the percentage of remodelled pulmonary arteries in male rats (placebo group  $3.4 \pm 0.2\%$  vs  $38.8 \pm 1.7\%$ , \*\*\*\* $p < 0.0001$ , FK506 group  $4.3 \pm 1.2\%$  vs  $37.0 \pm 2.2\%$ , \*\*\*\* $p < 0.0001$ ,  $n=4$ ). However, FK506 treatment ( $0.05\text{mg/kg/day}$ ) had no significant effect on the percentage of remodelled pulmonary arteries (Figure 3.6).

A.



B.

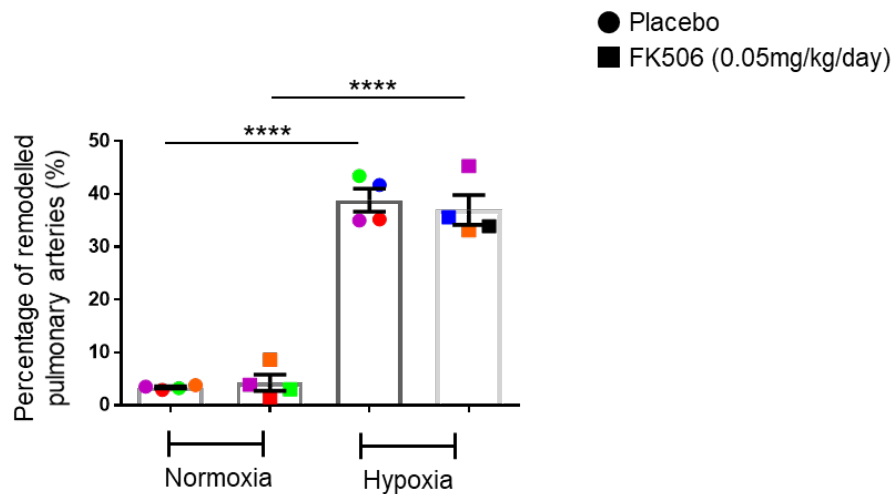


**Figure 3.6. The effect of hypoxia and FK506 treatment on pulmonary artery remodelling.**

Male rats housed under normoxia or hypoxia and treated with placebo or FK506 (0.05mg/kg/day). A) Representative images of pulmonary arteries under each condition. B) Quantification of the percentage of pulmonary arteries that appear remodelled with a double elastic lamina.  $n=4$ , \*\*\*\* $p<0.0001$ . Statistical analysis was performed using one-way ANOVA followed by Bonferroni post-hoc test. Data is displayed with the bar representing the mean  $\pm$  S.E.M. The measurement from each individual animal is also represented. Scale bar = 25 $\mu$ M, magnification = x40.

### **3.2.6 FK506 did not reverse pulmonary artery remodelling in hypoxic female rats**

Pulmonary artery remodelling was calculated in the same way for female rats. Again, hypoxia significantly increased the percentage of remodelled pulmonary arteries in female rats (placebo group  $3.4 \pm 0.9\%$  vs  $37.8 \pm 5.8\%$ ,  $***p < 0.001$ , FK506 group  $3.7 \pm 1.2\%$  vs  $34.1 \pm 1.3\%$ ,  $***p < 0.0001$ ,  $n=3-4$ ). However, FK506 treatment ( $0.05\text{mg/kg/day}$ ) had no significant effect on the percentage of remodelled pulmonary arteries (Figure 3.7).

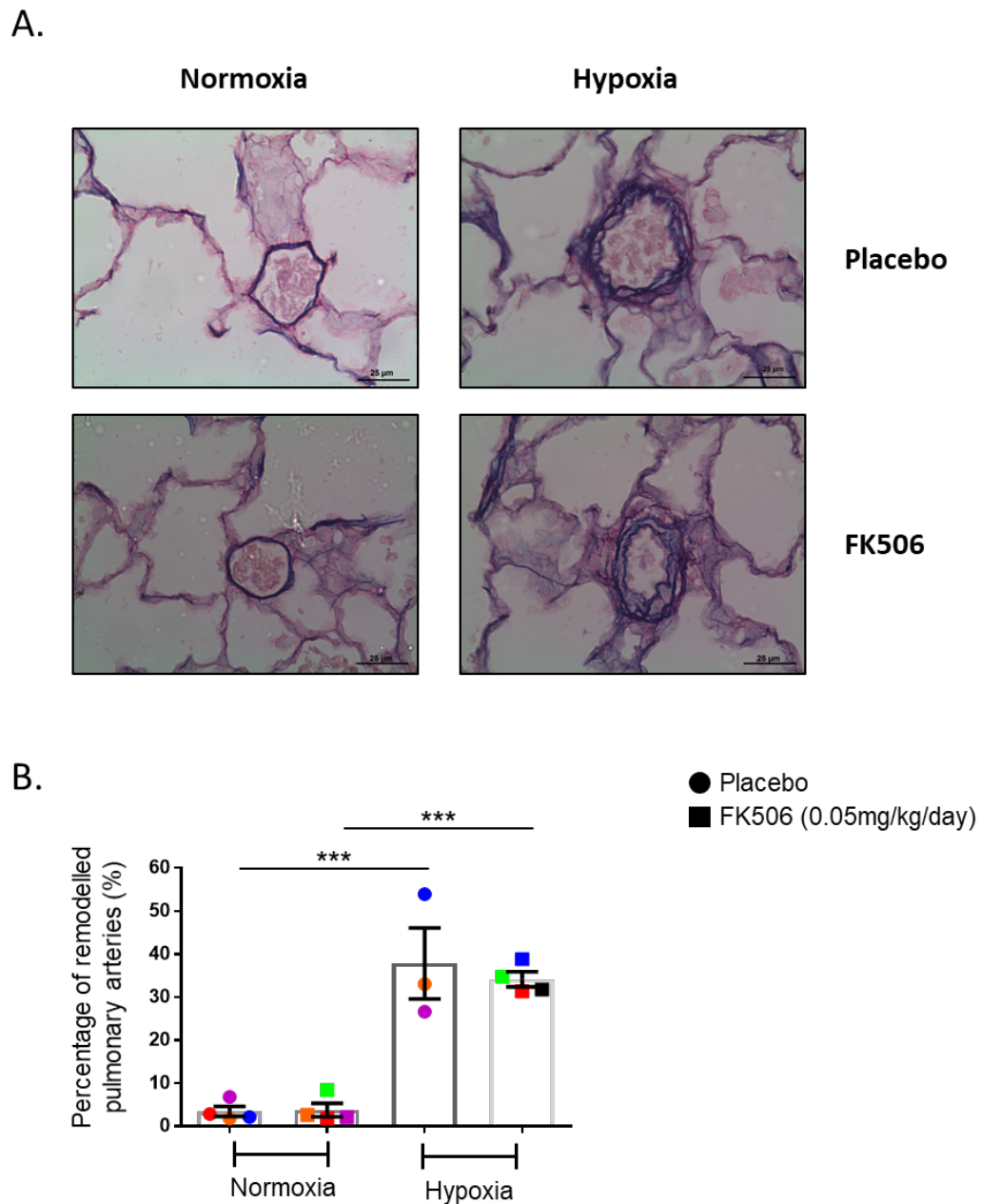


**Figure 3.7. The effect of hypoxia and FK506 treatment on pulmonary artery remodelling.**

Female rats housed under normoxia or hypoxia and treated with placebo or FK506 (0.05mg/kg/day). A) Representative images of pulmonary arteries under each condition. B) Quantification of the percentage of pulmonary arteries that appear remodelled with a double elastic lamina.  $n=3-4$ ,  $***p<0.001$ . Statistical analysis was performed using one-way ANOVA followed by Bonferroni post-hoc test. Data is displayed with the bar representing the mean  $\pm$  S.E.M. The measurement from each individual animal is also represented. Scale bar =  $25\mu\text{M}$ , magnification =  $\times 40$ .

### 3.2.7 Systemic blood pressure in male rats is not influenced by treatment with FK506

It was important to assess the effect of FK506 treatment on the systemic circulation. Assessment of systemic blood pressures would ensure that any effects of FK506 were specific for the pulmonary circulatory system and were not the result of FK506 influencing the systemic circulation. Mean systemic arterial pressure (normoxia placebo  $69.1 \pm 4.2$  mmHg, normoxia FK506  $74.3 \pm 4.7$  mmHg, hypoxia placebo  $87.2 \pm 2.9$  mmHg, hypoxia FK506  $78.8 \pm 9.8$  mmHg,  $n=4-6$ ) (Figure 3.8A), pulse pressure (normoxia placebo  $33.4 \pm 2.4$  mmHg, normoxia FK506  $32.9 \pm 1.8$  mmHg, hypoxia placebo  $26.3 \pm 1.6$  mmHg, hypoxia FK506  $30.5 \pm 3.1$  mmHg,  $n=4-6$ ) (Figure 3.8B), systolic pressure (normoxia placebo  $88.5 \pm 3.4$  mmHg, normoxia FK506  $93.0 \pm 3.5$  mmHg, hypoxia placebo  $101.3 \pm 2.2$  mmHg, hypoxia FK506  $95.2 \pm 8.0$  mmHg,  $n=4-6$ ) (Figure 3.8C) and diastolic pressure (normoxia placebo  $55.1 \pm 4.1$  mmHg, normoxia FK506  $60.1 \pm 4.6$  mmHg, hypoxia placebo  $75.1 \pm 2.9$  mmHg, hypoxia FK506  $64.7 \pm 10.2$  mmHg,  $n=4-6$ ) (Figure 3.8D) (mmHg) are all displayed. These measurements were within the expected ranges for the concentration of isoflurane used to anaesthetise the animals (Yang, 2014). There were no differences in any parameter between hypoxia or normoxia in animals on placebo. Furthermore, treatment with FK506 had no significant effect on any of these parameters under normoxic or hypoxic conditions. Therefore, any effect of FK506 on the pulmonary phenotype could be assumed to be pulmonary specific and there are no off target or non-specific effects of this treatment on the systemic circulation.

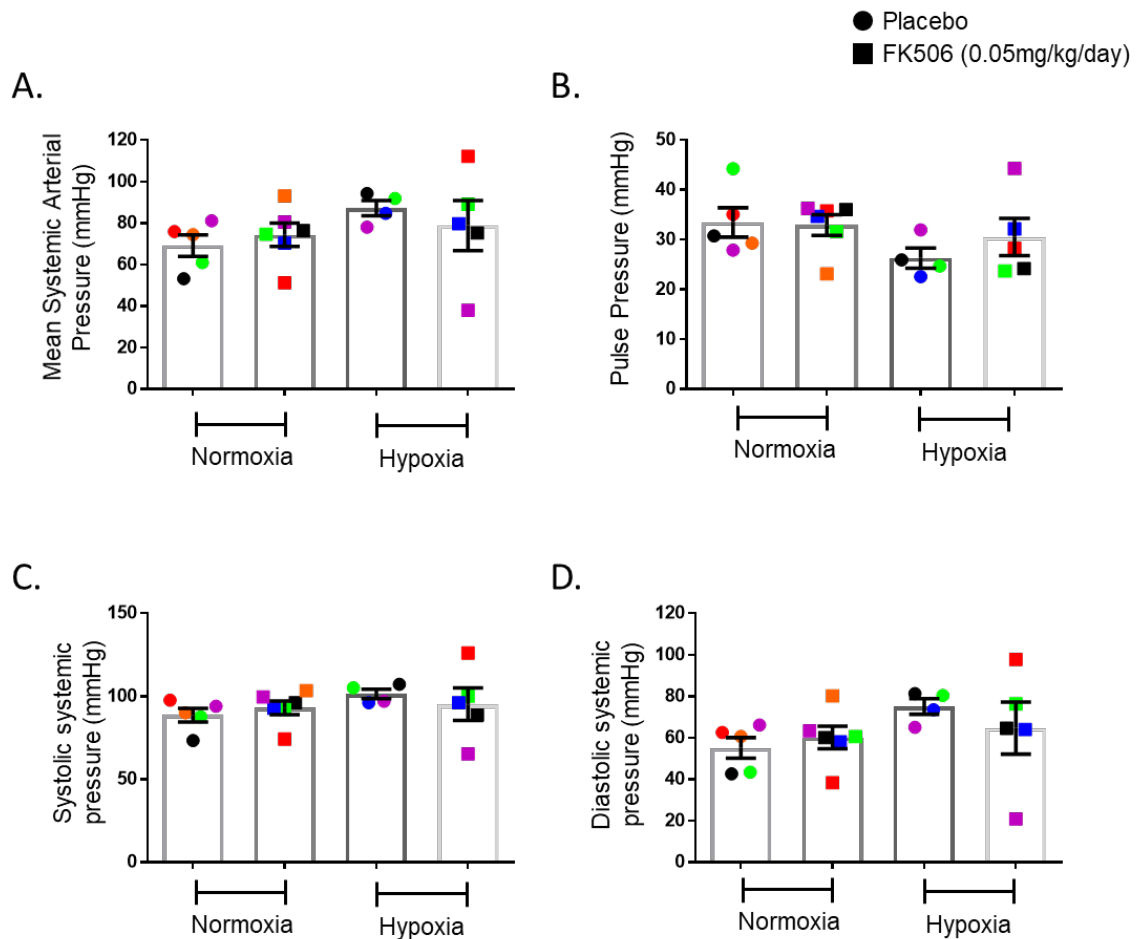


**Figure 3.8.** The effect of hypoxia and treatment with FK506 (0.05mg/kg/day) on systemic pressure in male rats.

Male rats were housed under normoxia or hypoxia and treated with placebo or FK506 (0.05mg/kg/day). A) Mean systemic arterial pressure (mmHg) B) Pulse pressure (mmHg). C) Systemic systolic pressure (mmHg). D) Systemic diastolic pressure (mmHg).  $n=4-6$ . Statistical analysis was performed using one-way ANOVA followed by Bonferroni post-hoc test. Data is displayed with the bar representing the mean  $\pm$  S.E.M. The measurement from each individual animal is also represented.

### **3.2.8 Systemic blood pressure in female rats is not affected by treatment with FK506 but hypoxia significantly influenced the systemic circulation**

The effect of FK506 on the systemic circulation was also assessed in the female animals. FK506 had no significant effect on the parameters of systemic blood pressure that were assessed, mean systemic arterial pressure (Figure 3.9A), pulse pressure (Figure 3.9B), systolic pressure (Figure 3.9C) and diastolic pressure (Figure 3.9D) (mmHg), under normoxic or hypoxic conditions. However, unlike the male rats, each of the parameters of systemic pressures was significantly affected by hypoxia in female rats. Hypoxia significantly increased mean systemic pressure (placebo group  $67.2 \pm 5.6$  mmHg vs  $96.8 \pm 2.3$  mmHg,  $**p < 0.01$ , FK506 group  $72.4 \pm 4.2$  mmHg vs  $103.8 \pm 2.4$  mmHg,  $***p < 0.0001$ ,  $n=5-6$ ), systolic pressure (placebo group  $85.1 \pm 4.2$  mmHg vs  $108.7 \pm 2.2$  mmHg,  $**p < 0.01$ , FK506 group  $86.5 \pm 3.6$  mmHg vs  $115.5 \pm 2.7$  mmHg,  $***p < 0.0001$ ,  $n=5-6$ ) and diastolic pressure (placebo group  $52.6 \pm 5.4$  mmHg vs  $84.2 \pm 2.3$  mmHg,  $***p < 0.001$ , FK506 group  $58.9 \pm 3.9$  mmHg vs  $91.2 \pm 2.3$  mmHg,  $***p < 0.0001$ ,  $n=5-6$ ). Correspondingly, pulse pressure was significantly decreased by hypoxia with the placebo treated group (placebo group  $32.5 \pm 1.7$  mmHg vs  $24.5 \pm 0.8$  mmHg,  $*p < 0.05$ ,  $n=5-6$ ).

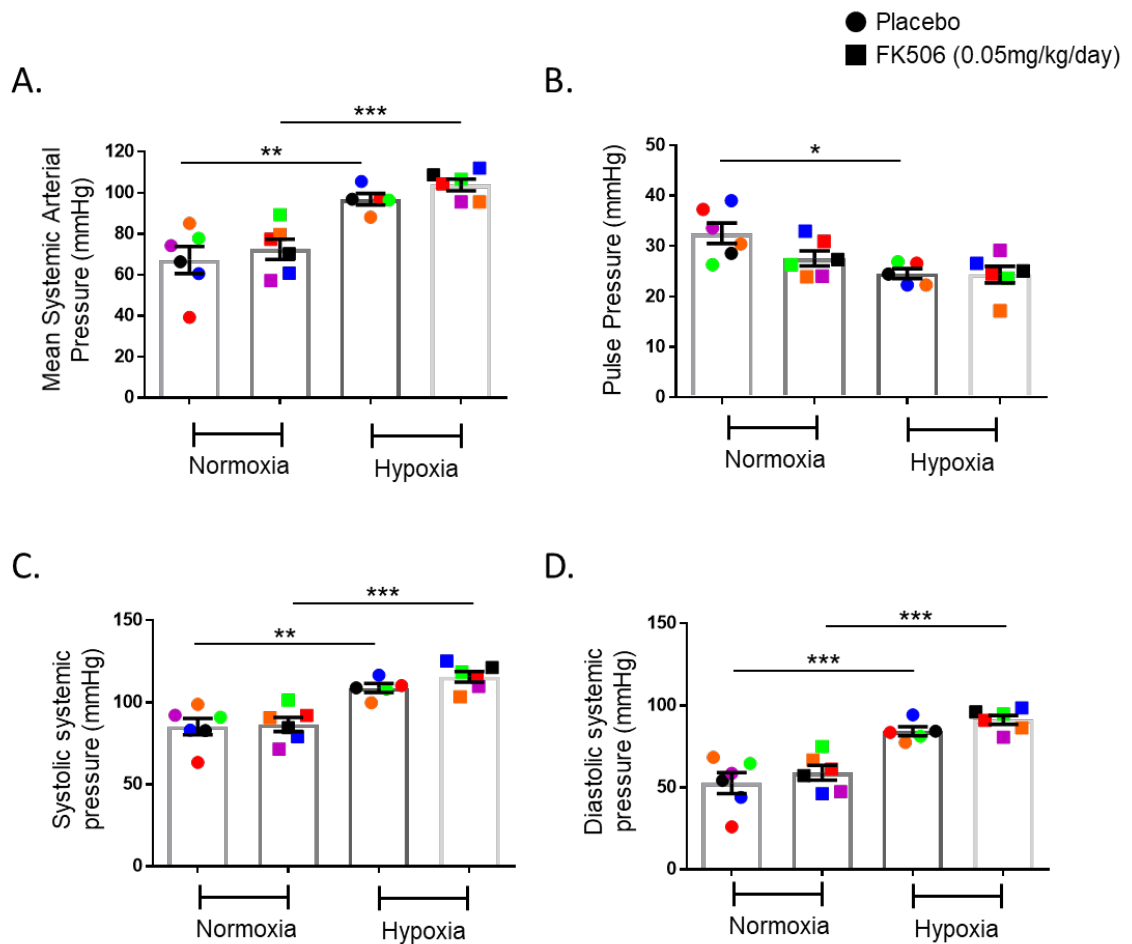


**Figure 3.9.** The effect of hypoxia and treatment with FK506 (0.05mg/kg/day) on systemic pressure in female rats.

Female rats were housed under normoxia or hypoxia and treated with placebo or FK506 (0.05mg/kg/day). A) Mean systemic arterial pressure (mmHg) B) Pulse pressure (mmHg). C) Systemic systolic (mmHg). D) Systemic diastolic pressure (mmHg).  $n=5-6$ ,  $*p<0.05$ ,  $**p<0.01$ ,  $***p<0.001$ . Statistical analysis was performed using one-way ANOVA followed by Bonferroni post-hoc test. Data is displayed with the bar representing the mean  $\pm$  S.E.M. The measurement from each individual animal is also represented.

### **3.2.9 Treatment with FK506 had no effect on LVSP in male rats housed in normoxic or hypoxic conditions**

Left ventricular systolic pressure (LVSP) was another parameter assessed in order to confirm that any effects of FK506 were RV-specific and not a result of an overall cardiac effect. There was no significant difference in LVSP across the 4 groups of male rats (normoxia placebo  $97.1 \pm 3.1$  mmHg, normoxia FK506  $102.5 \pm 3.6$  mmHg, hypoxia placebo  $106.4 \pm 3.1$  mmHg, hypoxia FK506  $98.9 \pm 4.8$  mmHg,  $n=4-6$ ) (Figure 3.10). This suggests that FK506 does not affect LVSP in male rats. Furthermore, hypoxia did not influence LVSP.

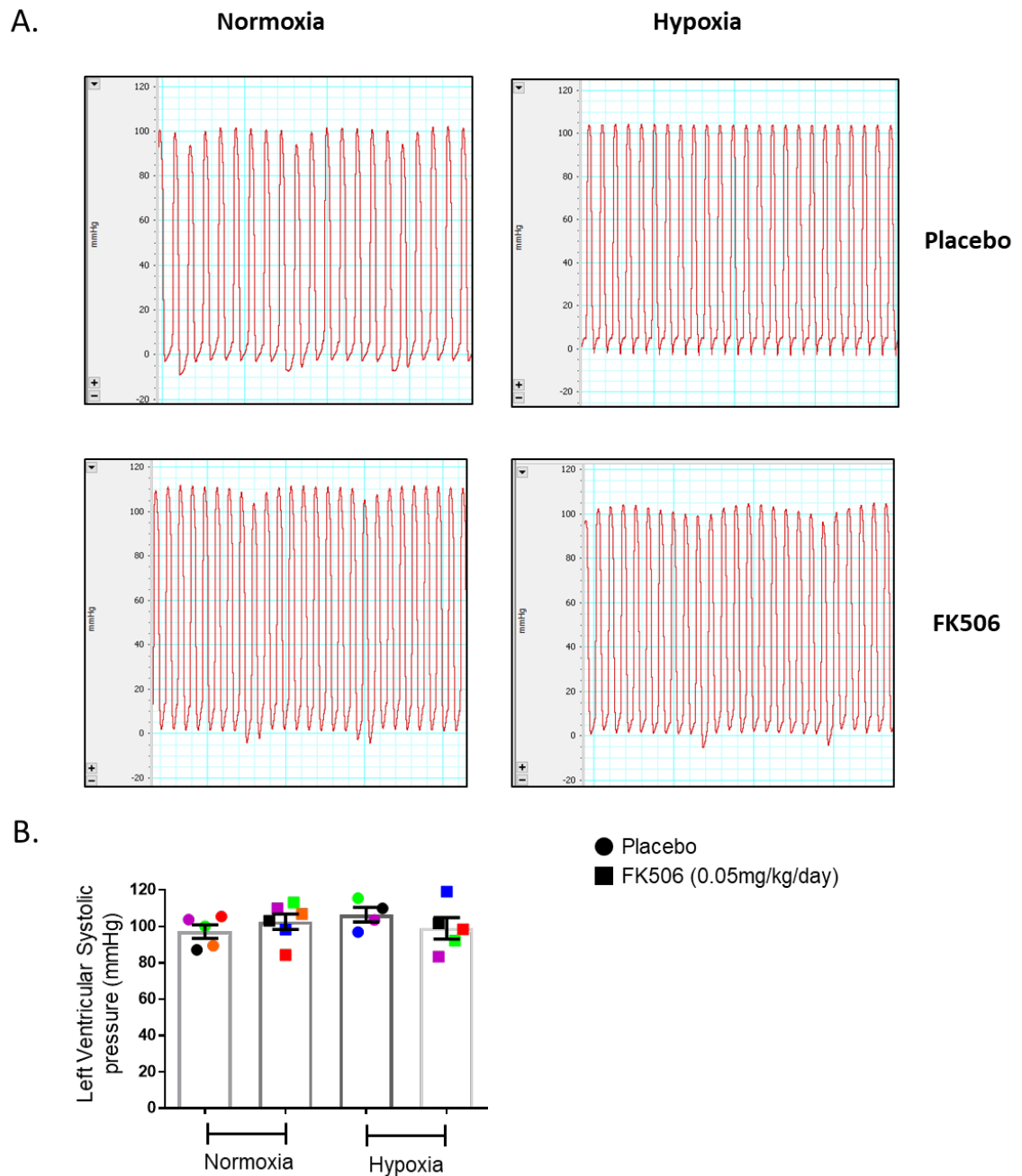


**Figure 3.10. Left Ventricular Systolic Pressure (LVSP) in male rats housed in normoxia or hypoxia and treated with placebo or FK506 (0.05mg/kg/day).**

A) Representative images showing the left ventricular systolic pressure traces collected by Millar PV loop system and AD Instruments software. B) LVSP (mmHg) in male rats housed in normoxia or hypoxia treated with placebo or FK506 (0.05mg/kg/day).  $n=4-6$ . Statistical analysis was performed using one-way ANOVA followed by Bonferroni post-hoc test. Data is displayed with the bar representing the mean  $\pm$  S.E.M. The measurement from each individual animal is also represented.

### **3.2.10 Treatment with FK506 had no effect on LVSP in female rats housed in normoxic or hypoxic conditions**

In female rats, treatment with FK506 did not influence LVSP. Consequently, it could be confirmed that any effect on RVSP would be the result of pulmonary or RV specific action of FK506 and not the result of an overall cardiac effect. There was a significant difference in LVSP between the normoxic and hypoxic female rats within the FK506 group ( $92.9 \pm 1.6$  mmHg vs  $113.6 \pm 2.1$  mmHg,  $**p < 0.01$ ,  $n=4-6$ ) (Figure 3.11). The difference in LVSP between the 2 groups appears to be a result of a reduced mean LVSP in the normoxic group in comparison to normal physiological levels of 120mmHg. This, therefore, suggests that these findings are not the result of hypoxia increasing LVSP in female rats.

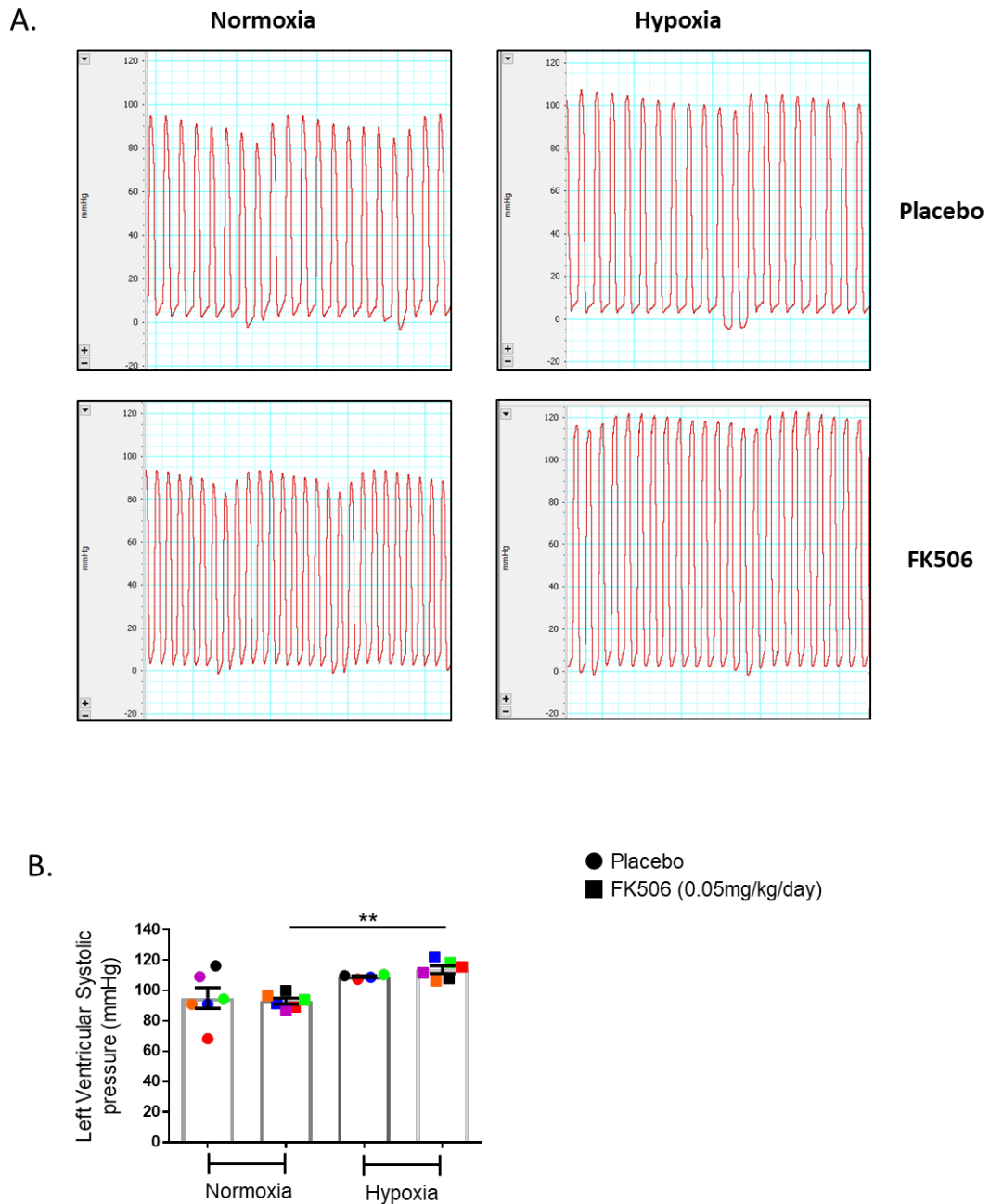


**Figure 3.11. Left Ventricular Systolic Pressure (LVSP) in female rats housed in normoxia or hypoxia and treated with placebo or FK506 (0.05mg/kg/day).**

A) Representative images showing the left ventricular systolic pressure traces collected by Millar PV loop system and AD Instruments software. B) LVSP (mmHg) in female rats housed in normoxia or hypoxia treated with placebo or FK506 (0.05mg/kg/day).  $n=4-6$ ,  $**p<0.01$ . Statistical analysis was performed using one-way ANOVA followed by Bonferroni post-hoc test. Data is displayed with the bar representing the mean  $\pm$  S.E.M. The measurement from each individual animal is also represented.

### 3.3 Discussion

The aim of this chapter was to characterise the chronic hypoxia model in male and female rats by assessing haemodynamics and the pathological changes in the pulmonary vasculature. This was necessary as this model of 5 week chronic hypoxia differed from the 4 week chronic hypoxia the lab had used previously (Docherty et al., 2019). However, it was felt to be important to replicate the successful 3 week dosing regimen of the published study by Spiekerkoetter et al. (2013) and therefore the rats had to remain in hypoxia for a total of 5 weeks. All parameters investigated indicated that the 5 week hypoxia regime had successfully induced a PH phenotype similar to that which the group had previously observed (Docherty et al., 2019). Hypoxia significantly increased RVSP along with the percentage of remodelled pulmonary arteries within the lung in both male and female rats. The effects of hypoxia on cardiac remodelling was also assessed however, cardiac-specific effects are discussed in Chapter 4. The effect of hypoxia on the systemic system as well as on the LV were also assessed. Hypoxia had no significant effect on LVSP in male rats. Within the FK506 treated group of female rats, there was a significant difference in LVSP between the normoxic and hypoxic groups. Systemic blood pressures were also significantly different between the normoxic and hypoxic groups. However, this is thought to be associated with a reduced LVSP in the normoxic group as the LVSP falls below the physiological level of 120 mmHg (Ross et al., 2010). Additionally, the systolic blood pressure and the diastolic blood pressure all fell below the expected physiological values of 120 mmHg and 80 mmHg (Ross et al., 2010). This could be associated with the concentration of anaesthetic or the duration of the procedure both of which have been shown to influence LVSP and systemic blood pressures (Redfors et al., 2014). It is well understood that increases in isoflurane concentration result in decreased systemic blood pressures (Conzen et al., 1992; Yang, 2014). The concentration and duration of isoflurane were dependent on each individual animal and therefore were very difficult to control for during the experiment. Previous experience within the lab has shown that obtaining appropriate haemodynamic pressure traces in the hypoxic animals can be technically more challenging and therefore the procedure can take longer and the animals are under anaesthetic for a longer period of time. This would ultimately affect systemic and LVSP pressures. A

closed chest approach was performed as the pressures obtained are more physiologically relevant than an open chested approach. However, there are challenges associated with this method. Positioning of the catheter in the correct position in the RV is more challenging and the conformational changes and increased pressure in the RV of hypoxic animals makes this increasingly challenging. This could be the result of many different factors including, cardiac remodelling, the animal's tolerance to anaesthetic or the investigator's skill on the day of the procedure. Systemic blood pressure could be measured by another method such as tail cuff or telemetry prior to terminal haemodynamic measurements. However, these methods come with their own caveats as they often induce stress in the animal which in turn can influence blood pressure.

The next aim of this study was to investigate the effect of FK506 (0.05 mg/kg/day) on the parameters of experimental PH in male and female rats. The aim was to insert the pellets when male and female rats weighed approximately 220 g as pellets were manufactured to release a dose of 0.05 mg/kg/day based on a body weight of 220 g. This weight was selected in order to keep in line with the previous study in which animals were started on the dosing regimen between 180-220g (Spiekerkoetter et al., 2013). Male and female rats gained weight throughout the study and there were significant differences in weight gain between normoxic and hypoxic groups. Therefore, the dose of FK506 would not have been consistently 0.05 mg/kg/day in all groups across the 3 weeks. This finding should be considered when assessing the effect of FK506 on the parameters of experimental PH. This dosing regimen was selected as it did not require daily dosing allowing the rats to be maintained in hypoxia for longer periods of time. Other studies performed by the group have utilised the slow-release pellets as a drug delivery method for 2-methoxyestradiol and this was shown to be successful in male and female rats regardless of weight gain (Docherty et al., 2019). In future, it would be important to collect blood samples from the rats and monitor the plasma concentration of FK506 to confirm the dosing method was appropriate.

Treatment with FK506 (0.05 mg/kg/day) in both male and female chronic hypoxia rats had no significant effect on parameters of experimental PH. Hypoxia significantly increased RVSP in both male and female rats, however,

FK506 did not significantly reverse this increase in RVSP. Although FK506 did not significantly reduce hypoxic RVSP, when comparing the male FK506 treated groups, there was no significant difference between normoxic and hypoxic RVSP whereas a significant difference was present between the equivalent female groups. Hypoxia significantly increased pulmonary artery remodelling in both male and female rats and FK506 did not significantly reverse this phenotype. The previous study in male rats utilising the monocrotaline and Sugen Hypoxia rat model showed that FK506 significantly reversed the PH phenotype (Spiekerkoetter et al., 2013). Additionally, the compassionate use of low dose FK506 in female PAH patients also suggested treatment had a positive effect on the clinical outcomes of the female patients (Spiekerkoetter et al., 2015). Therefore, it was expected that FK506 would significantly affect RVSP and pulmonary artery remodelling in both male and female chronic hypoxia rats in the current study and the aim was to investigate potential sex-specific effects of FK506. The dose and the dosing period were replicated from the Spiekerkoetter et al. (2013) study however, the delivery of FK506 and the rat model differed. The previous study had used an osmotic mini-pump for delivery of FK506 in each of the animal models (Sugen hypoxia and the monocrotaline rat model) (Spiekerkoetter et al., 2013) which differed from the use of slow-releasing pellets for FK506 delivery in the chronic hypoxia rat model used in this study. The design of osmotic mini-pumps would mean that a constant dose of FK506 would have delivered across the 3 weeks dosing period also.

Each group within the study had  $n=6$  based on availability of the hypobaric chambers and the limited space within the chambers. These  $n$  numbers were similar to related published studies, e.g. the Spiekerkoetter et al. (2013) study had  $n=6-8$  in the monocrotaline rat model groups and  $n=8$  in the Sugen Hypoxia rat model groups (Spiekerkoetter et al., 2013). However, power calculations performed using the data generated in the study in this thesis suggested  $n=10$  would allow an experimental power of 78% to detect 15 mmHg change in pressure assuming 5% significance level (InVivoStat software). Therefore, in order to fully determine the effect of FK506 on parameters of PAH it would be necessary to increase the  $n$  numbers of this study in the future.

The final aim of this part of the study was to assess the effects of FK506 treatment (0.05mg/kg/day) on systemic and left ventricular pressure in order to identify any potential off target, systemic effects. FK506 (0.05mg/kg/day) had no significant effect on LVSP or systemic blood pressures in male or female rats. We investigated these parameters in order to confirm that any effects of FK506 on RVSP were specific to the pulmonary circulation and not the result of an overall systemic effect.

In summary, investigation of the 5 week chronic hypoxia rat model showed that this model was able to induce an experimental PH phenotype, specifically increased RVSP and pulmonary artery remodelling. This confirmed that this model could be used as a rodent model for PH phenotype in future studies and also allowed the investigation of the effect of FK506 on PH phenotype. FK506 at 0.05 mg/kg/day did not significantly reverse the increased RVSP or pulmonary artery remodelling in this model. In addition, FK506 did not affect any of the measurements associated with systemic blood pressure or LVSP. In future, it would be important to continue with this investigation and confirm if the lack of response to FK506 was associated with the rodent model selected and the dosing regimen. As previous studies have shown FK506 to be successful in improving the PH phenotype (Spiekerkoetter et al., 2013; Spiekerkoetter et al., 2015) this data perhaps highlight that the correct protocol is critical in the success of this therapy. These data suggest that further investigation of FK506 as a potential therapeutic for the treatment of PAH must be conducted. Furthermore, the potential sex-specific effects of FK506 still need to be fully elucidated.

## **Chapter 4**

### **4 Sex differences in right ventricle in experimental pulmonary hypertension and the effect of FK506 treatment.**

## 4.1 Introduction

In pulmonary hypertension, remodelling of the RV is initiated by increased afterload. Increased afterload results from the pathological changes that take place in the pulmonary vasculature creating a high pressure, high resistance system. Initially, the RV remodels in an attempt to maintain cardiac output and right ventricular ejection fraction (RVEF) by increasing the RV wall mass to compensating for increased wall stress, a process known as hypertrophy (Lahm et al., 2018; Fang et al., 2012). In the early stages of disease these adaptations are sufficient to maintain cardiac function. In later stage disease, increases in RV wall mass are no longer able to maintain RV function. At this point, maladaptive remodelling occurs, and the RV dilates and becomes fibrotic leading to impaired right heart function (Vonk-Noordegraaf et al., 2013). Cardiomyocyte function is also thought to be impaired by this process as a result of extracellular matrix alterations, electrical remodelling and the production of reactive oxygen species (Bogaard et al., 2009; Piao et al., 2010). The response of the RV is one of the key factors which determines the clinical outcome of the patient (Vonk-Noordegraaf and Galie, 2011). RV failure is the main cause of mortality in PAH patients (Chin et al., 2005).

Although the role of the RV in determining prognosis for PAH is well understood, there is still a great need to develop our understanding of the pathological processes which occur in the RV. It is not appropriate to extrapolate findings from the investigation of pathological remodelling in the LV to the RV. It has been shown that the two ventricles exhibit key structural differences and differential responses to oxidative stress and activation of apoptotic processes which result in a more rapid progression of RV failure than LV failure (Reddy and Bernstein, 2015). A greater understanding of disease development can be gained from investigating how these maladaptive processes in the RV are influenced by factors known to be important in PAH such as sex and BMPR2 signalling. Recent clinical studies have identified a role for sex and BMPR2 in RV function in PAH patients (Jacobs et al., 2014; Kawut et al., 2009; Evans et al., 2016a; van der Bruggen et al., 2016). The poorer survival rates of male PAH patients are thought to be associated with a more rapid decrease in RV function (Jacobs et al., 2014; Kawut et al., 2009). Patients harbouring a BMPR2 mutation have been described as having poorer haemodynamic profiles at diagnosis (Evans et al.,

2016a) and in particular a greater degree of RV impairment even when experiencing similar afterload (van der Bruggen et al., 2016). However, there are still very few studies that have been conducted in this area of research.

Moreover, there are currently no therapies available to treat PAH patients that specifically target the RV. Current therapies are all targeted to the pulmonary vasculature and aim to counteract the vasoconstrictive environment. Although these therapies contribute to decreased RV afterload, they do not act directly on the RV and their effect on the clinical outcomes associated with the RV are likely to be limited (Handoko et al., 2010). Therefore, there is a need to understand the effect of potential PAH therapies on the RV.

The aims of this chapter were:

To characterise the 5 week chronic hypoxia rat model with regard to the RV.

To investigate the effect of FK506 treatment on right ventricular parameters of experimental PH.

To investigate the effect of hypoxia and FK506 treatment on gene expression profiles in the male and female rat RV.

To perform a direct comparison between the male and female gene expression profiles in the RV under normoxic and hypoxic conditions.

To develop an *in vitro* model to study the effects of sex on cardiac fibroblasts and cardiomyocytes from RV of male and female rats and an *in vivo* model to investigate the role of sex in right heart dysfunction independent of pathological changes in the pulmonary vasculature.

## 4.2 Results

As described previously, Sprague Dawley rats were housed in a hypobaric hypoxic chamber for 35 days. Subcutaneous pellets releasing FK506 at a dose of 0.05 mg/kg/day or placebo were inserted at the back of the neck subcutaneously on day 14 of the study. Following recovery from this procedure, the rats were then returned to the hypobaric hypoxic chamber for the remainder of the study. Controls which were both age and sex matched were housed in normoxia and were treated with the same dosing protocol. The study ended on day 35 with haemodynamic assessment using the Millar PV loop system. Following this, the heart, lung and other tissue types were collected for protein, RNA and histological analysis (Figure 4.1).

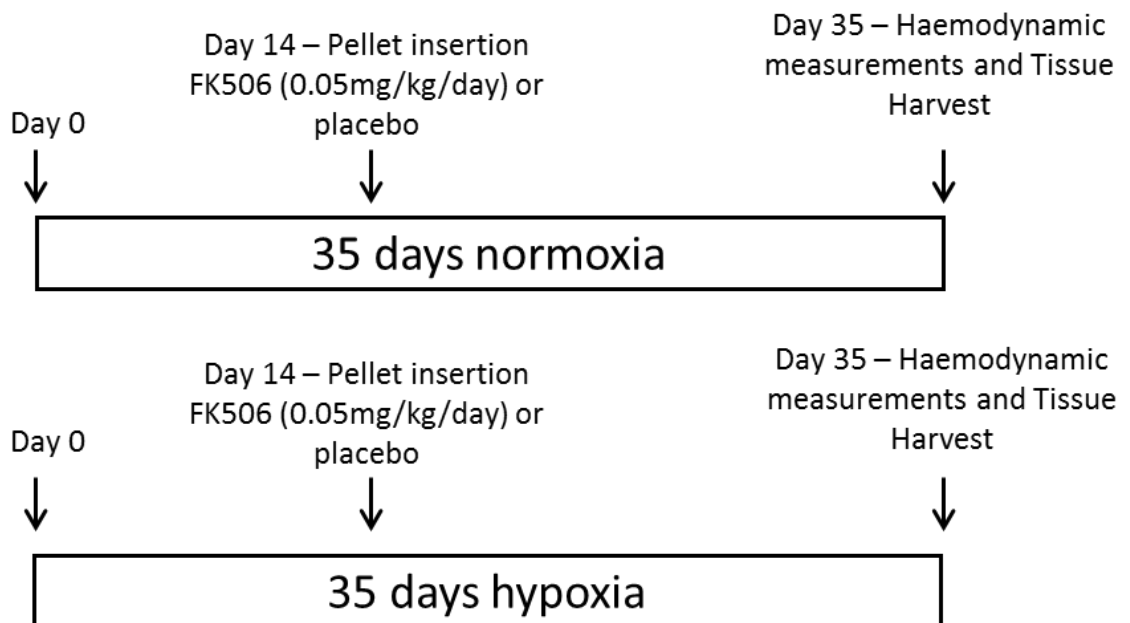


*Figure 4.1 - Schematic diagram showing FK506 study protocol and dosing regimen.*

*Male and female Sprague Dawley rats were kept in normoxic or hypoxic conditions for a period of 35 days. On day 14, FK506 pellets (0.05 mg/kg/day) or placebo pellets were administered, and the rats returned to normoxia or hypoxia. On day 35 haemodynamic measurements were collected and the animals humanely killed prior to tissue harvesting.*

#### 4.2.1 The effect of hypoxia and FK506 treatment on right ventricular hypertrophy in male rats

Following haemodynamic assessment, the heart was removed and the right ventricle (RV) was finely dissected from the left ventricle + septum (LV+S). The RV and LV+S were weighed separately and the mass recorded. Hypoxia significantly increased RV mass (mg) in both the placebo and FK506 groups (placebo group  $212.9 \pm 8.7$  mg vs  $478.3 \pm 24.3$  mg, \*\*\*\* $p < 0.0001$ , FK506 group  $209.3 \pm 4.6$  mg vs  $395.1 \pm 17.3$  mg, \*\*\*\* $p < 0.0001$ ,  $n=6$ ) and RV mass corrected for body weight (RV mass/body weight (mg/g)) in male rats (placebo group  $0.61 \pm 0.01$  vs  $1.43 \pm 0.07$ , \*\*\*\* $p < 0.0001$ , FK506 group  $209.3 \pm 4.6$  vs  $395.1 \pm 17.3$ , \*\*\*\* $p < 0.0001$ ,  $n=6$ ) (Figure 4.2). The effect of FK506 treatment (0.05mg/kg/day) on RV mass and RV mass/body weight was also investigated. FK506 significantly reduced RV mass ( $478.3 \pm 24.3$  mg vs  $395.1 \pm 17.3$  mg, \* $p < 0.05$ ,  $n=6$ ) and RV mass/body weight ( $1.43 \pm 0.07$  vs  $1.22 \pm 0.03$ , \* $p < 0.05$ ,  $n=6$ ) in hypoxic male rats. The standard measurement for right ventricular hypertrophy in experimental models within the pulmonary hypertension field is the Fulton's index (RV mass/LV+S mass) (Fulton et al., 1952). When Fulton's index was calculated hypoxia significantly increased RV/LV+S in male rats (placebo group  $0.28 \pm 0.01$  vs  $0.55 \pm 0.02$ , \*\*\*\* $p < 0.0001$ , FK506 group  $0.27 \pm 0.01$  vs  $0.50 \pm 0.01$ , \*\*\*\* $p < 0.0001$ ,  $n=6$ ). However, FK506 treatment had no significant effect on RV/LV+S in the hypoxic group. It was thought that this could be associated with a change in LV+S mass across the different experimental groups. Comparison of LV+S mass (mg)/body weight (g) showed LV+S mass/body weight is significantly increased in hypoxic male rats treated with placebo ( $2.2 \pm 0.1$  vs  $2.6 \pm 0.1$ , \* $p < 0.05$ ,  $n=6$ ) but not in those treated with FK506.

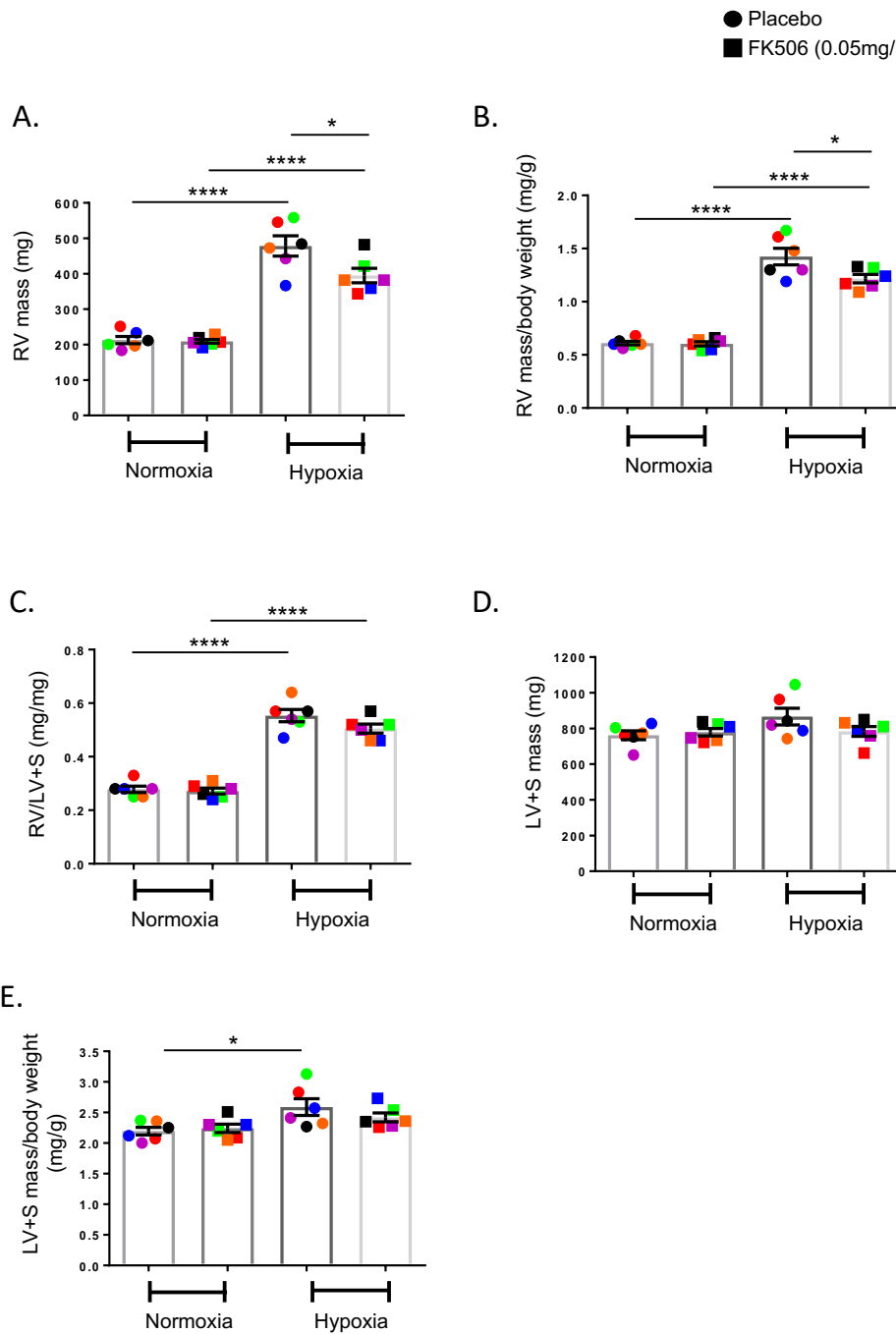


**Figure 4.2.** The effect of hypoxia and treatment with FK506 on right and left ventricular mass in male rats.

Male rats were housed in normoxia or hypoxia and treated with placebo or FK506 (0.05 mg/kg/day). A) RV mass (mg). B) RV mass/body weight (mg/g). C) RV/LV+S. D) LV+S mass (mg) E) LV+S mass/body weight (mg/g).  $n=6$ ,  $*p<0.05$ ,  $****p<0.0001$ . Statistical analysis was performed using one-way ANOVA followed by Bonferroni post-hoc test. Data is displayed with the bar representing the mean  $\pm$  S.E.M. The measurement from each individual animal is also represented.

#### 4.2.2 The effect of hypoxia and FK506 treatment on right ventricular hypertrophy in female rats

The same investigation was carried out on the RV and LV+S tissue collected from female rats. As was identified in the male rats, hypoxia significantly increased RV mass (mg) in both placebo and FK506 groups (placebo group  $176.4 \pm 7.3$  mg vs  $331.6 \pm 25.8$  mg, \*\*\*\* $p < 0.0001$ , FK506 group  $160.3 \pm 5.7$  mg vs  $285.2 \pm 13.9$  mg, \*\*\* $p < 0.001$ ,  $n=6$ ) and RV mass corrected for body weight (RV mass/body weight (mg/g)) in female rats (placebo group  $0.68 \pm 0.02$  vs  $1.31 \pm 0.09$ , \*\*\*\* $p < 0.0001$ , FK506 group  $0.62 \pm 0.03$  vs  $1.22 \pm 0.06$ , \*\*\*\* $p < 0.0001$ ,  $n=6$ ) (Figure 4.3). FK506 treatment had no significant effect on RV mass or RV mass/body weight in female rats. The Fulton's index (RV mass/LV+S mass) showed hypoxia significantly increased RV/LV+S (placebo group  $0.30 \pm 0.01$  vs  $0.52 \pm 0.02$ , \*\*\*\* $p < 0.0001$ , FK506 group  $0.28 \pm 0.01$  vs  $0.51 \pm 0.02$ , \*\*\*\* $p < 0.0001$ ,  $n=6$ ). FK506 treatment had no significant effect on RV/LV+S. There were no significant differences in LV+S mass or LV+S mass/body weight (mg/g) across the 4 experimental groups of female rats.

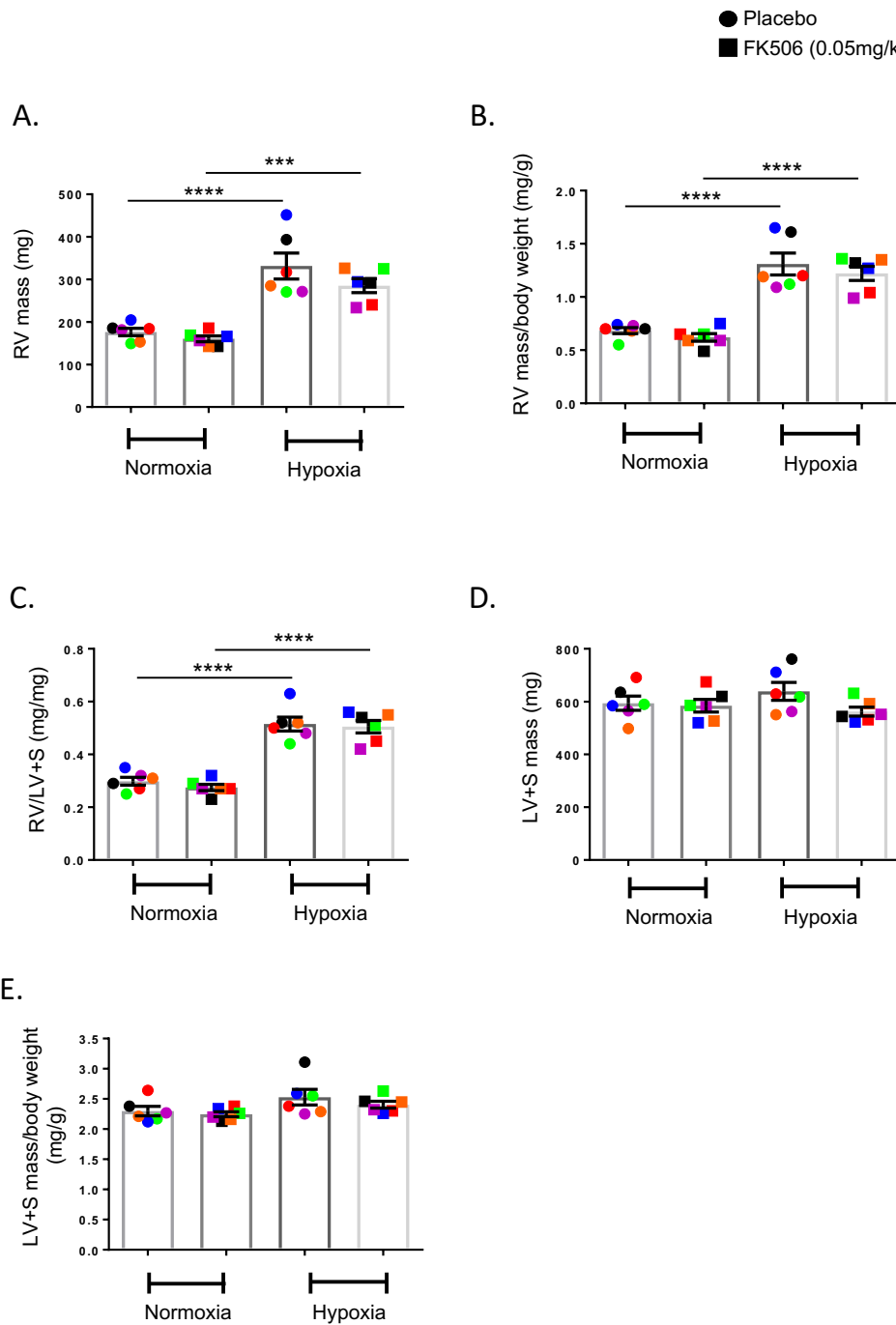


**Figure 4.3. The effect of hypoxia and treatment with FK506 on right and left ventricular mass in female rats.**

Female rats were housed in normoxia or hypoxia and treated with placebo or FK506 (0.05 mg/kg/day). A) RV mass (mg). B) RV mass/body weight (mg/g). C) RV/LV+S. D) LV+S mass (mg) E) LV+S mass/body weight (mg/g).  $n=6$ , \*\*\* $p<0.001$ , \*\*\*\* $p<0.0001$ . Statistical analysis was performed using one-way ANOVA followed by Bonferroni post-hoc test. Data is displayed with the bar representing the mean  $\pm$  S.E.M. The measurement from each individual animal is also represented.

### **4.2.3 Sex differences in right ventricular remodelling in experimental pulmonary hypertension**

The finding that treatment with FK506 (0.05 mg/kg/day) reduced RV mass and RV mass/body weight in male rats but not female rats highlighted a potential sex-specific effect of FK506 in the RV. As a result, it was important to investigate potential sex-dependent signalling within the RV which could influence RV remodelling in response to hypoxia and FK506 treatment. It was determined that initial investigations should involve a gene expression study as changes in gene expression may highlight signalling pathways that play a key role in the response of the RV. Candidate signalling pathways were selected based on genes and pathways known to be important in PAH and cardiac remodelling and the expression of genes within these pathways were investigated. The genes selected included those in the BMPR2 and transforming growth factor- $\beta$  (TGFB) pathway as well as those involved in cardiac hypertrophy and fibrosis. Initially, the effect of hypoxia on gene expression was investigated in male and female RV to understand the response to hypoxia at a mRNA level. Secondly, the effect of FK506 treatment on gene expression in the male and female rat RV was studied to identify a potential pathway involved in the action of FK506 which could lead to the reduction of RV mass in male rats. Finally, there was a direct comparison between the data collected from male and female rat RV under normoxic or hypoxic conditions. This comparison allowed identification of sex specific differences in gene expression. The data is displayed as part of the separate male and female studies and then again as part of the male vs female direct comparison.

### **4.2.4 Identification of an appropriate housekeeping gene for RV gene expression analysis**

After the mass of the RV and LV tissue had been recorded, the tissue was snap frozen in liquid nitrogen to allow it to be used for gene expression analysis. Firstly, the most consistent housekeeping gene across the different experimental groups had to be determined. A stable housekeeping gene is required in order to normalise the gene of interest with regard to the concentration of cDNA added to the experimental set up and the efficiency of the PCR reaction. It is possible that hypoxia, sex or treatment with FK506 could influence the expression of a

housekeeping gene and therefore this had to be determined prior to beginning the experiment. Three housekeeping genes -  $\beta$ 2-microglobulin (B2m), Peptidyl-prolyl cis-trans isomerase B (Ppib) and  $\beta$ -actin - were investigated by measuring the mRNA expression from RV tissue across all the experimental groups using TaqMan quantitative real-time PCR (qRT-PCR) method. The cycle threshold (CT) values and the standard deviation across the CT values was assessed across all of the study groups (Figure 4.4). B-actin showed the most variation across the groups with standard deviation of 0.73. B2M and Ppib showed similar standard deviation across the groups at 0.68 and 0.67 respectively. B2M showed lower CT values which was deemed more appropriate for a housekeeping gene. Therefore, B2M was selected as the housekeeping gene for all further gene expression analysis work.

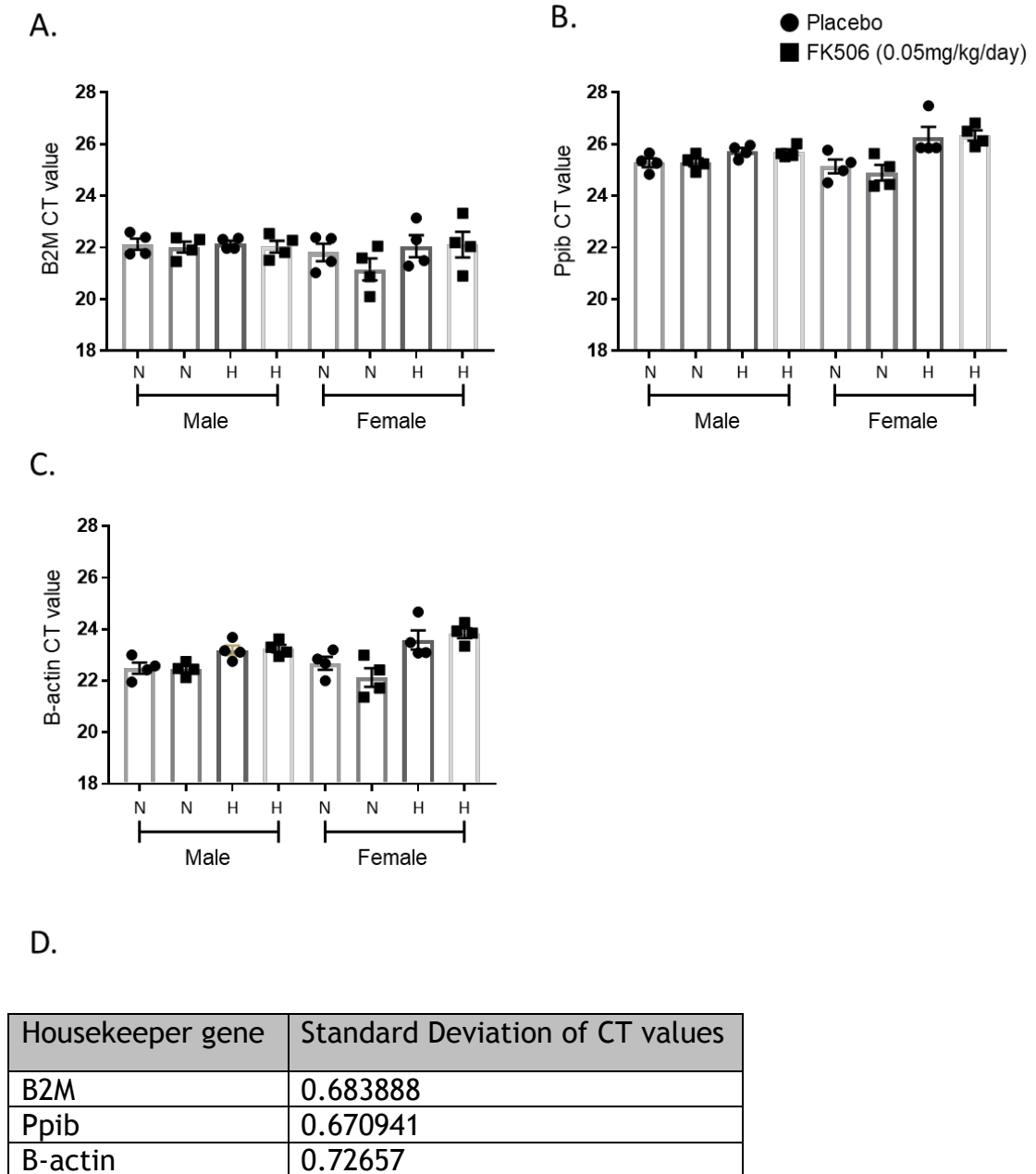


**Figure 4.4 . Identification of the most appropriate housekeeping gene for qRT-PCR analysis of RV tissue.**

TaqMan qRT-PCR was performed on RV tissue collected from each of the study groups to measure the mRNA expression of 3 potential housekeeping genes B2M, Ppib and B-actin. A) B2M CT values B) Ppib CT values. C) B-actin CT values D) Standard deviation of the CT values across all the samples for each of the housekeeper genes. n=4 per group repeated in triplicate. Data is displayed with the bar representing the mean  $\pm$  S.E.M. The measurement from each individual animal is also represented. No statistical analysis was performed. N = normoxic group, H = hypoxic group.

#### 4.2.5 The effect of hypoxia on the expression of genes involved in *Bmpr2* and *Tgf $\beta$* pathway in RV tissue from male rats

The first pathways to be investigated were the BMPR2 and TGF $\beta$  pathways. The expression of *Bmpr2*, *Smad 1*, *Id1*, *Id3*, *Tgfb1* and Tgf $\beta$ R1 genes was investigated by qRT-PCR. Firstly, the aim was to assess the effect of hypoxia on the expression of these genes (Figure 4.5). RV tissue from male rats treated with placebo was selected for this analysis. qRT-PCR showed that hypoxia significantly decreased the expression of *Bmpr2* ( $0.042 \pm 0.003$  vs  $0.025 \pm 0.003$ , \*\* $p < 0.01$ ,  $n=4$ ) and *Id3* ( $0.032 \pm 0.004$  vs  $0.017 \pm 0.002$ , \*\* $p < 0.001$ ,  $n=4$ ). Additionally, hypoxia significantly increased expression of *Tgfb1* ( $0.035 \pm 0.002$  vs  $0.049 \pm 0.005$ , \* $p < 0.05$ ,  $n=4$ ). However, hypoxia had no significant effect on the expression of *Smad1*, *Id1* or transforming growth factor  $\beta$  Receptor 1 (*TgfbR1*).

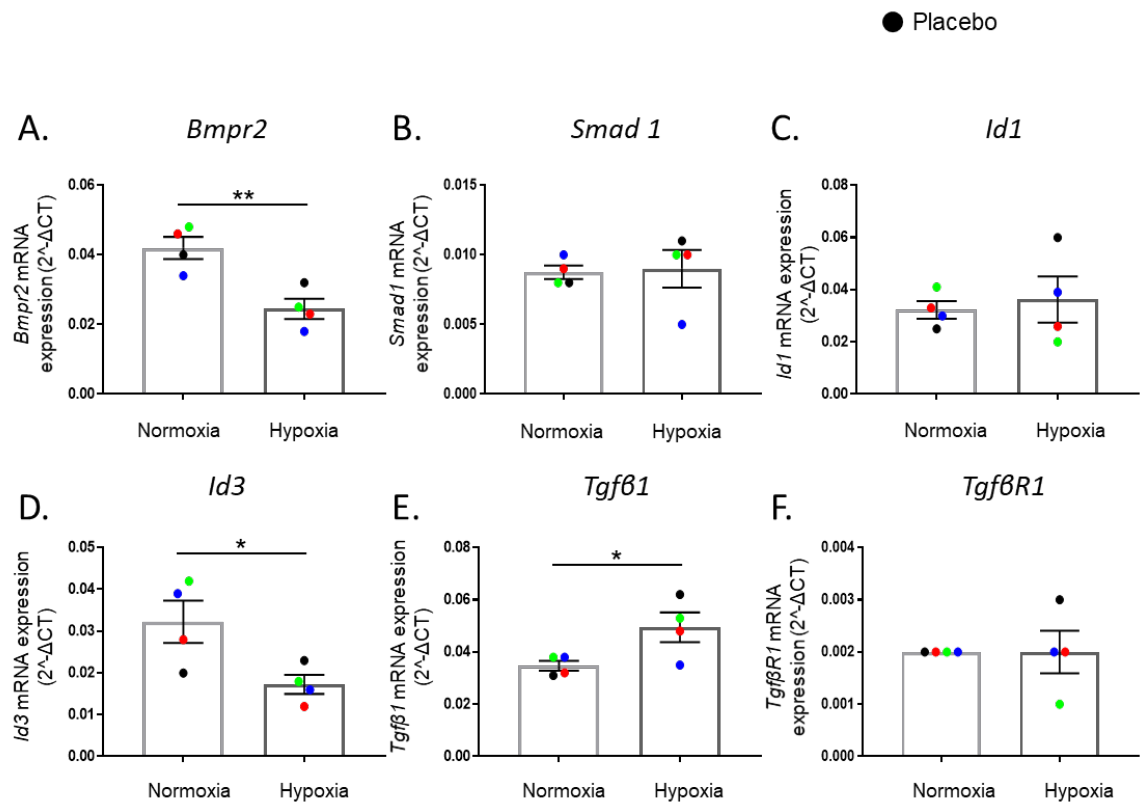


**Figure 4.5.** The effect of hypoxia on the gene expression of *Tgfβ* pathway and *Bmpr2* pathway in the male RV.

TaqMan qRT-PCR was performed on RV tissue harvested from male rats maintained in normoxia or hypoxia and treated with placebo. A) *Bmpr2* gene expression. B) *Smad1* gene expression C) *Id1* gene expression D) *Id3* mRNA expression. E) *Tgfβ1* gene expression F) *TgfβR1* gene expression. Data is displayed as 2<sup>-ΔCT</sup> and data was normalised to the expression of *B2M*. n=4 per group, repeated in triplicate. Statistical analysis was performed using an unpaired *t* test \**p*<0.05, \*\**p*<0.01. Data is displayed to show each individual *n* number and the bar represents the mean ± S.E.M.

#### 4.2.6 The effect of hypoxia on the expression of genes involved in cardiac remodelling in RV tissue from male rats

Assessment of the effect of hypoxia on the expression of genes associated with cardiac remodelling was also conducted. Collagen type 1 alpha 1 chain (*Col1a1*), collagen type 3 alpha 1 chain (*Col3a1*) and connective tissue growth factor (*Ctgf*) were used as gene expression markers of cardiac fibrosis. Natriuretic Peptide A (*Nppa*), Natriuretic Peptide B (*Nppb*) and Myosin heavy chain 7 (*Myh7*) were used as gene expression markers of cardiac hypertrophy. These results show that hypoxia significantly increased the expression of *Ctgf* ( $0.045 \pm 0.005$  vs  $0.192 \pm 0.043$ , \* $p < 0.05$ ,  $n=4$ ), *Nppb* ( $0.065 \pm 0.022$  vs  $0.233 \pm 0.050$ , \* $p < 0.05$ ,  $n=4$ ) and *Myh7* ( $0.219 \pm 0.011$  vs  $1.291 \pm 0.205$ , \*\*  $p < 0.01$ ,  $n=4$ ) in RV of male rats treated with placebo (Figure 4.6). Hypoxia also significantly decreased the expression of *Col3a1* ( $0.848 \pm 0.012$  vs  $0.571 \pm 0.078$ , \* $p < 0.05$ ,  $n=4$ ). These results suggest that at the end point of this study (35 days), hypoxia significantly affects the expression of markers of cardiac fibrosis and hypertrophy in male rats.

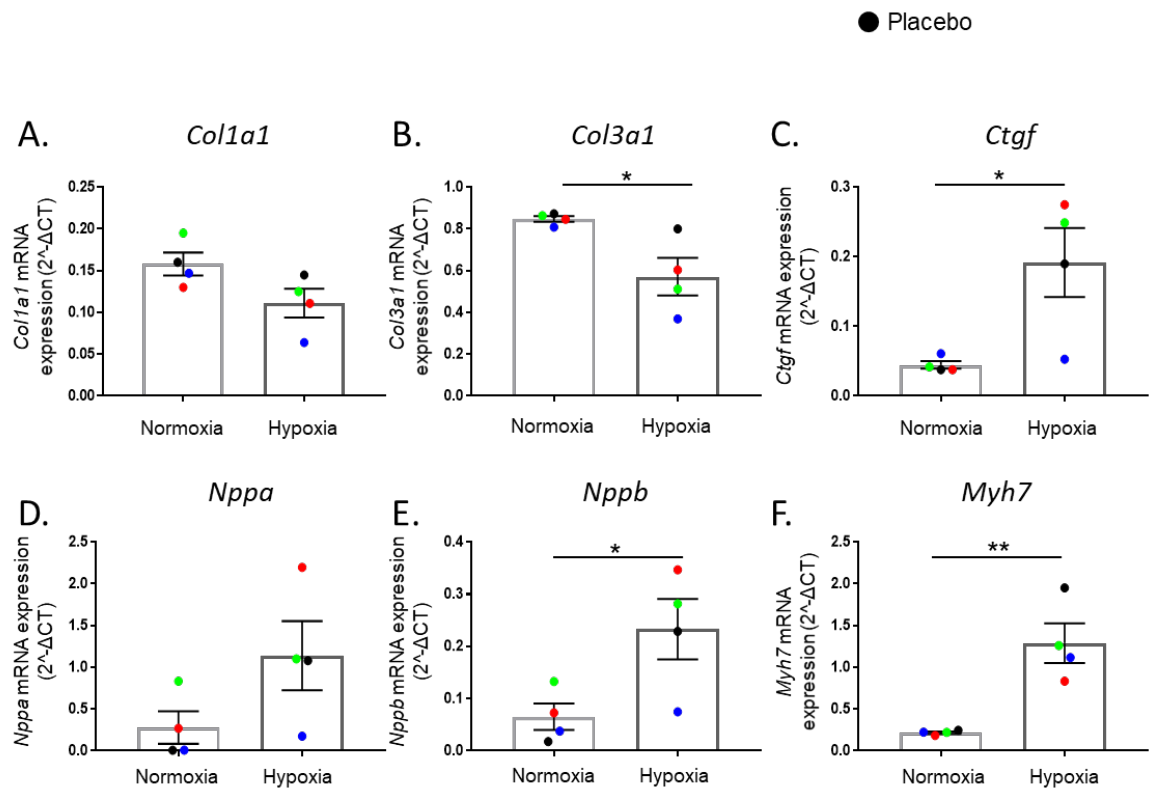


**Figure 4.6.** The effect of hypoxia on the expression of gene involved in cardiac hypertrophy and cardiac fibrosis in the male RV.

TaqMan qRT-PCR was performed on RV tissue harvested from male rats maintained in normoxia or hypoxia and treated with placebo. A) *Col1a1* gene expression. B) *Col3a1* gene expression C) *Ctgf* gene expression D) *Nppa* gene expression. E) *Nppb* gene expression F) *Myh7* gene expression. Data is displayed as  $2^{-\Delta CT}$  and data was normalised to the expression of *B2M*.  $n=4$  per group, repeated in triplicate. Statistical analysis was performed using un-paired *t* test \* $p < 0.05$ , \*\*  $p < 0.01$ . Data is displayed to show each individual  $n$  number and the bar represents the mean  $\pm$  S.E.M.

#### **4.2.7 The effect of hypoxia on the expression of genes involved in *Bmpr2* and *Tgf $\beta$* pathway in RV tissue from female rats**

The same investigation was performed in RV tissue harvested from female rats housed in normoxic and hypoxic conditions and treated with placebo. Hypoxia significantly reduced the gene expression of *Bmpr2* in the RV of female rats also ( $0.046 \pm 0.004$  vs  $0.027 \pm 0.003$ , \* $p < 0.05$ ,  $n=4$ ) (Figure 4.7). Hypoxia did not significantly affect the expression of any of the other genes of interest - *Smad1*, *Id1*, *Id3*, *Tgf $\beta$ 1* or *TgfBR1*.

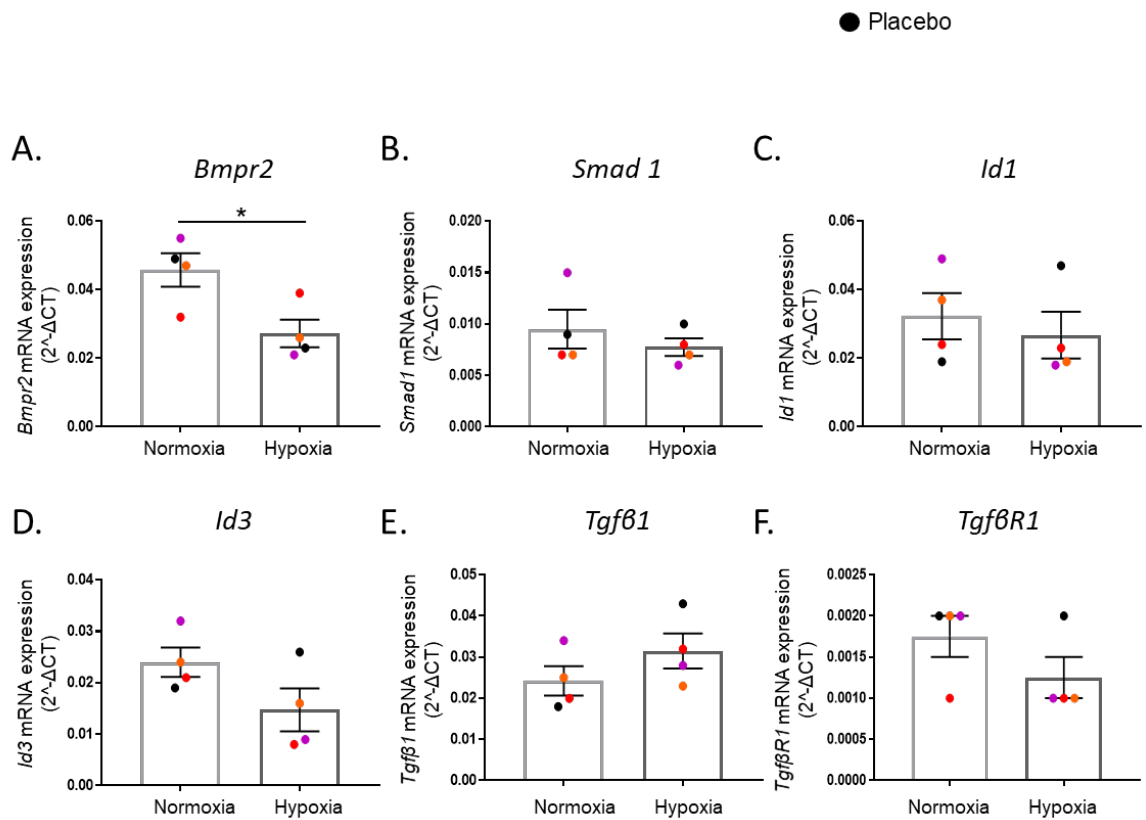


**Figure 4.7.** The effect of hypoxia on the gene expression of *Tgfβ* pathway and *Bmpr2* pathway in the female RV.

TaqMan qRT-PCR was performed on RV tissue harvested from female rats maintained in normoxia or hypoxia and treated with placebo. A) *Bmpr2* gene expression. B) *Smad1* gene expression C) *Id1* gene expression D) *Id3* gene expression. E) *Tgfβ1* gene expression F) *TgfβR1* gene expression. Data is displayed as  $2^{-\Delta CT}$  and data was normalised to the expression of *B2M*.  $n=4$  per group, repeated in triplicate. Statistical analysis was performed using un-paired *t* test  $*p<0.05$ . Data is displayed to show each individual  $n$  number and the bar represents the mean  $\pm$  S.E.M.

#### **4.2.8 The effect of hypoxia on the expression of genes involved in cardiac remodelling in RV tissue from female rats**

The effect of hypoxia on genes associated with cardiac remodelling were also investigated in the female RV. In the RV of female rats, hypoxia only significantly increases the expression of the hypertrophy marker *Myh7* ( $0.134 \pm 0.030$  vs  $0.577 \pm 0.098$ ,  $**p < 0.01$ ,  $n=4$ ) (Figure 4.8). Therefore, hypoxia had no significant effect on the expression of any of the genes associated with cardiac fibrosis at day 35 of hypoxia exposure.

● Placebo

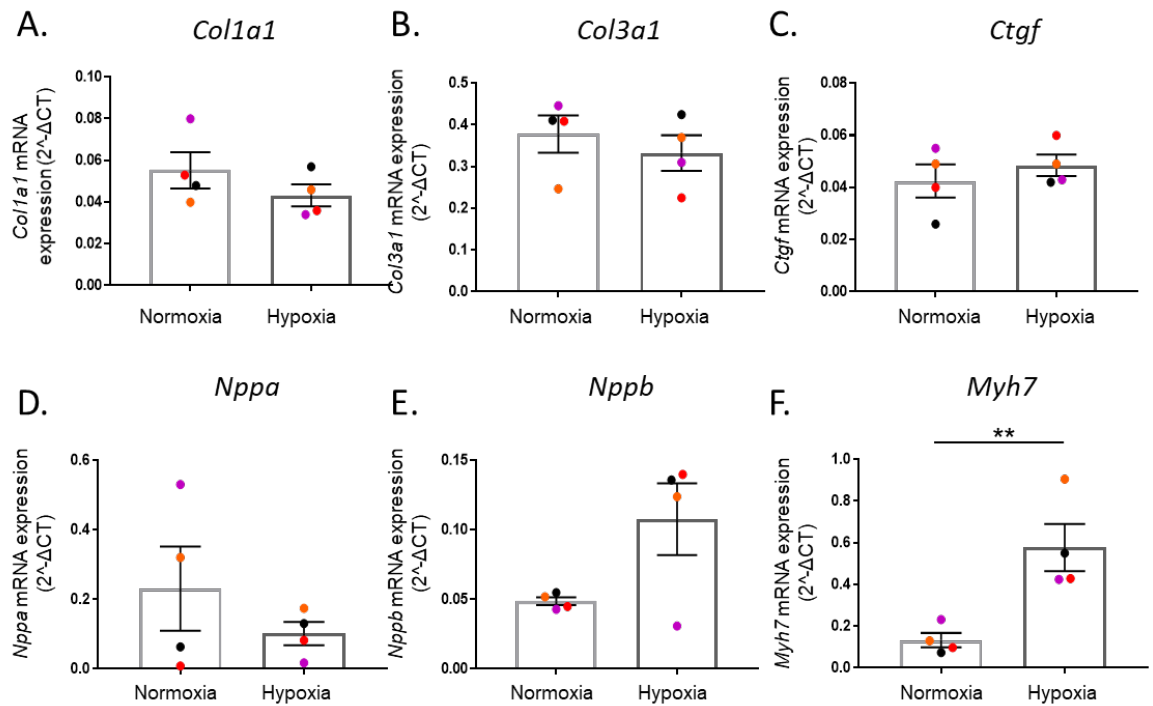


**Figure 4.8.** The effect of hypoxia on the expression of gene involved in cardiac hypertrophy and cardiac fibrosis in the female RV.

TaqMan qRT-PCR was performed on RV tissue harvested from female rats maintained in normoxia or hypoxia and treated with placebo. A) *Col1a1* gene expression. B) *Col3a1* gene expression C) *Ctgf* gene expression D) *Nppa* gene expression. E) *Nppb* gene expression F) *Myh7* gene expression. Data is displayed as 2<sup>-ΔCT</sup> and data was normalised to the expression of B2M. n=4 per group, repeated in triplicate. Statistical analysis was performed using un-paired t test, \*\* p<0.01. Data is displayed to show each individual n number and the bar represents the mean ± S.E.M.

#### 4.2.9 The effect of FK506 treatment on the expression of *Bmpr2* and *Tgfβ1* in RV tissue from male and female rats

This study showed that FK506 treatment significantly reduced RV mass in male rats independent of a reduction in RVSP suggesting that FK506 could have been acting directly on the myocardium. The expression of *Bmpr2* and *Tgfβ1* was assessed in order to identify the effect of FK506 treatment. Figure 4.5 showed *Tgfβ1* was significantly increased in the male RV under hypoxia. FK506 treatment (0.05 mg/kg/day) significantly reduced the expression of *Tgfβ1* in the male RV ( $0.049 \pm 0.005$  vs  $0.030 \pm 0.002$ , \* $p < 0.05$ ,  $n=4$ ) (Figure 4.9). This finding was specific to the male RV, which could be linked to the male specific reduction in RV mass as a result of FK506 treatment. There was no significant effect of FK506 on *Bmpr2* expression in the male or female RV.

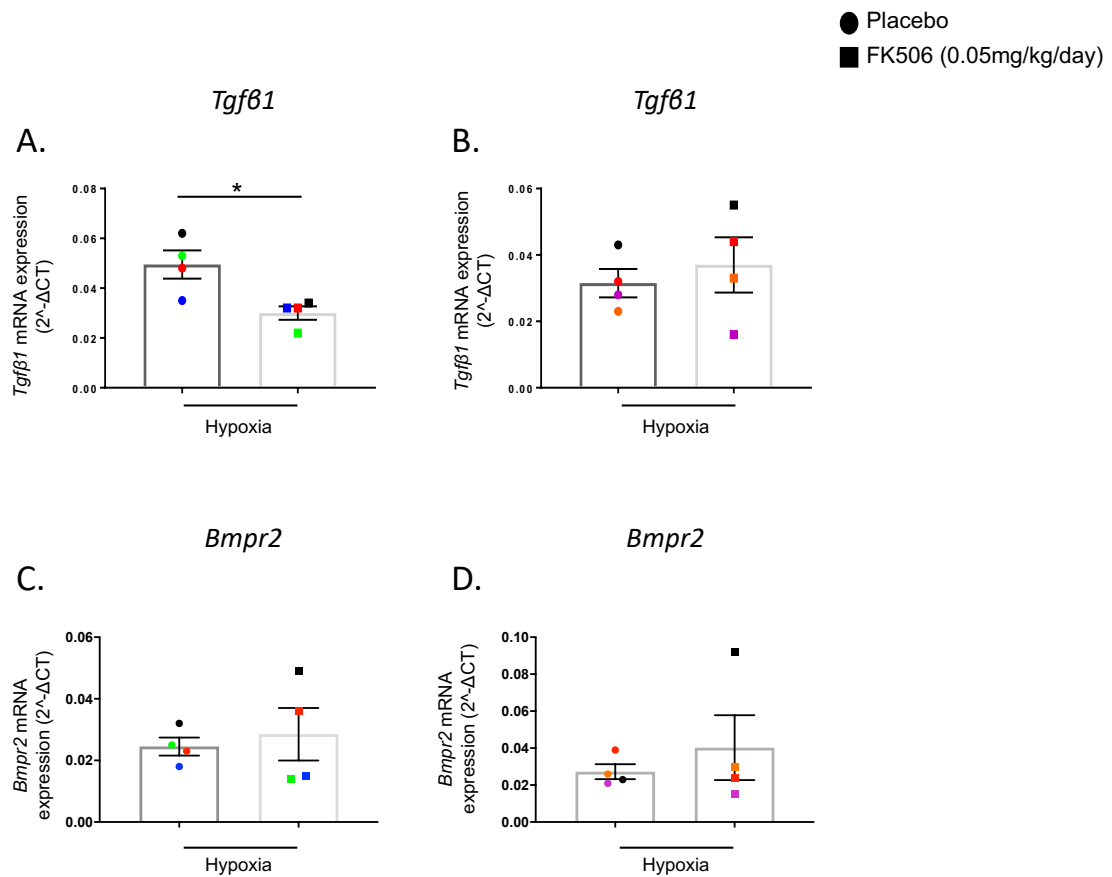


**Figure 4.9. FK506 treatment significantly reduces expression of Tgfβ1 in the male hypoxic RV.**

TaqMan qRT-PCR was performed on RV tissue harvested from male and female rats maintained in hypoxia and treated with FK506 (0.05 mg/kg/day) or placebo. A) Tgfβ1 gene expression in the male RV. B) Tgfβ1 gene expression in the female RV. C) Bmpr2 gene expression in the male RV. D) Bmpr2 gene expression in the female RV. Data is displayed as  $2^{-\Delta CT}$  and data was normalised to the expression of B2M. n=4 per group, repeated in triplicate. Statistical analysis was performed using unpaired t test \*p<0.05. Data is displayed to show each individual n number and the bar represents the mean  $\pm$  S.E.M.

#### **4.2.10 The effect of FK506 treatment on the expression of cardiac remodelling associated genes in the male RV**

Having identified that FK506 treatment significantly reduced the expression of *Tgfβ1* in the hypoxic male RV, the aim was to assess the expression of genes involved in cardiac remodelling. It was hypothesised that a reduction in *Tgfβ1* expression may result in changes in expression of *Col1a1*, *Col3a1*, *Ctgf*, *Nppa*, *Nppb* and *Myh7*. However, the expression of these genes was not significantly affected by FK506 treatment (Figure 4.10). Although, there was a trend that FK506 treatment reduced the expression of *Ctgf* with the reduction close to statistical significance ( $0.192 \pm 0.043$  vs  $0.069 \pm 0.015$ ,  $n=4$ ,  $p= 0.0583$ ).

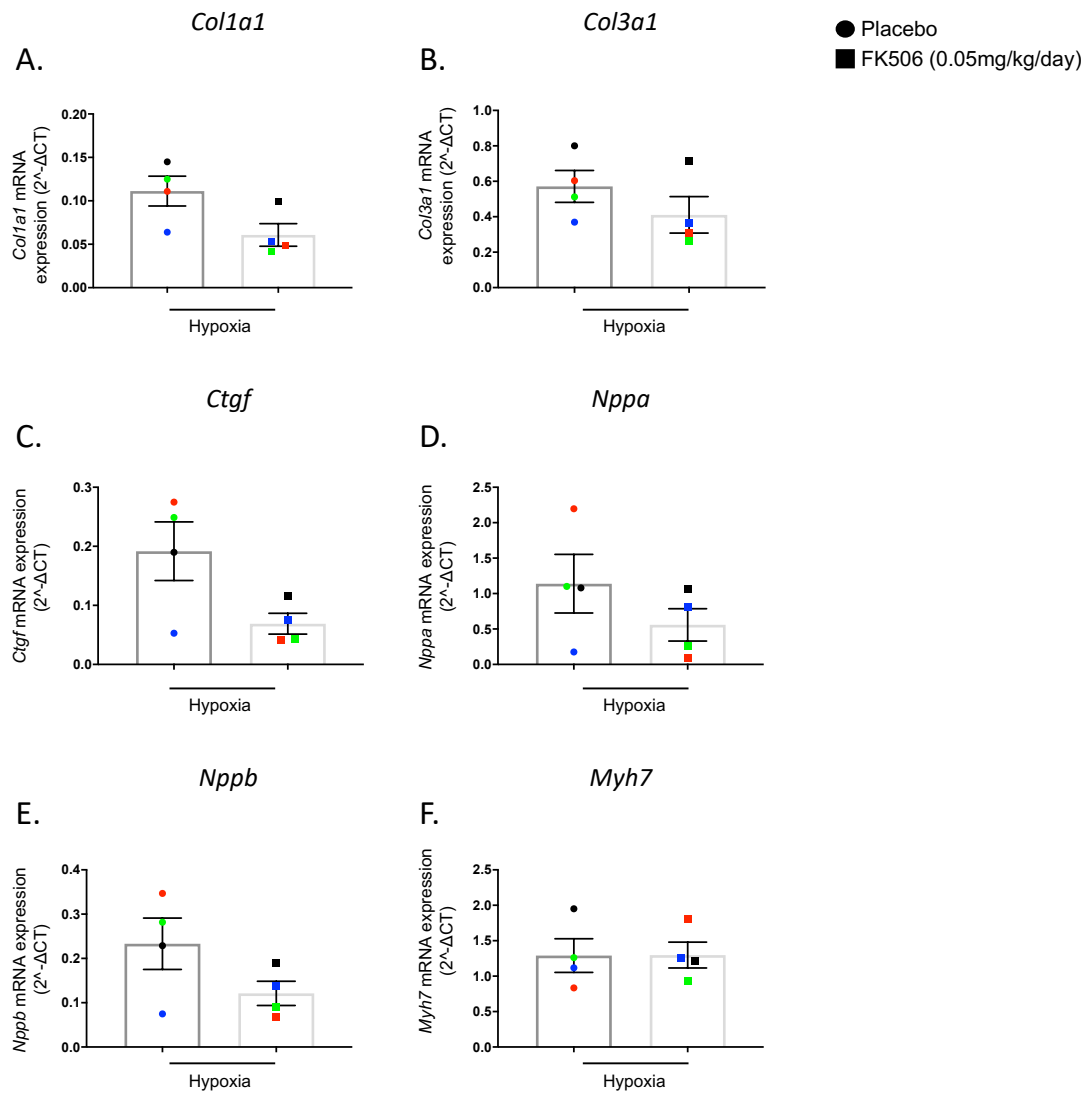


**Figure 4.10** FK506 treatment has no significant effect on the expression of genes involved in cardiac remodelling.

TaqMan qRT-PCR was performed on RV tissue harvested from male rats maintained in hypoxia and treated with FK506 (0.05 mg/kg/day) or placebo. Male RV gene expression A) Col1a1. B) Col3a1. C) Ctgf. D) Nppa. E) Nppb. F) Myh7. Data is displayed as  $2^{-\Delta CT}$  and data was normalised to the expression of B2M.  $n=4$  per group, repeated in triplicate. Statistical analysis was performed using unpaired  $t$  test. Data is displayed to show each individual  $n$  number and the bar represents the mean  $\pm$  S.E.M.

#### 4.2.11 Differential gene expression between the male and female normoxic RV.

The gene expression study had identified changes in gene expression as a result of hypoxia that appeared to be specific to the male RV. It was important then to perform a direct comparison between the male and female RV in order to interrogate and further understand how these changes in gene expression are related to sex. The data used for this comparison was displayed in previous figures when investigating the effect of hypoxia and FK506 on gene expression. Firstly, a comparison between RV tissue from male and female rats housed in normoxia and treated with placebo would highlight any sex-specific differences in gene expression under basal conditions (Figure 4.11). Expression of genes associated with the *Bmpr2* pathway - *Bmpr2*, *Smad1*, *Id1* and *Id3* - were not differentially expressed between male and female RV. However, *Tgfβ1* was significantly increased in the male RV compared to the female RV ( $0.035 \pm 0.002$  vs  $0.024 \pm 0.003$ , \* $p < 0.05$ ,  $n=4$ ). Additionally, genes involved in cardiac remodelling *Col1a1* ( $0.158 \pm 0.012$  vs  $0.055 \pm 0.008$ , \*\*\* $p < 0.001$ ,  $n=4$ ) and *Col3a1* ( $0.848 \pm 0.12$  vs  $0.378 \pm 0.039$ , \*\*\*\* $p < 0.0001$ ,  $n=4$ ) displayed significantly increased gene expression in the male RV. None of the genes associated with cardiac hypertrophy - *Nppa*, *Nppb* and *Myh7* were differentially expressed between the male and female RV.

● Placebo

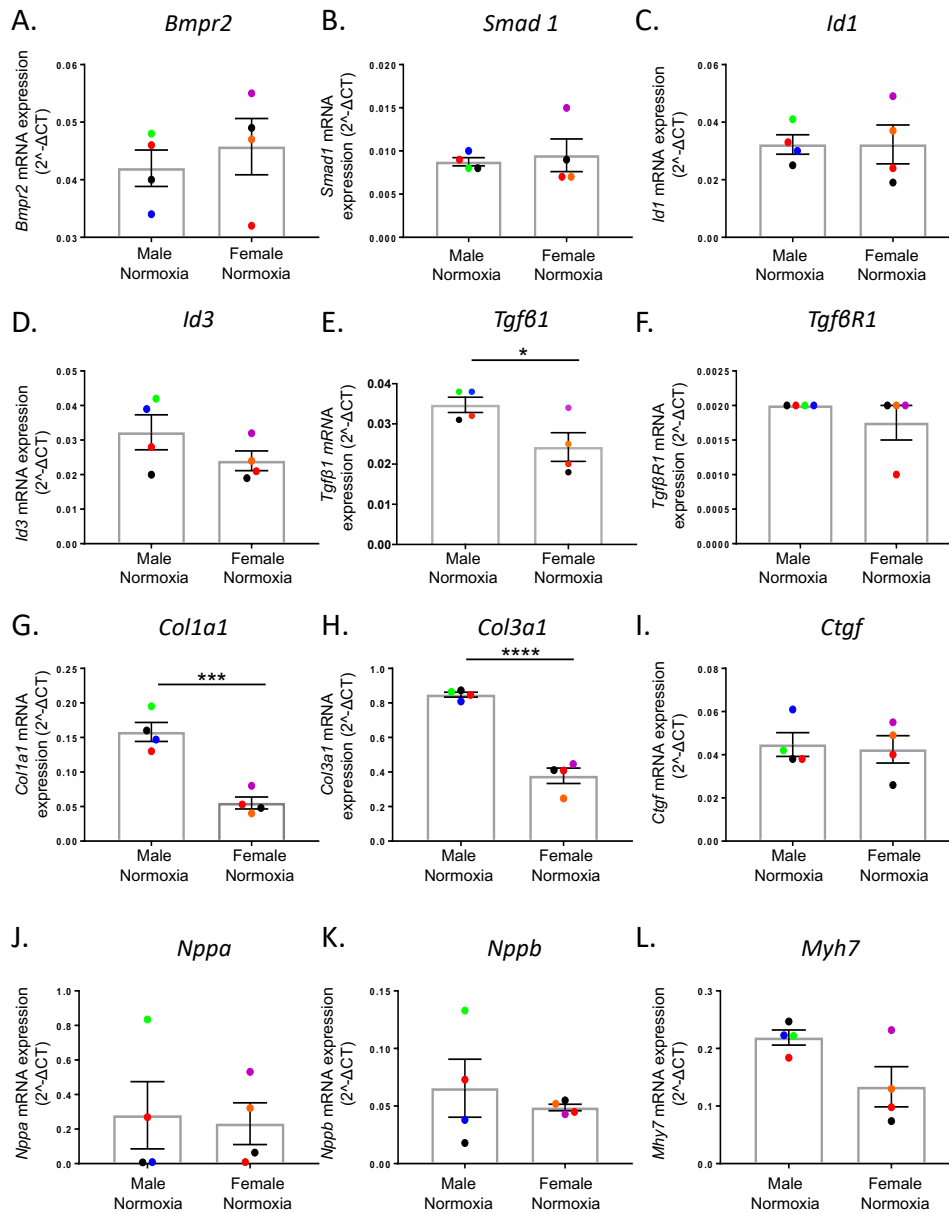


**Figure 4.11. Differential gene expression between the male and female normoxic RV.**

TaqMan qRT-PCR was performed on RV tissue harvested from male and female rats maintained in normoxia and treated with placebo. Gene expression of A) *Bmpr2*. B) *Smad1*. C) *Id1*. D) *Id3*. E) *Tgfb1*. F) *TgfbR1*. G) *Col1a1*. H) *Col3a1*. I) *Ctgf*. J) *Nppa*. K) *Nppb*. L) *Myh7*. Data is displayed as 2<sup>-ΔCT</sup> and data was normalised to the expression of B2M. n=4 per group, repeated in triplicate. Statistical analysis was performed using unpaired t test \*p<0.05, \*\*\* p<0.001, \*\*\*\* p<0.0001. Data is displayed to show each individual n number and the bar represents the mean ± S.E.M.

#### 4.2.12 Differential gene expression between the male and female hypoxic RV.

The final aim of the gene expression study was to compare the hypoxic male and female RV directly. Again, this data has been displayed in previous figures when investigating the effect of hypoxia and FK506 on gene expression. Similar to the normoxic RV, expression of *Bmpr2*, *Smad1*, *Id1* and *Id3*, genes involved in Bmpr2 signalling, were not differentially expressed between male and female. Again, there were differences in the level of *Tgfb1* expression between the male and female RV. *Tgfb1* expression was significantly increased in the hypoxic male RV compared to the female RV ( $0.049 \pm 0.005$  vs  $0.031 \pm 0.004$ , \* $p < 0.05$ ,  $n=4$ ). Furthermore, genes associated with cardiac hypertrophy and cardiac remodelling were also significantly increased in the hypoxic male RV, specifically - *Col1a1* ( $0.111 \pm 0.015$  vs  $0.043 \pm 0.005$ , \*\* $p < 0.01$ ,  $n=4$ ), *Ctgf* ( $0.192 \pm 0.043$  vs  $0.048 \pm 0.004$ , \* $p < 0.05$ ,  $n=4$ ), *Nppa* ( $1.139 \pm 0.385$  vs  $0.102 \pm 0.029$ , \* $p < 0.05$ ,  $n=4$ ) and *Myh7* ( $1.291 \pm 0.205$  vs  $0.577 \pm 0.098$ , \* $p < 0.05$ ,  $n=4$ ) (Figure 4.12).

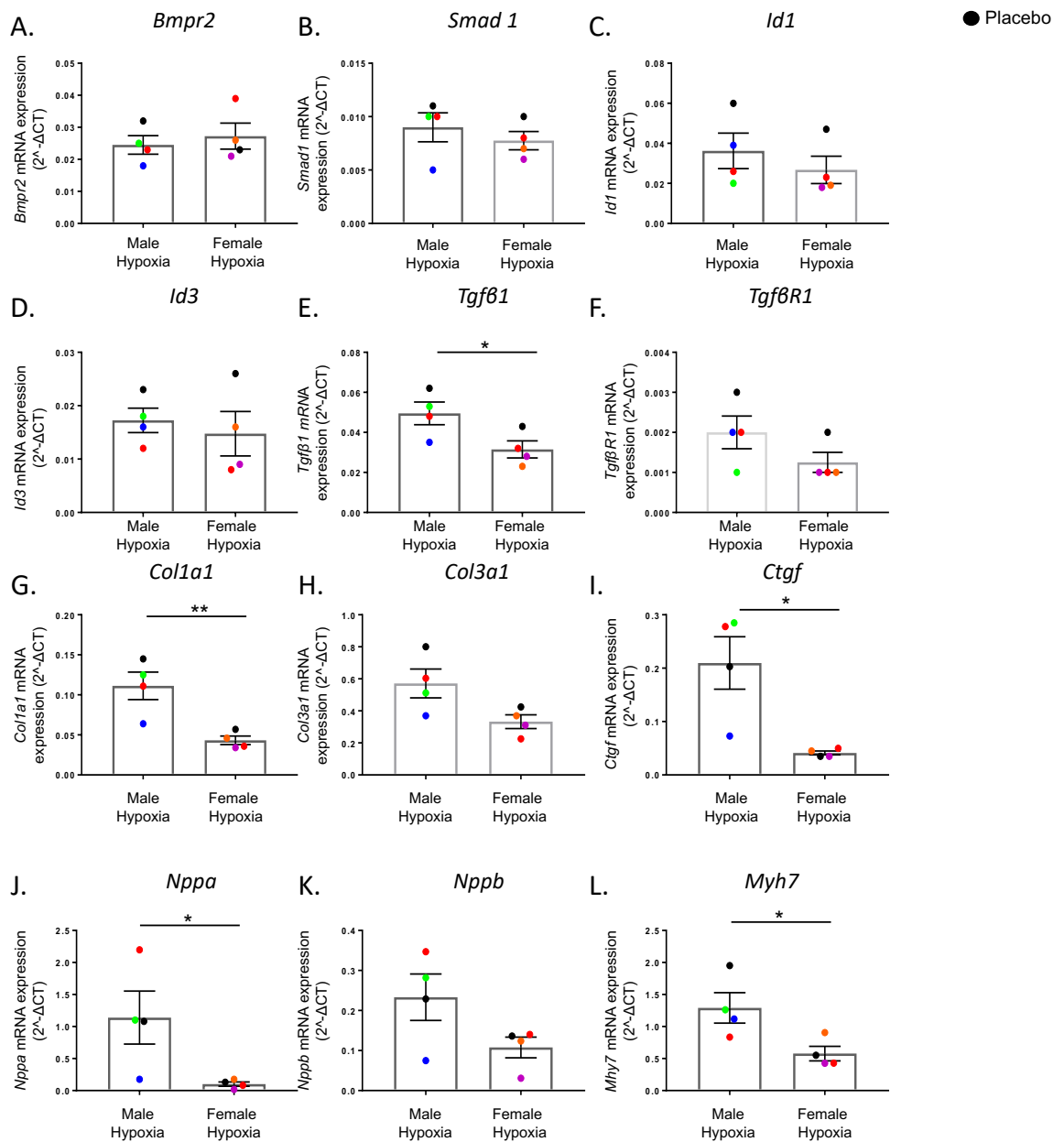


**Figure 4.12. Differential gene expression between the male and female hypoxic RV.**

TaqMan qRT-PCR was performed on RV tissue harvested from male and female rats maintained in normoxia and treated with placebo. Gene expression of A) *Bmpr2*. B) *Smad1*. C) *Id1*. D) *Id3*. E) *Tgfb1*. F) *TgfbR1*. G) *Col1a1*. H) *Col3a1*. I) *Ctgf*. J) *Nppa*. K) *Nppb*. L) *Myh7*. Data is displayed as 2<sup>-ΔCT</sup> and data was normalised to the expression of B2M. n=4 per group, repeated in triplicate. Statistical analysis was performed using unpaired t test \*p<0.05, \*\* p<0.01. Data is displayed to show each individual n number and the bar represents the mean ± S.E.M.

#### **4.2.13 Development of *in vitro* models to investigate the role of sex in the right ventricle.**

The results from the *in vivo* study highlighted that there is a need to develop our understanding of the role of sex in signalling pathways within the RV. Identifying an appropriate *in vitro* model would allow further studies to be conducted and these pathways to be investigated in more detail. Gene expression studies in the male and female rat RV had highlighted sex-specific differences in normoxic, basal conditions as well as sex-specific differences in response to hypoxia. *In vitro* models could also help to determine if these sex-specific differences were exclusive to cardiac fibroblasts or cardiomyocytes.

#### **4.2.14 Investigation of neonatal rat cardiac fibroblasts**

Neonatal rat cardiac fibroblasts (NRCFs) were considered as an *in vitro* model for these studies. The isolation of NRCFs was a protocol that was well established within the lab. Therefore, the initial aim was to investigate key signalling pathways in NRCFs isolated from Wistar Kyoto (WKY) rats. To briefly describe the isolation protocol, at 3-5 days both male and female neonatal rat pups were culled and the hearts collected. Sexing of the pups was not possible at the neonatal stage so male and female pups were combined for the purposes of this investigation. The ventricles were carefully dissected and enzymatically digested. NRCFs were then isolated by plating the cells on poly-l-lysine coated cell culture dishes for 1 hour before washing the dish to remove the neonatal cardiomyocytes that had not adhered. This method can result in low level contamination with cardiomyocytes, however, the subsequent DMEM media used promotes proliferation of the NRCFs and not the cardiomyocytes.

As it was not possible to isolate male and female NRCFs, initially, the aim was to investigate the effect of estrogen on the expression of genes in key signalling pathways in NRCFs. Estrogen acting via ER- $\beta$  has been shown to inhibit Ang II stimulated cardiac fibrosis and cardiac hypertrophy *in vivo* and *in vitro* models (Pedram et al., 2010; Hoa et al., 2018). In mouse models, estrogen has also been shown to inhibit Ang II stimulated increases in *Tgfb1* (Pedram et al., 2010).

Prior to beginning cell culture stimulations, cells were serum starved in phenol red free media. Phenol red can act as a weak estrogenic mimic therefore in all

cell culture stimulations involving estrogen, phenol red free media was used from the quiescence stage onwards. Angiotensin II (Ang II) (100nM) was used as a pathological stimulus in the NRCFs and the effect of  $\beta$ -estradiol (E2) at 1 nM or 10 nM concentrations was investigated. As the *in vivo* study had highlighted sex-specific differences in *Tgf- $\beta$ 1* expression under normoxic and hypoxic conditions, the expression of *Tgf- $\beta$ 1* was the first to be investigated (Figure 4.13).

Stimulation with Ang II did not affect the expression of *Tgf- $\beta$ 1* in NRCFs.

Furthermore, the addition of E2 at 1 nM or 10 nM had no significant effect on the gene expression of *Tgf- $\beta$ 1*. An extension of these studies was planned within the NRCFs, however, further investigation was required to characterise these cells and their responses before the effect of estrogen on pathological responses could be determined.

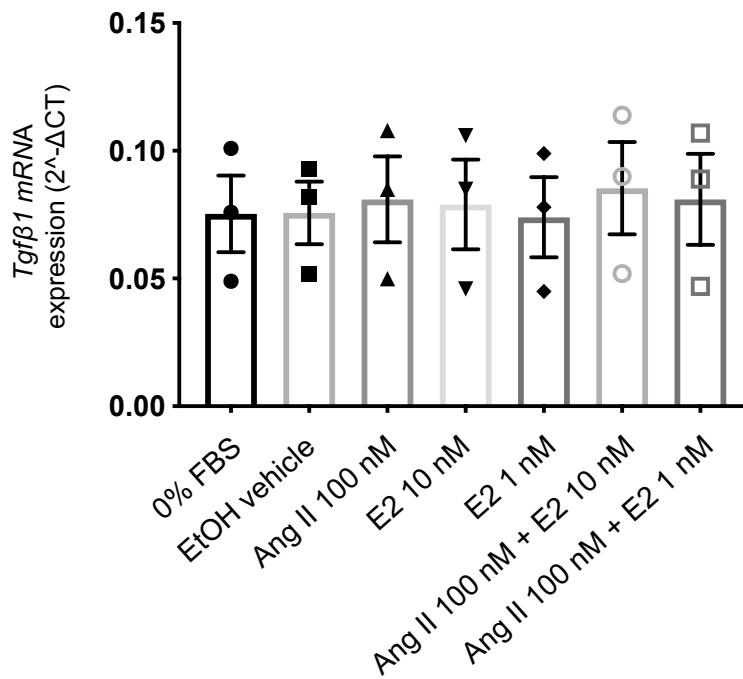


**Figure 4.13** The effect of estrogen on Tgf-β1 gene expression in Ang II stimulated NRCFs.

Neonatal rat cardiac fibroblasts (NRCFs) were isolated and cultured from neonatal rat ventricles. Cells were stimulated by Ang II 100 nM ± E2 at 10 nM or 1 nM for 24 hr. Tgf-β1 gene expression was assessed using TaqMan qRT-PCR. Data is displayed as 2<sup>-ΔCT</sup> and data was normalised to the expression of B2M. n=3, repeated in triplicate. Data is displayed to show each individual n number and the bar represents the mean ± S.E.M. EtOH = ethanol, E2 = 17β-estradiol.

### 4.3 Discussion

The first aim of this study was to investigate the effect of hypoxia on the RV in the 5-week chronic hypoxia model. The results showed hypoxia significantly increased RV mass, RV mass/body weight and RV/LV+S in male and female rats. This finding completed the investigation of the 5 week chronic hypoxia model carried out in Chapter 3 and confirms its success as an experimental model of PH.

The next aim was to investigate the sex dependent effects of treatment with FK506 on RV remodelling. The previous *in vivo* studies were only completed in male models of the disease (Spiekerkoetter et al., 2013). It was hypothesised that females may respond differently to FK506 induced increases in *BMPR2* expression as their basal levels could be lower. The findings discussed in Chapter 3 showed RVSP and pulmonary artery remodelling were not significantly affected by FK506 treatment in male or female rats. The RV investigation highlighted a sex-specific response in the effect of FK506 on RV mass independent of changes in RVSP. RV mass and RV mass/body weight were significantly reduced by FK506 treatment in male rat RV but not female RV. Treatment did not significantly alter the Fulton's index (RV/LV+S) which is the standard measure of RVH within the PH research field (Fulton et al., 1952). However, this was thought to be associated with an increase in LV+S mass/body weight within the hypoxic placebo treated male rats which affected the ratio measurement. This may be why FK506 treatment significantly reduces RV mass and RV mass/body weight in male rats but does not significantly affect the Fulton's index. This also suggests that hypoxia had induced LV remodelling either independently or secondary to RV remodelling. If tibial length had been measured during this study, a more appropriate measurement of RVH would have been RV mass (mg)/tibial length (mm) as this would have removed any potential interference of LV remodelling (Li et al., 2016b; Hardziyenka et al., 2011). However, this result does suggest that FK506 treatment has the potential to effect RV remodelling in male rats only, highlighting a possible sex-dependent effect of FK506.

The recent Spiekerkoetter et al. study (Spiekerkoetter et al., 2013) showed FK506 treatment significantly improved parameters of experimental pulmonary hypertension in several different male models of the disease via *BMPR2*

activation. Right ventricular hypertrophy (RVH) was reduced following a 3 week dosing period with FK506 (0.05 mg/kg/day). The group also completed a phase II clinical trial with compassionate use of low dose FK506 in 3 patients (Spiekerkoetter et al., 2015). This preliminary study showed increased cardiac function in the patients treated with FK506 as well as a reduction in the time spent in hospital due to RV failure. However, it is not understood if the improved RV function is secondary to FK506 effects on the pulmonary vasculature or if FK506 directly targets the RV.

Following these findings, it was important to further investigate the sex-specific effects of hypoxia and FK506 treatment on the RV. This was performed by assessing gene expression within the RV. It was hypothesised that significant changes in gene expression could highlight key pathways involved in sex-specific hypoxia-induced remodelling of the RV and sex-specific effects of FK506 on the RV. The gene expression study identified that hypoxia significantly increased *Tgfb1* gene expression in the male RV. FK506 treatment significantly reduced *Tgfb1* expression under hypoxic conditions. A finding which was not replicated in the female RV tissue. *Tgfb1* is known to play a role in the development of cardiac fibrosis and cardiac hypertrophy and therefore a reduction in the expression of *Tgfb1* could be associated with a reduction in cardiac hypertrophy and therefore RV mass. However, further characterisation of the effect of FK506 on the TGF $\beta$  pathway is required. Studies in human foreskin fibroblasts cultured have shown that treatment with FK506 can reduce the expression of *Tgfb1* and this leads to a reduction in collagen production (Lan et al., 2014). FK506 did not significantly reduce the expression of the genes associated with collagen and fibrosis - *Col1a1*, *Col3a1* or *Ctgf* in this study. However, the expression of many of the collagen genes are time dependent (Manabe et al., 2002; Friddle et al., 2000; van den Bosch et al., 2006) and it could be hypothesised that at another time point during the dosing period that FK506 treatment would have significantly affected gene expression. Furthermore, in future it would be important to also examine the protein expression as this would provide a better indication of collagen levels within the tissue at that time.

Another key finding of this study was that hypoxia significantly reduced the expression of *Bmpr2* in both the male and female RV. To our knowledge this is the first time this has been shown in male and female chronic hypoxia rats. Mutations in the *BMPR2* gene are one of the most well established genetic risk factors for developing PAH (Machado et al., 2009). Despite dysfunctional *BMPR2* signalling being well characterised in the lung, the downstream effects in the RV are not as well understood. A recent clinical study suggested *BMPR2* mutation carriers have poorer RV function despite similar cardiac adaptation in mutation carrier and non-carrier groups (Van Der Bruggen *et al.*, 2016). Unfortunately, this study did not stratify the results depending on gender. It does suggest, however, that *BMPR2* signalling influences RV function. Furthermore, a transgenic mouse model expressing RV specific mutant *BMPR2* displays impaired hypertrophy of the RV in response to increased RVSP (Hemnes *et al.*, 2014). This suggests that in the absence of functional *BMPR2*, the RV's ability to compensate for increased afterload is diminished. FK506 treatment had no significant effect on *Bmpr2* expression in the male or female RV, therefore, further work is required in order to assess if FK506 treatment affects *Bmpr2* signalling in the RV and consequently how this affects RV function in a PH model.

This study also highlighted several sex-specific differences in gene expression in the RV under hypoxic conditions. Interestingly these differences in expression were in *Tgfb1* and genes associated with cardiac fibrosis and cardiac hypertrophy. These processes that are known to be highly influenced by *Tgfb1* (Khan and Sheppard, 2006) (Rosenkranz, 2004). *Col1a1*, *Ctgf*, *Nppa* and *Myh7* were all significantly increased at a gene expression level in the male hypoxic RV compared with the female hypoxic RV. These results suggest that the male and female RV have differential responses to hypoxia. In order to further validate this finding, it would be important to examine the protein expression of each of these genes. Estrogen acting via estrogen receptor  $\beta$  (ER- $\beta$ ) has been shown to inhibit Ang II and endothelin-1 (ET-1) stimulated increases in *Tgfb1* and cardiac fibrosis in mouse models (Pedram et al., 2010). Additionally, estrogen acting via ER- $\beta$  has also been shown to reduce Ang II stimulated cardiac hypertrophy in neonatal cardiomyocyte cell models and female rodent models (Hoa et al., 2018). The published study showed cardiac hypertrophy was inhibited by the action of estrogen maintaining expression of transcription factor Krüppel-like

factor 15 (Klf15). However, studies investigating the action of estrogen specifically in the RV are lacking. The initial aim of the *in vitro* studies was to investigate the effects of E2 and estrogen metabolites on gene expression in Ang II stimulated neonatal rat cardiac fibroblasts. Previous studies had shown that Ang II increases the expression of *Tgf $\beta$ 1* in rat cardiac fibroblasts (Pedram et al., 2010; Lee et al., 1995) therefore it was expected that *Tgf $\beta$ 1* expression would have been increased. However, Ang II stimulation did not increase expression of Tgf $\beta$ 1 in this experiment and therefore, further characterisation of these cells has to be carried out before investigations can continue.

Currently, there are no treatments available that target RV dysfunction in PAH despite it being the main cause of mortality in PAH patients. Therefore, there is a real need to develop our understanding of the molecular mechanisms underlying RV dysfunction in order to identify potential therapeutic targets. Poorer male patient survival rates are thought to be associated with increased and accelerated RV dysfunction compared to females (Jacobs et al., 2014; Kawut et al., 2009). Clinical studies in control groups have suggested that higher estrogen levels are associated with increased RV function (Ventetuolo et al., 2011; Ventetuolo et al., 2016b). However, the role of estrogen in PAH is controversial as it has been shown to play a pathogenic role in both experimental animal studies (White et al., 2011; Mair et al., 2014b) and clinical studies (Ventetuolo et al., 2016a). This therefore adds to the complexity of identifying potential estrogen-associated therapeutic targets as therapies would have to be targeted to the RV specifically. Investigations into the effect of sex and estrogen on the RV could help develop our understanding of why females tend to have better RV function and perhaps even identify new RV-specific therapeutic targets.

## **Chapter 5**

### **5 The role of sex and estrogen in the development of experimental pulmonary hypertension and their effect in the RV**

## 5.1 Introduction

The most significant risk factor in the development of PAH is the female sex. Although more women develop PAH, males who do develop the disease tend to have poorer outcomes (Shapiro et al., 2012). This is thought to be associated with a quicker decline in RV function (Jacobs et al., 2014; Kawut et al., 2009). Therefore, the role of sex hormones, particularly estrogen, in the development and progression of PAH remains one of high interest within pre-clinical and clinical studies. Experimental studies investigating the role of estrogen in PAH have produced conflicting results. *In vivo* studies have shown estrogen to be protective in the pulmonary vasculature in chronic hypoxia (Xu et al., 2010; Lahm et al., 2012) and monocrotaline models of disease (Farhat et al., 1993). However, the opposing theory is that estrogen exacerbates disease progression within the lungs and reduced levels of estrogen could prevent or reverse the pathophysiology of disease (Mair et al., 2014b; White et al., 2011; Wright et al., 2015). This hypothesis was investigated in the Smad 1 (+/-) mouse model in which the females spontaneously develop a PH phenotype at approximately 6 months of age. Ovariectomy in the Smad1 (+/-) mouse model prevented an increase in RVSP and RV/LV+S, however, the same study also showed that ovariectomy in wild-type mice resulted in increased RVSP and RV/LV+S (Mair et al., 2015). The contradictory evidence surrounding the role of estrogen is known within the field as the “estrogen paradox” (Lahm et al., 2014).

Therapies that could manipulate endogenous estrogen production have also been utilised to investigate the role of estrogen. Anastrozole, a drug which was initially developed as a therapy for hormone receptor positive breast cancer, reduces the production of endogenous estrogen by inhibiting the action of the enzyme aromatase (Baum et al., 2002; Geisler et al., 1996). Aromatase catalyses the production of 17 $\beta$ -estradiol from the male sex hormone testosterone as well as the production of estrone (E1) from androstenedione (Grodin et al., 1973). Aromatase was found to be expressed in the PSMCs of both female animal models and female PAH patients (Mair et al., 2014b; Wright et al., 2015). This finding added more weight to the hypothesis that treatment with Anastrozole could improve parameters of PH. Inhibition of aromatase within the chronic hypoxia mouse model and the SuHx rat model reversed the PH phenotype associated with these models (Mair et al., 2014b). This involved reduced RVSP

and RVH as measured by RV/LV+S. This finding was specific to female mice and rats. Male chronic hypoxia mice and SuHx rats showed no improvement in these parameters when treated with the same dose of anastrozole (Mair et al., 2014b). Inhibition of endogenous estrogen has also been shown to improve metabolic dysfunction associated with disease in the Bmpr2 mutant mouse model (Chen et al., 2017).

Anastrozole safety and tolerability studies have now been conducted in PAH patient populations including male and female patients (Kawut et al., 2017). This Phase II clinical trial suggested Anastrozole was well tolerated and safe within the PAH patient populations and it was capable of reducing 17 $\beta$ -estradiol levels by approximately 40% after 3 months of treatment. Anastrozole treatment improved 6 min walk distance, a measure which indicates exercise tolerance of the patients and has been recognised as the primary clinical outcome used during the assessment of PAH patients (Demir and Küçüköğlü, 2015). However, it was not capable of improving any of the other clinical parameters of PAH such as functional class or the number of adverse events experienced by the patient group. The results were also not stratified based on sex. Given the sex-specific responses identified in pre-clinical models, this could have been an interesting measurement. Importantly, treatment with anastrozole had no detrimental effect on parameters of RV function. Although reversal of the pathophysiological state in the lungs could result in reduced afterload and therefore improved RV parameters, there is also the risk that inhibiting endogenous estrogen production could have direct detrimental effects in the RV as estrogen has been shown to be cardioprotective (Iorga et al., 2017). The outcomes of the small clinical study did justify a larger and longer Phase II clinical trial known as PHANTOM (NCT03229499) which is currently recruiting patients.

As well as a role for the production of 17 $\beta$ -estradiol, the metabolism of estrogen has also been shown to be important in PAH animal models and patient groups. It is thought that the estrogen metabolite 16 $\alpha$ -OHE1 is the most potent of the estrogen metabolites as it binds the receptor covalently (Swanek and Fishman, 1988). Furthermore, PAH patients have been shown to exhibit estrogen metabolism that tends to produce 16 $\alpha$ -OHE1 (Austin et al., 2009; West et al., 2008; Dempsey et al., 2013).

The RV-associated outcomes of inhibiting estrogen production are still not fully elucidated. It is important to understand the effect of Anastrozole on the RV as RV function is thought to determine clinical outcomes for PAH patients. Furthermore, an understanding of the inhibition of estrogen production in the pulmonary circulation and the RV may help to uncover the “estrogen paradox” that exists in PAH.

The aims of this chapter include:

To investigate the effect of treatment with Anastrozole (3 mg/kg/day) on the right ventricle in male and female chronic hypoxia mice.

To compare RV gene and protein expression profiles in male and female mice.

To investigate the effect of estrogen on the migration of PASMCs explanted from male and female rats.

## 5.2 Results

C57Bl/6 male and female mice were recruited to this study at 6-8 weeks old. Mice were housed in the hypobaric hypoxic chamber maintained at 550 mbar for 28 days. On day 14 of the study, administration of Anastrozole (3 mg/kg/day) or the equivalent volume of vehicle (1% CMC) was initiated. Anastrozole (3 mg/kg/day) or vehicle (1% CMC) was administered by daily i.p. injections for the last 14 days of the study. Age and sex-matched controls animals were housed in normoxic conditions and followed the same dosing regimen of Anastrozole (3 mg/kg/day) or vehicle (1% CMC). On day 28 of the study the male and normoxic animals were humanely culled and a tissue harvest was performed.

Haemodynamic assessment was performed on the female hypoxic mice before the mice were humanely culled and tissue harvested (Figure 5.1). Initially, the main aim of this study was to assess the effects of Anastrozole in the female RV as Anastrozole had been shown to be effective in reducing RV/LV+S in female mice only (Mair et al., 2014b). For this reason, full haemodynamic assessment was performed in the female hypoxic mice only. In future, haemodynamic assessment would be performed on male and female normoxic and hypoxic animals.

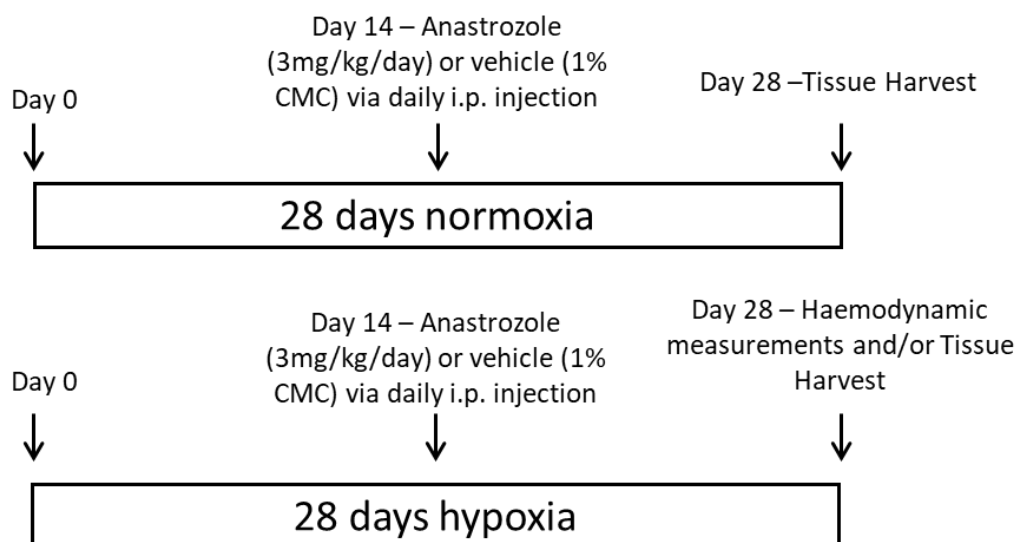


**Figure 5.1- Schematic diagram showing Anastrozole study protocol and dosing regimen.**

*Male and Female C57Bl/6 mice were kept in normoxia or hypoxia for a period of 28 days. On day 14 daily intra-peritoneal (i.p.) injections of Anastrozole (3mg/kg/day) or vehicle (1% CMC) began in normoxic and hypoxic mice for the remainder of the 28 days. On day 28 tissue was harvested from the normoxic group and the male hypoxic group. Haemodynamic assessment and tissue harvest were completed for the female hypoxic group.*

### 5.2.1 Investigation of the effect of Anastrozole on RVSP and BMPR2 expression in the female mouse lung

A previous study by the group had shown treatment with Anastrozole (3 mg/kg/day) significantly reduced RVSP (mmHg) as well as RVH in female chronic hypoxia mouse model (Mair et al., 2014b). Therefore, the aim was to confirm this finding in the current study and investigate the effect of anastrozole treatment on the RV.

All mice were humanely culled on day 28 and tissue was harvested from all animals. Only the hypoxic mice were haemodynamically assessed at day 28 prior to cull, haemodynamic assessment was not performed on normoxic mice. Haemodynamic measurement of RVSP in the female hypoxic vehicle treated and anastrozole treated groups showed no significant difference in RVSP between the 2 groups (Figure 5.2A).

A previous study had shown that chronic hypoxia significantly reduced the expression of BMPR2 in the lung at both a gene and protein level and BMPR2 expression was restored with Anastrozole treatment (Mair et al., 2014b). Therefore, to investigate the differential effect of treatment with anastrozole (3 mg/kg/day) in the current study, gene expression and protein expression of BMPR2 was investigated by TaqMan qRT-PCR and western blot, respectively.

Gene expression analysis showed *BMPR2* was significantly lower in the hypoxic vehicle treated group in comparison with the normoxic group ( $0.224 \pm 0.020$  vs  $0.341 \pm 0.023$ ,  $n=4$ ,  $*p<0.05$ ) (Figure 5.2B). However, Anastrozole was not able to restore gene expression of BMPR2 as there was no significant difference in expression between hypoxic vehicle and anastrozole treated groups.

Densitometric analysis of the western blot was used to compare BMPR2 protein expression in each of the groups (Figure 5.2D). There was no significant difference in BMPR2 protein expression across the groups.

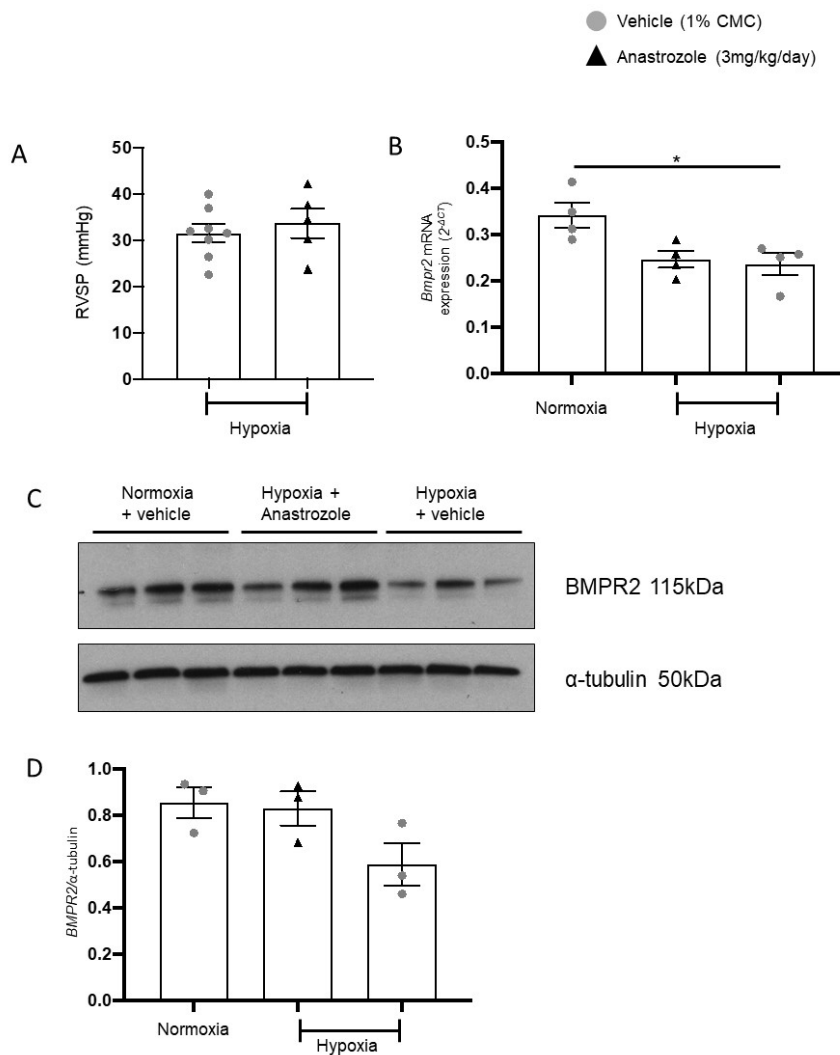


**Figure 5.2.** RVSP and lung BMPR2 expression in the female chronic hypoxia mouse model.

Female mice were maintained in normoxia and hypoxia and treated with Anastrozole (3 mg/kg/day) or vehicle (1% CMC). A) RVSP (mmHg) in female hypoxic mice treated with Anastrozole or vehicle.  $n=5-8$ . B) BMPR2 gene expression. TaqMan qRT-PCR was performed on lung tissue harvested from normoxic and hypoxic female mice treated with Anastrozole or vehicle. Data is displayed as  $2^{-\Delta CT}$  and data was normalised to the expression of B2M.  $n=4$  per group, repeated in triplicate. Statistical analysis was performed using one-way ANOVA followed by Bonferroni post-hoc test. C) BMPR2 protein expression in the lung. Representative immunoblots. D) Densitometric analysis of BMPR2 protein expression in the lung.  $\alpha$ -tubulin was used as a loading control.  $n=3$  per group. Data is displayed to show each individual  $n$  number and the bar represents the mean  $\pm$  S.E.M.

### 5.2.2 Treatment with Anastrozole had no significant effect on RV or LV+S mass in the chronic hypoxia female mouse model

The previous study also showed that Anastrozole treatment significantly reduced RVH as measured by RV/LV+S in female chronic hypoxia mice (Mair et al., 2014b). Therefore, the heart was harvested at the end of the study. The atria and vessels were removed, and the RV carefully dissected from the LV+S. The RV and LV+S mass was recorded. Hypoxia significantly increased RV mass ( $20.04 \pm 1.40$  vs  $27.39 \pm 0.84$  mg,  $n=5$ ,  $**p<0.01$ ) and RV mass corrected for body weight (RV mass/body weight) ( $1.02 \pm 0.07$  vs  $1.46 \pm 0.03$  mg/g,  $n=5$   $***p<0.001$ ) in the vehicle group only (Figure 5.3). However, there was no significant difference between the vehicle and anastrozole treated hypoxic groups. RV/LV+S ratio was significantly increased in both hypoxic treatment groups compared to their normoxic controls (vehicle treated:  $0.26 \pm 0.02$  vs  $0.41 \pm 0.01$ ,  $n=5$ ,  $****p<0.0001$ , Anastrozole treated:  $0.28 \pm 0.01$  vs  $0.38 \pm 0.01$ ,  $n=4-5$ ,  $***p<0.001$ ). However, within the vehicle treated group, LV+S mass was significantly lower in the hypoxic animals ( $78.52 \pm 2.23$  vs  $67.25 \pm 2.34$  mg,  $n=5$ ,  $*p<0.05$ ) and within the anastrozole treated group LV+S mass/body weight was significantly decreased in the hypoxic animals ( $4.09 \pm 0.21$  vs  $3.45 \pm 0.08$ ,  $n=4-5$ ,  $*p<0.05$ ). LV+S mass was not significantly different between the hypoxic vehicle and hypoxic anastrozole groups.

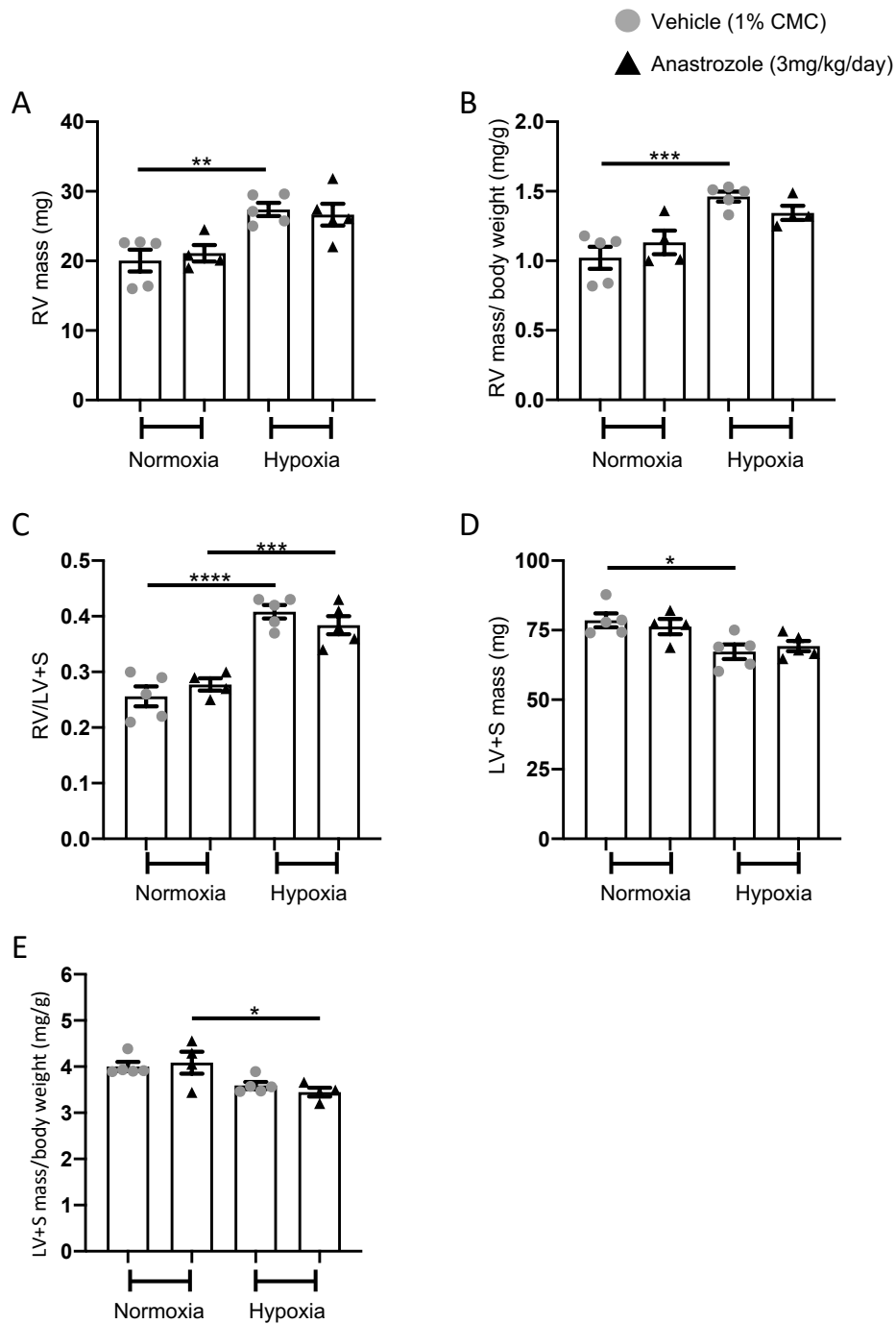


**Figure 5.3. The effect of hypoxic and treatment with Anastrozole (3mg/kg/day) on RV and LV+S mass in female C56Bl/6 mice.**

Mice were housed in normoxic or hypoxic conditions for 28 days and administered Anastrozole (3mg/kg/day) or vehicle (1% CMC) for the final 14 days. A) RV mass (mg) B) RV mass/body weight (mg/g). C) RV/LV+S. D) LV+S mass (mg) E) LV+S mass/body weight (mg/g).  $n=4-5$ , \* $p<0.05$ , \*\* $p<0.01$ , \*\*\* $p<0.001$ , \*\*\*\* $p<0.0001$ . Statistical analysis was performed using one-way ANOVA followed by Bonferroni post-hoc test. Data is displayed to show each individual  $n$  number and the bar represents the mean  $\pm$  S.E.M.

### 5.2.3 Anastrozole does not significantly affect RV or LV+S mass in male chronic hypoxia mice

The protocol at the end of the 28-day study varied slightly for the male mice. After the body weight was recorded, the mice were humanely culled, and tissue harvested. The heart was dissected in the same manner as the female mice - RV was finely dissected from the LV+S. RV mass and LV+S mass was recorded (Figure 5.4). Hypoxia did not significantly increase RV mass in the vehicle or anastrozole treated groups. However, when RV mass was corrected for body weight (RV mass (mg)/body weight (g)), hypoxia had a significant effect in the vehicle treated group ( $0.91 \pm 0.03$  vs  $1.26 \pm 0.05$  mg/g,  $n=5$ ,  $*p<0.05$ ). The Fulton's index RV/LV+S was significantly increased in both hypoxic groups compared to their normoxic counterparts (vehicle treated:  $0.24 \pm 0.01$  vs  $0.37 \pm 0.01$ ,  $n=5$ ,  $****p<0.0001$  anastrozole treated:  $0.23 \pm 0.004$  vs  $0.39 \pm 0.01$ ,  $n=4-5$ ,  $****p<0.0001$ ). However once again, hypoxia significantly affected the LV+S. LV+S mass measurements showed that LV+S mass and LV+S mass corrected for body weight was significantly decreased in the Anastrozole treated hypoxic group compared to normoxia (LV+S mass:  $117.88 \pm 10.60$  vs  $87.18 \pm 2.80$  mg,  $n=4-5$ ,  $**p<0.01$ , LV+S mass/body weight  $4.48 \pm 0.36$  vs  $3.40 \pm 0.08$  mg/g,  $n=4-5$ ,  $**p<0.01$ ). There was no significant difference in LV+S mass between the different treatment groups.

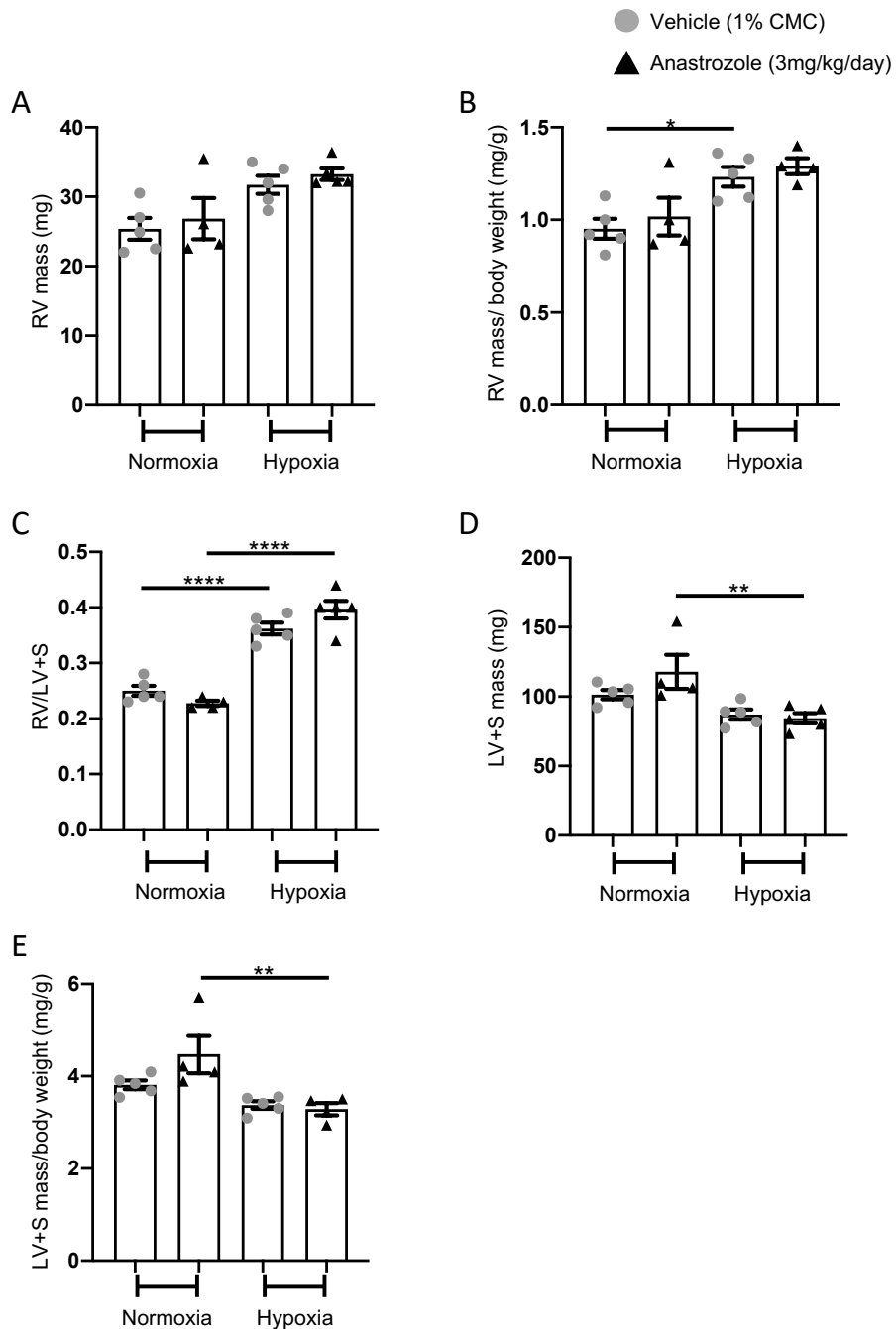


**Figure 5.4.** The effect of hypoxic and treatment with Anastrozole (3mg/kg/day) on RV and LV+S mass in male C56Bl/6 mice.

Mice were housed in normoxic or hypoxic conditions and administered Anastrozole (3mg/kg/day) or vehicle (1% CMC). RV mass (mg) B) RV mass/body weight (mg/g). C) RV/LV+S. D) LV+S mass (mg) E) LV+S mass/body weight (mg/g).  $n=4-5$ ,  $*p<0.05$ ,  $**p<0.01$ ,  $****p<0.0001$ . Statistical analysis was performed using one-way ANOVA followed by Bonferroni post-hoc test. Data is displayed to show each individual  $n$  number and the bar represents the mean  $\pm$  S.E.M.

#### 5.2.4 Expression studies in the male and female mouse RV.

As described, the previous study by the lab group had shown treatment with Anastrozole (3 mg/kg/day) was capable of significantly decreasing RVSP and RVH in the female chronic hypoxia mouse model (Mair et al., 2014b). Therefore, the aim prior to commencing the study was to investigate the effect of Anastrozole on the RV. However, in this current study Anastrozole had no significant effect on RVSP or RV/LV+S. For this reason, it was determined that the effect of Anastrozole on the RV was not the most informative investigation at this stage. Sex-specific expression profiles in the rat RV had been identified during the rat RV investigation. Therefore, the aim was to conduct a similar analysis in this mouse model in order to identify if these findings were apparent in different rodents.

#### 5.2.5 Protein expression of Id1 and Id3 is significantly different between the male and female normoxic RV

BMPR2 dysfunction is the strongest risk factor in the development of PAH (Fessel et al., 2011) and recent studies have also shown that increased RV dysfunction is associated with BMPR2 mutation (van der Bruggen et al., 2016) indicating that BMPR2 signalling in the RV could influence clinical outcomes. Therefore, investigation of BMPR2 signalling in the RV could develop our understanding of how this could impact clinical outcomes. The gene expression of *Bmpr2*, *Smad1*, *Id1* and *Id3* gene expression was compared in male and female normoxic RV. There were no significant differences in the gene expression of the BMPR2 pathway components between the male and female normoxic RV (Figure 5.5). When the protein expression was compared, analysis showed that expression of ID1 and ID3 was significantly downregulated in the female RV compared to the male RV (ID1  $0.00073 \pm 0.00032$  vs  $0.00330 \pm 0.00041$ , n=5, \*\*p<0.001, ID3  $0.00189 \pm 0.00044$  vs  $0.00380 \pm 0.00029$ , n=5, \*\*p<0.001) (Figure 5.6).

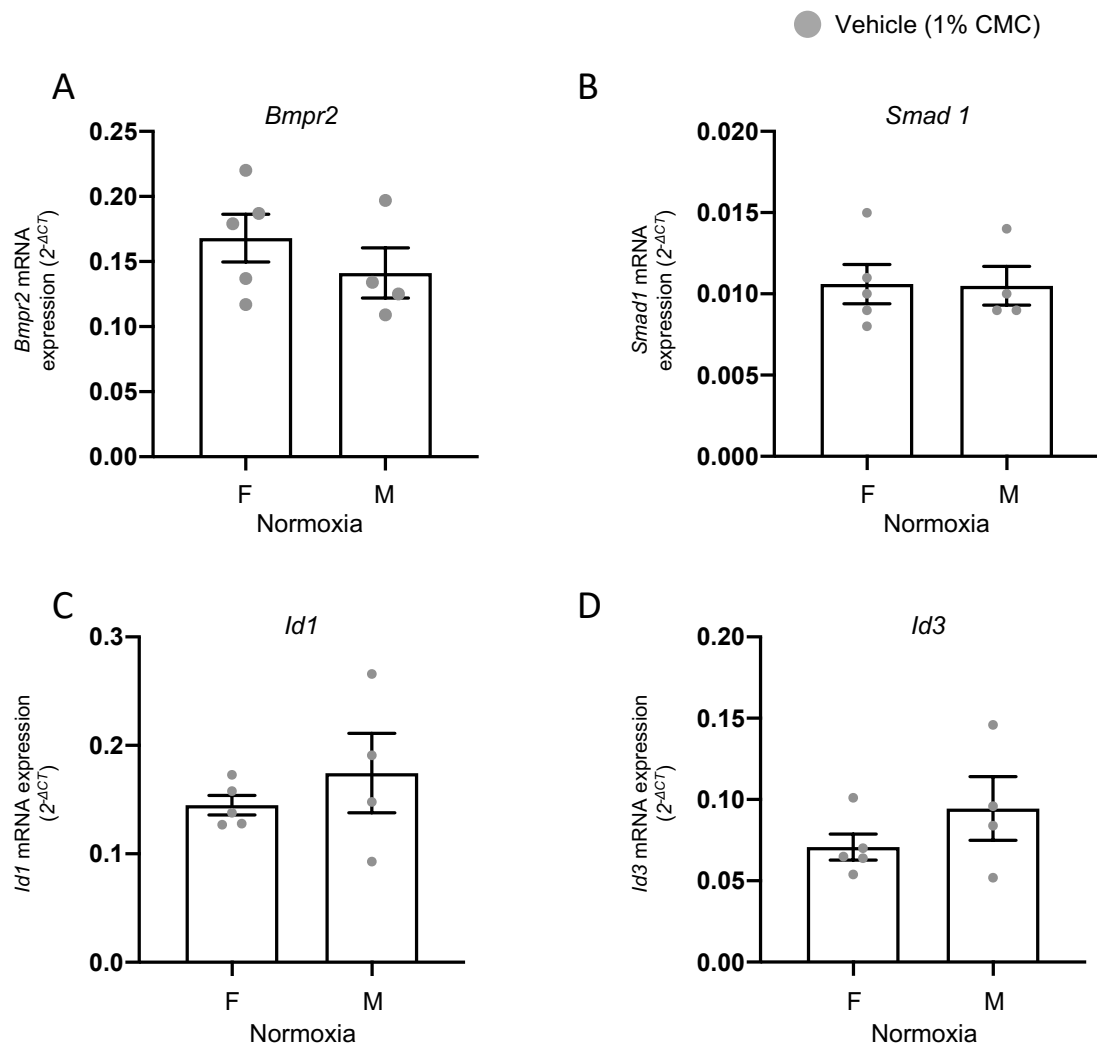


**Figure 5.5. Differential gene expression between the male and female normoxic mouse RV.**

TaqMan qRT-PCR was performed on RV tissue harvested from male and female mice maintained in normoxia and treated with vehicle (1% CMC). A direct comparison between normoxic male and normoxic female RV is carried out for each of the genes investigated. A) *Bmpr2* gene expression. B) *Smad1* gene expression C) *Id1* gene expression D) *Id3* gene expression. E) *CYP1b1* gene expression. Data is displayed as  $2^{-\Delta CT}$  and data was normalised to the expression of B2M.  $n=4-5$  per group, repeated in triplicate. Statistical analysis was performed using un-paired *t* test  $*p<0.05$ . Data is displayed to show each individual *n* number and the bar represents the mean  $\pm$  S.E.M.

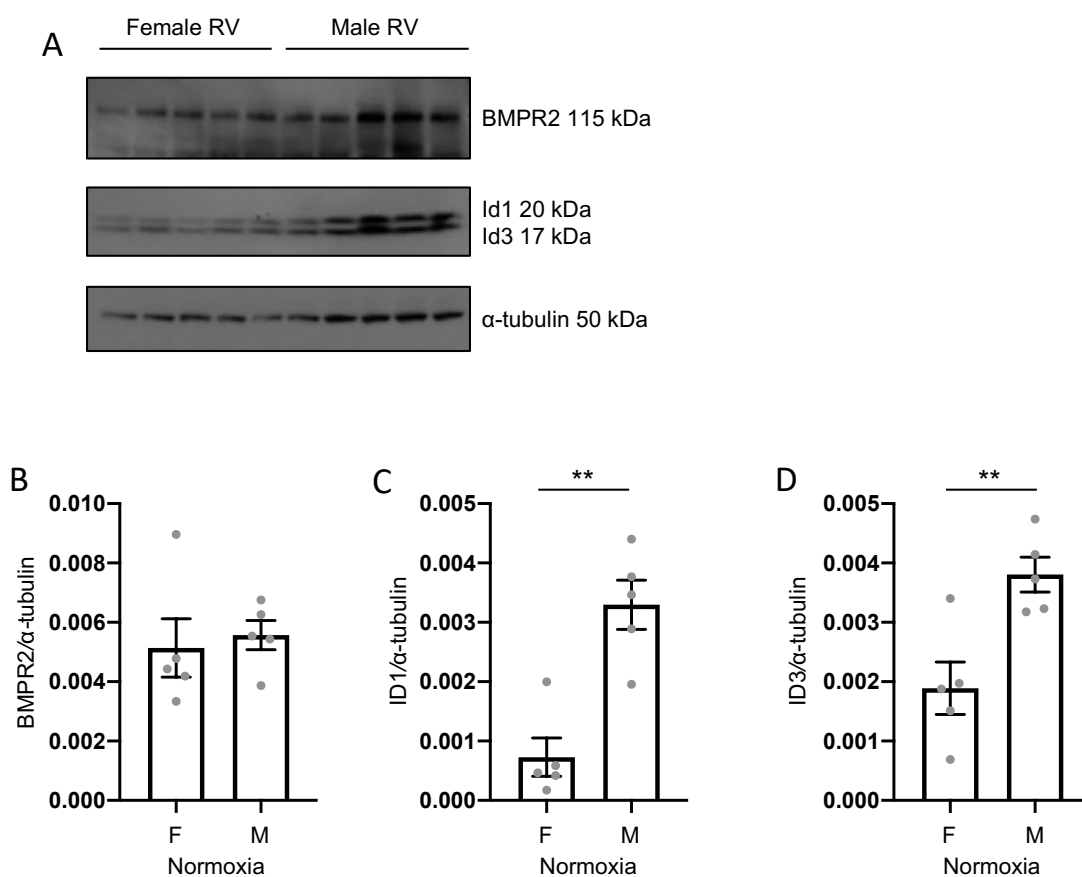


**Figure 5.6 Protein expression of BMPR2, ID1 and ID3 in the normoxic male and female mouse RV.**

Male and female mice were maintained in normoxia and treated with vehicle (1% CMC). Protein expression in the RV was investigated by western blot. A) Representative immunoblot. Densitometric analysis of B) BMPR2 C) ID1 and D) ID3 protein expression in the RV.  $\alpha$ -tubulin was used as a loading control.  $n=5$  per group, 1 technical replicate. Statistical analysis was performed using unpaired  $t$  test  $**p<0.01$ . Data is displayed to show each individual  $n$  number and the bar represents the mean  $\pm$  S.E.M.

### **5.2.6 CYP1b1, ER- $\alpha$ and Aromatase are expressed in the male and female mouse RV but expression is not significantly different between males and females**

Next the expression of proteins involved in the production and metabolism of estrogen as well as the estrogen signalling pathway were investigated. The gene expression of *Cyp1b1* was compared in normoxic male and female mouse RV by TaqMan qRT-PCR. There was no significant difference in *Cyp1b1* expression between males and females (Figure 5.7). Following this, the protein expression of CYP1B1, ER- $\alpha$  and Aromatase were all investigated by western blot in the male and female RV. The key finding was that both the male and female mouse RV express each of these proteins (Figure 5.8). However, densitometric analysis did not show any significant difference in the expression of CYP1b1, ER- $\alpha$  or aromatase between the male and female mouse RV.

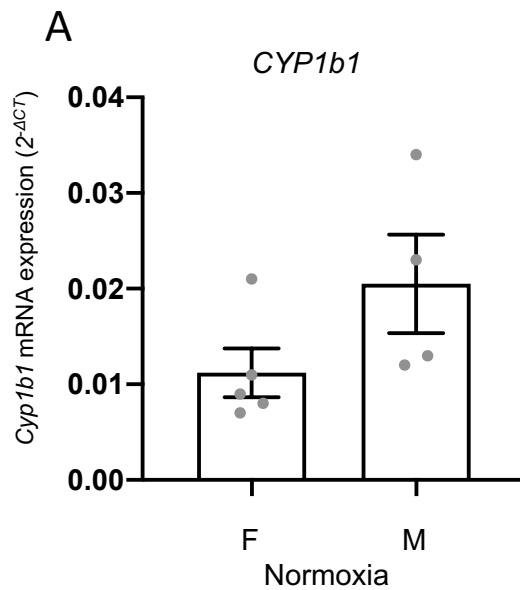


**Figure 5.7.** *Cyp1b1* gene expression in the male and female normoxic mouse RV.

TaqMan qRT-PCR was performed on RV tissue harvested from male and female mice maintained in normoxia and treated with vehicle (1% CMC). A direct comparison between normoxic male and normoxic female RV was carried out. A) *CYP1b1* gene expression. Data is displayed as  $2^{-\Delta CT}$  and data was normalised to the expression of B2M.  $n=4-5$  per group, repeated in triplicate. Statistical analysis was performed using un-paired  $t$  test  $*p<0.05$ . Data is displayed to show each individual  $n$  number and the bar represents the mean  $\pm$  S.E.M.

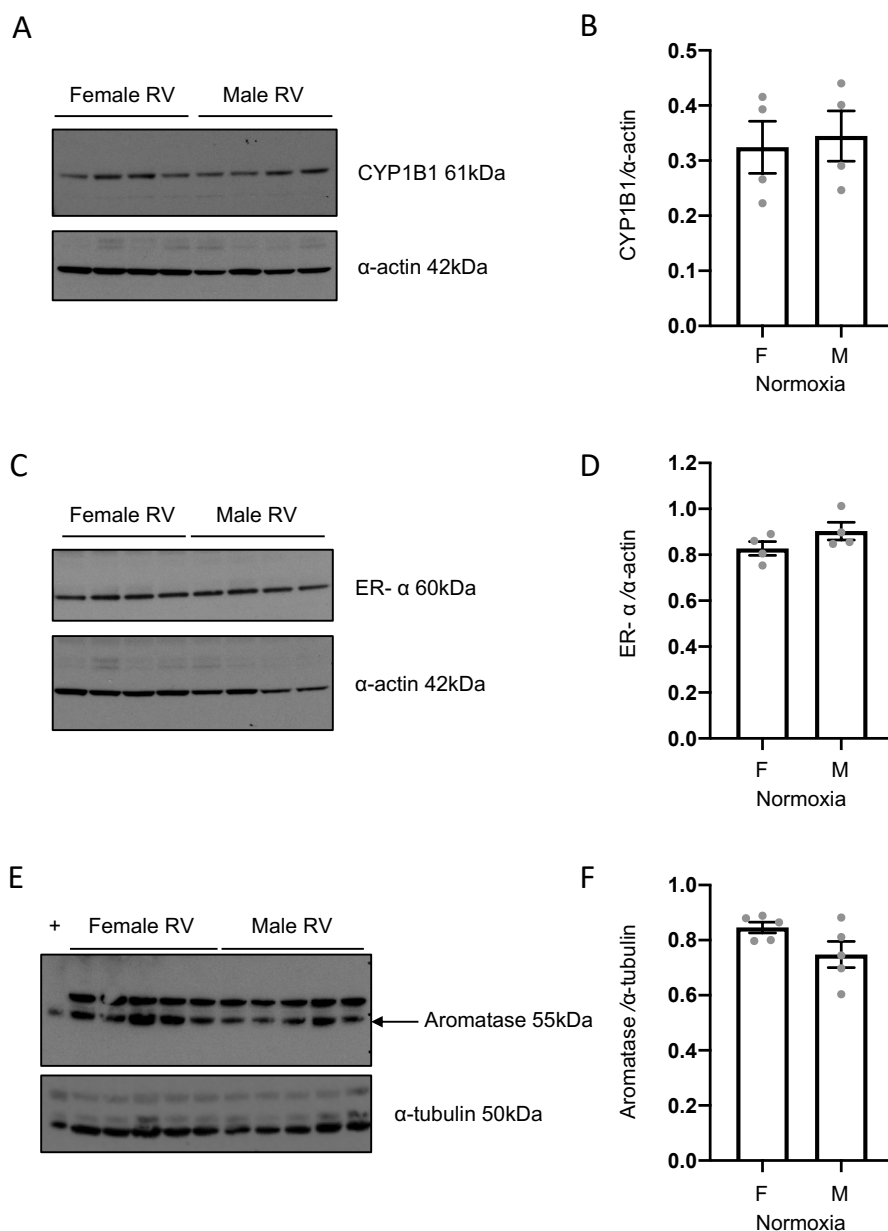


**Figure 5.8 Protein expression in the male and female mouse normoxic RV.**

Male and female mice were maintained in normoxia and treated with vehicle (1% CMC). Protein expression in the RV was investigated by western blot. A) CYP1b1 expression - representative immunoblot B) Densitometric analysis of CYP1b1 protein expression in the RV. C) ER- $\alpha$  expression - representative immunoblot. D) Densitometric analysis of ER- $\alpha$  protein expression in the RV.  $\alpha$ -actin was used as a loading control.  $n=4$  per group. E) Aromatase expression - representative immunoblot. Positive control (+) - mouse uterus tissue. F) Densitometric analysis of Aromatase protein expression in the RV.  $\alpha$ -tubulin was used as a loading control,  $n=5$  per group, 1 technical replicate. Data is displayed to show each individual  $n$  number and the bar represents the mean  $\pm$  S.E.M.

## **5.2.7 Investigation of the effect of estrogen on the migration of pulmonary artery smooth muscle cells**

### **5.2.7.1 The expression of ER- $\alpha$ and ER- $\beta$ in male and female rat PASMCs.**

The final aim of this chapter was to investigate the effect of estrogen on the migration of PASMCs. Briefly, the left lung lobe was removed from male and female rat post-mortem and the main pulmonary artery (PA) dissected from the lung. The PA was digested using a solution including elastase and collagenase and the resultant cells were filtered and plated for cell culture purposes.

Prior to investigating the effect of estrogen, it was necessary to confirm expression of estrogen receptors ER- $\alpha$  and ER- $\beta$  in male and female rat PASMCs under basal conditions. Protein was extracted from the cells and the expression of the estrogen receptors was confirmed using western blot (Figure 5.9). Both male and female rat PASMCs expressed ER- $\alpha$  and ER- $\beta$ .

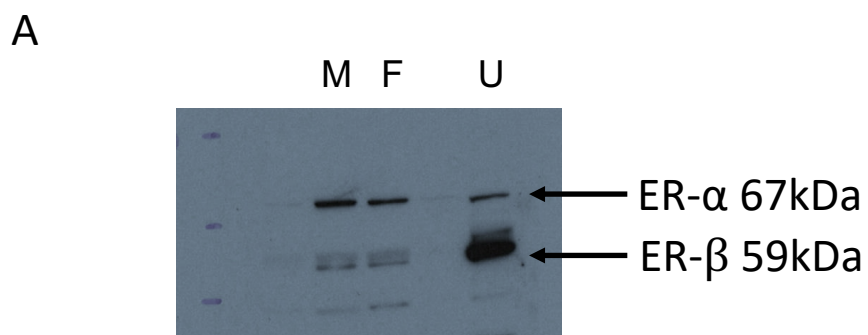


*Figure 5.9. Expression of ER- $\alpha$  and ER- $\beta$  in male and female rat PSMCs.*

*The protein expression of ER- $\alpha$  and ER- $\beta$  in male (M) and female (F) rat PSMCs under basal conditions was assessed by western blot. A) Representative immunoblot showing the expression of ER- $\alpha$  and ER- $\beta$ . Uterus (U) was used as a positive control. This was performed by Dr. Katie Harvey.*

### 5.2.7.2 The effect of varying serum conditions on the migration of rat PSMCs.

The aim of this assay was to assess PSMC migration in response to stimulation with  $17\beta$ -estradiol and estrogen metabolite,  $16\alpha$ -OHE1. As estrogens were being added to these cells as a stimulant the DMEM and serum used in the cell culture experiments had to be optimised. Fetal bovine serum has been shown to contain estrogens (Reynolds et al., 1982) therefore, a charcoal stripping process can be performed on FBS to remove any endogenous estrogenic compounds from the serum. Charcoal is used to strip non-polar compounds from FBS including hormones. Additionally, phenol red present in most DMEM has been shown to act as a weak estrogenic mimic (Welshons et al., 1988). Consequently, FBS and phenol red media can influence cell culture estrogen stimulations and it is favourable to use charcoal stripped FBS in phenol red free DMEM when performing hormone stimulations. Therefore, prior to beginning cell stimulations with estrogen the effect of varying DMEM media and serum conditions on cell migration was tested.

First, cells were allowed to reach full confluence before a physical scratch was induced in the cell monolayer. Images at 0 hr (the time the scratch was induced) and at 24 hr were captured. The bottom of the well was marked to ensure the same area of the scratch was captured at each time point. The area of a small section of the scratch indicated by the line drawn on the bottom of the well was measured at 0 hr and 24 hr and the % wound closure calculated  $0 - 24 \text{ hr area} / 0 \text{ Hr} * 100$ .

The migration assay showed that 10% FBS in phenol red free DMEM induced the greatest migratory response in male PSMCs (78% wound closure, n=1) (Figure 5.10, Figure 5.11). Both 10% charcoal stripped serum in phenol red free DMEM and 10% FBS in phenol red DMEM were capable of inducing a migratory response (44%, 57% wound closure, n=1), however, this was to a lesser extent. The 1% serum controls were similar across the 3 different groups (22%, 20% and 27% wound closure, n=1).

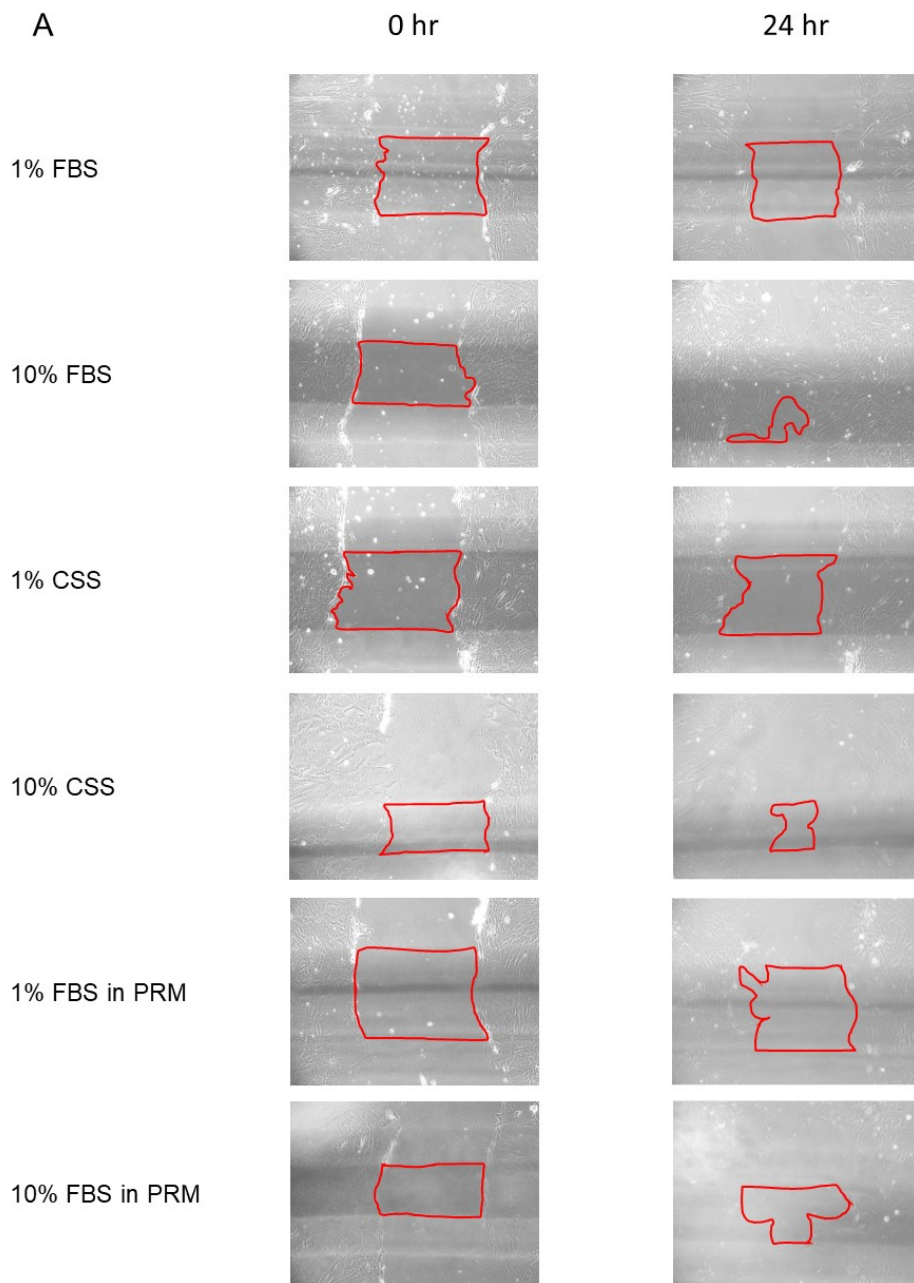


**Figure 5.10.** *The effect of serum and DMEM on the migration of male rat PASCs.*

Rat PASCs were grown to a confluent monolayer and serum starved for 24 Hr before a scratch was induced in the monolayer. Cells were grown in varying conditions - 1% fetal bovine serum (FBS), 10% FBS, 1% charcoal stripped serum (CSS), 10% CSS, 1% FBS in phenol red media (PRM) and 10% FBS in PRM for 24 hr. The area of a section of the scratch was measured at 0 hr and again at 24 hr. The % wound closure is calculated by  $0 \text{ hr} - 24 \text{ hr area} / 0 \text{ hr} * 100$ . n=1. A) Representative images highlighting the area of the scratch at 0 hr and 24 hr times points.

A

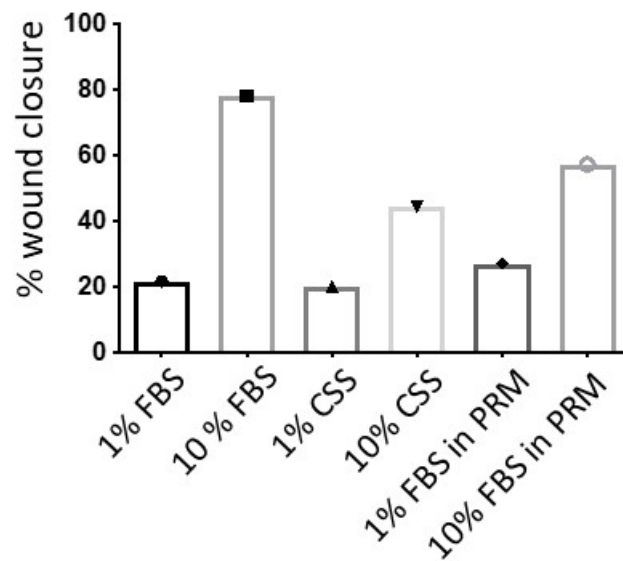


**Figure 5.11.** *The effect of serum and DMEM on the migration of male rat PASCs.*

Rat PASCs were grown to a confluent monolayer and serum starved for 24 Hr before a scratch was induced in the monolayer. Cells were grown in varying conditions - 1% fetal bovine serum (FBS), 10% FBS, 1% charcoal stripped serum (CSS), 10% CSS, 1% FBS in phenol red media (PRM) and 10% FBS in PRM for 24 hr. The area of a section of the scratch was measured at 0 hr and again at 24 hr. The % wound closure is calculated by  $0 \text{ hr} - 24 \text{ hr area} / 0 \text{ hr} * 100$ .  $n=1$ . A) % wound closure for each of the conditions. Data is displayed to show the individual  $n$  number.

### 5.2.7.3 The effect of $17\beta$ -estradiol and $16\alpha$ -OHE1 on the migration of PSMCs

Having confirmed that the use of phenol red free DMEM and charcoal stripped serum should not prevent the migration of PSMCs, the subsequent aim was to stimulate male and female PSMCs with E2 and  $16\alpha$ -OHE1 at physiologically relevant concentrations and assess the migration of the cells. Male and female PSMCs were stimulated with  $17\beta$ -estradiol (E2) at 1 nM and 10 nM and  $16\alpha$ -OHE1 at 1 nM and 10 nM for 24 hr (Figure 5.12). Similar to the previous assay, a scratch was induced in the cell monolayer at 0 hr and the area of a section of the scratch at 0 hr and 24 hr measured from images captured and the % wound closure calculated. However, the 10% charcoal stripped serum positive control did not induce an increased % wound closure as was expected in either the male or the female PSMCs. Furthermore, there was no significant effect of E2 or  $16\alpha$ -OHE1 on % wound closure in the female PSMCs. Migration analysis was only carried out in n=1 for the male PSMCs and therefore, it is not possible to comment on statistically significant results.

As investigation of the effect of FBS vs charcoal stripped serum had shown FBS was capable of inducing migration of PSMCs to a greater extent than charcoal stripped serum, the experiment was repeated utilising FBS (Figure 5.13). Cell stimulations were carried out in 1% FBS and 10% FBS was used as a positive control. 10% FBS significantly increased % wound closure compared to the 1% FBS basal control in female PSMCs (female  $13.89 \pm 2.02$  vs  $81.82 \pm 3.65$  %, n=3, \*\*\*\*p<0.0001). The success of the positive control confirmed the cells were capable of migration and the assay design was able to detect % wound closure. However, both E2 (1 nM) and  $16\alpha$ -OHE (1 nM) did not affect % wound closure in female PSMCs. The ethanol (EtOH) vehicle control was not significantly different from the 1% FBS control indicating that the EtOH vehicle does not affect the migration of these cells.

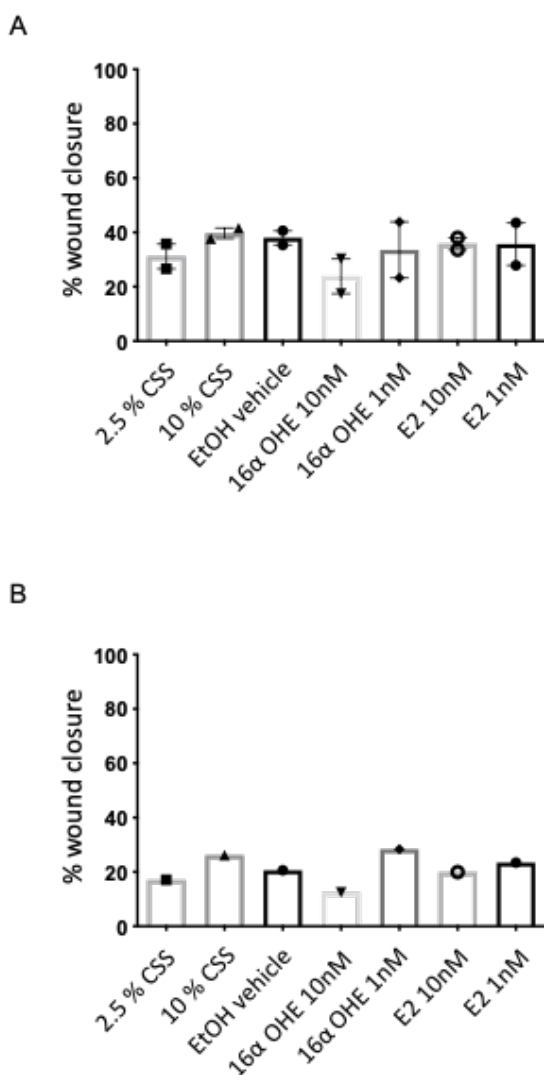


**Figure 5.12.** The effect of 17 $\beta$ -estradiol and 16 $\alpha$ -OHE1 on the migration of male and female rat pulmonary artery smooth muscle cells in charcoal stripped serum.

Rat PASMCs were grown to a confluent monolayer and serum starved for 24 Hr before a scratch was induced in the monolayer. Cells were stimulated for 24 Hrs with 16 $\alpha$ -OHE1 1nM, 16 $\alpha$ -OHE1 10nM, 17 $\beta$ -estradiol (E2) 1nM or E2 10nM for 24hours in 2.5% charcoal stripped serum (CSS) DMEM. The area of a section of the scratch was measured at 0 hr and again at 24 hr. The % wound closure is calculated by  $0 \text{ hr} - 24 \text{ hr area} / 0 \text{ hr} * 100$ . A) Female rat PASMCs. n=2. B) Male rat PASMCs. n=1. Data is displayed to show each individual n number and the bar represents the mean  $\pm$  S.E.M.

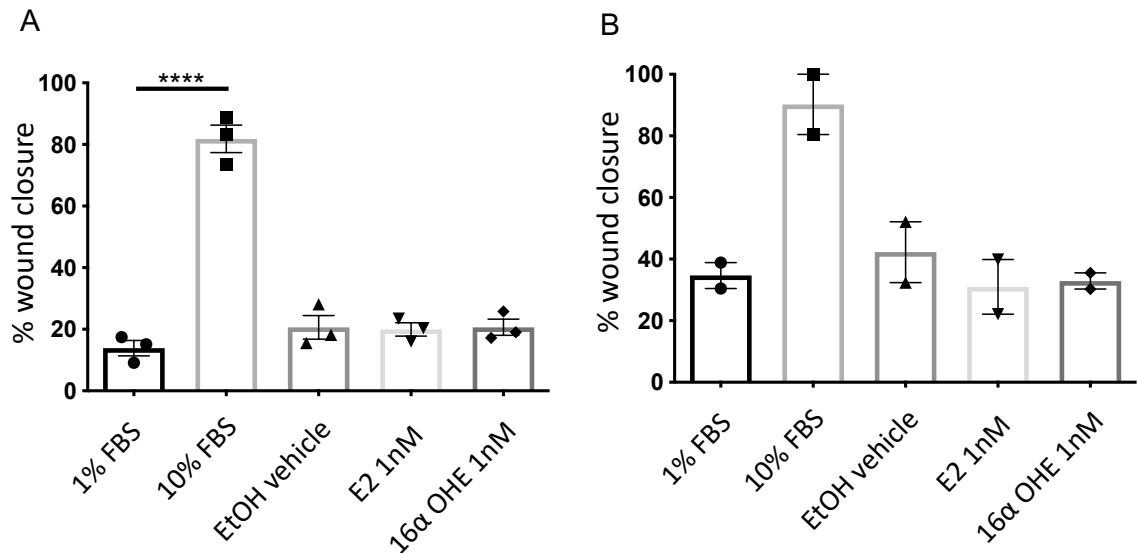


**Figure 5.13.** The effect of 17 $\beta$ -estradiol and 16 $\alpha$ -OHE1 on the migration of male and female rat pulmonary artery smooth muscle cells in charcoal stripped serum and FBS.

Rat PAMSCs were grown to a confluent monolayer and serum starved for 24 hr before a scratch was induced in the monolayer. Cells were stimulated for 24 hr with 16 $\alpha$ -OHE1 1nM, 16 $\alpha$ -OHE1 10nM, 17 $\beta$ -estradiol (E2) 1nM or E2 10nM for 24 hr in 2.5% charcoal stripped serum (CSS) DMEM. The area of a section of the scratch was measured at 0 hr and again at 24 hr. The % wound closure is calculated by  $0 \text{ hr} - 24 \text{ hr area} / 0 \text{ hr} \times 100$ . A) Female rat PAMSCs.  $n=3$  \*\*\*\* $p < 0.0001$ . B) Male rat PAMSCs  $n=2$ . Statistical analysis was performed using one-way ANOVA followed by Bonferroni post-hoc test. Data is displayed to show each individual  $n$  number and the bar represents the mean  $\pm$  S.E.M.

### 5.3 Discussion

Despite an increasing number of studies in the area, the role of estrogen in the development and progression of PAH is still not fully elucidated. Recent literature has indicated a pathogenic effect of estrogen in the pulmonary vasculature (Mair et al., 2014b; White et al., 2012; Rajkumar et al., 2010). Further complexity is added to interrogating the role of estrogen as studies have also shown contradictory effects in the lung and the right ventricle. Animal studies have highlighted a protective effect of estrogen in the RV with females of the SuHx rat model displaying improved cardiac output and RVEF (Liu et al., 2014; Frump et al., 2015). Inhibiting the production of endogenous estrogens with the use of aromatase inhibitors, such as Anastrozole, is being investigated as potential therapeutics for the treatment of PAH. The effect of these therapies on the RV has to be carefully monitored as ultimately RV dysfunction is the main cause of mortality in the PAH patient population.

In this chapter, the key aim was to investigate the role of estrogen in the development of PH and in the RV. Initially, the effect of Anastrozole on PH phenotype was assessed. The chronic hypoxia mouse model was utilised as Anastrozole was effective at reducing RVSP and RVH in female mice of this rodent model (Mair et al., 2014b). In the current study, treatment with Anastrozole (3 mg/kg/day) did not significantly reduce RVSP or RVH in female mice. RVH in male mice was not influenced by the administration of Anastrozole similar to the finding by Mair et al. (2014). The chronic hypoxic model and the dosing protocol were identical between the 2 studies. However, the current study involved lower *n* numbers in each of the groups compared to the 8-10 animals per group in the previous study. There was a slight trend emerging in the female hypoxic group that the Anastrozole treated group had lower RV/LV+S compared to the vehicle treated group. An increase in *n* numbers in this study may have been able to statistically confirm or refute this trend. Although, the RVSP in both the vehicle and Anastrozole treated female mice was similar. In an attempt to identify if Anastrozole had been effective in these mice, lung BMPR2 expression levels were investigated. Previous studies have shown hypoxia decreases lung BMPR2 expression and Anastrozole is capable of restoring expression (Mair et al., 2014b). Gene and protein expression analysis did not provide evidence to confirm this effect of Anastrozole. Measuring circulating

estrogen levels within the plasma of the female mice at the end of the study would have allowed confirmation that Anastrozole treatment was effective at inducing a reduction in endogenous estrogen production.

The hypothesis at the beginning of this study was that Anastrozole treatment would significantly reduce RVH in the female mice and the studies following would further investigate the effect of Anastrozole on RV signalling pathways. However, as Anastrozole had no significant effect on RVH the aim of the study was adapted to focus on sex-specific differences in gene and protein expression in the normoxic RV. This investigation combined with the data produced in the rat model (Chapter 3), would confirm if sex-specific differences were apparent across multiple rodent models. An understanding of the male and female RV under normal conditions could identify key differences in signalling pathways that may account for the differing responses in the diseased state.

Once again, the BMPR2 pathway was selected as a candidate pathway as mutations in the BMPR2 gene is one of the most well-established risk factors for developing PAH. Despite dysfunctional BMPR2 signalling being well characterised in the lung, the downstream effects in the RV are not so well understood. The results of the current study showed that although there was no significant difference in the gene expression of the BMPR2 pathway, at a protein level Id1 and Id3 were significantly reduced in the female mouse RV. These results suggest that under normal physiological conditions BMPR2 signalling is downregulated in the female RV. Downregulation of the BMPR2 signalling pathway has been identified in female PSMCs compared to male PSMCs (Mair et al., 2015). It was suggested this could be related to the predisposition of the female sex to develop PAH. This finding is concordant in that female RV also showed downregulation of the downstream components of the BMPR2 signalling pathway and therefore could also contribute to female susceptibility. Additionally, the disparity between gene expression and protein levels suggests that there could be differential post-translational modifications in male and female RV. Further studies would be required to confirm and fully understand the significance of this finding however it does highlight that there are significant, gender-specific differences between the male and female RV. Importantly, these changes occur in a pathway that has been identified as having

a key role in the development of PAH. To further develop this hypothesis, key assessments would involve a comparison of the BMPR2 pathway expression in male and female RV in the chronic hypoxia mouse model. Additionally, it may also be beneficial to assess RV function in male and female mutant BMPR2 transgenic mice with conditional KO in lung vs heart.

The ability of the RV to synthesise and metabolise estrogen and also the potential for estrogen signalling within the RV was assessed. In order to do this, the expression of CYP1B1, ER- $\alpha$  and aromatase was investigated. Gene expression analysis showed the expression of *Cyp1b1* was similar between male and female RV. Expression of aromatase, CYP1b1 and ER- $\alpha$  proteins confirmed the potential for the synthesis, metabolism and signalling of estrogens with the male and female mouse RV. The protein expression was not significantly different between the sexes. Currently, estrogen synthesis, metabolism and signalling in the right ventricle specifically are largely unexplored. Additionally, the effect of treatment with Anastrozole on the RV of PAH patients is not fully elucidated. Although, the Phase II clinical trials conducted by Kawut et al. (2017) did show that Anastrozole treatment did not negatively impact the parameters of RV functionality assessed (Kawut et al., 2017). The ongoing clinical trial being carried out by the same group, will provide a larger patient group in which this can be confirmed. Having highlighted the potential for differential BMPR2 signalling in the male and female mouse RV, the effect of Anastrozole on BMPR2 signalling in the RV of pre-clinical models of disease could be an interesting focus for future studies.

Finally, the ability of E2 and 16 $\alpha$ -OHE1 to stimulate migration of male and female rat PSMCs was assessed. Preliminary studies highlighted that 10% CSS media was able to stimulate migration of male or female rat PSMCs but not to the same extent as 10% FBS. Initial cell culture stimulations were carried out in CSS but assessment of the migration of these cells showed no difference across any of the conditions including the 10% CSS which was included as a positive control. The effect of the positive control differed from the preliminary investigations, however it does perhaps suggest that the charcoal stripping process removes factors from the FBS that contribute to the migratory potential of cells. The process removes lipophilic molecules from the serum such

as growth factors (Tu et al., 2018). Although it is preferable that cell culture experiments involving estrogen be carried out in CSS, the final stimulations were performed using FBS to supplement the DMEM. This could be a limitation of this work as we do not know how any endogenous hormones in the FBS will influence the effect of E2 and 16 $\alpha$ -OHE1.

When supplementing the DMEM with 1% FBS, E2 (1 nM) and 16 $\alpha$ -OHE1 (1 nM) had no significant effect on the migration of female RPASMCs. Although statistical analysis could not be completed on the male RPASMCs data, the trend is the same in that E2 and 16 $\alpha$ -OHE1 had no effect on migration. These concentrations of E2 and 16 $\alpha$ -OHE1 were selected as they are physiologically relevant. E2 circulating levels in pre-menopausal women range from 30-400 pg/mL depending on the stage of the menstrual cycle (Becker, 2008), however levels are much lower in posts-menopausal women at < 10pg/mL (Modugno et al., 2006). 16 $\alpha$ -OHE1 circulating levels range from 295 pg/mL in post-menopausal women to 360 pg/mL in pre-menopausal women (Arslan et al., 2014; Modugno et al., 2006; Jernstrom et al., 2003). E2 and 16 $\alpha$ -OHE1, at the same concentration used in this study (1 nM), induce proliferation of PSMCs (Wright et al., 2015; White et al., 2012), however, there is very little known about the effect of estrogen or estrogen metabolites on the migration of PSMCs. In vascular smooth muscle cells E2 at a concentration of 10 nM reduces TNF- $\alpha$  induced proliferation and migration (Li et al., 2016a). E2 at 10 nM concentration has also been shown to inhibit lipopolysaccharide induced vascular SMC migration and serum induced migration in rat aortic VSMCs (Jiang et al., 2010; Zheng et al., 2015). PSMCs have a different phenotype and behaviour to other vascular beds with regards to proliferation and therefore it is possible their migratory response is also different (Frid et al., 1997). E2 (10 nM) has been shown to stimulate migration in other cell types such as endometriotic epithelial cells (Qi et al., 2018). Future studies could follow to assess whether E2 and 16 $\alpha$ -OHE1 have an inhibitory effect on the migration of PSMCs.

In summary, this data highlighted sex-dependent differences in the protein expression of ID1 and ID3, the downstream proteins involved in BMPR2 signalling. Although these findings are preliminary, they do fit with the hypothesis that basal differences in BMPR2 signalling may contribute to the susceptibility of

females to the development of PAH. Moreover, investigation of rat PASMCs highlighted that E2 and 16 $\alpha$ -OHE1 are not capable of stimulating migration in either male or female cells under the conditions utilised. As therapeutics targeting BMPR2 and estrogen synthesis are currently under investigation for the treatment of PAH, it is important to enhance our understanding of their potential effects in the pulmonary vasculature and RV.

## **6 General Discussion**

## 6.1 General Discussion

PAH is a devastating and currently incurable disease which results from pathological remodelling of the pulmonary vasculature. These pathological changes lead to an increased afterload experienced by the RV which eventually results in right heart dysfunction and ultimately right heart failure. PAH registries have identified key characteristics of the patient population which have influenced the study of this disease. The REVEAL registry highlighted approximately 80% of the PAH population are female (Badesch et al., 2010). This suggested that females were more susceptible to disease and indicated a role for female sex hormones in the development of disease. Subsequent research has followed which has uncovered pathogenic effects of estrogen in the pulmonary vasculature (Mair et al., 2014b; White et al., 2012; Rajkumar et al., 2010). However, there have been contradictory studies which have indicated a protective effect for estrogen in the lung (Xu et al., 2010; Lahm et al., 2012; Umar et al., 2011). The effect of estrogen on the RV is largely unexplored.

The other major risk factor in the development of PAH is abnormal BMPR2 signalling (Fessel et al., 2011). Mutations in BMPR2 have been identified in both heritable and idiopathic versions of the disease (Machado et al., 2009). Patients harbouring BMPR2 mutations are more likely to present with worse disease progression at a younger age (Evans et al., 2016a). Aberrant BMPR2 signalling results in a decrease in anti-proliferative ID1 and ID3 which act as inhibitors of DNA binding preventing differentiation and proliferation (Morrell et al., 2009). BMPR2 dysfunction is better understood in the lung where it is known to lead to increased proliferation of PASMCs. Sex differences in the expression of BMPR2 have been identified which could also be related to increased susceptibility in females (Mair et al., 2015). However, the role of BMPR2 in the RV is not well understood.

Current therapies are all targeted towards the increased vasoconstriction present in the PAH lung (Ryan et al., 2015). There is a real need to identify new therapeutic targets which are capable of reversing the pathological remodelling of the pulmonary vasculature or the dysfunction of the RV.

The key aims of this thesis were to investigate the sex-dependent and RV-specific effects of potential PAH therapies that are undergoing clinical trials. It is more common in rare, orphan diseases such as PAH that drugs licensed for another uses are considered as potential therapies. A recent study identified that FK506, an FDA approved drug currently licensed for use as an immunosuppressant in organ transplantation, was able to increase the expression of BMPR2 (Spiekerkoetter et al., 2013). Investigations in three different rodent models showed FK506 treatment improved the key parameters of PH disease phenotype. However, there was a need to identify the sex-dependent effects of this therapy as this had not yet been investigated. Published studies have identified sex-specific differences in the BMPR2 pathway in rodent models as well as human PSMCs with females displaying lower levels of expression (Mair et al., 2015). Although this sex difference has not been fully elucidated in the chronic hypoxia rat model it was hypothesised that female rats may respond differently to FK506-induced increases in BMPR2 expression as their basal levels could be lower.

Chapter 3 investigated the effects of FK506 treatment on the development of PAH. During this investigation the 5-week chronic hypoxia rat model was characterised as this model had not previously been used within the lab group. This model was confirmed as an appropriate model for the investigation as all the PH phenotype parameters measured corresponded to previous models utilised by the lab (Docherty et al., 2019; Mair et al., 2014; Dean et al., 2018). Treatment with FK506 had not previously been investigated in this rodent model. FK506 was not capable of reducing RVSP or pulmonary artery remodelling. The slow releasing pellets which were utilised to administer FK506, released the drug at a dose appropriate to their weight at the beginning of the study. One limitation of this study was that the concentration of FK506 did not increase with the weight gain of the animals throughout the 3-week dosing period. Additionally, weight gain was lower in the female rats across the 3-week dosing period as a result it would not be appropriate to directly compare males and females as it is likely the doses were not equivalent. This could have been further investigated had plasma FK506 concentrations have been monitored at the end of the study. Other studies by the lab group have utilised slow releasing pellets for the administration of 2-methoxyestradiol in male and female rats and

effects have been apparent in males and females regardless of the inevitable greater weight gain in male animals (Docherty et al., 2019).

Chapter 4 focused on a cardiac-specific investigation of the sex specific effects of FK506 treatment. It is currently unknown if FK506 treatment affects BMPR2 signalling in the RV and consequently how this affects RV function in a PH model. RV/LV+S significantly increased in hypoxia, however, treatment with FK506 did not influence RV/LV+S measurements. When RV mass was assessed in isolation, there was a significant decrease in the FK506 treated hypoxic group in males only. This finding was also apparent when the RV mass was corrected for body weight. Although RV/LV+S is the standard measure within the field, it may have more been appropriate to measure tibial length in this study to confirm the effects of FK506 on the male RV (Yin et al., 1982). This reduction in RV mass was also independent of any significant changes in RVSP, which could suggest a direct effect of FK506 on the RV. Furthermore, this was a sex-dependent effect as FK506 had no significant effect on RV mass, RV mass/body weight or RV/LV+S in the female hypoxic rats. Treatment with FK506 also significantly reduced the expression of *Tgfβ1* in the male hypoxic RV. As the role of *Tgfβ1* in cardiac fibrosis and cardiac hypertrophy is well established (Khan and Sheppard, 2006; Rosenkranz, 2004), the effect of FK506 on the gene expression of markers of hypertrophy and fibrosis was investigated. FK506 treatment did not alter gene expression of these markers, however, it is understood that the expression of these genes is time dependent (Manabe et al., 2002; van den Bosch et al., 2006; Friddle et al., 2000) and therefore further investigations are required. To further elucidate the effect of FK506 on the RV, cellular hypertrophy measured by wheat germ agglutinin staining and collagen deposition measured by picosirius red staining could be utilised (Fattah et al., 2016; McCarroll et al., 2018).

The investigations in this chapter also involved a comparison between the RV gene expression profiles in normoxia vs hypoxia and male vs female. There were several key differences identified, consequently, it was important to identify patterns in gene expression which could influence the response of the RV in disease. Hypoxia significantly reduced *Bmpr2* gene expression in the male and female RV, a finding which is important in the study of PAH. A recent clinical study showed BMPR2 mutation carriers have poorer RV function despite similar

cardiac adaptation in mutation carrier and non-carrier groups (van der Bruggen et al., 2016) suggesting that BMPR2 signalling has an effect on RV function. Furthermore, mutations in BMPR2 have also been shown to impair RVH in a transgenic mouse model (Hemnes et al., 2014). Reduced expression of BMPR2 in the hypoxic RV may also contribute to impaired function.

Next, *Tgfβ1* emerged from the expression profiles as a gene influenced by hypoxia and sex. *Tgfβ1* expression was significantly higher in males under normoxic and hypoxic conditions. Hypoxia induced expression of *Tgfβ1* in the males only. This could be related to the FK506 dependent reduction in RV mass and *Tgfβ1* expression previously discussed. Investigations of genes involved in cardiac hypertrophy and fibrosis were once again conducted. In normoxia, *Col1a1* and *Col3a1* were significantly upregulated in males and *Col1a1*, *Ctgf*, *Nppa* and *Myh7* were increased in males following exposure to hypoxia. Although these are very preliminary investigations, they begin to identify potential differential *Tgfβ1*-mediated effects in the male RV that are not present in the female RV. Our understanding of the significance of this finding is limited as only changes in gene expression have been identified. This hypothesis would have to be further investigated in isolated male and female cardiac myocytes and fibroblasts through investigation of *Tgfβ1* signalling.

The final results chapter aimed to investigate the effect of endogenous estrogen on the development of PH. Published studies showed treatment with Anastrozole was capable of reversing the PH phenotype in female mice (Mair et al., 2014b; Chen et al., 2017). In contrast, Anastrozole treatment in the current study did not significantly affect RVSP or RVH. The expression of the BMPR2 pathway was investigated in normoxic mice similar to the previous study in rats (Chapter 4). Similar to the rat study, *Bmpr2*, *Smad1*, *Id1* and *Id3* gene expression were not significantly different between males and females. However, the mouse study presented in Chapter 5 also investigated protein expression. This showed that ID1 and Id3 were significantly down-regulated in the female RV. Protein expression analysis should also be carried out in the rat tissue to confirm this finding across different species. Protein investigations also showed that proteins involved in estrogen synthesis, metabolism and signalling (Aromatase, CYP1B1 and ER-α) are all expressed in both the male and female mouse RV. Finally, the

ability of E2 and 16 $\alpha$ -OHE1 to induce migration of male and female rat PSMCs was assessed. The conclusion of this work was that E2 and 16 $\alpha$ -OHE1 did not stimulate migration of PSMCs. One limitation of the migration assay design was that proliferation of the PSMCs was not inhibited. Therefore, it would not have been possible to differentiate between the effects of PSMCs proliferation and migration on % wound closure. As there was no significant effect on % wound closure, the role of proliferation was not considered. E2 at a concentration of 10 nM has been shown to inhibit migration of smooth muscle cells in other vascular beds (Li et al., 2016a; Jiang et al., 2010; Zheng et al., 2015). These investigations should be extended in the future to investigate a potential inhibitory effect of E2 and 16 $\alpha$ -OHE1 on cell migration in response to classical agonists such as TGF $\beta$ .

## 6.2 Future perspective

The need to develop our understanding of the RV encouraged the development of the surgical pulmonary artery banding (PAB) rat model during these investigations. The method development is described in Appendix 7.2. The surgical procedure was particularly challenging and only sham surgeries have been performed successfully. The major challenges associated with this surgery are that the pulmonary artery is very thin walled and fragile and the RV is unable to withstand stress while the pulmonary artery is being manipulated during surgery (Tarnavski et al. 2004). The aim of developing this model was to compare RV function and RV phenotype in male and female rats, allowing the influence of sex and estrogen on the response of the RV to increased afterload to be investigated. This RV dysfunction model would provide a unique opportunity to investigate the pulmonary-independent effects of increased afterload and the pulmonary independent effects of estrogen on the RV. Using other rodent models, it would prove difficult to decipher the effect of estrogen on RV structure and function as it could be secondary to effects on the pulmonary vasculature or as the result of a direct effect on the RV.

Initial *in vitro* investigations were carried out in neonatal rat cardiac fibroblasts which were routinely used in the lab (Flores-Munoz et al., 2012). However, studies that could be carried out in these cells were limited due to the inability to culture the cells based on sex or to isolate and culture RV cells. Therefore, a protocol for the isolation of adult rat RV cardiomyocytes was another method under development during this PhD thesis. The development of this model is described in Appendix 7.1. The isolation of viable adult myocytes is more challenging than neonatal cardiac cells. The isolation of neonatal cells is technically less demanding and the cells are more suited to culturing (Louch et al., 2011). Isolation of adult RV cardiomyocytes presented a challenge as current protocols within the lab were optimised to the successful isolation of LV cardiomyocytes. Isolation of adult RV cardiomyocytes results in a lower cell yield than that of the LV, maximising the number of viable isolated cardiomyocytes was one of the key aims during method development. Successful development would have provided a model which allowed investigation of cardiomyocytes in a sex-specific manner. Key investigations that could have been conducted

included: investigation of the sex-dependent effects of *Tgf $\beta$ 1* and the effect of FK506 treatment on isolated cardiomyocytes.

Currently, there are no treatments available that target RV dysfunction in PAH, despite this being the main cause of mortality in PAH patients. There is a real need to develop our understanding of the molecular mechanisms underlying RV dysfunction in order to identify potential therapeutic targets. Poorer male patient survival rates are thought to be associated with increased and accelerated RV dysfunction compared to females (Jacobs et al., 2014; Kuwat et al., 2009). Investigations into the effect of estrogen on the RV could help develop our understanding of why females tend to have better RV function and identify new RV-specific therapeutic targets. Clinical studies in control groups have suggested that higher estrogen levels are associated with increased RV function (Ventetuolo et al., 2011; Ventetuolo et al., 2015b). However, there is added complexity to estrogen-targeted therapeutics as estrogen has been shown to play a pathogenic role in both experimental animal studies (Mair et al., 2014b; White et al., 2011) and clinical studies (Ventetuolo et al., 2015). Targeting therapies specifically to the pulmonary vasculature or the RV could be a solution.

This thesis highlights that there are key differences between the male and female RV under basal conditions and in response to hypoxia which require further investigation. It is possible that sex-specific RV signalling contributes to the differences in disease progression in males and females. In the development of new PAH therapeutics, it is essential the sex-specific responses are investigated. In future, it may be beneficial to the clinical outcomes of PAH patients to stratify therapy depending on sex and to develop therapies that selectively target the lung or RV to reduce disease morbidity and mortality.

## 7 Appendices

### 7.1 Development of a protocol to isolate cardiomyocytes from the adult rat right ventricle

Initial investigations were performed in neonatal rat cardiac fibroblasts (NRCFs). This cell type was selected for early stage studies as they are technically easy to work with. Also, NRCFs have increased proliferative potential compared to adult cells due to their neonatal rat heart origin (Porrello et al., 2011; Zogbi et al., 2014; Alkass et al., 2015). Although, it was understood that NRCFs were not the most appropriate model as it was not possible to isolate male and female cells or RV and LV cells. Sexing of neonatal pups is challenging and cell yields from the neonatal RV would have been low for complete *in vitro* investigations. The lab had developed successful protocols for the isolation of adult rat LV cardiomyocytes. The aim of this work was to adapt this protocol to successfully isolate viable RV cardiomyocytes. This would allow a model in which RV-derived cardiomyocytes could be investigated. It would also allow studies in male and female cells to be carried out in order to investigate sex-specific effects. The key challenge with this protocol development was ensuring that an appropriate number of cells were isolated that were still viable.

To summarise the isolation protocol, Wistar Hans rats were culled and the hearts rapidly excised and transferred to a chilled Krebs solution. A Langendorff perfusion was set up and the hearts were cannulated via the aorta. An enzymatic digestion involving Collagenase Type I (0.7 mg/mL) and protease (0.06 mg/mL) in Krebs solution was performed. Following digestion, a 0.5% BSA in Krebs solution was perfused through the heart which acted to halt the enzymatic digestion. Optimising the protocol involved identifying and selecting the most appropriate time periods for both the enzymatic digestion and the 0.5% BSA solution perfusion. Often the enzymatic activity of the collagenase Type I is batch dependent. The batch used in this current study was 260 units/mg. Following the perfusion step, the heart was cut down from the Langendorff set up and the RV dissected from the LV. It was from this point forward that the RV and LV cells were isolated. The tissue was then gently agitated to release the cells from the tissue mass. This was performed in a step by step process which involved removing the cell suspension and adding further 0.5% BSA solution. The

cells were then examined under the microscope to identify the number of viable rod-shaped cardiomyocytes. The viable rod-shaped cells and the non-viable ball shaped cells (Powell and Twist, 1976) in the field of view were counted (Figure 7.1). A haemocytometer was not used for cell counting due to the size of cardiomyocytes. A representative cell population was not seen in the haemocytometer.

The aim of this protocol development was to alter the time period of the enzymatic digestion and the 0.5% BSA perfusion step in order to determine the time period that resulted in the highest yield of viable cardiomyocytes to allow further downstream studies to be carried out. Table 12 shows the development of the protocol using cells derived from the RV of male Wistar Hans rats. As the protocol had not been optimised for RV cells it was important to vary the protocol significantly in order to identify the best time periods for the perfusion steps. The enzymatic digestion time period was varied between 3.5 mins and 10 mins. The 0.5% BSA perfusion step was varied between 0 mins and 4 mins. This approach identified a 5.5 mins enzymatic digestion followed by 2 mins 0.5% BSA perfusion resulted in the highest percentage of rod cells (Table 12). Protocol development was initially carried out in male RV cells. Once the optimal perfusion times had been identified, the protocol was repeated in cells derived from female rat RV (Table 13). This protocol resulted in a similar percentage of rod-shaped viable cardiomyocytes and therefore these perfusion time periods were deemed appropriate. The next steps in this protocol development would have been to begin the addition of calcium chloride ( $\text{CaCl}_2$ ) in incremental stages and assess the percentage of viable cells when 1mM  $\text{CaCl}_2$  was reached. It is necessary to increase the calcium concentration within the cells in order to culture the cells for further experimentation.

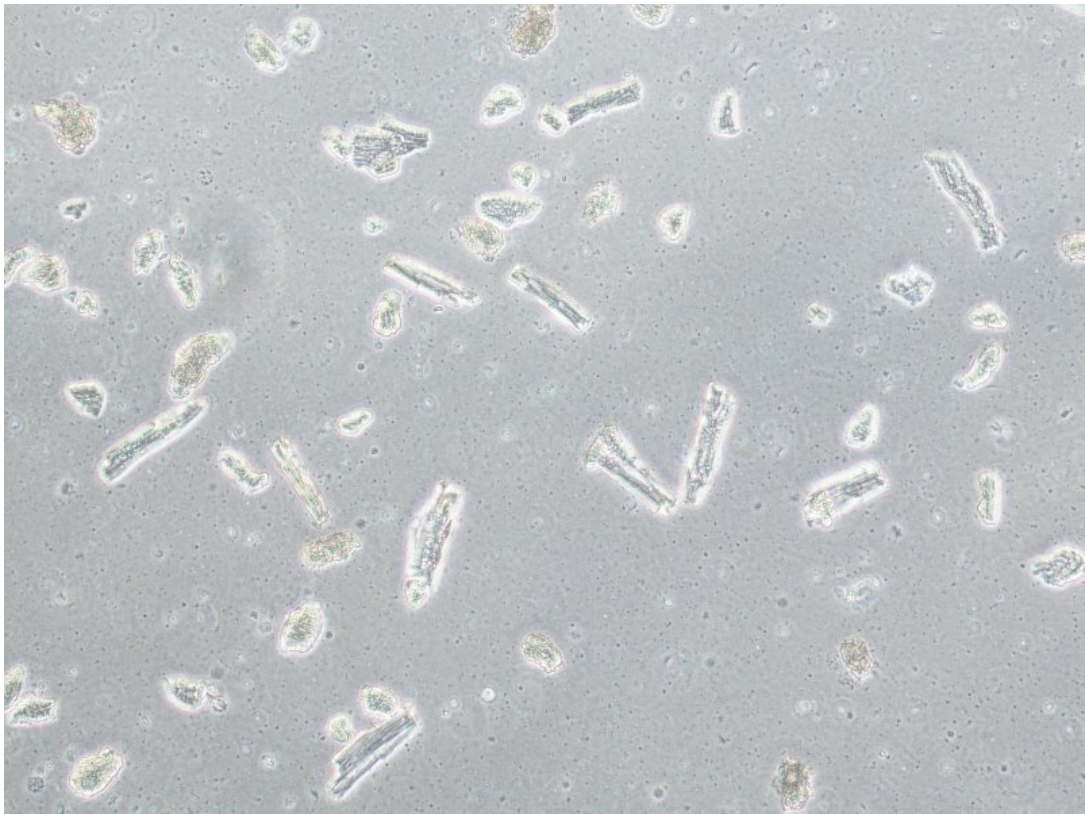


*Figure 7.1 Representative image showing the rod shaped and ball shaped cells following adult rat RV cardiomyocyte isolation protocol.*

The resulting rod and ball shaped cardiomyocytes isolated from the RV of adult Wistar Hans rats.

Enzyme time (mins)	BSA time (mins)	Mean no. of rods	Mean no. of Balls	Mean Total no. of cells	Mean Rod %
03:30	04:00	8.5	55.5	64.0	13.2
04:00	04:00	13.5	136.0	149.5	8.9
04:30	02:00	19.0	104.0	123.0	15.7
04:30	02:00	1.0	74.0	75.0	0.8
05:00	00:00	9.1	79.6	88.7	10.3
05:15	00:00	41.0	150.0	191.0	21.5
05:30	02:00	27	49	76.0	35.5
05:30	02:00	17.4	91.6	109.0	16.2
05:30	03:00	19.0	90.4	109.4	17.7
10:00	00:00	8.0	98.5	106.5	7.5

**Table 12. Development of adult rat RV cardiomyocyte isolation in Wistar Hans male rats.**

*Cardiomyocyte isolation experiments were performed in male Wistar Hans rats. The time of the enzyme perfusion (0.7 mg/mL collagenase and 0.06 mg/mL protease in Krebs solution) on the Langendorff set up was varied in each isolation experiment to optimise the protocol. The time of the 0.5% BSA solution perfusion on the Langendorff set up was also varied in each isolation to optimise the protocol. Cells from the RV were dropped onto a microscope slide and the cells in a field of view were counted. The number of rod-shaped and ball shaped cells were counted and the rod % was calculated. Several fields of view were counted and the mean values calculated. Cells were counted at 0mM calcium chloride (CaCl<sub>2</sub>).*

Enzyme time (mins)	BSA time (mins)	Mean no. of rods	Mean no. of Balls	Mean Total no. of cells	Mean Rod %
05:30	02:00	36	88	124.0	29.0

***Table 13. Development of adult rat RV cardiomyocyte isolation in Wistar Hans female rat.***

*Cardiomyocyte isolation experiment performed in a female Wistar Hans rat. 05:30 mins enzyme perfusion (0.7 mg/mL collagenase and 0.06 mg/mL protease in Krebs solution) and 02:00 mins 0.5% BSA solution perfusion on the Langendorff set up. Cells from the RV were dropped onto a microscope slide and the cells in a field of view were counted. The number of rod-shaped and ball shaped cells were counted and the rod % was calculated. Several fields of view were counted and the mean values calculated. Cells were counted at 0 mM calcium chloride (CaCl<sub>2</sub>).*

## 7.2 Development of the pulmonary artery banding rat model

As the study developed the central focus was on the effect of sex, BMPR2 and potential PAH therapies on the RV. There was a need to investigate changes in the RV in isolation rather than secondary to the pulmonary vasculature. For this reason, we began to work towards developing a pulmonary artery banding (PAB) rat model at the University of Glasgow. This model would allow investigation of the pulmonary-independent effects of sex on the development of right heart dysfunction developing our understanding of some of the sex paradoxes that exist in pulmonary hypertension. Additionally, it provides an experimental model to investigate the cardiac-specific effects of PH therapies and could help identify therapies that would improve right heart function. This could ultimately contribute to improving mortality rates within the PAH population.

The early stages of model development were carried out as part of this study. A study by Tarnavski et al. in 2004 describes the PAB surgical procedure in a mouse model (Tarnavski et al., 2004). The PAB rat model protocol we aimed to develop was based on this method. The sham surgery also underwent development to act as a control. The protocol which was under development is detailed in Table 14. Briefly, the rat was intubated and positioned on the sterile, surgical table. A left lateral thoracotomy at the second intercostal space was performed in order to expose the pulmonary artery. The pulmonary artery was bluntly dissected from the aorta. This step was technically challenging as it was important to ensure extreme care was taken not to damage to pulmonary artery or the aorta. A suture was then positioned under the pulmonary artery with the use of a ligation aid before the suture was tied to constrict the artery. A 19G blunted needle positioned alongside the pulmonary artery was used to determine the diameter of the constriction. The sham surgery involved the same process of positioning the suture under the pulmonary artery, but the suture was then removed without being tied. Finally, the wound was closed before the intubation tube was removed and the animal was transferred to a recovery cage. The recovery of the animal was closely monitored.

Step	Description
Preparation	Prepare sterile field and sterile instruments.
Anaesthetics	Intubate and ventilate - approx. 3% isoflurane in oxygen. Ventilator - 60 breaths per min with 4ml tidal volume.
Analgesics	Prior to the beginning of surgery - Subcutaneous injection of: Buprenorphine (0.05mg/kg) and Rimadyl (8mg/kg). Rib injections: Ropivacaine (4.5mg/kg).
Thoracotomy	Left thoracotomy at the second intercostal space to expose the top of the heart, aorta and pulmonary artery.
Isolation of PA	Isolate the pulmonary artery from the aorta by blunt dissection. Position the ligation aid with the piece of suture in between the aorta and pulmonary artery. Using forceps stretch the connective tissue over the tip of the ligation aid until the ligation aid breaks the through the connective tissue.
Banding	Pull the suture through the ligation aid and remove the ligation aid ensuring that the suture remains under the pulmonary artery. Place blunted 19G needle on top of the artery and tie the suture around the artery to the diameter of the needle.
Suturing	Intercostal layer, muscle layer, subcutaneous layer (x2) and skin.
Recovery	Turn off isoflurane and continue to administer oxygen. Once the rat can breathe on its own, disconnect from ventilator while keeping the intubation tube in place. When convinced the rat is able to make a full recovery remove intubation tube.
Post-Surgery care	Maintain in heated box post-surgery. When the rat has fully recovered it can be return to the cage. Post-surgery - for 2 days administer Buprenorphine (0.05mg/kg) in Nutella (am and pm).

*Table 14. Development of the pulmonary artery banding rat model protocol.*

Unfortunately, due to other constraints with the project, only 2 sham surgeries were carried out. 1 male Wistar rat and 1 male Sprague Dawley rat successfully recovered from the sham surgery. Both animals had a satisfactory recovery and incisions that healed well post-surgery. The male rats were haemodynamically assessed post-surgery as an assessment of model development. One rat was assessed at 4 weeks and the other at 6 weeks post-surgery. RVSP, LVSP and SAP were recorded (Table 15). RV mass was recorded and RVH calculated using the standard measure in the pulmonary hypertension field  $RV/LV+S$ . The RVH measurements were consistent with male rats housed in normoxic conditions (Dean et al., 2016; Docherty et al., 2019) suggesting that the surgical procedure had not resulted in right ventricular hypertrophy. However, the RVSP of the male sham rats was slightly elevated in comparison with normoxic rats, previous studies have shown normoxic rats with RVSP of approximately 30 mmHg (Docherty et al., 2019; Mair et al., 2014b). This suggests that manipulation of the pulmonary artery during the surgical procedure could have induced a physiological response associated with the trauma which lead to an increase in RVSP, however, further sham surgeries would have to be carried out in order to investigate this fully. The pulmonary artery was not collected following haemodynamic assessment, however, in future it may be possible to histologically analyse the PA in the sham animals to try and identify any damage or remodelling.

During the development of this model, it was identified that the method by which the pulmonary artery was constricted could be improved. Although the study by Tarnavski et al. (2004) described a method of using a blunted needle placed alongside the pulmonary artery as a guide for the diameter of the constriction, it was thought there would be variability in the constriction diameter using this method. Another method is to use a surgical clip to constrict the artery. Investigations of right heart dysfunction after pulmonary artery banding with a clip either 0.5 mm and 0.6 mm in diameter showed that 0.1 mm of a difference in the diameter of the clip was the difference between severe right heart failure and right heart dysfunction (Andersen et al., 2014). It is unlikely that this level of accuracy could be achieved by tying a suture and therefore the surgical clip would allow the most reproducible results.

	Sham Rat 1	Sham Rat 2
Weeks post-surgery haemodynamic assessment was carried out	4	6
Strain	Sprague Dawley	Wistar
Weight at PAB surgery (g)	300	259
Weight at haemodynamic measurements (g)	350.9	364.8
RVSP (mmHg)	40.96	35.19
Mean Systemic Arterial Pressure (mmHg)	56.69	97.54
LVSP (mmHg)	87	109.8
RV mass (mg)	221.25	139.3
RVH (RV/LV+S)	0.26	0.23

***Table 15. Summary of the phenotype and haemodynamic measurements of Pulmonary Artery Banding Sham surgery model.***

## Bibliography

- ABE, K., TOBA, M., ALZOUBI, A., ITO, M., FAGAN, K. A., COOL, C. D., VOELKEL, N. F., MCMURTRY, I. F. & OKA, M. 2010. Formation of plexiform lesions in experimental severe pulmonary arterial hypertension. *Circulation*, 121, 2747-54.
- ALKASS, K., PANULA, J., WESTMAN, M., WU, T. D., GUERQUIN-KERN, J. L. & BERGMANN, O. 2015. No Evidence for Cardiomyocyte Number Expansion in Preadolescent Mice. *Cell*, 163, 1026-36.
- ANDERSEN, S., SCHULTZ, J. G., ANDERSEN, A., RINGGAARD, S., NIELSEN, J. M., HOLMBOE, S., VILDBRAD, M. D., DE MAN, F. S., BOGAARD, H. J., VONK-NOORDEGRAAF, A. & NIELSEN-KUDSK, J. E. 2014. Effects of bisoprolol and losartan treatment in the hypertrophic and failing right heart. *J Card Fail*, 20, 864-73.
- ANDERSSON, C., LYDRUP, M. L., FERNO, M., IDVALL, I., GUSTAFSSON, J. & NILSSON, B. O. 2001. Immunocytochemical demonstration of oestrogen receptor beta in blood vessels of the female rat. *J Endocrinol*, 169, 241-7.
- ARSLAN, A. A., KOENIG, K. L., LENNER, P., AFANASYEVA, Y., SHORE, R. E., CHEN, Y., LUNDIN, E., TONIOLO, P., HALLMANS, G. & ZELENIUCH-JACQUOTTE, A. 2014. Circulating estrogen metabolites and risk of breast cancer in postmenopausal women. *Cancer Epidemiol Biomarkers Prev*, 23, 1290-7.
- ASAKI, T., KUWANO, K., MORRISON, K., GATFIELD, J., HAMAMOTO, T. & CLOZEL, M. 2015. Selexipag: An Oral and Selective IP Prostacyclin Receptor Agonist for the Treatment of Pulmonary Arterial Hypertension. *J Med Chem*, 58, 7128-37.
- AUSTIN, E. D., COGAN, J. D., WEST, J. D., HEDGES, L. K., HAMID, R., DAWSON, E. P., WHEELER, L. A., PARL, F. F., LOYD, J. E. & PHILLIPS, J. A., 3RD 2009. Alterations in oestrogen metabolism: implications for higher penetrance of familial pulmonary arterial hypertension in females. *Eur Respir J*, 34, 1093-9.
- AUSTIN, E. D., HAMID, R., HEMNES, A. R., LOYD, J. E., BLACKWELL, T., YU, C., PHILLIPS III, J. A., GADDIPATI, R., GLADSON, S., GU, E., WEST, J. & LANE, K. B. 2012. BMPR2 expression is suppressed by signaling through the estrogen receptor. *Biol Sex Differ*, 3, 6.
- AUSTIN, E. D. & LOYD, J. E. 2014. The genetics of pulmonary arterial hypertension. *Circ Res*, 115, 189-202.
- AWDISH, R. & CAJIGAS, H. 2016. Definition, epidemiology and registries of pulmonary hypertension. *Heart Fail Rev*, 21, 223-8.
- BADESCH, D. B., RASKOB, G. E., ELLIOTT, C. G., KRICHMAN, A. M., FARBER, H. W., FROST, A. E., BARST, R. J., BENZA, R. L., LIOU, T. G., TURNER, M., GILES, S., FELDKIRCHER, K., MILLER, D. P. & MCGOON, M. D. 2010. Pulmonary arterial hypertension: baseline characteristics from the REVEAL Registry. *Chest*, 137, 376-87.
- BARAKAT, R., OAKLEY, O., KIM, H., JIN, J. & KO, C. J. 2016. Extra-gonadal sites of estrogen biosynthesis and function. *BMB Rep*, 49, 488-96.
- BARST, R. J., RUBIN, L. J., LONG, W. A., MCGOON, M. D., RICH, S., BADESCH, D. B., GROVES, B. M., TAPSON, V. F., BOURGE, R. C., BRUNDAGE, B. H., KOERNER, S. K., LANGLEBEN, D., KELLER, C. A., MURALI, S., URETSKY, B. F., CLAYTON, L. M., JOBSIS, M. M., BLACKBURN, S. D., SHORTINO, D. & CROW, J. W. 1996. A comparison of continuous intravenous epoprostenol

- (prostacyclin) with conventional therapy for primary pulmonary hypertension. *N Engl J Med*, 334, 296-301.
- BAUER, M., WILKENS, H., LANGER, F., SCHNEIDER, S. O., LAUSBERG, H. & SCHAFERS, H. J. 2002. Selective upregulation of endothelin B receptor gene expression in severe pulmonary hypertension. *Circulation*, 105, 1034-6.
- BAUM, M., BUDZAR, A. U., CUZICK, J., FORBES, J., HOUGHTON, J. H., KLIJN, J. G. & SAHMOUD, T. 2002. Anastrozole alone or in combination with tamoxifen versus tamoxifen alone for adjuvant treatment of postmenopausal women with early breast cancer: first results of the ATAC randomised trial. *Lancet*, 359, 2131-9.
- BECKER, J. B. 2008. *Sex differences in the brain: from genes to behavior*, Oxford, Oxford University Press.
- BEHR, J. & RYU, J. H. 2008. Pulmonary hypertension in interstitial lung disease. *Eur Respir J*, 31, 1357-67.
- BJORNSTROM, L. & SJOBERG, M. 2005. Mechanisms of estrogen receptor signaling: convergence of genomic and nongenomic actions on target genes. *Mol Endocrinol*, 19, 833-42.
- BLENCK, C. L., HARVEY, P. A., RECKELHOFF, J. F. & LEINWAND, L. A. 2016. The Importance of Biological Sex and Estrogen in Rodent Models of Cardiovascular Health and Disease. *Circ Res*, 118, 1294-312.
- BLOCK, E. R., PATEL, J. M. & EDWARDS, D. 1989. Mechanism of hypoxic injury to pulmonary artery endothelial cell plasma membranes. *Am J Physiol*, 257, C223-31.
- BOGAARD, H. J., ABE, K., VONK NOORDEGRAAF, A. & VOELKEL, N. F. 2009. The right ventricle under pressure: cellular and molecular mechanisms of right-heart failure in pulmonary hypertension. *Chest*, 135, 794-804.
- BOGAARD, H. J., MIZUNO, S., HUSSAINI, A. A., TOLDO, S., ABBATE, A., KRASKAUSKAS, D., KASPER, M., NATARAJAN, R. & VOELKEL, N. F. 2011. Suppression of histone deacetylases worsens right ventricular dysfunction after pulmonary artery banding in rats. *Am J Respir Crit Care Med*, 183, 1402-10.
- BORGENDORFF, M. A., DICKINSON, M. G., BERGER, R. M. & BARTELD, B. 2015a. Right ventricular failure due to chronic pressure load: What have we learned in animal models since the NIH working group statement? *Heart Fail Rev*, 20, 475-91.
- BORGENDORFF, M. A., KOOP, A. M., BLOKS, V. W., DICKINSON, M. G., STEENDIJK, P., SILLJE, H. H., VAN WIECHEN, M. P., BERGER, R. M. & BARTELD, B. 2015b. Clinical symptoms of right ventricular failure in experimental chronic pressure load are associated with progressive diastolic dysfunction. *J Mol Cell Cardiol*, 79, 244-53.
- BROUCHET, L., KRUST, A., DUPONT, S., CHAMBON, P., BAYARD, F. & ARNAL, J. F. 2001. Estradiol accelerates reendothelialization in mouse carotid artery through estrogen receptor-alpha but not estrogen receptor-beta. *Circulation*, 103, 423-8.
- BURKE, D. L., FRID, M. G., KUNRATH, C. L., KAROOR, V., ANWAR, A., WAGNER, B. D., STRASSHEIM, D. & STENMARK, K. R. 2009. Sustained hypoxia promotes the development of a pulmonary artery-specific chronic inflammatory microenvironment. *Am J Physiol Lung Cell Mol Physiol*, 297, L238-50.
- CHEN, X., AUSTIN, E. D., TALATI, M., FESSEL, J. P., FARBER-EGGER, E. H., BRITAIN, E. L., HEMNES, A. R., LOYD, J. E. & WEST, J. 2017. Oestrogen

- inhibition reverses pulmonary arterial hypertension and associated metabolic defects. *Eur Respir J* [Online], 50. Available: <http://dx.doi.org/10.1183/13993003.02337-2016> [Accessed 18 August 2020].
- CHEN, Z., YUHANNA, I. S., GALCHEVA-GARGOVA, Z., KARAS, R. H., MENDELSON, M. E. & SHAUL, P. W. 1999. Estrogen receptor alpha mediates the nongenomic activation of endothelial nitric oxide synthase by estrogen. *J Clin Invest*, 103, 401-6.
- CHIN, K. M., KIM, N. H. & RUBIN, L. J. 2005. The right ventricle in pulmonary hypertension. *Coron Artery Dis*, 16, 13-8.
- CHRISTMAN, B. W., MCPHERSON, C. D., NEWMAN, J. H., KING, G. A., BERNARD, G. R., GROVES, B. M. & LOYD, J. E. 1992. An imbalance between the excretion of thromboxane and prostacyclin metabolites in pulmonary hypertension. *N Engl J Med*, 327, 70-5.
- CLAPHAM, K. R., SINGH, I., CAPUANO, I. S., RAJAGOPAL, S. & CHUN, H. J. 2019. MEF2 and the Right Ventricle: From Development to Disease. *Front Cardiovasc Med*, 6, 29.
- COGAN, J., AUSTIN, E., HEDGES, L., WOMACK, B., WEST, J., LOYD, J. & HAMID, R. 2012. Role of BMPR2 alternative splicing in heritable pulmonary arterial hypertension penetrance. *Circulation*, 126, 1907-16.
- COLEMAN, R. A., SMITH, W. L. & NARUMIYA, S. 1994. International Union of Pharmacology classification of prostanoid receptors: properties, distribution, and structure of the receptors and their subtypes. *Pharmacol Rev*, 46, 205-29.
- COLVIN, K. L. & YEAGER, M. E. 2014. Animal Models of Pulmonary Hypertension: Matching Disease Mechanisms to Etiology of the Human Disease. *J Pulm Respir Med* [Online], 4. Available: <http://dx.doi.org/10.4172/2161-105X.1000198> [Accessed 18 August 2020].
- CONZEN, P. F., VOLLMAR, B., HABAZETTL, H., FRINK, E. J., PETER, K. & MESSMER, K. 1992. Systemic and regional hemodynamics of isoflurane and sevoflurane in rats. *Anesth Analg*, 74, 79-88.
- COOKE, P. S., NANJAPPA, M. K., KO, C., PRINS, G. S. & HESS, R. A. 2017. Estrogens in Male Physiology. *Physiol Rev*, 97, 995-1043.
- COOL, C. D., STEWART, J. S., WERAHERA, P., MILLER, G. J., WILLIAMS, R. L., VOELKEL, N. F. & TUDER, R. M. 1999. Three-Dimensional Reconstruction of Pulmonary Arteries in Plexiform Pulmonary Hypertension Using Cell-Specific Markers. *The American Journal of Pathology*, 155, 411-419.
- CUI, J., SHEN, Y. & LI, R. 2013. Estrogen synthesis and signaling pathways during ageing: from periphery to brain. *Trends Mol Med*, 19, 197-209.
- DAVIE, N., HALEEN, S. J., UPTON, P. D., POLAK, J. M., YACOUB, M. H., MORRELL, N. W. & WHARTON, J. 2002. ET(A) and ET(B) receptors modulate the proliferation of human pulmonary artery smooth muscle cells. *Am J Respir Crit Care Med*, 165, 398-405.
- DEAN, A., NILSEN, M., LOUGHLIN, L., SALT, I. P. & MACLEAN, M. R. 2016. Metformin Reverses Development of Pulmonary Hypertension via Aromatase Inhibition. *Hypertension*, 68, 446-54.
- DELL'ITALIA, L. J. 1991. The right ventricle: anatomy, physiology, and clinical importance. *Curr Probl Cardiol*, 16, 653-720.
- DEMIR, R. & KÜÇÜKOĞLU, M. S. 2015. Six-minute walk test in pulmonary arterial hypertension. *Anatol J Cardiol*, 15, 249-254.
- DEMPSIE, Y., MACRITCHIE, N. A., WHITE, K., MORECROFT, I., WRIGHT, A. F., NILSEN, M., LOUGHLIN, L., MAIR, K. M. & MACLEAN, M. R. 2013.

- Dexfenfluramine and the oestrogen-metabolizing enzyme CYP1B1 in the development of pulmonary arterial hypertension. *Cardiovasc Res*, 99, 24-34.
- DENG, Z., HAGHIGHI, F., HELLEBY, L., VANTERPOOL, K., HORN, E. M., BARST, R. J., HODGE, S. E., MORSE, J. H. & KNOWLES, J. A. 2000. Fine mapping of PPH1, a gene for familial primary pulmonary hypertension, to a 3-cM region on chromosome 2q33. *Am J Respir Crit Care Med*, 161, 1055-9.
- DEWACHTER, L., ADNOT, S., FADEL, E., HUMBERT, M., MAITRE, B., BARLIER-MUR, A. M., SIMONNEAU, G., HAMON, M., NAEIJE, R. & EDDAHIBI, S. 2006. Angiopoietin/Tie2 pathway influences smooth muscle hyperplasia in idiopathic pulmonary hypertension. *Am J Respir Crit Care Med*, 174, 1025-33.
- DIAS, C. A., ASSAD, R. S., CANEO, L. F., ABDUCH, M. C., AIELLO, V. D., DIAS, A. R., MARCIAL, M. B. & OLIVEIRA, S. A. 2002. Reversible pulmonary trunk banding. II. An experimental model for rapid pulmonary ventricular hypertrophy. *J Thorac Cardiovasc Surg*, 124, 999-1006.
- DOCHERTY, C. K., NILSEN, M. & MACLEAN, M. R. 2019. Influence of 2-Methoxyestradiol and Sex on Hypoxia-Induced Pulmonary Hypertension and Hypoxia-Inducible Factor-1-alpha. *J Am Heart Assoc*, 8, e011628.
- ELLIOTT, F. M. & REID, L. 1965. Some new facts about the pulmonary artery and its branching pattern. *Clin Radiol*, 16, 193-8.
- ELLIOTT, W. H., TAN, Y., LI, M. & TAN, W. 2015. High Pulsatility Flow Promotes Vascular Fibrosis by Triggering Endothelial EndMT and Fibroblast Activation. *Cellular and Molecular Bioengineering*, 8, 285-295.
- EMA. 2017. *EMA concludes safety review of Upravi* [Online]. Available: [https://www.ema.europa.eu/en/documents/press-release/ema-concludes-safety-review-uptravi\\_en.pdf](https://www.ema.europa.eu/en/documents/press-release/ema-concludes-safety-review-uptravi_en.pdf) [Accessed 18 August 2020].
- EVANS, J. D., GIRERD, B., MONTANI, D., WANG, X. J., GALIE, N., AUSTIN, E. D., ELLIOTT, G., ASANO, K., GRUNIG, E., YAN, Y., JING, Z. C., MANES, A., PALAZZINI, M., WHEELER, L. A., NAKAYAMA, I., SATOH, T., EICHSTAEDT, C., HINDERHOFER, K., WOLF, M., ROSENZWEIG, E. B., CHUNG, W. K., SOUBRIER, F., SIMONNEAU, G., SITBON, O., GRAF, S., KAPTOGE, S., DI ANGELANTONIO, E., HUMBERT, M. & MORRELL, N. W. 2016a. BMPR2 mutations and survival in pulmonary arterial hypertension: an individual participant data meta-analysis. *Lancet Respir Med*, 4, 129-37.
- EVANS, N. J., BAYLISS, A. L., REALE, V. & EVANS, P. D. 2016b. Characterisation of Signalling by the Endogenous GPER1 (GPR30) Receptor in an Embryonic Mouse Hippocampal Cell Line (mHippoE-18). *PLoS One*, 11, e0152138.
- FABER, M. J., DALINGHAUS, M., LANKHUIZEN, I. M., STEENDIJK, P., HOP, W. C., SCHOEMAKER, R. G., DUNCKER, D. J., LAMERS, J. M. & HELBING, W. A. 2006. Right and left ventricular function after chronic pulmonary artery banding in rats assessed with biventricular pressure-volume loops. *Am J Physiol Heart Circ Physiol*, 291, H1580-6.
- FANG, Y. H., PIAO, L., HONG, Z., TOTH, P. T., MARSBOOM, G., BACHE-WIIG, P., REHMAN, J. & ARCHER, S. L. 2012. Therapeutic inhibition of fatty acid oxidation in right ventricular hypertrophy: exploiting Randle's cycle. *J Mol Med (Berl)*, 90, 31-43.
- FARBER, H. W., MILLER, D. P., POMS, A. D., BADESCH, D. B., FROST, A. E., MUROS-LE ROUZIC, E., ROMERO, A. J., BENTON, W. W., ELLIOTT, C. G., MCGOON, M. D. & BENZA, R. L. 2015. Five-Year outcomes of patients enrolled in the REVEAL Registry. *Chest*, 148, 1043-54.

- FARHAT, M. Y., CHEN, M. F., BHATTI, T., IQBAL, A., CATHAPERMAL, S. & RAMWELL, P. W. 1993. Protection by oestradiol against the development of cardiovascular changes associated with monocrotaline pulmonary hypertension in rats. *Br J Pharmacol*, 110, 719-23.
- FATTAH, C., NATHER, K., MCCARROLL, C. S., HORTIGON-VINAGRE, M. P., ZAMORA, V., FLORES-MUNOZ, M., MCARTHUR, L., ZENTILIN, L., GIACCA, M., TOUYZ, R. M., SMITH, G. L., LOUGHREY, C. M. & NICKLIN, S. A. 2016. Gene Therapy With Angiotensin-(1-9) Preserves Left Ventricular Systolic Function After Myocardial Infarction. *J Am Coll Cardiol*, 68, 2652-2666.
- FESSEL, J. P., LOYD, J. E. & AUSTIN, E. D. 2011. The genetics of pulmonary arterial hypertension in the post-BMP2 era. *Pulm Circ*, 1, 305-319.
- FILARDO, E. J., QUINN, J. A., BLAND, K. I. & FRACKELTON, A. R., JR. 2000. Estrogen-induced activation of Erk-1 and Erk-2 requires the G protein-coupled receptor homolog, GPR30, and occurs via trans-activation of the epidermal growth factor receptor through release of HB-EGF. *Mol Endocrinol*, 14, 1649-60.
- FILARDO, E. J., QUINN, J. A., FRACKELTON, A. R., JR. & BLAND, K. I. 2002. Estrogen action via the G protein-coupled receptor, GPR30: stimulation of adenylyl cyclase and cAMP-mediated attenuation of the epidermal growth factor receptor-to-MAPK signaling axis. *Mol Endocrinol*, 16, 70-84.
- FLORES-MUNOZ, M., WORK, L. M., DOUGLAS, K., DENBY, L., DOMINCZAK, A. F., GRAHAM, D. & NICKLIN, S. A. 2012. Angiotensin-(1-9) attenuates cardiac fibrosis in the stroke-prone spontaneously hypertensive rat via the angiotensin type 2 receptor. *Hypertension*, 59, 300-7.
- FRID, M. G., DEMPSEY, E. C., DURMOWICZ, A. G. & STENMARK, K. R. 1997. Smooth muscle cell heterogeneity in pulmonary and systemic vessels. Importance in vascular disease. *Arterioscler Thromb Vasc Biol*, 17, 1203-9.
- FRIDDLE, C. J., KOGA, T., RUBIN, E. M. & BRISTOW, J. 2000. Expression profiling reveals distinct sets of genes altered during induction and regression of cardiac hypertrophy. *Proc Natl Acad Sci U S A*, 97, 6745-50.
- FRUMP, A. L., GOSS, K. N., VAYL, A., ALBRECHT, M., FISHER, A., TURSUNOVA, R., FIERST, J., WHITSON, J., CUCCI, A. R., BROWN, M. B. & LAHM, T. 2015. Estradiol improves right ventricular function in rats with severe angioproliferative pulmonary hypertension: effects of endogenous and exogenous sex hormones. *Am J Physiol Lung Cell Mol Physiol*, 308, L873-90.
- FULTON, R. M., HUTCHINSON, E. C. & JONES, A. M. 1952. Ventricular weight in cardiac hypertrophy. *Br Heart J*, 14, 413-20.
- FUNG, J. J. & STARZL, T. E. 1995. FK506 in solid organ transplantation. *Ther Drug Monit*, 17, 592-5.
- GALIE, N., BARBERA, J. A., FROST, A. E., GHOFRANI, H. A., HOEPER, M. M., MCLAUGHLIN, V. V., PEACOCK, A. J., SIMONNEAU, G., VACHIERY, J. L., GRUNIG, E., OUDIZ, R. J., VONK-NOORDEGRAAF, A., WHITE, R. J., BLAIR, C., GILLIES, H., MILLER, K. L., HARRIS, J. H., LANGLEY, J. & RUBIN, L. J. 2015. Initial Use of Ambrisentan plus Tadalafil in Pulmonary Arterial Hypertension. *N Engl J Med*, 373, 834-44.
- GALIE, N., BRUNDAGE, B. H., GHOFRANI, H. A., OUDIZ, R. J., SIMONNEAU, G., SAFDAR, Z., SHAPIRO, S., WHITE, R. J., CHAN, M., BEARDSWORTH, A., FRUMKIN, L. & BARST, R. J. 2009a. Tadalafil therapy for pulmonary arterial hypertension. *Circulation*, 119, 2894-903.

- GALIE, N., GHOFRANI, H. A., TORBICKI, A., BARST, R. J., RUBIN, L. J., BADESCH, D., FLEMING, T., PARPIA, T., BURGESS, G., BRANZI, A., GRIMMINGER, F., KURZYNA, M. & SIMONNEAU, G. 2005. Sildenafil citrate therapy for pulmonary arterial hypertension. *N Engl J Med*, 353, 2148-57.
- GALIE, N., HOEPER, M. M., HUMBERT, M., TORBICKI, A., VACHIERY, J. L., BARBERA, J. A., BEGHETTI, M., CORRIS, P., GAINE, S., GIBBS, J. S., GOMEZ-SANCHEZ, M. A., JONDEAU, G., KLEPETKO, W., OPITZ, C., PEACOCK, A., RUBIN, L., ZELLWEGER, M. & SIMONNEAU, G. 2009b. Guidelines for the diagnosis and treatment of pulmonary hypertension: the Task Force for the Diagnosis and Treatment of Pulmonary Hypertension of the European Society of Cardiology (ESC) and the European Respiratory Society (ERS), endorsed by the International Society of Heart and Lung Transplantation (ISHLT). *Eur Heart J*, 30, 2493-537.
- GALIE, N., HUMBERT, M., VACHIERY, J. L., GIBBS, S., LANG, I., TORBICKI, A., SIMONNEAU, G., PEACOCK, A., VONK NOORDEGRAAF, A., BEGHETTI, M., GHOFRANI, A., GOMEZ SANCHEZ, M. A., HANSMANN, G., KLEPETKO, W., LANCELLOTTI, P., MATUCCI, M., MCDONAGH, T., PIERARD, L. A., TRINDADE, P. T., ZOMPATORI, M., HOEPER, M., ABOYANS, V., VAZ CARNEIRO, A., ACHENBACH, S., AGEWALL, S., ALLANORE, Y., ASTEGGIANO, R., PAOLO BADANO, L., ALBERT BARBERA, J., BOUVAIST, H., BUENO, H., BYRNE, R. A., CARERJ, S., CASTRO, G., EROL, C., FALK, V., FUNCK-BRENTANO, C., GORENFLO, M., GRANTON, J., IUNG, B., KIELY, D. G., KIRCHHOF, P., KJELLSTROM, B., LANDMESSER, U., LEKAKIS, J., LIONIS, C., LIP, G. Y., ORFANOS, S. E., PARK, M. H., PIEPOLI, M. F., PONIKOWSKI, P., REVEL, M. P., RIGAU, D., ROSENKRANZ, S., VOLLER, H. & LUIS ZAMORANO, J. 2016. 2015 ESC/ERS Guidelines for the diagnosis and treatment of pulmonary hypertension: The Joint Task Force for the Diagnosis and Treatment of Pulmonary Hypertension of the European Society of Cardiology (ESC) and the European Respiratory Society (ERS): Endorsed by: Association for European Paediatric and Congenital Cardiology (AEPC), International Society for Heart and Lung Transplantation (ISHLT). *Eur Heart J*, 37, 67-119.
- GALL, H., FELIX, J. F., SCHNECK, F. K., MILGER, K., SOMMER, N., VOSWINCKEL, R., FRANCO, O. H., HOFMAN, A., SCHERMULY, R. T., WEISSMANN, N., GRIMMINGER, F., SEEGER, W. & GHOFRANI, H. A. 2017. The Giessen Pulmonary Hypertension Registry: Survival in pulmonary hypertension subgroups. *J Heart Lung Transplant*, 36, 957-967.
- GARCIA DE VINUESA, A., ABDELILAH-SEYFRIED, S., KNAUS, P., ZWIJSEN, A. & BAILLY, S. 2016. BMP signaling in vascular biology and dysfunction. *Cytokine Growth Factor Rev*, 27, 65-79.
- GEISLER, J., KING, N., DOWSETT, M., OTTESTAD, L., LUNDGREN, S., WALTON, P., KORMESET, P. O. & LØNNING, P. E. 1996. Influence of anastrozole (Arimidex), a selective, non-steroidal aromatase inhibitor, on in vivo aromatisation and plasma oestrogen levels in postmenopausal women with breast cancer. *Br J Cancer*, 74, 1286-91.
- GEVA, T., POWELL, A. J., CRAWFORD, E. C., CHUNG, T. & COLAN, S. D. 1998. Evaluation of regional differences in right ventricular systolic function by acoustic quantification echocardiography and cine magnetic resonance imaging. *Circulation*, 98, 339-45.
- GIAID, A., YANAGISAWA, M., LANGLEBEN, D., MICHEL, R. P., LEVY, R., SHENNIB, H., KIMURA, S., MASAKI, T., DUGUID, W. P. & STEWART, D. J. 1993.

- Expression of endothelin-1 in the lungs of patients with pulmonary hypertension. *N Engl J Med*, 328, 1732-9.
- GODFRAIND, T. 2017. Discovery and Development of Calcium Channel Blockers. *Front Pharmacol* [Online], 8. Available: <http://dx.doi.org/10.3389/fphar.2017.00286> [Accessed 18 August 2020].
- GOMEZ-ARROYO, J., SALEEM, S. J., MIZUNO, S., SYED, A. A., BOGAARD, H. J., ABBATE, A., TARASEVICIENE-STEWART, L., SUNG, Y., KRASKAUSKAS, D., FARKAS, D., CONRAD, D. H., NICOLLS, M. R. & VOELKEL, N. F. 2012. A brief overview of mouse models of pulmonary arterial hypertension: problems and prospects. *Am J Physiol Lung Cell Mol Physiol*, 302, L977-91.
- GONZALEZ DE VALDIVIA, E., BROSELID, S., KAHN, R., OLDE, B. & LEEB-LUNDBERG, L. M. F. 2017. G protein-coupled estrogen receptor 1 (GPER1)/GPR30 increases ERK1/2 activity through PDZ motif-dependent and -independent mechanisms. *J Biol Chem*, 292, 9932-9943.
- GOOD, R. B., GILBANE, A. J., TRINDER, S. L., DENTON, C. P., COGHLAN, G., ABRAHAM, D. J. & HOLMES, A. M. 2015. Endothelial to Mesenchymal Transition Contributes to Endothelial Dysfunction in Pulmonary Arterial Hypertension. *Am J Pathol*, 185, 1850-8.
- GRODIN, J. M., SIITERI, P. K. & MACDONALD, P. C. 1973. Source of estrogen production in postmenopausal women. *J Clin Endocrinol Metab*, 36, 207-14.
- HALL, J. M., COUSE, J. F. & KORACH, K. S. 2001. The multifaceted mechanisms of estradiol and estrogen receptor signaling. *J Biol Chem*, 276, 36869-72.
- HANDOKO, M. L., DE MAN, F. S., ALLAART, C. P., PAULUS, W. J., WESTERHOF, N. & VONK-NOORDEGRAAF, A. 2010. Perspectives on novel therapeutic strategies for right heart failure in pulmonary arterial hypertension: lessons from the left heart. *Eur Respir Rev*, 19, 72-82.
- HARADA, N., SASANO, H., MURAKAMI, H., OHKUMA, T., NAGURA, H. & TAKAGI, Y. 1999. Localized expression of aromatase in human vascular tissues. *Circ Res*, 84, 1285-91.
- HARDZIYENKA, M., CAMPAN, M. E., REESINK, H. J., SURIE, S., BOUMA, B. J., GROENINK, M., KLEMENS, C. A., BEEKMAN, L., REMME, C. A., BRESSER, P. & TAN, H. L. 2011. Right ventricular failure following chronic pressure overload is associated with reduction in left ventricular mass: evidence for atrophic remodeling. *J Am Coll Cardiol*, 57, 921-8.
- HELDRING, N., PIKE, A., ANDERSSON, S., MATTHEWS, J., CHENG, G., HARTMAN, J., TUJAGUE, M., STROM, A., TREUTER, E., WARNER, M. & GUSTAFSSON, J. A. 2007. Estrogen receptors: how do they signal and what are their targets. *Physiol Rev*, 87, 905-31.
- HEMNES, A. R., BRITTAIN, E. L., TRAMMELL, A. W., FESSEL, J. P., AUSTIN, E. D., PENNER, N., MAYNARD, K. B., GLEAVES, L., TALATI, M., ABSI, T., DISALVO, T. & WEST, J. 2014. Evidence for right ventricular lipotoxicity in heritable pulmonary arterial hypertension. *Am J Respir Crit Care Med*, 189, 325-34.
- HEMNES, A. R. & HUMBERT, M. 2017. Pathobiology of pulmonary arterial hypertension: understanding the roads less travelled. *Eur Respir Rev* [Online], 26. Available: <https://doi.org/10.1183/16000617.0093-2017> [Accessed 1 September 2020].
- HESEL, M. H., STEENDIJK, P., DEN ADEL, B., SCHUTTE, C. I. & VAN DER LAARSE, A. 2006. Characterization of right ventricular function after monocrotaline-induced pulmonary hypertension in the intact rat. *Am J Physiol Heart Circ Physiol*, 291, H2424-30.

- HIRATA, M., OUSAKA, D., ARAI, S., OKUYAMA, M., TARUI, S., KOBAYASHI, J., KASAHARA, S. & SANO, S. 2015. Novel Model of Pulmonary Artery Banding Leading to Right Heart Failure in Rats. *Biomed Res Int*, 2015, 753210.
- HISLOP, A. & REID, L. 1976. New findings in pulmonary arteries of rats with hypoxia-induced pulmonary hypertension. *Br J Exp Pathol*, 57, 542-54.
- HLASTALA, M. P. & BERGER, A. J. 2001. *Physiology of Respiration*, New York, USA, Oxford University Press.
- HOA, N., GE, L., KORACH, K. S. & LEVIN, E. R. 2018. Estrogen receptor beta maintains expression of KLF15 to prevent cardiac myocyte hypertrophy in female rodents. *Mol Cell Endocrinol*, 470, 240-250.
- HOPPER, R. K., MOONEN, J. R., DIEBOLD, I., CAO, A., RHODES, C. J., TOJAIS, N. F., HENNIGS, J. K., GU, M., WANG, L. & RABINOVITCH, M. 2016. In Pulmonary Arterial Hypertension, Reduced BMPR2 Promotes Endothelial-to-Mesenchymal Transition via HMGA1 and Its Target Slug. *Circulation*, 133, 1783-94.
- HUANG, W., YEN, R. T., MCLAURINE, M. & BLEDSOE, G. 1996. Morphometry of the human pulmonary vasculature. *J Appl Physiol (1985)*, 81, 2123-33.
- HUMBERT, M., GUIGNABERT, C., BONNET, S., DORFMULLER, P., KLINGER, J. R., NICOLLS, M. R., OLSCHESKI, A. J., PULLAMSETTI, S. S., SCHERMULY, R. T., STENMARK, K. R. & RABINOVITCH, M. 2019. Pathology and pathobiology of pulmonary hypertension: state of the art and research perspectives. *Eur Respir J* [Online], 53. Available: <http://dx.doi.org/10.1183/13993003.01887-2018> [Accessed 18 August 2020].
- HUMBERT, M., SEGAL, E. S., KIELY, D. G., CARLSEN, J., SCHWIERIN, B. & HOEPER, M. M. 2007. Results of European post-marketing surveillance of bosentan in pulmonary hypertension. *Eur Respir J*, 30, 338-44.
- HUMBERT, M., SITBON, O., CHAOUAT, A., BERTOCCHI, M., HABIB, G., GRESSIN, V., YAICI, A., WEITZENBLUM, E., CORDIER, J. F., CHABOT, F., DROMER, C., PISON, C., REYNAUD-GAUBERT, M., HALOUN, A., LAURENT, M., HACHULLA, E., COTTIN, V., DEGANI, B., JAIS, X., MONTANI, D., SOUZA, R. & SIMONNEAU, G. 2010. Survival in patients with idiopathic, familial, and anorexigen-associated pulmonary arterial hypertension in the modern management era. *Circulation*, 122, 156-63.
- HUMBERT, M., SITBON, O., CHAOUAT, A., BERTOCCHI, M., HABIB, G., GRESSIN, V., YAICI, A., WEITZENBLUM, E., CORDIER, J. F., CHABOT, F., DROMER, C., PISON, C., REYNAUD-GAUBERT, M., HALOUN, A., LAURENT, M., HACHULLA, E. & SIMONNEAU, G. 2006. Pulmonary arterial hypertension in France: results from a national registry. *Am J Respir Crit Care Med*, 173, 1023-30.
- IORGA, A., CUNNINGHAM, C. M., MOAZENI, S., RUFFENACH, G., UMAR, S. & EGHBALI, M. 2017. The protective role of estrogen and estrogen receptors in cardiovascular disease and the controversial use of estrogen therapy. *Biol Sex Differ* [Online], 8. Available: <http://dx.doi.org/10.1186/s13293-017-0152-8> [Accessed 18 August 2020].
- JACOBS, W., VAN DE VEERDONK, M. C., TRIP, P., DE MAN, F., HEYMANS, M. W., MARCUS, J. T., KAWUT, S. M., BOGAARD, H. J., BOONSTRA, A. & VONK NOORDEGRAAF, A. 2014. The right ventricle explains sex differences in survival in idiopathic pulmonary arterial hypertension. *Chest*, 145, 1230-1236.

- JASMIN, J. F., LUCAS, M., CERNACEK, P. & DUPUIS, J. 2001. Effectiveness of a nonselective ET(A/B) and a selective ET(A) antagonist in rats with monocrotaline-induced pulmonary hypertension. *Circulation*, 103, 314-8.
- JERNSTROM, H., KLUG, T. L., SEPKOVIC, D. W., BRADLOW, H. L. & NAROD, S. A. 2003. Predictors of the plasma ratio of 2-hydroxyestrone to 16alpha-hydroxyestrone among pre-menopausal, nulliparous women from four ethnic groups. *Carcinogenesis*, 24, 991-1005.
- JIANG, P., XU, J., ZHENG, S., HUANG, J., XIANG, Q., FU, X. & WANG, T. 2010. 17beta-estradiol down-regulates lipopolysaccharide-induced MCP-1 production and cell migration in vascular smooth muscle cells. *J Mol Endocrinol*, 45, 87-97.
- JING, Z. C., PARIKH, K., PULIDO, T., JERJES-SANCHEZ, C., WHITE, R. J., ALLEN, R., TORBICKI, A., XU, K. F., YEHLE, D., LALIBERTE, K., ARNESON, C. & RUBIN, L. J. 2013. Efficacy and safety of oral treprostinil monotherapy for the treatment of pulmonary arterial hypertension: a randomized, controlled trial. *Circulation*, 127, 624-33.
- JOHANSEN, A. K. 2014. *Estrogen metabolism in pulmonary arterial hypertension*. PhD Thesis, University of Glasgow.
- JONES, P. L., COWAN, K. N. & RABINOVITCH, M. 1997. Tenascin-C, proliferation and subendothelial fibronectin in progressive pulmonary vascular disease. *Am J Pathol*, 150, 1349-60.
- KASIMIR, M. T., SEEBACHER, G., JAKSCH, P., WINKLER, G., SCHMID, K., MARTA, G. M., SIMON, P. & KLEPETKO, W. 2004. Reverse cardiac remodelling in patients with primary pulmonary hypertension after isolated lung transplantation. *Eur J Cardiothorac Surg*, 26, 776-81.
- KATO, K., WAKAI, J., OZAWA, K., SEKIGUCHI, M. & KATAHIRA, K. 2016. Different sensitivity to the suppressive effects of isoflurane anesthesia on cardiorespiratory function in SHR/Izm, WKY/Izm, and Crl:CD (SD) rats. *Exp Anim*, 65, 393-402.
- KAWUT, S. M., AL-NAAMANI, N., AGERSTRAND, C., ROSENZWEIG, E. B., ROWAN, C., BARST, R. J., BERGMANN, S. & HORN, E. M. 2009. Determinants of Right Ventricular Ejection Fraction in Pulmonary Arterial Hypertension\*. *Chest*, 135, 752-9.
- KAWUT, S. M., ARCHER-CHICKO, C. L., DEMICHELE, A., FRITZ, J. S., KLINGER, J. R., KY, B., PALEVSKY, H. I., PALMISCIANO, A. J., PATEL, M., PINDER, D., PROPERT, K. J., SMITH, K. A., STANCZYK, F., TRACY, R., VAIDYA, A., WHITTENHALL, M. E. & VENTETUOLO, C. E. 2017. Anastrozole in Pulmonary Arterial Hypertension. A Randomized, Double-Blind, Placebo-controlled Trial. *Am J Respir Crit Care Med*, 195, 360-368.
- KAY, J. M., HARRIS, P. & HEATH, D. 1967. Pulmonary hypertension produced in rats by ingestion of *Crotalaria spectabilis* seeds. *Thorax*, 22, 176-9.
- KELLY, C. M. & BUZDAR, A. U. 2010. Anastrozole. *Expert Opin Drug Saf*, 9, 995-1003.
- KHAN, R. & SHEPPARD, R. 2006. Fibrosis in heart disease: understanding the role of transforming growth factor-beta in cardiomyopathy, valvular disease and arrhythmia. *Immunology*, 118, 10-24.
- KHOSLA, S., ATKINSON, E. J., MELTON, L. J., 3RD & RIGGS, B. L. 1997. Effects of age and estrogen status on serum parathyroid hormone levels and biochemical markers of bone turnover in women: a population-based study. *J Clin Endocrinol Metab*, 82, 1522-7.

- KOVACS, A., LAKATOS, B., TOKODI, M. & MERKELY, B. 2019. Right ventricular mechanical pattern in health and disease: beyond longitudinal shortening. *Heart Fail Rev*, 24, 511-520.
- LAHM, T., ALBRECHT, M., FISHER, A. J., SELEJ, M., PATEL, N. G., BROWN, J. A., JUSTICE, M. J., BROWN, M. B., VAN DEMARK, M., TRULOCK, K. M., DIEUDONNE, D., REDDY, J. G., PRESSON, R. G. & PETRACHE, I. 2012. 17beta-Estradiol attenuates hypoxic pulmonary hypertension via estrogen receptor-mediated effects. *Am J Respir Crit Care Med*, 185, 965-80.
- LAHM, T., DOUGLAS, I. S., ARCHER, S. L., BOGAARD, H. J., CHESLER, N. C., HADDAD, F., HEMNES, A. R., KAWUT, S. M., KLINE, J. A., KOLB, T. M., MATHAI, S. C., MERCIER, O., MICHELAKIS, E. D., NAEIJE, R., TUDER, R. M., VENTETUOLO, C. E., VIEILLARD-BARON, A., VOELKEL, N. F., VONK-NOORDEGRAAF, A. & HASSOUN, P. M. 2018. Assessment of Right Ventricular Function in the Research Setting: Knowledge Gaps and Pathways Forward. An Official American Thoracic Society Research Statement. *Am J Respir Crit Care Med*, 198, e15-e43.
- LAHM, T., TUDER, R. M. & PETRACHE, I. 2014. Progress in solving the sex hormone paradox in pulmonary hypertension. *Am J Physiol Lung Cell Mol Physiol*, 307, L7-26.
- LAN, C. C., FANG, A. H., WU, P. H. & WU, C. S. 2014. Tacrolimus abrogates TGF-beta1-induced type I collagen production in normal human fibroblasts through suppressing p38MAPK signalling pathway: implications on treatment of chronic atopic dermatitis lesions. *J Eur Acad Dermatol Venereol*, 28, 204-15.
- LARKIN, E. K., NEWMAN, J. H., AUSTIN, E. D., HEMNES, A. R., WHEELER, L., ROBBINS, I. M., WEST, J. D., PHILLIPS, J. A., 3RD, HAMID, R. & LOYD, J. E. 2012. Longitudinal analysis casts doubt on the presence of genetic anticipation in heritable pulmonary arterial hypertension. *Am J Respir Crit Care Med*, 186, 892-6.
- LAU, E. M. T., GIANNOULATOU, E., CELERMAJER, D. S. & HUMBERT, M. 2017. Epidemiology and treatment of pulmonary arterial hypertension. *Nat Rev Cardiol*, 14, 603-614.
- LEE, A. A., DILLMANN, W. H., MCCULLOCH, A. D. & VILLARREAL, F. J. 1995. Angiotensin II stimulates the autocrine production of transforming growth factor-beta 1 in adult rat cardiac fibroblasts. *J Mol Cell Cardiol*, 27, 2347-57.
- LEE, J. K., KODAMA, I., HONJO, H., ANNO, T., KAMIYA, K. & TOYAMA, J. 1997. Stage-dependent changes in membrane currents in rats with monocrotaline-induced right ventricular hypertrophy. *Am J Physiol*, 272, H2833-42.
- LEE, J. K., NISHIYAMA, A., KAMBE, F., SEO, H., TAKEUCHI, S., KAMIYA, K., KODAMA, I. & TOYAMA, J. 1999. Downregulation of voltage-gated K(+) channels in rat heart with right ventricular hypertrophy. *Am J Physiol*, 277, H1725-31.
- LI, H., CHENG, Y., SIMONCINI, T. & XU, S. 2016a. 17beta-Estradiol inhibits TNF-alpha-induced proliferation and migration of vascular smooth muscle cells via suppression of TRAIL. *Gynecol Endocrinol*, 32, 581-6.
- LI, W. Q., LI, X. H., DU, J., ZHANG, W., LI, D., XIONG, X. M. & LI, Y. J. 2016b. Rutaecarpine attenuates hypoxia-induced right ventricular remodeling in rats. *Naunyn Schmiedebergs Arch Pharmacol*, 389, 757-67.

- LINDNER, V., KIM, S. K., KARAS, R. H., KUIPER, G. G., GUSTAFSSON, J. A. & MENDELSON, M. E. 1998. Increased expression of estrogen receptor-beta mRNA in male blood vessels after vascular injury. *Circ Res*, 83, 224-9.
- LINDSEY, S. H., CARVER, K. A., PROSSNITZ, E. R. & CHAPPELL, M. C. 2011. Vasodilation in response to the GPR30 agonist G-1 is not different from estradiol in the mRen2.Lewis female rat. *J Cardiovasc Pharmacol*, 57, 598-603.
- LING, Y., JOHNSON, M. K., KIELY, D. G., CONDLIFFE, R., ELLIOT, C. A., GIBBS, J. S., HOWARD, L. S., PEPKE-ZABA, J., SHEARES, K. K., CORRIS, P. A., FISHER, A. J., LORDAN, J. L., GAINE, S., COGHLAN, J. G., WORT, S. J., GATZOULIS, M. A. & PEACOCK, A. J. 2012. Changing demographics, epidemiology, and survival of incident pulmonary arterial hypertension: results from the pulmonary hypertension registry of the United Kingdom and Ireland. *Am J Respir Crit Care Med*, 186, 790-6.
- LIU, A., SCHREIER, D., TIAN, L., EICKHOFF, J. C., WANG, Z., HACKER, T. A. & CHESLER, N. C. 2014. Direct and indirect protection of right ventricular function by estrogen in an experimental model of pulmonary arterial hypertension. *Am J Physiol Heart Circ Physiol*, 307, H273-83.
- LIU, Z. H., KANJO, Y. & MIZUTANI, S. 2009. Urinary excretion rates of natural estrogens and androgens from humans, and their occurrence and fate in the environment: a review. *Sci Total Environ*, 407, 4975-85.
- LOUCH, W. E., SHEEHAN, K. A. & WOLSKA, B. M. 2011. Methods in cardiomyocyte isolation, culture, and gene transfer. *J Mol Cell Cardiol*, 51, 288-98.
- LOYD, J. E., BUTLER, M. G., FOROUD, T. M., CONNEALLY, P. M., PHILLIPS, J. A., 3RD & NEWMAN, J. H. 1995. Genetic anticipation and abnormal gender ratio at birth in familial primary pulmonary hypertension. *Am J Respir Crit Care Med*, 152, 93-7.
- MACHADO, R. D., ALDRED, M. A., JAMES, V., HARRISON, R. E., PATEL, B., SCHWALBE, E. C., GRUENIG, E., JANSSEN, B., KOEHLER, R., SEEGER, W., EICKELBERG, O., OLSCHIEWSKI, H., ELLIOTT, C. G., GLISSMEYER, E., CARLQUIST, J., KIM, M., TORBICKI, A., FIJALKOWSKA, A., SZEWCZYK, G., PARMA, J., ABRAMOWICZ, M. J., GALIE, N., MORISAKI, H., KYOTANI, S., NAKANISHI, N., MORISAKI, T., HUMBERT, M., SIMONNEAU, G., SITBON, O., SOUBRIER, F., COULET, F., MORRELL, N. W. & TREMBATH, R. C. 2006. Mutations of the TGF-beta type II receptor BMPR2 in pulmonary arterial hypertension. *Hum Mutat*, 27, 121-32.
- MACHADO, R. D., EICKELBERG, O., ELLIOTT, C. G., GERACI, M. W., HANAOKA, M., LOYD, J. E., NEWMAN, J. H., PHILLIPS, J. A., 3RD, SOUBRIER, F., TREMBATH, R. C. & CHUNG, W. K. 2009. Genetics and genomics of pulmonary arterial hypertension. *J Am Coll Cardiol*, 54, S32-42.
- MACLEAN, M. R., MCCULLOCH, K. M. & BAIRD, M. 1994. Endothelin ETA- and ETB-receptor-mediated vasoconstriction in rat pulmonary arteries and arterioles. *J Cardiovasc Pharmacol*, 23, 838-45.
- MAIR, K. M., HARVEY, K. Y., HENRY, A. D., HILLYARD, D. Z., NILSEN, M. & MACLEAN, M. R. 2019. Obesity alters oestrogen metabolism and contributes to pulmonary arterial hypertension. *Eur Respir J* [Online], 53. Available: <http://dx.doi.org/10.1183/13993003.01524-2018> [Accessed 18 August 2020].
- MAIR, K. M., JOHANSEN, A. K., WRIGHT, A. F., WALLACE, E. & MACLEAN, M. R. 2014a. Pulmonary arterial hypertension: basis of sex differences in incidence and treatment response. *Br J Pharmacol*, 171, 567-79.

- MAIR, K. M., WRIGHT, A. F., DUGGAN, N., ROWLANDS, D. J., HUSSEY, M. J., ROBERTS, S., FULLERTON, J., NILSEN, M., LOUGHLIN, L., THOMAS, M. & MACLEAN, M. R. 2014b. Sex-dependent influence of endogenous estrogen in pulmonary hypertension. *Am J Respir Crit Care Med*, 190, 456-67.
- MAIR, K. M., YANG, X. D., LONG, L., WHITE, K., WALLACE, E., EWART, M. A., DOCHERTY, C. K., MORRELL, N. W. & MACLEAN, M. R. 2015. Sex affects bone morphogenetic protein type II receptor signaling in pulmonary artery smooth muscle cells. *Am J Respir Crit Care Med*, 191, 693-703.
- MANABE, I., SHINDO, T. & NAGAI, R. 2002. Gene expression in fibroblasts and fibrosis: involvement in cardiac hypertrophy. *Circ Res*, 91, 1103-13.
- MCCARROLL, C. S., HE, W., FOOTE, K., BRADLEY, A., MCGLYNN, K., VIDLER, F., NIXON, C., NATHER, K., FATTAH, C., RIDDELL, A., BOWMAN, P., ELLIOTT, E. B., BELL, M., HAWKSBY, C., MACKENZIE, S. M., MORRISON, L. J., TERRY, A., BLYTH, K., SMITH, G. L., MCBRIDE, M. W., KUBIN, T., BRAUN, T., NICKLIN, S. A., CAMERON, E. R. & LOUGHREY, C. M. 2018. Runx1 Deficiency Protects Against Adverse Cardiac Remodeling After Myocardial Infarction. *Circulation*, 137, 57-70.
- MCLAUGHLIN, V. V., BENZA, R. L., RUBIN, L. J., CHANNICK, R. N., VOSWINCKEL, R., TAPSON, V. F., ROBBINS, I. M., OLSCHESKI, H., RUBENFIRE, M. & SEEGER, W. 2010. Addition of inhaled treprostinil to oral therapy for pulmonary arterial hypertension: a randomized controlled clinical trial. *J Am Coll Cardiol*, 55, 1915-22.
- MCMURTRY, I. F., DAVIDSON, A. B., REEVES, J. T. & GROVER, R. F. 1976. Inhibition of hypoxic pulmonary vasoconstriction by calcium antagonists in isolated rat lungs. *Circ Res*, 38, 99-104.
- MEDAROV, B. I. & JUDSON, M. A. 2015. The role of calcium channel blockers for the treatment of pulmonary arterial hypertension: How much do we actually know and how could they be positioned today? *Respir Med*, 109, 557-64.
- MENDELSON, M. E. & KARAS, R. H. 1999. The protective effects of estrogen on the cardiovascular system. *N Engl J Med*, 340, 1801-11.
- MENDES-FERREIRA, P., SANTOS-RIBEIRO, D., ADAO, R., MAIA-ROCHA, C., MENDES-FERREIRA, M., SOUSA-MENDES, C., LEITE-MOREIRA, A. F. & BRAS-SILVA, C. 2016. Distinct right ventricle remodeling in response to pressure overload in the rat. *Am J Physiol Heart Circ Physiol*, 311, H85-95.
- MEYRICK, B. & REID, L. 1980. Ultrastructural findings in lung biopsy material from children with congenital heart defects. *Am J Pathol*, 101, 527-42.
- MEYRICK, B. O. & REID, L. M. 1982. Crotalaria-induced pulmonary hypertension. Uptake of 3H-thymidine by the cells of the pulmonary circulation and alveolar walls. *Am J Pathol*, 106, 84-94.
- MILLER, P. J. 1971. An elastin stain. *Med Lab Technol*, 28, 148-9.
- MIYAUCHI, T., YORIKANE, R., SAKAI, S., SAKURAI, T., OKADA, M., NISHIKIBE, M., YANO, M., YAMAGUCHI, I., SUGISHITA, Y. & GOTO, K. 1993. Contribution of endogenous endothelin-1 to the progression of cardiopulmonary alterations in rats with monocrotaline-induced pulmonary hypertension. *Circ Res*, 73, 887-97.
- MODUGNO, F., KIP, K. E., COCHRANE, B., KULLER, L., KLUG, T. L., ROHAN, T. E., CHLEBOWSKI, R. T., LASSER, N. & STEFANICK, M. L. 2006. Obesity, hormone therapy, estrogen metabolism and risk of postmenopausal breast cancer. *Int J Cancer*, 118, 1292-301.
- MORRELL, N. W., ADNOT, S., ARCHER, S. L., DUPUIS, J., JONES, P. L., MACLEAN, M. R., MCMURTRY, I. F., STENMARK, K. R., THISTLETHWAITE, P. A.,

- WEISSMANN, N., YUAN, J. X. & WEIR, E. K. 2009. Cellular and molecular basis of pulmonary arterial hypertension. *J Am Coll Cardiol*, 54, S20-31.
- NATHAN, L., PERVIN, S., SINGH, R., ROSENFELD, M. & CHAUDHURI, G. 1999. Estradiol inhibits leukocyte adhesion and transendothelial migration in rabbits in vivo : possible mechanisms for gender differences in atherosclerosis. *Circ Res*, 85, 377-85.
- NEWMAN, J. H., TREMBATH, R. C., MORSE, J. A., GRUNIG, E., LOYD, J. E., ADNOT, S., COCCOLO, F., VENTURA, C., PHILLIPS, J. A., 3RD, KNOWLES, J. A., JANSSEN, B., EICKELBERG, O., EDDAHIBI, S., HERVE, P., NICHOLS, W. C. & ELLIOTT, G. 2004. Genetic basis of pulmonary arterial hypertension: current understanding and future directions. *J Am Coll Cardiol*, 43, 33s-39s.
- NICOLLS, M. R., MIZUNO, S., TARASEVICIENE-STEWART, L., FARKAS, L., DRAKE, J. I., AL HUSSEINI, A., GOMEZ-ARROYO, J. G., VOELKEL, N. F. & BOGAARD, H. J. 2012. New models of pulmonary hypertension based on VEGF receptor blockade-induced endothelial cell apoptosis. *Pulm Circ*, 2, 434-42.
- NOVELLA, S., PEREZ-CREMADES, D., MOMPEON, A. & HERMENEGILDO, C. 2019. Mechanisms underlying the influence of oestrogen on cardiovascular physiology in women. *J Physiol*, 597, 4873-4886.
- OLSCHEWSKI, H., ROSE, F., GRUNIG, E., GHOFRANI, H. A., WALMRATH, D., SCHULZ, R., SCHERMULY, R., GRIMMINGER, F. & SEEGER, W. 2001. Cellular pathophysiology and therapy of pulmonary hypertension. *J Lab Clin Med*, 138, 367-77.
- OTTO, C., FUCHS, I., KAUSELMANN, G., KERN, H., ZEVIK, B., ANDREASEN, P., SCHWARZ, G., ALTMANN, H., KLEWER, M., SCHOOR, M., VONK, R. & FRITZEMEIER, K. H. 2008. GPR30 does not mediate estrogenic responses in reproductive organs in mice. *Biol Reprod*, 80, 34-41.
- PARE, G., KRUST, A., KARAS, R. H., DUPONT, S., ARONOVITZ, M., CHAMBON, P. & MENDELSON, M. E. 2002. Estrogen receptor-alpha mediates the protective effects of estrogen against vascular injury. *Circ Res*, 90, 1087-92.
- PEACOCK, A. J., MURPHY, N. F., MCMURRAY, J. J., CABALLERO, L. & STEWART, S. 2007. An epidemiological study of pulmonary arterial hypertension. *Eur Respir J*, 30, 104-9.
- PEDRAM, A., RAZANDI, M., O'MAHONY, F., LUBAHN, D. & LEVIN, E. R. 2010. Estrogen receptor-beta prevents cardiac fibrosis. *Mol Endocrinol*, 24, 2152-65.
- PIAO, L., FANG, Y. H., CADETE, V. J., WIETHOLT, C., URBONIENE, D., TOTH, P. T., MARSBOOM, G., ZHANG, H. J., HABER, I., REHMAN, J., LOPASCHUK, G. D. & ARCHER, S. L. 2010. The inhibition of pyruvate dehydrogenase kinase improves impaired cardiac function and electrical remodeling in two models of right ventricular hypertrophy: resuscitating the hibernating right ventricle. *J Mol Med (Berl)*, 88, 47-60.
- PINSKY, M. R. 1984. Instantaneous venous return curves in an intact canine preparation. *J Appl Physiol Respir Environ Exerc Physiol*, 56, 765-71.
- PINSKY, M. R. 2016. The right ventricle: interaction with the pulmonary circulation. *Crit Care*, 20, 266.
- PINSKY, M. R., DESMET, J. M. & VINCENT, J. L. 1992. Effect of positive end-expiratory pressure on right ventricular function in humans. *Am Rev Respir Dis*, 146, 681-7.

- PORRELLO, E. R., MAHMOUD, A. I., SIMPSON, E., HILL, J. A., RICHARDSON, J. A., OLSON, E. N. & SADEK, H. A. 2011. Transient regenerative potential of the neonatal mouse heart. *Science*, 331, 1078-80.
- POWELL, T. & TWIST, V. W. 1976. A rapid technique for the isolation and purification of adult cardiac muscle cells having respiratory control and a tolerance to calcium. *Biochem Biophys Res Commun*, 72, 327-33.
- QI, S., YAN, L., LIU, Z., MU, Y. L., LI, M., ZHAO, X., CHEN, Z. J. & ZHANG, H. 2018. Melatonin inhibits 17beta-estradiol-induced migration, invasion and epithelial-mesenchymal transition in normal and endometriotic endometrial epithelial cells. *Reprod Biol Endocrinol*, 16, 62.
- RABINOVITCH, M. 1998. Elastase and the pathobiology of unexplained pulmonary hypertension. *Chest*, 114, 213s-224s.
- RABINOVITCH, M. 2008. Molecular pathogenesis of pulmonary arterial hypertension. *J Clin Invest*, 118, 2372-9.
- RABINOVITCH, M., BOTHWELL, T., HAYAKAWA, B. N., WILLIAMS, W. G., TRUSLER, G. A., ROWE, R. D., OLLEY, P. M. & CUTZ, E. 1986. Pulmonary artery endothelial abnormalities in patients with congenital heart defects and pulmonary hypertension. A correlation of light with scanning electron microscopy and transmission electron microscopy. *Lab Invest*, 55, 632-53.
- RABINOVITCH, M., GAMBLE, W., NADAS, A. S., MIETTINEN, O. S. & REID, L. 1979. Rat pulmonary circulation after chronic hypoxia: hemodynamic and structural features. *Am J Physiol*, 236, H818-27.
- RAJKUMAR, R., KONISHI, K., RICHARDS, T. J., ISHIZAWAR, D. C., WIECHERT, A. C., KAMINSKI, N. & AHMAD, F. 2010. Genomewide RNA expression profiling in lung identifies distinct signatures in idiopathic pulmonary arterial hypertension and secondary pulmonary hypertension. *Am J Physiol Heart Circ Physiol*, 298, H1235-48.
- RANCHOUX, B., ANTIGNY, F., RUCKER-MARTIN, C., HAUTEFORT, A., PECHOUX, C., BOGAARD, H. J., DORFMULLER, P., REMY, S., LECERF, F., PLANTE, S., CHAT, S., FADEL, E., HOUSSAINI, A., ANEGON, I., ADNOT, S., SIMONNEAU, G., HUMBERT, M., COHEN-KAMINSKY, S. & PERROS, F. 2015. Endothelial-to-mesenchymal transition in pulmonary hypertension. *Circulation*, 131, 1006-18.
- REDDY, S. & BERNSTEIN, D. 2015. The vulnerable right ventricle. *Curr Opin Pediatr*, 27, 563-8.
- REDFORS, B., SHAO, Y. & OMEROVIC, E. 2014. Influence of anesthetic agent, depth of anesthesia and body temperature on cardiovascular functional parameters in the rat. *Lab Anim*, 48, 6-14.
- REDINGTON, A. N., RIGBY, M. L., SHINEBOURNE, E. A. & OLDERSHAW, P. J. 1990. Changes in the pressure-volume relation of the right ventricle when its loading conditions are modified. *Br Heart J*, 63, 45-9.
- REYNOLDS, H., NATHAN, P., SRIVASTAVA, L. S. & HESS, E. V. 1982. Release of estradiol from fetal bovine serum by rat thymus, spleen, kidney, lung and lung macrophage cultures. *Endocrinology*, 110, 2213-5.
- RICH, S. 2012. Right ventricular adaptation and maladaptation in chronic pulmonary arterial hypertension. *Cardiol Clin*, 30, 257-69.
- RICH, S. & BRUNDAGE, B. H. 1987. High-dose calcium channel-blocking therapy for primary pulmonary hypertension: evidence for long-term reduction in pulmonary arterial pressure and regression of right ventricular hypertrophy. *Circulation*, 76, 135-41.
- RICH, S., DANTZKER, D. R., AYRES, S. M., BERGOFKY, E. H., BRUNDAGE, B. H., DETRE, K. M., FISHMAN, A. P., GOLDRING, R. M., GROVES, B. M.,

- KOERNER, S. K. & ET AL. 1987. Primary pulmonary hypertension. A national prospective study. *Ann Intern Med*, 107, 216-23.
- RICH, S., KAUFMANN, E. & LEVY, P. S. 1992. The effect of high doses of calcium-channel blockers on survival in primary pulmonary hypertension. *N Engl J Med*, 327, 76-81.
- RIZZO, A. N., FRAIDENBURG, D. R. & YUAN, J. X. 2015. *Pulmonary Vascular Anatomy*, Berlin, Heidelberg, Springer.
- ROCKMAN, H. A., ONO, S., ROSS, R. S., JONES, L. R., KARIMI, M., BHARGAVA, V., ROSS, J., JR. & CHIEN, K. R. 1994. Molecular and physiological alterations in murine ventricular dysfunction. *Proc Natl Acad Sci U S A*, 91, 2694-8.
- ROSENBERG, H. C. & RABINOVITCH, M. 1988. Endothelial injury and vascular reactivity in monocrotaline pulmonary hypertension. *Am J Physiol*, 255, H1484-91.
- ROSENKRANZ, S. 2004. TGF-beta1 and angiotensin networking in cardiac remodeling. *Cardiovasc Res*, 63, 423-32.
- ROSS, B., MCINTOSH, M., RODAROS, D., HEBERT, T. E. & ROHLICEK, C. V. 2010. Systemic arterial pressure at maturity in rats following chronic hypoxia in early life. *Am J Hypertens*, 23, 1228-33.
- ROTH, R. A., DOTZLAF, L. A., BARANYI, B., KUO, C. H. & HOOK, J. B. 1981. Effect of monocrotaline ingestion on liver, kidney, and lung of rats. *Toxicol Appl Pharmacol*, 60, 193-203.
- RYAN, J. J., HUSTON, J., KUTTY, S., HATTON, N. D., BOWMAN, L., TIAN, L., HERR, J. E., JOHRI, A. M. & ARCHER, S. L. 2015. Right ventricular adaptation and failure in pulmonary arterial hypertension. *Can J Cardiol*, 31, 391-406.
- RYBALKIN, S. D., YAN, C., BORNFELDT, K. E. & BEAVO, J. A. 2003. Cyclic GMP phosphodiesterases and regulation of smooth muscle function. *Circ Res*, 93, 280-91.
- SAKUMA, M., ISHIGAKI, H., KOMAKI, K., OIKAWA, Y., KATOH, A., NAKAGAWA, M., HOZAWA, H., YAMAMOTO, Y., TAKAHASHI, T. & SHIRATO, K. 2002. Right ventricular ejection function assessed by cineangiography--Importance of bellows action. *Circ J*, 66, 605-9.
- SAKURAI, T., YANAGISAWA, M., INOUE, A., RYAN, U. S., KIMURA, S., MITSUI, Y., GOTO, K. & MASAKI, T. 1991. cDNA cloning, sequence analysis and tissue distribution of rat preproendothelin-1 mRNA. *Biochem Biophys Res Commun*, 175, 44-7.
- SAMAVAT, H. & KURZER, M. S. 2015. Estrogen metabolism and breast cancer. *Cancer Lett*, 356, 231-43.
- SANZ, J., CONROY, J. & NARULA, J. 2012. Imaging of the right ventricle. *Cardiol Clin*, 30, 189-203.
- SATO, K., WEBB, S., TUCKER, A., RABINOVITCH, M., O'BRIEN, R. F., MCMURTRY, I. F. & STELZNER, T. J. 1992. Factors influencing the idiopathic development of pulmonary hypertension in the fawn hooded rat. *Am Rev Respir Dis*, 145, 793-7.
- SCHMITTGEN, T. D. & LIVAK, K. J. 2008. Analyzing real-time PCR data by the comparative CT method. *Nature Protocols*, 3, 1101-1108.
- SEO, B., OEMAR, B. S., SIEBENMANN, R., VON SEGESSER, L. & LUSCHER, T. F. 1994. Both ETA and ETB receptors mediate contraction to endothelin-1 in human blood vessels. *Circulation*, 89, 1203-8.
- SHAPIRO, S., TRAIGER, G. L., TURNER, M., MCGOON, M. D., WASON, P. & BARST, R. J. 2012. Sex differences in the diagnosis, treatment, and outcome of patients with pulmonary arterial hypertension enrolled in the registry to

- evaluate early and long-term pulmonary arterial hypertension disease management. *Chest*, 141, 363-373.
- SHEEHAN, F. & REDINGTON, A. 2008. The right ventricle: anatomy, physiology and clinical imaging. *Heart*, 94, 1510-5.
- SHEIKH, A. Q., LIGHTHOUSE, J. K. & GREIF, D. M. 2014. Recapitulation of developing artery muscularization in pulmonary hypertension. *Cell Rep*, 6, 809-17.
- SHIMODA, L. A. & LAURIE, S. S. 2013. Vascular remodeling in pulmonary hypertension. *J Mol Med (Berl)*, 91, 297-309.
- SIMONNEAU, G., MONTANI, D., CELERMAJER, D. S., DENTON, C. P., GATZOULIS, M. A., KROWKA, M., WILLIAMS, P. G. & SOUZA, R. 2019. Haemodynamic definitions and updated clinical classification of pulmonary hypertension. *Eur Respir J* [Online], 53. Available: <http://dx.doi.org/10.1183/13993003.01913-2018> [Accessed 18 August 2020].
- SITBON, O., HUMBERT, M., JAIS, X., IOOS, V., HAMID, A. M., PROVENCHER, S., GARCIA, G., PARENT, F., HERVE, P. & SIMONNEAU, G. 2005. Long-term response to calcium channel blockers in idiopathic pulmonary arterial hypertension. *Circulation*, 111, 3105-11.
- SITBON, O., SATTLER, C., BERTOLETTI, L., SAVALE, L., COTTIN, V., JAIS, X., DE GROOTE, P., CHAOUAT, A., CHABANNES, C., BERGOT, E., BOUVAIST, H., DAUPHIN, C., BOURDIN, A., BAUER, F., MONTANI, D., HUMBERT, M. & SIMONNEAU, G. 2016. Initial dual oral combination therapy in pulmonary arterial hypertension. *Eur Respir J*, 47, 1727-36.
- SOUTHGATE, L., MACHADO, R. D., GRAF, S. & MORRELL, N. W. 2020. Molecular genetic framework underlying pulmonary arterial hypertension. *Nat Rev Cardiol*, 17, 85-95.
- SPIEKERKOETTER, E., SUNG, Y. K., SUDHEENDRA, D., BILL, M., ALDRED, M. A., VAN DE VEERDONK, M. C., VONK NOORDEGRAAF, A., LONG-BOYLE, J., DASH, R., YANG, P. C., LAWRIE, A., SWIFT, A. J., RABINOVITCH, M. & ZAMANIAN, R. T. 2015. Low-Dose FK506 (Tacrolimus) in End-Stage Pulmonary Arterial Hypertension. *Am J Respir Crit Care Med*, 192, 254-7.
- SPIEKERKOETTER, E., SUNG, Y. K., SUDHEENDRA, D., SCOTT, V., DEL ROSARIO, P., BILL, M., HADDAD, F., LONG-BOYLE, J., HEDLIN, H. & ZAMANIAN, R. T. 2017. Randomised placebo-controlled safety and tolerability trial of FK506 (tacrolimus) for pulmonary arterial hypertension. *Eur Respir J* [Online], 50. Available: <http://dx.doi.org/10.1183/13993003.02449-2016> [Accessed 18 August 2020].
- SPIEKERKOETTER, E., TIAN, X., CAI, J., HOPPER, R. K., SUDHEENDRA, D., LI, C. G., EL-BIZRI, N., SAWADA, H., HAGHIGHAT, R., CHAN, R., HAGHIGHAT, L., DE JESUS PEREZ, V., WANG, L., REDDY, S., ZHAO, M., BERNSTEIN, D., SOLOW-CORDERO, D. E., BEACHY, P. A., WANDLESS, T. J., TEN DIJKE, P. & RABINOVITCH, M. 2013. FK506 activates BMPR2, rescues endothelial dysfunction, and reverses pulmonary hypertension. *J Clin Invest*, 123, 3600-13.
- ST CROIX, C. M. & STEINHORN, R. H. 2016. New Thoughts about the Origin of Plexiform Lesions. *Am J Respir Crit Care Med*, 193, 484-5.
- STAMPFER, M. & GRODSTEIN, F. 1994. Cardioprotective effect of hormone replacement therapy. Is not due to selection bias. *Bmj*, 309, 808-9.
- STENMARK, K. R., FAGAN, K. A. & FRID, M. G. 2006. Hypoxia-induced pulmonary vascular remodeling: cellular and molecular mechanisms. *Circ Res*, 99, 675-91.

- STENMARK, K. R., MEYRICK, B., GALIE, N., MOOI, W. J. & MCMURTRY, I. F. 2009. Animal models of pulmonary arterial hypertension: the hope for etiological discovery and pharmacological cure. *Am J Physiol Lung Cell Mol Physiol*, 297, L1013-32.
- STRICKER, R., EBERHART, R., CHEVAILLER, M. C., QUINN, F. A. & BISCHOF, P. 2006. Establishment of detailed reference values for luteinizing hormone, follicle stimulating hormone, estradiol, and progesterone during different phases of the menstrual cycle on the Abbott ARCHITECT analyzer. *Clin Chem Lab Med*, 44, 883-7.
- SWANECK, G. E. & FISHMAN, J. 1988. Covalent binding of the endogenous estrogen 16 alpha-hydroxyestrone to estradiol receptor in human breast cancer cells: characterization and intranuclear localization. *Proc Natl Acad Sci U S A*, 85, 7831-5.
- SZTRYMF, B., COULET, F., GIRERD, B., YAICI, A., JAIS, X., SITBON, O., MONTANI, D., SOUZA, R., SIMONNEAU, G., SOUBRIER, F. & HUMBERT, M. 2008. Clinical outcomes of pulmonary arterial hypertension in carriers of BMP2 mutation. *Am J Respir Crit Care Med*, 177, 1377-83.
- TARASEVICIENE-STEWART, L., KASAHARA, Y., ALGER, L., HIRTH, P., MC MAHON, G., WALTENBERGER, J., VOELKEL, N. F. & TUDER, R. M. 2001. Inhibition of the VEGF receptor 2 combined with chronic hypoxia causes cell death-dependent pulmonary endothelial cell proliferation and severe pulmonary hypertension. *Faseb j*, 15, 427-38.
- TARNAVSKI, O., MCMULLEN, J. R., SCHINKE, M., NIE, Q., KONG, S. & IZUMO, S. 2004. Mouse cardiac surgery: comprehensive techniques for the generation of mouse models of human diseases and their application for genomic studies. *Physiological Genomics*, 16, 349-360.
- TEDFORD, R. J. 2014. Determinants of right ventricular afterload (2013 Grover Conference series). *Pulm Circ*, 4, 211-9.
- TEICHERT-KULISZEWSKA, K., KUTRYK, M. J., KULISZEWSKI, M. A., KAROUBI, G., COURTMAN, D. W., ZUCCO, L., GRANTON, J. & STEWART, D. J. 2006. Bone morphogenetic protein receptor-2 signaling promotes pulmonary arterial endothelial cell survival: implications for loss-of-function mutations in the pathogenesis of pulmonary hypertension. *Circ Res*, 98, 209-17.
- THIES, R. L. & AUTOR, A. P. 1991. Reactive oxygen injury to cultured pulmonary artery endothelial cells: mediation by poly(ADP-ribose) polymerase activation causing NAD depletion and altered energy balance. *Arch Biochem Biophys*, 286, 353-63.
- THOMAS, M. P. & POTTER, B. V. 2013. The structural biology of oestrogen metabolism. *J Steroid Biochem Mol Biol*, 137, 27-49.
- THOMAS, P., PANG, Y., FILARDO, E. J. & DONG, J. 2005. Identity of an estrogen membrane receptor coupled to a G protein in human breast cancer cells. *Endocrinology*, 146, 624-32.
- THOMPSON, K. & RABINOVITCH, M. 1996. Exogenous leukocyte and endogenous elastases can mediate mitogenic activity in pulmonary artery smooth muscle cells by release of extracellular-matrix bound basic fibroblast growth factor. *J Cell Physiol*, 166, 495-505.
- TODOROVICH-HUNTER, L., JOHNSON, D. J., RANGER, P., KEELEY, F. W. & RABINOVITCH, M. 1988. Altered elastin and collagen synthesis associated with progressive pulmonary hypertension induced by monocrotaline. A biochemical and ultrastructural study. *Lab Invest*, 58, 184-95.

- TOFOVIC, S. P. & JACKSON, E. K. 2020. Estradiol Metabolism: Crossroads in Pulmonary Arterial Hypertension. *Int J Mol Sci* [Online], 21. Available: <http://dx.doi.org/10.3390/ijms21010116> [Accessed 18 August 2020].
- TOFOVIC, S. P., ZHANG, X., ZHU, H., JACKSON, E. K., RAFIKOVA, O. & PETRUSEVSKA, G. 2008. 2-Ethoxyestradiol is antimitogenic and attenuates monocrotaline-induced pulmonary hypertension and vascular remodeling. *Vascul Pharmacol*, 48, 174-83.
- TU, C., FIANDALO, M. V., POP, E., STOCKING, J. J., AZABDAFTARI, G., LI, J., WEI, H., MA, D., QU, J., MOHLER, J. L., TANG, L. & WU, Y. 2018. Proteomic Analysis of Charcoal-Stripped Fetal Bovine Serum Reveals Changes in the Insulin-like Growth Factor Signaling Pathway. *J Proteome Res*, 17, 2963-2977.
- TYBERG, J. V., TAICHMAN, G. C., SMITH, E. R., DOUGLAS, N. W., SMISETH, O. A. & KEON, W. J. 1986. The relationship between pericardial pressure and right atrial pressure: an intraoperative study. *Circulation*, 73, 428-32.
- UMAR, S., IORGA, A., MATORI, H., NADADUR, R. D., LI, J., MALTESE, F., VAN DER LAARSE, A. & EGHBALI, M. 2011. Estrogen rescues preexisting severe pulmonary hypertension in rats. *Am J Respir Crit Care Med*, 184, 715-23.
- VAN DEN BOSCH, B. J., LINDSEY, P. J., VAN DEN BURG, C. M., VAN DER VLIES, S. A., LIPS, D. J., VAN DER VUSSE, G. J., AYOUBI, T. A., DOEVENDANS, P. A. & SMEETS, H. J. 2006. Early and transient gene expression changes in pressure overload-induced cardiac hypertrophy in mice. *Genomics*, 88, 480-8.
- VAN DER BRUGGEN, C. E., HAPPE, C. M., DORFMULLER, P., TRIP, P., SPRUIJT, O. A., ROL, N., HOEVENAARS, F. P., HOUWELING, A. C., GIRERD, B., MARCUS, J. T., MERCIER, O., HUMBERT, M., HANDOKO, M. L., VAN DER VELDEN, J., VONK NOORDEGRAAF, A., BOGAARD, H. J., GOUMANS, M. J. & DE MAN, F. S. 2016. Bone Morphogenetic Protein Receptor Type 2 Mutation in Pulmonary Arterial Hypertension: A View on the Right Ventricle. *Circulation*, 133, 1747-60.
- VANDERPOOL, R. R., KIM, A. R., MOLTHEN, R. & CHESLER, N. C. 2011. Effects of acute Rho kinase inhibition on chronic hypoxia-induced changes in proximal and distal pulmonary arterial structure and function. *J Appl Physiol (1985)*, 110, 188-98.
- VENTETUOLO, C. E., BAIRD, G. L., BARR, R. G., BLUEMKE, D. A., FRITZ, J. S., HILL, N. S., KLINGER, J. R., LIMA, J. A., OUYANG, P., PALEVSKY, H. I., PALMISCIANO, A. J., KRISHNAN, I., PINDER, D., PRESTON, I. R., ROBERTS, K. E. & KAWUT, S. M. 2016a. Higher Estradiol and Lower Dehydroepiandrosterone-Sulfate Levels Are Associated with Pulmonary Arterial Hypertension in Men. *Am J Respir Crit Care Med*, 193, 1168-75.
- VENTETUOLO, C. E., MITRA, N., WAN, F., MANICHAIKUL, A., BARR, R. G., JOHNSON, C., BLUEMKE, D. A., LIMA, J. A., TANDRI, H., OUYANG, P. & KAWUT, S. M. 2016b. Oestradiol metabolism and androgen receptor genotypes are associated with right ventricular function. *Eur Respir J*, 47, 553-63.
- VENTETUOLO, C. E., OUYANG, P., BLUEMKE, D. A., TANDRI, H., BARR, R. G., BAGIELLA, E., CAPPOLA, A. R., BRISTOW, M. R., JOHNSON, C., KRONMAL, R. A., KIZER, J. R., LIMA, J. A. & KAWUT, S. M. 2011. Sex hormones are associated with right ventricular structure and function: The MESA-right ventricle study. *Am J Respir Crit Care Med*, 183, 659-67.
- VONK NOORDEGRAAF, A. & GALIE, N. 2011. The role of the right ventricle in pulmonary arterial hypertension. *Eur Respir Rev*, 20, 243-53.

- VONK NOORDEGRAAF, A., WESTERHOF, B. E. & WESTERHOF, N. 2017. The Relationship Between the Right Ventricle and its Load in Pulmonary Hypertension. *J Am Coll Cardiol*, 69, 236-243.
- VONK-NOORDEGRAAF, A., HADDAD, F., CHIN, K. M., FORFIA, P. R., KAWUT, S. M., LUMENS, J., NAEIJE, R., NEWMAN, J., OUDIZ, R. J., PROVENCHER, S., TORBICKI, A., VOELKEL, N. F. & HASSOUN, P. M. 2013. Right heart adaptation to pulmonary arterial hypertension: physiology and pathobiology. *J Am Coll Cardiol*, 62, D22-33.
- VRTAČNIK, P., OSTANEK, B., MENCEJ-BEDRAČ, S. & MARC, J. 2014. The many faces of estrogen signaling. *Biochem Med (Zagreb)*, 24, 329-42.
- WANG, R. N., GREEN, J., WANG, Z., DENG, Y., QIAO, M., PEABODY, M., ZHANG, Q., YE, J., YAN, Z., DENDULURI, S., IDOWU, O., LI, M., SHEN, C., HU, A., HAYDON, R. C., KANG, R., MOK, J., LEE, M. J., LUU, H. L. & SHI, L. L. 2014. Bone Morphogenetic Protein (BMP) signaling in development and human diseases. *Genes Dis*, 1, 87-105.
- WELSHONS, W. V., WOLF, M. F., MURPHY, C. S. & JORDAN, V. C. 1988. Estrogenic activity of phenol red. *Mol Cell Endocrinol*, 57, 169-78.
- WEST, J., COGAN, J., GERACI, M., ROBINSON, L., NEWMAN, J., PHILLIPS, J. A., LANE, K., MEYRICK, B. & LOYD, J. 2008. Gene expression in BMPR2 mutation carriers with and without evidence of pulmonary arterial hypertension suggests pathways relevant to disease penetrance. *BMC Med Genomics*, 1, 45.
- WHITE, K., DEMPSIE, Y., NILSEN, M., WRIGHT, A. F., LOUGHLIN, L. & MACLEAN, M. R. 2011. The serotonin transporter, gender, and 17beta oestradiol in the development of pulmonary arterial hypertension. *Cardiovasc Res*, 90, 373-82.
- WHITE, K., JOHANSEN, A. K., NILSEN, M., CIUCLAN, L., WALLACE, E., PATON, L., CAMPBELL, A., MORECROFT, I., LOUGHLIN, L., MCCLURE, J. D., THOMAS, M., MAIR, K. M. & MACLEAN, M. R. 2012. Activity of the estrogen-metabolizing enzyme cytochrome P450 1B1 influences the development of pulmonary arterial hypertension. *Circulation*, 126, 1087-98.
- WILSON, D. W., SEGALL, H. J., PAN, L. C. & DUNSTON, S. K. 1989. Progressive inflammatory and structural changes in the pulmonary vasculature of monocrotaline-treated rats. *Microvasc Res*, 38, 57-80.
- WRIGHT, A. F., EWART, M. A., MAIR, K., NILSEN, M., DEMPSIE, Y., LOUGHLIN, L. & MACLEAN, M. R. 2015. Oestrogen receptor alpha in pulmonary hypertension. *Cardiovasc Res*, 106, 206-16.
- XIONG, J. 2015. To be EndMT or not to be, that is the question in pulmonary hypertension. *Protein Cell*, 6, 547-50.
- XU, D. Q., LUO, Y., LIU, Y., WANG, J., ZHANG, B., XU, M., WANG, Y. X., DONG, H. Y., DONG, M. Q., ZHAO, P. T., NIU, W., LIU, M. L., GAO, Y. Q. & LI, Z. C. 2010. Beta-estradiol attenuates hypoxic pulmonary hypertension by stabilizing the expression of p27kip1 in rats. *Respir Res*, 11, 182.
- XU, W., KANEKO, F. T., ZHENG, S., COMHAIR, S. A., JANOCHA, A. J., GOGGANS, T., THUNNISSEN, F. B., FARVER, C., HAZEN, S. L., JENNINGS, C., DWEIK, R. A., ARROLIGA, A. C. & ERZURUM, S. C. 2004. Increased arginase II and decreased NO synthesis in endothelial cells of patients with pulmonary arterial hypertension. *Faseb j*, 18, 1746-8.
- YANAGISAWA, M., KURIHARA, H., KIMURA, S., TOMOBE, Y., KOBAYASHI, M., MITSUI, Y., YAZAKI, Y., GOTO, K. & MASAKI, T. 1988. A novel potent vasoconstrictor peptide produced by vascular endothelial cells. *Nature*, 332, 411-5.

- YANG, C. F. C., M. Y-C.; CHEN, T-I.; CHENG, C-F. 2014. Dose-dependent effects of isoflurane on cardiovascular function in rats. *Tzu Chi Medical Journal*, 26, lvsp119-122.
- YANG, J., LI, X., LI, Y., SOUTHWOOD, M., YE, L., LONG, L., AL-LAMKI, R. S. & MORRELL, N. W. 2013. Id proteins are critical downstream effectors of BMP signaling in human pulmonary arterial smooth muscle cells. *Am J Physiol Lung Cell Mol Physiol*, 305, L312-21.
- YIN, F. C., SPURGEON, H. A., RAKUSAN, K., WEISFELDT, M. L. & LAKATTA, E. G. 1982. Use of tibial length to quantify cardiac hypertrophy: application in the aging rat. *Am J Physiol*, 243, H941-7.
- YUAN, J. X. J. & RUBIN, L. J. 2001. Pathophysiology of pulmonary hypertension. *Respiratory-Circulatory Interactions in Health and Disease*, 447-478.
- ZHENG, S., CHEN, X., HONG, S., LONG, L., XU, Y., SIMONCINI, T. & FU, X. 2015. 17beta-Estradiol inhibits vascular smooth muscle cell migration via up-regulation of striatin protein. *Gynecol Endocrinol*, 31, 618-24.
- ZOGBI, C., SATURI DE CARVALHO, A. E., NAKAMUTA, J. S., CACERES VDE, M., PRANDO, S., GIORGI, M. C., ROCHITTE, C. E., MENEGHETTI, J. C. & KRIEGER, J. E. 2014. Early postnatal rat ventricle resection leads to long-term preserved cardiac function despite tissue hypoperfusion. *Physiol Rep* [Online], 2. Available: <http://dx.doi.org/10.14814/phy2.12115> [Accessed 18 August 2020].